

# UC San Diego

## UC San Diego Electronic Theses and Dissertations

### Title

The role of BCL2 family genes in chronic myeloid leukemia stem cells

### Permalink

<https://escholarship.org/uc/item/4td3353v>

### Author

Goff, Daniel Jacob

### Publication Date

2012

Peer reviewed|Thesis/dissertation

UNIVERSITY OF CALIFORNIA, SAN DIEGO

**The role of BCL2 family genes in chronic myeloid leukemia stem cells**

A dissertation submitted in partial satisfaction of the requirements for the  
degree Doctor of Philosophy

in

Biomedical Sciences

by

Daniel Jacob Goff

Committee in charge:

Professor Catriona Jamieson, Chair  
Professor Lawrence Goldstein, Co-Chair  
Professor Dwayne Stupack  
Professor David Traver  
Professor Dong-Er Zhang

2012

Copyright

Daniel Jacob Goff, 2012

All rights reserved.

The Dissertation of Daniel Jacob Goff is approved, and it is acceptable in quality and form for publication on microfilm and electronically:

---

---

---

---

Co-Chair

---

Chair

University of California, San Diego

2012

## **DEDICATION**

This work is dedicated to my family: To Dad for sparking my interest in science and for your constant advice; to Mom for your endless encouragement and support; and to my wife and best friend, Elly, for pushing me to be the best person I can be - how lucky I am to have fallen in mutual weirdness with you.

## **EPIGRAPH**

A scientist in his laboratory is not only a technician: he is also a child placed before natural phenomena which impress him like a fairy tale.

*Marie Curie*

## TABLE OF CONTENTS

Signature page .....	iii
Dedication.....	iv
Epigraph .....	v
Table of Contents .....	vi
List of Abbreviations .....	viii
List of Figures .....	x
List of Tables .....	xvii
Acknowledgements .....	xviii
Vita .....	xxiv
Abstract of the Dissertation .....	xxvi
1. Introduction.....	1
1.1. Cancer stem cells: the malignant 1%.....	3
1.1.1. Stochastic versus cancer stem cell-driven malignancy .....	3
1.1.2. Cancer stem cell biology .....	5
1.2. Chronic myeloid leukemia: a paradigm for cancer stem cell-driven malignancy .....	11
1.2.1. Normal and malignant hematopoiesis .....	12
1.2.2. Chronic myeloid leukemia biology .....	16
1.2.3. Treatment of CML .....	19
1.2.4. The role of leukemic stem cells in CML.....	22
1.3. Apoptosis deregulation: a potent mechanism for therapy-resistance in cancer .....	27
1.3.1. Apoptosis versus necrosis.....	28
1.3.2. Mechanisms of apoptosis .....	29
1.3.3. The BCL2 gene family .....	34
1.3.4. BCL2 family regulation .....	38
1.3.5. BCL2 family deregulation in cancer and CML .....	40
1.3.6. Molecular targeting of the BCL2 family .....	43
1.4. Summary: targeting the BCL2 family in CML LSC.....	45
2. Niche targeting of human blast crisis leukemia stem cells with a novel pan-BCL2 inhibitor .....	47
2.1. Introduction .....	49
2.2. Results .....	52

2.2.1. Pro-survival BCL2 family expression is increased in primary CML LSC with progression to BC .....	52
2.2.2. The bone marrow niche protects BC LSC from the TKI, dasatinib	67
2.2.3. Bone marrow LSC are induced into quiescence by TKI-treatment	74
2.2.4. Dasatinib-resistant LSC express pro-survival BCL2 family genes	80
2.2.5. BC LSC are sensitive to sabutoclax, a pan-BCL2 family inhibitor.	85
2.2.6. Sabutoclax sensitizes marrow-niche engrafted BC LSC to dasatinib	93
2.3. Summary and discussion.....	102
2.4. Materials and Methods.....	109
2.4.1. Patient sample preparation and FACS sorting .....	109
2.4.2. Quantitative RT-PCR.....	109
2.4.3. Transcriptome sequencing and analysis .....	111
2.4.4. BCL2 and MCL1 FACS-protein analyses .....	112
2.4.5. <i>In vivo</i> analyses.....	112
2.4.6. DiR staining and measurement by FACS.....	114
2.4.7. FACS cell cycle analysis .....	114
2.4.8. Bone marrow IHC and IF.....	115
2.4.9. Nanofluidic phospho-proteomic immunoassay.....	117
2.4.10. RT-PCR apoptosis array .....	118
2.4.11. Bone marrow BCL2 and MCL1 IHC analysis .....	118
2.4.12. SL/M2 co-culture .....	119
2.4.13. Competitive peptide displacement assays .....	119
2.4.14. <i>In vitro</i> drug treatment and apoptosis analysis.....	120
2.4.15. Colony assays .....	121
2.4.16. Lentivirus transduction .....	121
2.4.17. <i>Ex vivo</i> drug treatment .....	121
2.4.18. Statistical analysis .....	122
3. Conclusions and future studies .....	124
3.1. Exploring further the role of individual BCL2 family genes in CML LSC survival and maintenance.....	126
3.2. The role of BCL2 family genes in CML progression.....	130
3.3. Mechanisms of BCL2 family upregulation in BC LSC .....	133
3.4. The role of the niche in regulating LSC survival.....	138
3.5. Optimizing BCL2 family inhibition for targeting BC LSC.....	149
3.6. Translating BCL2 inhibition to other CSC-driven malignancies.....	154
3.7. Summary .....	157
Appendix.....	158
References .....	163



## LIST OF ABBREVIATIONS

<b>CSC</b>	cancer stem cell
<b>LSC</b>	leukemic stem cell
<b>HSC</b>	hematopoietic stem cell
<b>MPP</b>	multipotent progenitor
<b>CMP</b>	common myeloid progenitor
<b>GMP</b>	granulocyte-macrophage progenitor
<b>MEP</b>	megakaryocyte-erythrocyte progenitor
<b>AML</b>	acute myeloid leukemia
<b>CML</b>	chronic myeloid leukemia
<b>ALL</b>	acute lymphoid leukemia
<b>CP</b>	chronic phase (CML)
<b>AP</b>	accelerated phase (CML)
<b>BC</b>	blast crisis (CML)
<b>TKI</b>	tyrosine kinase inhibitor
<b>Caspase</b>	cysteinyI aspartic-acid protease
<b>IAP</b>	inhibitor of apoptosis
<b>BCL2</b>	B-cell lymphoma 2
<b>MCL1</b>	Myeloid cell leukemia sequence 1
<b>BCLX</b>	B-cell lymphoma-extra large
<b>BFL1</b>	BCL2-related protein A1 (BCL2A1)
<b>MOMP</b>	mitochondrial outer-membrane permeabilization
<b>FACS</b>	fluorescence-activated cell sorting

**FMO** fluorescence minus one control

**MACS** magnetic-activated cell sorting

**IHC** immunohistochemistry

**IF** immunofluorescence

## LIST OF FIGURES

<b>Figure 1.1</b> .....	4
<i>Two models of tumor heterogeneity and propagation: a)</i> in the stochastic or clonal evolution model sub-clones are derived from the cell of origin and from each other via random mutagenesis. Every clone is genetically different and can form a tumor independently. <i>b)</i> In the cancer stem cell model only a unique subset of cells is...	
<b>Figure 1.2</b> .....	5
<i>Traditional versus CSC targeted therapy: a)</i> traditional cancer therapies seek to kill every possible tumor cell. Unfortunately, as CSC are the most resistant to such therapy, they survive treatment and drive relapse. <i>b)</i> With CSC targeted therapy the goal is to eliminate the tumor by eradicating its malignant source. After the CSC...	
<b>Figure 1.3</b> .....	7
<i>Method for assaying CSC tumorigenicity and self-renewal:</i> Putative CSC are isolated from bulk cells and transplanted separately into immunodeficient mice. Only cells with tumorigenic ability will form tumors in the transplanted animals. CSC can then be re-isolated from the tumors and serially transplanted into secondary recipients. Only...	
<b>Figure 1.4</b> .....	15
<i>Overview of hematopoiesis and HSC biology:</i> The HSC life cycle is balanced between quiescence, self-renewal and differentiation. Quiescence protects the fidelity of the stem cell pool while self-renewal expands and maintains the stem cell population. However, in order to produce mature blood cells HSC must differentiate...	
<b>Figure 1.5</b> .....	26
<i>Evolution of CML and development of blast crisis LSC: a)</i> Normal HSC proliferate and differentiate in a highly regulated manner. Acquisition of BCR-ABL generates chronic phase LSC <i>(b)</i> , which have unregulated proliferation and differentiation and produce abnormally high numbers of myeloid cells. Over time, additional oncogenic...	
<b>Figure 1.6</b> .....	31
<i>Overview of the two main pathways of apoptosis: a)</i> The extrinsic pathway is activated by extracellular ligands such as FAS and TNF. These ligands bind to and activate death receptors on the cell surface. This triggers a signaling cascade mediated by death domain-containing proteins, such as FADD, that culminates in...	
<b>Figure 1.7</b> .....	37
<i>Overview of BCL2 family protein organization:</i> BCL2 family proteins fall into 4 different functional groups. These subgroups groups regulate mitochondrial outer-membrane permeabilization (MOMP) by heterodimerization. In the absence of pro-survival stimuli, pore-formers and activators are free and interact with each other to...	
<b>Figure 2.1</b> .....	59
<i>FACS, progenitor analysis scheme:</i> Representative FACS plots of a BC sample showing the gating scheme used for progenitor analysis and sorting.	

<b>Figure 2.2</b> .....	59
<i>BC samples are enriched in granulocyte-macrophage progenitors (GMP). Left: Representative FACS plots of lineage negative cells (top row) and myeloid progenitors (bottom row) in normal, CP and BC samples. Right: Quantification of myeloid progenitor types in normal (n=4), CP (n=8) and BC (n=8) samples.</i>	
<b>Figure 2.3</b> .....	60
<i>BC progenitors express high levels of BCL2 family mRNAs. a) qRT-PCR of pro-survival (long isoforms) BCL2, MCL1, BCLX, BFL1 and BCR-ABL mRNAs in primary CP (black, n=13) and BC (red, n=11) progenitors. b) CP and BC expression compared to that of normal (black, n=16) progenitors. All values are normalized to...</i>	
<b>Figure 2.4</b> .....	61
<i>The MCL1 L:S isoform balance is switched in normal versus CML progenitors. a) RT-qPCR of MCL1<sub>L</sub> and MCL1<sub>S</sub> in normal, CP and BC progenitors. b) MCL1<sub>L</sub>:MCL1<sub>S</sub> ratio in normal (n=7), CP (n=8) and BC progenitors. c) Whole transcriptome sequencing of FACS-sorted progenitor cells from a normal and a BC sample...</i>	
<b>Figure 2.5</b> .....	62
<i>BCLX<sub>L</sub> but not other BCL2 family member mRNA expression is correlated with BCR-ABL expression in CML progenitors. a) Correlation between BCR-ABL mRNA expression and BCLX<sub>L</sub> mRNA expression in progenitors. Left: Primary CP and BC samples (n=20). Right: BCR-ABL transduced normal progenitor colonies (n=12)...</i>	
<b>Figure 2.6</b> .....	63
<i>BCL2 family protein expression is increased in BC progenitors and is correlated with CD123<sup>+</sup> cell expansion. a) Representative FACS histograms of BCL2 and MCL1 protein expression in CP versus BC progenitors. b) Quantitative intracellular FACS analysis of total BCL2 and MCL1 protein in primary CP and BC progenitors. BCL2...</i>	
<b>Figure 2.7</b> .....	64
<i>Normal, CP and BC progenitors differentially express apoptosis genes. a) Clustering of expression of apoptosis related genes in normal (n=3), CP CML (n=7) and BC CML (n=5) progenitors measured by RNA sequencing analysis. Heat-map shows relative fragments per kilobase of exon per million fragments mapped (FPKM)...</i>	
<b>Figure 2.8</b> .....	65
<i>BCL2 family gene expression is generally increased in CML compared to normal progenitors. Relative fold expression of BCL2 family genes in CP (n=7) and BC (n=5) compared to normal (n=3) progenitors measured by RNA sequencing analysis. Graph shows mean +/- SEM for each gene relative to normal progenitors, which are set at 1.</i>	
<b>Figure 2.9</b> .....	66
<i>Normal, CP and BC progenitors differentially express apoptosis-gene splice isoforms. a) Clustering of splice isoform expression in normal (n=3), CP (n=7) and BC (n=5) progenitors. Heat-map shows relative FPKM. Two splice isoforms of RIPK2, which are oppositely upregulated and downregulated, are highlighted in blue. b) Table of...</i>	

<b>Figure 2.10</b> .....	69
<i>Experimental design for measuring the effects of dasatinib on BC LSC in vivo: a)</i> Peripheral blood mononuclear cells (PBMC) were isolated using a ficoll- gradient and CD34 <sup>+</sup> cells were purified using magnetic bead selection (MACS). 50-100,000 CD34 <sup>+</sup> cells were transplanted into neonatal RAG2 <sup>-/-</sup> γ <sub>c</sub> <sup>-/-</sup> mice <sup>33</sup> . <i>b)</i> After a 6-8 week...	
<b>Figure 2.11</b> .....	70
<i>Transplanted BC CML cells form myeloid sarcomas and engraft all hematopoietic niches. a)</i> Representative photographs of control and BC LSC transplanted animals. The arrow denotes a large, subcutaneous myeloid sarcoma. <i>b)</i> Representative FACS plots of total human engraftment (CD45 <sup>+</sup> cells, top row) and progenitor engraftment...	
<b>Figure 2.12</b> .....	72
<i>Bone marrow engrafted BC LSC, but not those in other niches, are resistant to dasatinib. a)</i> Total human CD45 engraftment in liver, spleen, blood, tumor, and bone marrow of BC transplanted mice (see Table 2.2 for n). <i>b)</i> Engraftment of CD45 <sup>+</sup> CD34 <sup>+</sup> CD38 <sup>+</sup> cells in the hematopoietic tissues (see Table 2.2 for n)...	
<b>Figure 2.13</b> .....	73
<i>Dasatinib treatment does not prevent BC CML relapse in secondary transplanted animals. a)</i> Representative FACS plots showing engraftment of CD45 <sup>+</sup> (top row) and CD34 <sup>+</sup> CD38 <sup>+</sup> (bottom row) cells in the marrow of mice that were serially transplanted with whole bone marrow derived from vehicle and dasatinib (25mg/kg) treated...	
<b>Figure 2.14</b> .....	73
<i>Dasatinib significantly reduces BCR-ABL activity in bone marrow engrafted LSC. a)</i> Quantitative proteomic analysis of phospho-CRKL (left) and β <sub>2</sub> microglobulin (right) in FACS-sorted BC progenitors engrafted in mouse bone marrow after treatment with vehicle or dasatinib. <i>b)</i> Quantification of total area under the curve (AUC) of...	
<b>Figure 2.15</b> .....	77
<i>Quiescent BC LSC are engrafted in both spleen and marrow but are more frequent in the spleen. a)</i> Representative FACS histograms of DiR signal retention in CD45 <sup>+</sup> CD38 <sup>+</sup> BC cells engrafted in tumor, spleen, and bone marrow at 18 weeks post-transplant. <i>b)</i> DiR mean fluorescence intensity (MFI) of CD45 <sup>+</sup> CD38 <sup>+</sup> BC cells...	
<b>Figure 2.16</b> .....	78
<i>Dasatinib treatment enriches for quiescent BC LSC in the marrow but not the spleen. a and c)</i> Representative FACS plots showing cell cycle analysis of CD45 <sup>+</sup> CD34 <sup>+</sup> CD38 <sup>+</sup> BC cells engrafted in spleen (top row) and bone marrow (bottom row) following vehicle and dasatinib treatment. <i>b and d)</i> Quantification of G2/S, G1...	
<b>Figure 2.17</b> .....	79
<i>Quiescent bone marrow niche LSC are enriched in the endosteal region. a and b)</i> Representative histological analyses of BC engrafted bone marrow showing H&E, human specific CD45, CD34, CD38 and Ki67 and pHis-H3 staining. The dotted lines delineate the endosteal region (defined as 5 cell widths (~50μm) from the marrow...	

<b>Figure 2.18</b> .....	82
<i>Marrow LSC differentially express BCL2 family genes compared to spleen LSC. a)</i> BCL2 family qRT-PCR array data of FACS-sorted progenitors from engrafted mice (n=3). The graph depicts fold expression in marrow-engrafted progenitors relative to spleen-engrafted progenitors, which are set at 1. All bars are mean +/- SEM...	
<b>Figure 2.19</b> .....	83
<i>Marrow CD34<sup>+</sup> LSC express BCL2 and MCL1 protein. a)</i> Representative immunohistochemical analyses of gross (top) and endosteal (bottom) engraftment of human CD34 <sup>+</sup> , BCL2 <sup>+</sup> and MCL1 <sup>+</sup> cells in mouse bone marrow. Scale bars equal 1mm in low-magnification images and 100µm in high-magnification images...	
<b>Figure 2.20</b> .....	84
<i>BCL2 family expressing BC LSC are more frequent in the epiphyseal region and are highly enriched following dasatinib treatment. a)</i> Quantification of CD34 <sup>+</sup> BCL2 <sup>+</sup> and CD34 <sup>+</sup> MCL1 <sup>+</sup> cells engrafted in the epiphysis and diaphysis of untreated BC engrafted bone marrow (n=3 per group). Statistical analyses are by unpaired t-test...	
<b>Figure 2.21</b> .....	87
<i>Experimental design for in vitro sabutoclax treatment: a)</i> CD34 <sup>+</sup> BC cells were isolated and purified by ficoll-gradient and MACS and cultured either alone or in the presence of SL/M2 stromal cells. <i>b)</i> CD34 <sup>+</sup> BC cells were treated with sabutoclax for 48 hours and apoptosis was measured by FACS. <i>c)</i> For the co-cultured cells, sabutoclax...	
<b>Figure 2.22</b> .....	88
<i>Sabutoclax inhibits multiple BCL2 family proteins with high potency. Fluorescence polarization assay analysis of ABT-737 (a) and sabutoclax (b) against BCL2, MCL1, BCLX<sub>L</sub> and BFL1 protein bound to a BIM peptide. Graph shows mean FITC fluorescence +/- SD from 2 replicate measurements.</i>	
<b>Figure 2.23</b> .....	89
<i>Sabutoclax induces caspase-3 cleavage in CML cells. a)</i> Percent of cleaved caspase-3 positive K562 cells following treatment with different doses of ABT-737 and sabutoclax. Graph shows mean +/- SEM from 3 independent experiments. <i>b)</i> Representative FACS plots of vehicle and sabutoclax treated BC cells. The top row...	
<b>Figure 2.24</b> .....	90
<i>Sabutoclax targets BC LSC in the context of a protective bone marrow microenvironment. a)</i> qRT-PCR of pro-survival BCL2 family transcripts in FACS-sorted BC progenitors after 1 week of culture in the presence of SL/M2 stroma (n=4 experiments) or SL/M2 conditioned media (n=2 experiments). Values are...	
<b>Figure 2.25</b> .....	91
<i>ABT-737 targets BC LSC in vitro. a)</i> FACS analysis of normal (n=5) and BC (n=5) progenitors cultured on SL/M2 bone marrow stroma in the presence of ABT-737. <i>b)</i> Total colonies formed by normal (n=2) and BC (n=3) progenitors following ABT-737 treatment in the presence and absence of SL/M2 stroma. Values for both graphs...	

<b>Figure 2.26</b> .....	92
<i>shRNA-mediated knockdown of BCL2 inhibits BC but not normal colony formation. a)</i> Representative FACS plots of untransduced versus sh-Control and sh-BCL2 transduced progenitors. <b>b)</b> Representative colonies from control or sh-BCL2 transduced progenitors. <b>c)</b> qRT-PCR of <i>BCL2<sub>L</sub></i> mRNA in HEK29T and K562 cell...	
<b>Figure 2.27</b> .....	95
<i>Experimental design for in vivo sabutoclax and combination treatment: CD34<sup>+</sup> BC cells were isolated by ficoll-gradient and MACS and transplanted into neonatal RAG2<sup>-/-</sup>γ<sub>c</sub><sup>-/-</sup> mice<sup>33</sup>. Following a 6-10 week engraftment period, the transplanted mice were split into cohorts and treated with sabutoclax (IP, 3 doses per week), dasatinib (oral...</i>	
<b>Figure 2.28</b> .....	95
<i>Sabutoclax targets engrafted BC LSC in vivo. a)</i> Representative FACS plots of BC cells engrafted in mouse bone marrow showing gating and measurement of human CD45 <sup>+</sup> cells and progenitors after treatment with either vehicle or sabutoclax for 2 weeks and compared to no-transplant control marrow (left column). <b>b)</b> Engraftment...	
<b>Figure 2.29</b> .....	97
<i>Sabutoclax targets quiescent, BCL2<sup>+</sup>MCL1<sup>+</sup> marrow LSC. a)</i> Representative images of BCL2 and MCL1 immunohistochemical staining in BC engrafted bone marrow following vehicle and sabutoclax treatment. The top row shows raw bright-field images while the bottom row shows pseudocoloring for quantification. Scale bars...	
<b>Figure 2.30</b> .....	98
<i>In vivo sabutoclax pre-treatment sensitizes BC LSC to dasatinib ex vivo. a)</i> Scheme and representative FACS plots of vehicle or sabuotclax pre-treated BC progenitors before and after <i>ex vivo</i> treatment with dasatinib for 1 week in SL/M2 co-culture. <b>b)</b> Frequency of live BC progenitors from vehicle (n=3) or sabutoclax (5mg/kg, n=3)...	
<b>Figure 2.31</b> .....	99
<i>Sabutoclax in combination with dasatinib targets marrow engrafted BC LSC. a)</i> Relative engraftment of BC progenitors in spleen, blood and bone marrow following treatment with vehicle (n=9), sabutoclax (1.25mg/kg, n=9), dasatinib (25mg/kg, n=9) and sabutoclax in combination with dasatinib (n=11). Graph shows mean +/- SEM...	
<b>Figure 2.32</b> .....	101
<i>Sabutoclax targets quiescent, BCL2<sup>+</sup> and MCL1<sup>+</sup> BC LSC enriched by dasatinib treatment. a)</i> IHC-based quantification of CD34 <sup>+</sup> Ki-67 <sup>+</sup> BC cells in the epiphysis and diaphysis of bone marrow treated with dasatinib alone (25mg/kg, n=3) and dasatinib + sabutoclax (1.25mg/kg, n=3). <b>b)</b> Frequency of CD34 <sup>+</sup> BCL2 <sup>+</sup> and CD34 <sup>+</sup> MCL1 <sup>+</sup> BC...	
<b>Figure 2.33</b> .....	107
<i>Proposed model for BCL2 family regulation of BC LSC survival and TKI-resistance: BC LSC are primed for apoptosis due to the prolonged effects of BCR-ABL, which induces genetic instability and oncogenic stress, and leads to the upregulation of regulators such as p53 and other pro-apoptotic genes. However, BC LSC fail to...</i>	

<b>Figure 2.34</b> .....	108
<i>Summary: Sabutoclax sensitizes bone marrow-niche engrafted BC LSC to dasatinib-mediated apoptosis. While transplanted BC progenitors engraft multiple hematopoietic niches, these cells are differentially sensitive to dasatinib depending on their <i>in vivo</i> location. Both progenitors and bulk CML cells are highly sensitive to...</i>	
<b>Figure 3.1</b> .....	129
<i>Apogossypol treatment induces "differentiation" of blast crisis progenitors. a) Representative FACS plots of vehicle and apogossypol treated blast crisis cells cultured <i>in vitro</i>. b) Quantification of lineage positive blast crisis cells following treatment with either vehicle or two different doses of apogossypol. Graph shows a...</i>	
<b>Figure 3.2</b> .....	132
<i>Effects of BCL2 overexpression on normal and chronic phase progenitor colony formation and replating: a) Representative bright-field and fluorescence images of empty vector and pCMV-BCL2 transfected HEK29T cells. b) Relative BCL2<sub>L</sub> mRNA expression in empty vector and pCMV-BCL2 transfected HEK293T cells...</i>	
<b>Figure 3.3</b> .....	136
<i>BCL2 protein expression in different primitive populations: a) BCL2 mean fluorescence intensity (MFI) of CD123<sup>-</sup> and CD123<sup>+</sup> progenitor fractions of 13 primary CML samples. Graph shows median with statistical analysis by Mann Whitney test. b) BCL2 MFI of stem (CD34<sup>+</sup>CD38<sup>-</sup>), progenitor (CD34<sup>+</sup>CD38<sup>+</sup>), CD123<sup>-</sup> progenitor...</i>	
<b>Figure 3.4</b> .....	137
<i>A novel deletion variant of GSK3β has impaired ability to downregulate BCL2 protein expression. a) Representative FACS plots showing BCL2 expression in CD34<sup>+</sup> myeloid sarcoma cells following transduction with GSK3β-full length and GSK3β-deletion encoding lentiviruses compared to control lentivirus. b) BCL2 MFI in...</i>	
<b>Figure 3.5</b> .....	137
<i>BCL2 protein variants can be detected and quantified using nanofluidic-proteomic analysis. a) Representative traces of BCL2 signal in control and pCMV-BCL2 transfected HEK293T cells. b) Quantification of β2M and different BCL2 protein peaks in control versus pCMV-BCL2 transfected HEK293T cells. Graph shows...</i>	
<b>Figure 3.6</b> .....	145
<i>Engraftment in the bone marrow niche alters the expression of the BCL2 family and other apoptosis genes in BC progenitors. a) Fold change of significantly differentially expressed splice isoforms in bone marrow engrafted BC progenitors (CD34<sup>+</sup>CD38<sup>+</sup> cells) versus pre-transplantation progenitors. BCL2 family isoforms are highlighted...</i>	
<b>Figure 3.7</b> .....	146
<i>Engraftment in the bone marrow niche alters the expression of apoptosis genes in BC stem cells. a) Fold change of significantly differentially expressed splice isoforms in bone marrow engrafted BC stem cells (CD34<sup>+</sup>CD38<sup>-</sup> cells) versus pre-transplantation stem cells. BCL2 family isoforms are highlighted in red. b) Summary of the top-10...</i>	



<b>Figure 3.8</b> .....	147
<i>The phenotype of engrafted BC CML cells are either niche-independent or niche-dependent, depending on the patient sample. a) Representative FACS plots showing the phenotype of human progenitor cells engrafted in the liver, spleen and bone marrow of BC transplanted mice. The top row shows patient B12 while the bottom...</i>	
<b>Figure 3.9</b> .....	148
<i>Bone marrow engrafted BC CML progenitors are consistently resistant to dasatinib regardless of the patient sample. Relative tissue engraftment of CD45<sup>+</sup> CD34<sup>+</sup>CD38<sup>+</sup> BC cells derived from two different patients following treatment with vehicle (n=5 and n=4 respectively) and dasatinib (25mg/kg, n=5 and n=4 respectively). Both graphs...</i>	
<b>Figure 3.10</b> .....	152
<i>Mice serially transplanted with treated bone marrow ultimately develop high-level leukemic engraftment. Representative FACS plots of mice serially transplanted with vehicle, sabutoclax, dasatinib and combination-treated whole bone marrow showing engraftment of human CD45<sup>+</sup> cells.</i>	
<b>Figure 3.11</b> .....	153
<i>Sabutoclax toxicity in single agent and combination treatment: a) Change in body weight of mice treated with vehicle (n=14 mice) versus sabutoclax (5mg/kg, n=14 mice). b) Local tissue inflammation observed at the site of sabutoclax injection (denoted by the arrow). A vehicle treated control mouse is included for comparison...</i>	
<b>Figure 3.12</b> .....	156
<i>Pro-survival BCL2 expression is increased in bone marrow engrafted prostate cancer cells following castration. qRT-PCR analysis showing relative BCL2<sub>L</sub> mRNA expression in prostate cancer cells harvested from the bone of intact (n=3) versus castrated (n=3) mice. Graph show mean +/- SEM. Statistical analysis is by unpaired...</i>	
<b>Figure A.1</b> .....	158
<i>BC progenitors differentially express several genes involved in cancer signaling. Diagram of common signaling pathways involved in cancer and demonstrating genes significantly different in BC (n=5) versus CP (n=7) progenitors. White = no change; Red = significantly increased expression; Green = significantly decreased expression.</i>	

## LIST OF TABLES

<b>Table 2.1</b> .....	57
CML patient sample characteristics	
<b>Table 2.2</b> .....	71
Frequency of engraftment of human leukemic cell populations in BC LSC transplanted mice	
<b>Table 2.3</b> .....	88
Characteristics of ABT-737 and sabutoclax and efficacy against normal and BC progenitors cultured <i>in vitro</i>	
<b>Table 2.4</b> .....	96
Sabutoclax effects on BC LSC engraftment <i>in vivo</i>	
<b>Table 2.5</b> .....	100
Sabutoclax + dasatinib combination effects on BC LSC engraftment <i>in vivo</i>	
<b>Table A.1</b> .....	159
Apoptosis genes significantly differentially expressed in normal versus BC progenitors	
<b>Table A.2</b> .....	160
Apoptosis genes significantly differentially expressed in normal versus CP progenitors	
<b>Table A.3</b> .....	162
Apoptosis genes significantly differentially expressed in CP versus BC progenitors	

## ACKNOWLEDGEMENTS

I thank my mentor Dr. Catriona Jamieson for her continuous and enthusiastic advice, help and mentorship throughout my graduate training. Dr. Jamieson embodies everything that a medical scientist should strive to be - an excellent and caring clinician, a creative and savvy researcher and a dedicated teacher.

My colleagues in Dr. Jamieson's lab have contributed tremendously to my development as a scientist and I thank them for their friendship and support and for their invaluable assistance with this work. I especially thank Dr. Kristen Smith who performed much of the confocal and fluorescence microscopy and FACS cell cycle analysis, worked closely with me on the *in vivo* combination experiments and greatly helped me focus and refine my thesis. Kristen was essentially a second mentor to me and I am grateful for her thoughtful critique of my work, her thorough experimental advice, and her critical input on my meeting abstracts and manuscript. I credit Ifat Geron and Annelie Schairer for teaching me how to do molecular biology in hematopoietic cells and for training me to do much of the *in vitro* and *in vivo* work detailed here. I also appreciate their suggestions and feedback on my thesis proposal and manuscript. Angela Court-Recart, Alice Shih and Heather Leu helped extensively with mouse experiments and I am indebted to them for their assistance with early-morning "sac-days" and weekend mouse dosing experiments. I also thank Angela for numerous stimulating scientific discussions and for her knowledge of and advice on data analysis and

presentation. Furthermore, I appreciate Angela, Alice and Heather's hard work in maintaining the mouse colony. I am grateful to Dr. Anil Sadarangani for his help with western blot analysis, phospho-proteomics and RNA sequencing experiments. Anil also worked tirelessly to secure patient samples from our various collaborators and helped significantly with grant and manuscript preparation and submission. I thank Ryan Chuang for his enthusiastic assistance with lentivector cloning, PCR and *in vitro* colony experiments. I could not have asked for a brighter and more motivated undergraduate student to work with. Dr. Larisa Balaian assisted with SL/M2 co-culture experiments and I am grateful for her expertise and knowledge of the micro-environmental niche. I thank Dr. Qingfei "Fay" Jiang and Dr. Wenxue Ma for their experimental advice, for assistance with mouse experiments and for critically reading my manuscript. I am also grateful to Fay for her help with writing this dissertation. Thanks to Rusty Wall and all others who helped with processing and banking of patient samples and to Dr. Kim-Hien Dao, Dr. Isabel Newton, Dr. Jennifer Black, Dr. Leslie Crews and Dr. Eva Hellqvist for their constant encouragement and career advice. I also thank Kim-Hien for cloning BCR-ABL lentivector, Isabel for her help with DiR experiments and Jenn, Rusty and Eva for their help with processing mouse tissue. I greatly appreciate the help of Kimberly Wilson who was always willing to sort out any odd administrative problems I encountered. I also thank Kim for scheduling my various thesis committee meetings and for her help with grant and manuscript submission. Finally, thanks to current and former students in the lab, Lilia

Earnest, Cayla Mason and Andrew Burch for their friendship and for contributing to such a fun work environment.

I would like to thank all of my colleagues and collaborators at various institutions in San Diego and abroad. At the Moores Cancer Center I thank Dr. Christian Barrett and Dr. Kelly Frazer who provided crucial assistance with RNA sequencing analysis, Dr. Christina Jamieson who generously helped with *in vivo* apoptosis analysis, Dr. Sheldon Morris who advised and assisted with all statistical analyses, and Dr. Ida Deichaite who helped with industry relations and grant submission. I also appreciate the expert assistance of Dennis Young with whom I spent countless hours analyzing and sorting samples at the Moores FACS core. At UCSD I want to thank Dr. Larry Goldstein and his graduate student Jessica Rusert for providing BCR-ABL lentivirus and for their overall advice and encouragement on this project. At the Sanford-Burnham Institute I thank Dr. Maurizio Pellecchia and his project scientists Dr. Jun Wei and Dr. Shinichi Kitada for providing the BCL2 inhibitors and instruction in how best to administer those compounds. I appreciate their expertise in troubleshooting some of the dosing related issues we encountered. I also thank Dr. John Reed and his project scientists Dr. Maryla Krajewska and Dr. Dayong Zhai who performed the BCL2 and MCL1 protein analysis on paraffin-embedded mouse bone marrow sections and the fluorescence polarization assays, respectively. Thanks to our collaborators Dr. Jason Gotlib at Stanford University, Dr. Mark Minden at Princess Margaret Hospital in Toronto and Dr. Giovanni Martinelli at the University of Bologna

who provided CML patient samples. I also appreciate the contributions of Dr. Marco Marra and Dr. Hye-Jung Chun at the Michael Smith Genome Sciences Center in Vancouver and Dr. Thomas Hudson, Dr. Kamran Shazand, Dr. John McPherson, Dr. Milica Volar and Dr. Richard De Borja at the Ontario Institute for Cancer Research who helped with RNA sequencing and analysis and interpretation of the very complex data. Finally, I want to thank Dr. Jamieson, Dr. Morris, Dr. Goldstein, Dr. Reed, Dr. Krajewska and Dr. Hudson for critically reading and editing our manuscript. I am extremely grateful to all of our collaborators for lending their expertise to this project and am humbled to work with such an array of talented scientists.

I wish to thank all of my international colleagues who invited me to present our work and whose advice, while often challenging, always improved the scope and detail of the project. I'd especially like to recognize Dr. Tomoki Naoe and Dr. Yosuke Minami who hosted me for the 2010 Global Center of Excellence Conference in Nagoya. Dr. Naoe and Dr. Minami also graciously allowed me to work in their lab and I appreciate the opportunity they gave me to discuss and exchange ideas with their students and colleagues at the Nagoya University Graduate School of Medicine.

I'd like to recognize the organizers and coordinators of my fellowship programs. Thanks to Dr. Marilyn Farquhar and the administrators of the UCSD Cancer Training Grant for sponsoring me as a graduate fellow for 2009-2010. Thanks to Dr. Goldstein, Jennifer Braswell, Heather Haber and the other administrators of the CIRM training grant for sponsoring me as a graduate

fellow for 2010-2012. I also wish to thank the other students and professors who attended the weekly CIRM journal clubs and the CIRM retreats for sharing their stem cell knowledge and for the interesting discussions.

Thanks to my friends in the MST program, especially Becca Saenz, Michael Lam and George Hightower for their support and friendship throughout these long years of graduate education. Also, thanks to Becca for allowing me to use her outstanding dissertation as a formatting reference for mine. I would like to thank Dr. Paul Insel, Mary Alice Kiisel and the UCSD MST program as well as Leanne Nordeman, Gina Butcher and the Biomedical Sciences Graduate Program for their guidance and help navigating between medical school and graduate school. I appreciate the advice of Dr. Ken Kaushansky and Dr. Joseph Vinetz who helped me come to a decision on which lab to join. Dr. Kaushansky also served as a member of my thesis committee until he moved to Stony Brook in 2010. Lastly, I wish to thank my thesis committee, Dr. Catriona Jamieson, Dr. Larry Goldstein, Dr. Dwayne Stupack, Dr. David Traver and Dr. Dong-Er Zhang for always being available for advice, for their encouragement and for helping me to become a successful scientist.

Finally, I want to acknowledge those who commented on, proofread and edited this dissertation. Specifically, thanks to my Mom, Sue Chasen, for proofreading amidst her adventures exploring the country. Thanks to Kristen Smith for all of her suggestions and editing. And thanks to my wife, Elly, for

her support and encouragement during the writing process and for her honest and helpful critique of this document.

Chapter 2, in part, has been submitted to Nature Medicine for publication. Daniel J. Goff, Angela Court-Recart, Alice Y. Shih, Anil Sadarangani, Christian L. Barrett, Hye-Jung Chun, Maryla Krajewska, Heather Leu, Jun Wei, Dayong Zhai, Ifat Geron, Qingfei Jiang, Ryan Chuang, Larisa Balaian, Jason Gotlib, Mark Minden, Giovanni Martinelli, Annelie E. Schairer, Wenxue Ma, Jessica Ruser, Kim-Hien Dao, Kamran Shazand, John D. McPherson, Peggy Wentworth, Christina A. M. Jamieson, Sheldon R. Morris, Lawrence S.B. Goldstein, Thomas J. Hudson, Marco Marra, Kelly A. Frazer, Kristen M. Smith, Maurizio Pellecchia, John C. Reed and Catriona H.M. Jamieson. "Niche targeting of human blast crisis leukemia stem cells with a novel pan-BCL2 inhibitor." The dissertation author is the primary investigator and author of the manuscript.



## VITA

- 2004 Bachelor of Science, University of California San Diego
- 2012 Doctor of Philosophy, University of California San Diego
- 2014 (Expected) Medical Doctor, University of California San Diego

## PUBLICATIONS

1. Kavalierchik E, **Goff D**, and Jamieson CHM. "Chronic myeloid leukemia stem cells." *Journal of Clinical Oncology*, 2008 June;26(17): 2911-2915
2. **Goff D** and Jamieson CHM. "Cycling toward elimination of leukemic stem cells." *Cell Stem Cell*, 2010 April 2; (6) 4:296-7
3. Kuwatsuka Y, Minami M, Minami Y, Sugimoto K, Hayakawa F, Miyata Y, Abe A, **Goff D**, Kiyoi H, and Naoe T. "The mTOR inhibitor, everolimus (RAD001), overcomes resistance to imatinib in quiescent Ph-positive acute lymphoblastic leukemia cells." *Blood Cancer Journal*, 2011 1, e17; doi:10.1038/bcj.2011.16
4. Raheem, O, Kulidjian A, Wu C, Jeong YB, Yamaguchi T, Smith KM, **Goff D**, Leu H, Morris SR, Cacalano NA, Masuda K, Jamieson CHM, Kane CJ, and Jamieson CA. "A novel patient-derived intra-femoral xenograft model of bone metastatic prostate cancer that recapitulates mixed osteolytic and osteoblastic lesions." *Journal of Translational Medicine*, 2011 Oct 28;9(1):185
5. **Goff DJ**, Court-Recart A, Shih AY, Sadarangani A, Barrett CL, Chun H, Krajewska M, Leu H, Wei J, Zhai D, Geron I, Jiang Q, Chuang R, Balaian L, Gotlib J, Minden M, Martinelli G, Schairer AE, Ma W, Rusert J, Dao K, Shazand K, McPherson JD, Wentworth P, Jamieson CA, Morris SR, Goldstein LSB, Hudson TJ, Marra M, Frazer KA, Smith KM, Pellicchia M, Reed JC, and Jamieson CHM. "Niche targeting of human blast crisis leukemia stem cells with a novel pan-BCL2 inhibitor." 2012, manuscript in review at *Nature Medicine*.
6. Ma W, Gutierrez A, **Goff DJ**, Geron I, Sadarangani A, Jamieson CA, Court-Recart A, Shih AY, Jiang Q, Wu CC, Li K, Smith KM, Gibson N, Deichaite I, Morris SR, Wei P, Carson DA, Look AT, and Jamieson CHM. "NOTCH1 signaling drives human T-cell acute lymphoblastic leukemia initiating cell survival and self-renewal." 2012, manuscript being prepared for submission for publication.

7. Jiang Q, Crews LA, Barrett CL, Chun H, **Goff DJ**, Minden M, Sadarangani A, Morris SR, Marra MA, Frazer KA, and Jamieson CHM. "RNA Editing Drives Malignant Progenitor Reprogramming in Chronic Myeloid Leukemia." 2012, manuscript being prepared for submission for publication.

#### **FIELDS OF STUDY**

Major Field: Leukemia Stem Cells

Studies in Hematopoiesis, Leukemia and Stem Cell Biology  
Professor Catriona Jamieson

## **ABSTRACT OF THE DISSERTATION**

### **The role of BCL2 family genes in chronic myeloid leukemia stem cells**

by

Daniel Jacob Goff

Doctor of Philosophy in Biomedical Sciences

University of California, San Diego, 2012

Professor Catriona Jamieson, Chair

Professor Lawrence Goldstein, Co-Chair

Leukemia stem cells (LSC) play a pivotal role in therapeutic resistance and progression of chronic myeloid leukemia (CML) to blast crisis (BC). Although effective for treating CML, BCR-ABL targeted tyrosine kinase inhibitors (TKIs) fail to expunge quiescent, niche-resident LSC that drive blastic transformation and relapse. While resistance to therapy occurs through diverse molecular mechanisms, cumulative evidence suggests that anti-apoptotic BCL2 family genes may contribute to CML progression and TKI

resistance as well as to normal hematopoietic stem and progenitor cell survival. However, the role of BCL2 family genes in human BC LSC maintenance has not yet been elucidated.

This dissertation investigates the importance of BCL2 family genes for the survival of CML LSC both *in vitro* and *in vivo* and in the context of the cytoprotective bone marrow niche. Our investigations begin with an examination of BCL2 family gene expression in purified, primary human CML and normal myeloid progenitors (CD34<sup>+</sup>CD38<sup>+</sup>lin<sup>-</sup>). Next, we examine the role of BCL2 expression and quiescence in promoting bone marrow niche-dependent cytoprotection of LSC in a mouse xenograft model of CML. We then investigate whether LSC are susceptible to BCL2 inhibition using pharmacological inhibitors as well as shRNA. Finally, the dissertation concludes with investigations into whether niche-dependent LSC protection LSC may be overcome by using a BCL2 inhibitor in combination with standard TKI-treatment.

CML LSC are found to upregulate multiple pro-survival BCL2 family genes upon progression to BC. Moreover, bone marrow niche-engrafted LSC are quiescent, upregulate BCL2, and are resistant to dasatinib, a potent TKI, compared to LSC in other hematopoietic niches. Notably, in both stromal coculture and xenotransplantation experiments LSC are significantly inhibited with a novel, small molecule pan-BCL2 inhibitor, sabutoclax, at doses that spare normal hematopoietic progenitors. Sabutoclax also sensitizes marrow-niche LSC to dasatinib, and combination treatment delays CML relapse in

serially transplanted mice. These data underscore the importance of pro-survival BCL2 genes in microenvironmental maintenance of malignant stem cells and suggest that niche targeted inhibition of BCL2 family proteins may serve as a vital component of a combined treatment strategy to eliminate quiescent, TKI-resistant LSC in human BC CML.

# 1. Introduction

Cancer has superseded heart disease as the leading cause of death for individuals younger than 85 in the United States and worldwide<sup>1,2</sup>. While significant advances in detection, diagnosis and treatment have led to an encouragingly consistent decline in incidence and mortality from a peak in 1990, more than 1.5 million new cancer cases are projected to occur in 2012 in the United States alone<sup>3</sup>. Moreover, as incidence is invariably linked with age<sup>4,5</sup>, cancer will be a significant source of morbidity as well as financial hardship as the life expectancy of our population continues to increase. Thus there remains a significant need to understand and develop better methods to treat and potentially cure cancer.

For some cancer types, including acute leukemia, pancreatic cancer and lung cancer there has been little improvement in 5-year survival since 1975<sup>3</sup>, and the main challenge is to devise effective treatments for the primary tumor. However, for many other cancers, vast improvements in treatment have made mortality less a direct result of the primary malignancy than a result of relapse and metastasis, which remain significant risks. While encouraging, this nevertheless implies that in many cases current anti-proliferative therapies do not completely eradicate all cancer cells, and over time therapy-resistant cells may resurrect the malignancy. This is inherently an evolutionary process in which the enormous selective pressure of treatment selects for small cohorts of resistant cells from a heterogeneous tumor<sup>6,7</sup>. It is therefore not surprising

that numerous studies show that relapsed tumors are often more aggressive and more therapy-resistant following both radiation and chemotherapy<sup>6-11</sup>. Therefore, a more comprehensive understanding of the molecular underpinnings of therapeutic resistance and relapse has become increasingly important.

In addition to therapeutic resistance mediated by the selection of certain clones, a vast array of data has recently been published supporting the existence of cancer stem cells that are intrinsically resistant to multiple forms of treatment<sup>12-15</sup>. Analogous to tissue specific adult stem cells that give rise to all the cells that make up an organ, cancer stem cells can self-renew and can regenerate the bulk of tumor cells that make up a cancer<sup>16-18</sup>. As opposed to targeting bulk tumor cells that will simply be restored over time, targeting cancer stem cells has the promise of completely eradicating a tumor by removing the source of malignant cells<sup>19</sup>. The elimination of cancer stem cells thus represents an exciting new strategy for curative cancer therapies.

## **1.1. Cancer stem cells: the malignant 1%**

### **1.1.1. Stochastic versus cancer stem cell-driven malignancy**

There currently exist two main models of cancer cell propagation: the clonal evolution model and the cancer stem cell model. In the clonal evolution model, a cancer is thought to come from a single oncogenically mutated cell of origin. As the cell of origin expands there is a stochastic accumulation of additional mutations in the daughter cells leading to the presence of a heterogeneous array of sub-clones with different genetic abnormalities (Figure 1.1a)<sup>20,21</sup>. Importantly, every clone retains the ability to continuously divide and give rise to a new tumor, and heterogeneity comes from selective pressure and random mutagenesis that generates new sub-clones. According to this model, certain sub-clones may be more or less malignant, but this is solely dependent upon the individual array of mutations present in that cell. Also, because essentially any cell has the potential to drive relapse, the best treatment strategy is to kill as many cells as possible. While there is substantial evidence in some cancers for a stochastic model where most cells are tumorigenic<sup>22,23</sup>, seminal experiments by John Dick and colleagues first demonstrated in acute myeloid leukemia (AML)<sup>24</sup> that tumorigenic potential may instead be limited to a certain population of cells, termed cancer stem cells (CSC), that give rise to other malignant cells through a cancer cell hierarchy<sup>25</sup>.



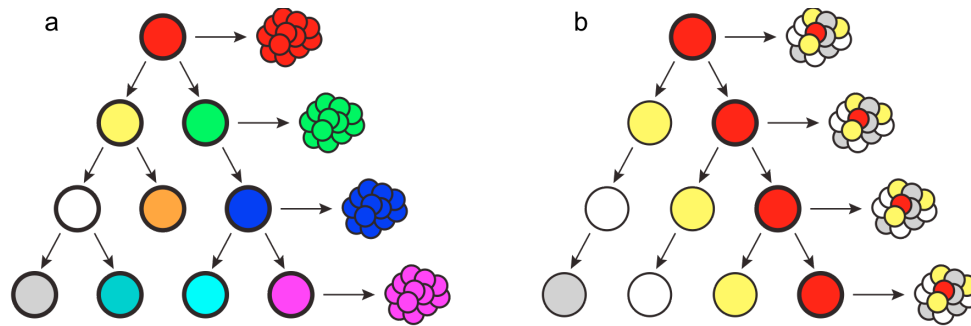


**Figure 1.1.** Two models of tumor heterogeneity and propagation: **a)** in the stochastic or clonal evolution model sub-clones are derived from the cell of origin and from each other via random mutagenesis. Every clone is genetically different and can form a tumor independently. **b)** In the cancer stem cell model only a unique subset of cells is tumorigenic. The other cancer cells are derived from the cell of origin in a hierarchical manner but they cannot form a new tumor independent of the cancer stem cell<sup>20,21,23,26</sup>.

In contrast to the clonal evolution model, the cancer stem cell model posits that the cell of origin is unique in its tumorigenic capacity and behaves like a stem cell from normal regenerating tissue<sup>27</sup>. Just as a normal organ is made up of differentiated cells derived from a limited stem cell pool, it is hypothesized that a cancer is made up of "differentiated" cancer cells derived from a rare malignant stem cell. Non-cancer stem cells may make up the bulk of the tumor but they themselves cannot generate a new tumor. Rather, the cancer is maintained by a continuously self-renewing CSC pool, and tumor heterogeneity comes from sequential and hierarchical differentiation that produces progeny of limited cancer forming ability (Figure 1.1b)<sup>17,23,25</sup>. This model is supported by observations in germ cell and hematopoietic cancers where differentiated cells are clearly derived from neoplastic cells<sup>28-31</sup>. In addition, data from several cancer studies have demonstrated that only a small, phenotypically unique population of cells can transplant disease into

immunodeficient animals<sup>24,32-34</sup>. Together these data suggest that, at least for some cancers, only a small subset of tumor cells may actually be responsible for maintaining the disease. This implies that instead of attempting to kill every last cancer cell, therapy may be more effective if it specifically targets "the malignant 1%": the CSC (Figure 1.2). Therefore, much research has recently focused on understanding the functional mechanisms that drive CSC-dependent cancers.

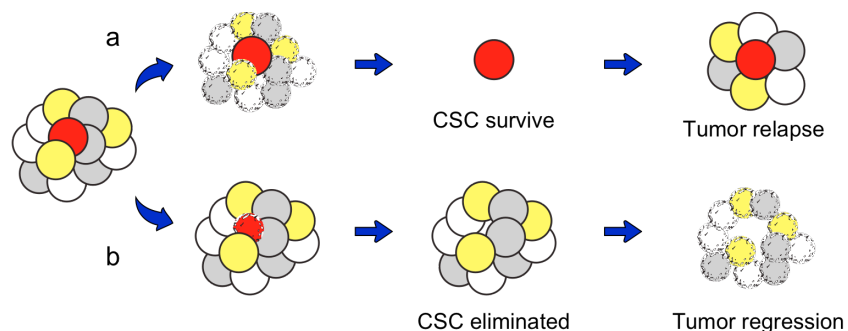


**Figure 1.2. Traditional versus CSC targeted therapy:** **a)** Traditional cancer therapies seek to kill every possible tumor cell. Unfortunately, as CSC are the most resistant to such therapy, they survive treatment and drive relapse. **b)** With CSC targeted therapy the goal is to eliminate the tumor by eradicating its malignant source. After the CSC population is lost the tumor will naturally regress because of the limited tumorigenicity of the remaining cells<sup>17,18,35,36</sup>.

### 1.1.2. Cancer stem cell biology

As in normal stem cells, the defining characteristic of CSC is self-renewal<sup>17</sup>. This trait is assayed experimentally by isolating the cells of interest, usually by fluorescence-activated cell sorting (FACS) or magnetic-activated cell sorting (MACS) using defined cell-surface markers, followed by transplantation into syngeneic (for transgenic models) or immunocompromised

(for xenograft models) mice. Transplanted CSC, which have self-renewal ability, will expand and generate a new tumor while non-CSC will not (Figure 1.3)<sup>17,36</sup>. Tumorigenic ability must be demonstrated serially for a cell to truly be considered a CSC. Serial transplantability distinguishes CSC from other cancer cells, which often have some degree of proliferative potential but not long term self-renewal ability<sup>17</sup>. In addition to self-renewal and differentiation, CSC have been ascribed other stem cell-like traits such as quiescence and radiation- and drug-resistance. For example, in chronic myeloid leukemia (CML), reversibly quiescent CSC have been identified<sup>37</sup> and have been shown to be genetically similar to non-proliferating hematopoietic stem cells<sup>38</sup>. CML CSC are also insensitive to standard therapy<sup>39</sup>. Likewise, a subset of quiescent, drug-resistant AML CSC has been identified in conjunction with the bone marrow niche<sup>40,41</sup>. Together these characteristics allow CSC to survive treatment and to contribute to cancer relapse (Figure 1.2).

Despite the similarity between CSC and normal stem cells it is important to note that CSC is a functional rather than a phenotypic definition: the ability of a cancer cell to serially generate a new malignancy following isolation from the primary tumor<sup>16</sup>. This can be somewhat confusing because it implies that CSC need not necessarily originate from normal stem cells. While there are clear examples such as AML where a mutated stem cell is indeed the cell of origin<sup>24,25,27</sup>, in other malignancies it has been shown that CSC are phenotypic progenitors with aberrant self-renewal potential<sup>42,43</sup>. This discrepancy suggests a few things: 1) CSC can be generated through various

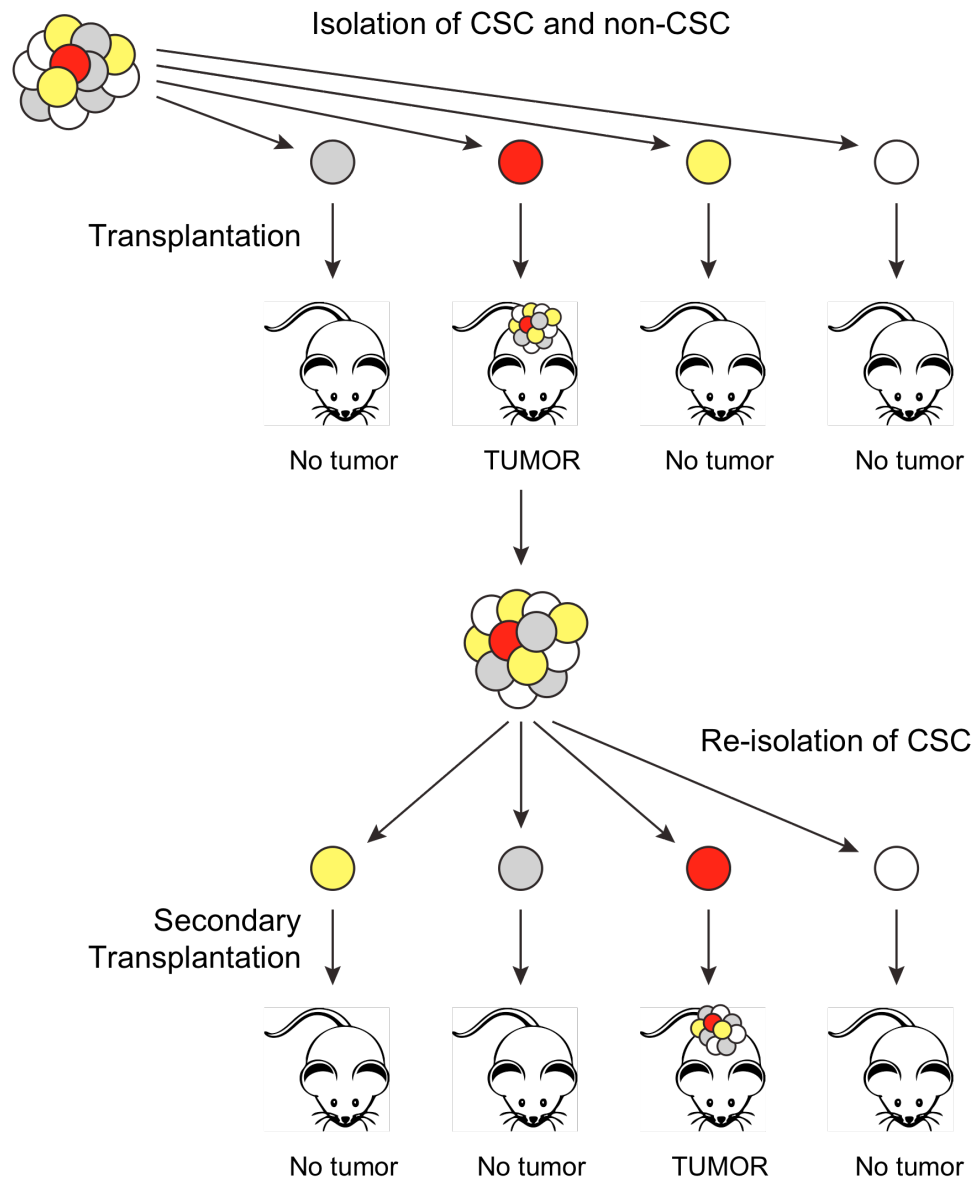


**Figure 1.3.** Method for assaying CSC tumorigenicity and self-renewal: Putative CSC are isolated from bulk cells and transplanted separately into immunodeficient mice. Only cells with tumorigenic ability will form tumors in the transplanted animals. CSC can then be re-isolated from the tumors and serially transplanted into secondary recipients. Only CSC, which are self-renewing, will form secondary tumors<sup>17,23,36</sup>.

genetic mutations that either directly change a normal stem cell into a malignant stem cell or that aberrantly confer "stem-ness" to a more differentiated cancer cell. 2) Theoretically any cell may have the potential to become a CSC provided that it can become self-renewing and able to recapitulate the heterogeneity of the original tumor. 3) The mechanisms of CSC generation and the phenotypic cell of origin are likely different depending on the specific cancer type.

While it is useful to think of CSC as a stable and phenotypically defined population for a particular cancer, it is important to note that CSC are dynamic and likely change in response to further mutagenesis and other selective pressure<sup>21</sup>. Both of these points are exemplified by CML CSC. In the chronic phase (CP) of disease CSC are thought to originate from a malignant hematopoietic stem cell<sup>32,44-47</sup>. As the disease progresses to the blast phase however, there is an accumulation of oncogenic mutations and the CSC phenotype changes to an aberrantly self-renewing myeloid progenitor<sup>36,42,43</sup>. An interesting implication is that CSC clones derived from different cells of origin may exist simultaneously. Also, because CSC are subject to evolutionary forces just like any other cell, random mutagenesis can generate sub-clones of a particular CSC that co-exist and compete with the parental clone<sup>21,26,48</sup>. Therefore the stochastic and CSC models are not mutually exclusive, and in CSC driven malignancies, clonal evolution likely occurs at the level of CSC.

Although there is abundant evidence for the importance of CSC in several cancers, the CSC model is not without controversy. First, there remain well-documented cases of cancers in which virtually all of the cells appear to be cancer-initiating<sup>22,49,50</sup>. A simple explanation is that some cancers follow a stochastic model while others follow a hierarchical model. Opponents of the CSC hypothesis also argue that estimates of CSC frequency are higher in transgenic mouse models than in xenograft models of the same cancer type<sup>50</sup>. Moreover, estimates of CSC frequency in human cancers in particular are shown to depend upon the degree of immuno-competence of host mice<sup>22,23</sup>. Because the identification and study of human CSC depends largely upon the ability of transplanted cells to survive in a foreign host, these results suggest that xenograft assays may significantly underestimate the true CSC population, which depends upon the availability of cytokines and other factors that are not necessarily functional across species<sup>49,50</sup>. Alternatively, xenograft studies may merely identify human cancer cells that can readily adapt to the mouse microenvironment<sup>36</sup>. These concerns have been partially addressed in genetically simpler cancers such as CML and B-cell acute lymphoblastic leukemia (B-ALL), where a single mutation in primitive stem cells can promote cancer formation, and where transgenic mouse model data concerning CSC phenotype and behavior mirrors human xenograft data<sup>31,36,42,43,51</sup>. Unfortunately, because of genetic complexity, transgenic models do not necessarily exist for many cancers. Undoubtedly, the current model systems for studying CSC are not perfect, and clearly the CSC field would benefit from

the development of models more permissive to human cells<sup>23</sup>. Indeed recent studies of normal hematopoiesis and leukemia in improved mouse models that use better injection methods, depletion of residual immunity or transgenic expression of human cytokines report higher frequencies of transplantable self-renewing cells<sup>52-54</sup>. Nevertheless, it is worth reiterating that the CSC definition does not depend upon the exact frequency of tumorigenic cells but upon their function and hierarchical organization<sup>16,55</sup>. Furthermore, these newer studies still identify cells with differential ability to transplant disease and with phenotypes consistent with previous studies. This suggests that while estimates of CSC frequency are likely to become more accurate with better models, the basic premise guiding the CSC model is still accurate, at least for leukemia.

Despite the hurdles involved in their research, CSC continue to be described in new cancers and there is now convincing evidence for CSC in a host of diverse malignancies including those of the brain<sup>56,57</sup>, lung<sup>58</sup>, breast<sup>33,59</sup> and colon<sup>60,61</sup>. These discoveries have undoubtedly contributed to our overall understanding of CSC biology and many deliver promise of new effective treatments for historically incurable cancers. Among the CSC-driven malignancies, CML in particular has proven to be a useful model system for the development of novel therapies directed at the elimination of CSC.

## **1.2. Chronic myeloid leukemia: a paradigm for cancer stem cell-driven malignancy**

The ability to study putative CSC is highly dependent upon the availability of functional and phenotypic markers to aid in the purification of cells via FACS. Research on leukemic stem cells (LSC), which draws on an abundance of knowledge of cell-surface markers garnered from years of study of the hematopoietic system, has therefore been at the forefront of the CSC field. Though significant advances have led to the discovery of CSC in an array of solid tumors, they are still arguably the best characterized in myeloid leukemias. Chronic myeloid leukemia (CML) makes a good CSC-model system in particular because its genetic cause is relatively simple and well documented. Also, CML progresses through readily distinguishable stages marked by specific changes in the LSC population. Studying CML LSC can therefore provide insight into the development and evolution of CSC in general. In addition, because CML has a molecularly targeted therapy, it is useful for modeling CSC responses to treatment. As CML LSC are derived from and share many characteristics with hematopoietic stem cells (HSC)<sup>62</sup>, their biology and resulting malignancy are best understood in comparison to normal HSC and hematopoiesis.



### 1.2.1. Normal and malignant hematopoiesis

Normal HSC constitute a relatively small pool of multipotent stem cells that reside in the bone marrow. As the primary self-renewing population of the hematopoietic system, HSC are responsible for maintaining the proper supply of various differentiated cells that carry out the primary functions of blood: supplying oxygen to tissue, maintaining innate and adaptive immunity and regulating clotting and healing following injury. The HSC pool exists throughout life because differentiated blood cells have a limited life span and must be continuously replenished. In normal homeostatic conditions HSC cell division is balanced between self-renewal, which maintains the HSC population over time, and differentiation, which gives rise to mature functional blood cells. At the single cell level this balance equates to cellular "choices" between symmetrical and asymmetrical division. These choices lead either to the generation of new HSC, which maintain the stem cell population, or to the generation of multipotent progenitors (MPP) that lack long-term self-renewal capacity but have increased proliferative potential (Figure 1.4)<sup>63</sup>. Another direction that an HSC can take is to stay quiescent, and at any time there are separate populations of both resting HSC as well as actively dividing HSC<sup>64</sup>. In the same way that quiescence may confer therapeutic resistance to CSC, quiescent stem cells are broadly more resistant to cytotoxic insults<sup>65</sup>, and this state may therefore be a crucial mechanism for preserving HSC longevity.

Differentiation is a one-way ticket, and following division from an HSC a normal hematopoietic progenitor may never again return to the long-term

self-renewing state. Instead, the newly formed progenitor progresses through sequential stages of expansion and differentiation. This process is characterized by another series of cellular "choices" that lead to hierarchical commitment to a particular hematopoietic lineage. There are two main paths of commitment that the MPP may take: myeloid, which leads to the development of red blood cells, platelets, granulocytes and leukocytes, or lymphoid, which leads to the development of B and T lymphocytes (summarized in Figure 1.4)<sup>63</sup>.

The balance of "choices" that guide HSC and progenitors to the different blood lineages is highly regulated by a complex gene transcriptional network. HSC self-renewal, for example, is maintained by expression of a unique set of transcription factors that promote multipotency. On the other hand, differentiation is induced by sequential activation or silencing of transcription factors that genetically promote lineage specification and commitment<sup>66,67</sup>. The genetic milieu in turn, is controlled by the integration of extracellular cytokine and hormonal signals, as well as direct cell-cell interactions from the bone marrow niche<sup>68,69</sup>. This regulation allows the hematopoietic system to dynamically respond to different situations such as blood loss and infection. For example, in response to anemia and hypoxia from acute blood loss, increased erythropoietin (EPO) released by kidney interstitial cells leads to an increase in progenitor expansion and commitment down the myeloid lineage resulting in increased erythropoiesis<sup>70</sup>. Because of the well-preserved hierarchical organization of the hematopoietic system,

aberrations in this regulatory network tend to result in over-accumulation or shortage of specific blood lineages. Likewise, blood malignancies often result from mutations in HSC or progenitors that dysregulate lineage-specific transcriptional programs and intracellular responses to differentiation signals<sup>67</sup>. Thus leukemias tend also to be lineage restricted and are characterized by over-accumulation of either myeloid or lymphoid cells depending on the regulatory cascade disrupted. A good example is polycythemia vera (PV), where mutation of the kinase JAK2 causes increased EPO responsiveness and intracellular signal transduction leading to skewed differentiation of progenitors down the myeloid lineage and over-accumulation of red blood cells<sup>71</sup>. Similarly, CML is characterized by over-accumulation of differentiated leukocytes and granulocytes due to dysregulated intracellular signaling and transcriptional regulation in BCR-ABL transformed HSC<sup>72</sup>.

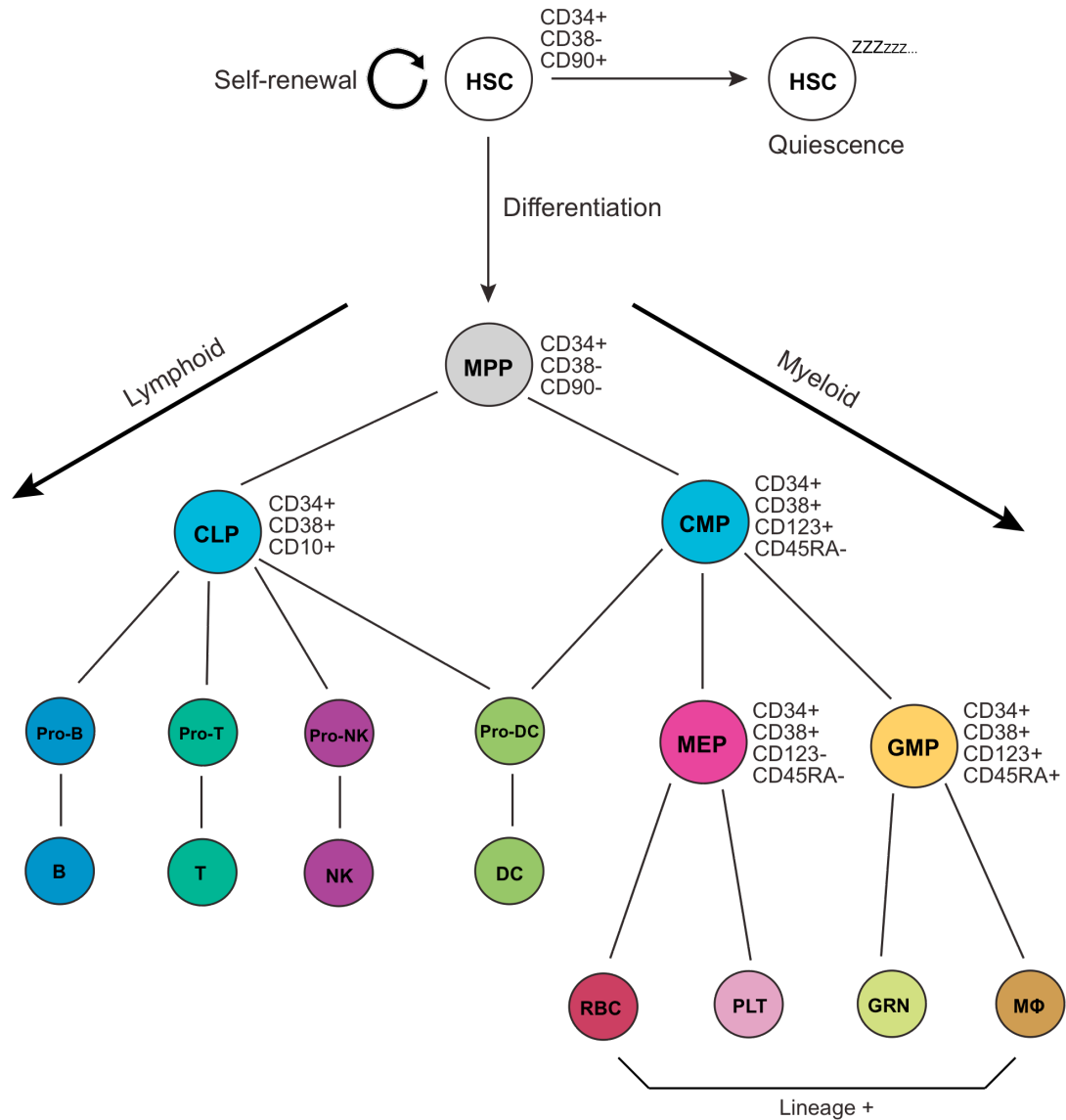


**Figure 1.4. Overview of hematopoiesis and HSC biology:** The HSC life cycle is balanced between quiescence, self-renewal and differentiation. Quiescence protects the fidelity of the stem cell pool while self-renewal expands and maintains the stem cell population. However, in order to produce mature blood cells HSC must differentiate. Differentiation is defined by loss of self-renewal ability and step-wise (via sequential cell-divisions) commitment to a particular lymphoid or myeloid lineage. Human surface markers, used for sorting the cells, are shown for the HSC and progenitor populations. **Abbreviations:** MPP=multipotent progenitor; CLP=common lymphoid progenitor; CMP=common myeloid progenitor; MEP=megakaryocyte-erythrocyte progenitor; GMP=granulocyte-macrophage progenitor; RBC=red blood cell; PLT=platelet; GRN=granulocyte; MΦ=macrophage; NK=natural killer cell; DC=dendritic cell<sup>63,67</sup>.

### 1.2.2. Chronic myeloid leukemia biology

CML, first recognized in patients with high leukocyte counts and splenomegaly, is a progressive myeloproliferative neoplasm with an incidence of about 1 in 100,000 cases per year<sup>72-76</sup>. Clinically, patients usually present in the chronic phase (CP) of disease, where they show over-accumulation of normally differentiated myeloid cells in peripheral blood along with other symptoms related to deficiency of normal hematopoiesis such as anemia and bleeding. Over a period of months to years the disease naturally progresses through an accelerated phase (AP) to an acute phase known as blast crisis (BC), which is much more aggressive, is associated with differentiation block characterized by accumulation of undifferentiated blasts (usually myeloid but can be lymphoid) in blood and bone marrow, and which without treatment is almost uniformly fatal<sup>72,73,76,77</sup>.

Although clinical CML was first described in the mid 1800s, it wasn't until 100 years later that its cellular and molecular biology were truly uncovered<sup>74,75</sup>. In a classic 1960 paper, Nowell and Hungerford described the presence of a characteristic abnormal chromosome in leukocytes from CML patients that they proposed was the cause of malignancy<sup>78</sup>. The Philadelphia Chromosome, as it became known, was the first example of a specific DNA abnormality that could be linked directly to cancer<sup>73,74</sup> and was later shown by Janet Rowley to be the result of a reciprocal translocation between chromosomes 9 and 22 [t(9:22)(q34;q31)]<sup>79</sup>. Subsequently, the 9:22

translocation was shown to create a fusion of the breakpoint cluster (*BCR*) and abelson (*c-ABL*) genes<sup>80-82</sup> that lead to the production of an abnormal chimeric *BCR-ABL* mRNA transcript and protein<sup>83,84</sup>. Clues to the oncogenic function of *BCR-ABL* came from cloning of the *c-ABL* gene, the normal homologue of *v-ABL*, which had been shown to be a proto-oncogene and encode a tyrosine kinase<sup>85,86</sup>. It was soon shown that *c-ABL* kinase activity was enhanced in *BCR-ABL* protein and promoted oncogenic cellular transformation<sup>87,88</sup>, and that transgenic expression of *BCR-ABL* in mouse hematopoietic cells could induce myeloid leukemia<sup>89,90</sup>. Thus, via the oncogenicity of *BCR-ABL*, the Philadelphia chromosome was proven to be the causative genetic abnormality of CML.

The most common *BCR-ABL* variant in CML is P210, made up of *BCR* exons 12-16 (the major breakpoint cluster) fused to the 5'-end of the *ABL* gene. As both genes normally encode ubiquitously expressed kinases (serine-threonine and tyrosine respectively) the *BCR-ABL* fusion protein is a kinase that contains features and regulatory domains from both parental proteins that define its overall function<sup>72,91</sup>. For example, the normal 5'-end of *ABL* contains SRC homology (SH) domains critical for the localization of the protein and physiologic regulation of the kinase domain. Upstream fusion of the *BCR* domain is thought to disrupt SH-domain-mediated regulation of the *ABL* kinase<sup>72,92</sup>. In addition, fused SH domains act as scaffolds that recruit adaptor proteins such as GRB2 that allow *BCR-ABL* to interact with and activate RAS, a regulator of cell proliferation<sup>93</sup>. Thus *BCR-ABL* functions as a constitutively

active ABL kinase, and its oncogenic mechanisms are linked to the activation of various ABL and non-ABL-dependent cellular pathways<sup>72,91,92</sup>.

A wide variety of proteins and pathways have been identified that mediate BCR-ABL-dependent pathogenesis. These include the kinase signaling pathways PI3K-AKT, JAK-STAT and RAS-MAPK, transcription factors such as MYC, and integrins involved in cell adhesion. BCR-ABL-induced alterations in these pathways lead to aberrant cell proliferation, cell cycle, apoptosis, adhesion and homing (exhaustively reviewed by Deininger, Druker, Melo and Barnes)<sup>73,91,94</sup>. For example, in addition to RAS, activation of PI3K-AKT signaling is required for BCR-ABL-mediated transformation and proliferation<sup>95,96</sup>. The PI3K and JAK-STAT pathways also contribute to growth factor independence and cell survival by intracellular activation of IL-3 signaling<sup>91</sup>. In addition to independence from soluble growth factors, CML cells proliferate despite niche-dependent inhibitory signals because of impaired adhesion and integrin signaling<sup>97-99</sup>. Finally, activation of these pathways in tandem contributes to apoptosis-resistance in CML cells (see section 1.3.5), which may be necessary to counterbalance the strong apoptotic stress induced by the concurrent activation of several oncogenic pathways<sup>91</sup>. Together, these data demonstrate the complexity of BCR-ABL-mediated carcinogenesis, but suggest that most of this oncogenic potential may be inhibited by targeting the common activator, BCR-ABL.

Most BCR-ABL-mediated signaling can be linked to the ABL kinase function of the fusion protein. However, downstream targets have also been

shown to depend somewhat on the transformed cell of origin as well as the exact variety of BCR-ABL protein present<sup>91</sup>. For example, the P190 and P230 variants of *BCR-ABL*, which come about from fusion of *ABL* to alternative *BCR* breakpoint cluster regions, have different leukemogenic potential<sup>100</sup>. Interestingly, these variants are more commonly associated with Philadelphia<sup>+</sup>-ALL and chronic neutrophilic leukemia and are rarely seen in CML<sup>72,91</sup>. Because all *BCR-ABL* variants contain essentially the same portion of *ABL*, these data suggest that the phenotypic consequences of *BCR-ABL* expression depend in part on the exact elements contributed by *BCR*. In addition, despite a common link to BCR-ABL for most tumorigenic pathways, BCR-ABL alone does not appear to be sufficient to promote advanced disease. This suggests that other mutagenic events or epigenetic changes, in addition to BCR-ABL expression, are necessary for CML progression and may be important to consider for treatment<sup>13,77,91,101,102</sup>. Nonetheless, *ABL* kinase activity has proved to be absolutely essential for CML development, and inhibition of BCR-ABL has become the cornerstone of anti-CML therapy.

### 1.2.3. Treatment of CML

Traditional therapies for CML included arsenic and splenic irradiation followed later by busulfan and hydroxyurea. These therapies, while somewhat effective in controlling symptoms, were by no means curative and did little to stop progression of the disease or extend patient survival<sup>74,103</sup>. More



successful treatments came first with the development of allogeneic bone marrow transplant in the 1970s<sup>103,104</sup>, followed by interferon-alpha treatment in the 1980s<sup>105</sup>, which induced more durable cytogenetic responses and, in the case of transplant, could be curative. However, interferon treatment was successful only for a subset of patients, while the use of transplant depended upon the availability of compatible donors. Therefore, despite major improvements, there was still need for a more ubiquitously effective therapy. The recognition of BCR-ABL as the key player in CML pathogenesis naturally led to the hypothesis that inhibition of BCR-ABL could be used as an effective therapeutic strategy. So, 40 years after the discovery of the Philadelphia chromosome, clinical trials began on the first BCR-ABL targeted tyrosine kinase inhibitor (TKI), imatinib<sup>106</sup>.

TKIs function as molecular mimetics that bind to the kinase domain of BCR-ABL and prevent binding of ATP<sup>73</sup>. This prevents BCR-ABL from phosphorylating downstream proteins and causes cell death in CML cells specifically<sup>107</sup>. Since being introduced clinically in 2001, TKIs have been tremendously successful and the 5-year survival rate of treated chronic phase patients now exceeds 80%. Even more impressive is that greater than 60% of these patients achieve long-term major cytogenetic responses<sup>108,109</sup>. For some, this has led to a new view of CML as more a manageable chronic condition than a deadly malignancy. Despite this dramatic success, Philadelphia<sup>+</sup> cells are still detectable in some patients treated with TKIs, including those who achieve major cytogenetic responses<sup>110,111</sup>. Worse, a

large proportion of patients who discontinue imatinib relapse<sup>112-114</sup>, a significant problem particularly for those patients who, for economic or clinical reasons, can't continue therapy. For those patients who are compliant, there is significant risk for the development of TKI resistance-imparting mutations in the *BCR-ABL* gene<sup>115,116</sup>. Moreover, a number of patients progress to BC even with treatment, which is clinically significant because the disease becomes much more malignant and refractory to continued TKI therapy<sup>77</sup>. These issues have been somewhat addressed by the recent development of newer and more potent TKIs that are even more effective in killing BCR-ABL<sup>+</sup> CML cells, albeit with significant side effects. Unfortunately, a substantial number of patients fail to respond to all TKIs<sup>76,77</sup>, and the only recognized curative therapy for CML remains bone marrow transplant<sup>103</sup>, which comes with significant risks of morbidity and mortality. Together these findings suggest the existence of a subset of CML leukemic stem cells that are intrinsically resistant to treatment and that can initiate progression and relapse following elimination of most of the disease. Without doubt, current treatments effectively kill bulk CML cells and dramatically slow disease progression. However, any curative therapy will have to invariably target the leukemic stem cell population critical for disease persistence.

#### 1.2.4. The role of leukemic stem cells in CML

Evidence for CML leukemic stem cells (LSC) first came from studies of chronic phase demonstrating that CML cells were clonal in origin and hierarchically derived from a cell that could generate both the myeloid and lymphoid lineages<sup>44-46</sup>. These data strongly suggested that HSC were the CML cells of origin and were later complemented by animal models demonstrating that transplanted human CD34<sup>+</sup> CML cells could engraft immunodeficient mice long-term<sup>32</sup>. That resistant LSC are the instigators of relapse was later evidenced by sensitive PCR analyses showing that residual disease is largely restricted to the stem cell compartment<sup>111</sup> and by direct analysis of BCR-ABL<sup>+</sup> HSC showing that these cells are insensitive to TKI treatment<sup>39,110,117,118</sup>. Recently, these observations have been further strengthened by mathematical models of clinical CML that support the clonal and hierarchical nature of the disease and the existence of a TKI-resistant LSC population<sup>119-121</sup>.

Based on the wealth of data indicating malignant HSC as the chronic phase cells of origin, it would be natural to assume that blast crisis CML is driven by increasingly malignant HSC. Yet blast crisis appears to actually be propagated by phenotypic hematopoietic progenitors. This is evidenced by data showing expansion of the granulocyte-macrophage progenitor (GMP) population in blast crisis, and demonstrating that malignant blast crisis GMP can both serially re-plate and serially transplant blast crisis CML in immunocompromised mice<sup>34,42</sup>. These results are further supported by data in syngeneic animal models where transgenic overexpression of BCR-ABL in

MPP leads to expansion of serially transplantable GMP<sup>43</sup>. Surprisingly, in some models malignant GMP are actually more potent at initiating disease than HSC<sup>34</sup>, suggesting that progenitors rather than HSC may be the key propagators of blast crisis CML. These data raise an important question: How do myeloid progenitors, normally a non-self-renewing population, become tumor-initiating LSC in blast crisis?

A hallmark of blast crisis is the appearance of new chromosomal abnormalities<sup>77</sup>. These are partially explained by the fact that long-term exposure to oncogenic kinases causes increased genetic instability and mutagenesis by induction of chronic DNA damage<sup>122</sup>. In CML this is exemplified by data showing that BCR-ABL induces the production of DNA-damaging reactive oxygen species (ROS)<sup>123,124</sup>. However, BCR-ABL also paradoxically increases DNA repair by prolongation of the G2/M phase of the cell cycle<sup>124-126</sup>. This apparent contradiction is explained eloquently by Radich who writes: "the combination of more DNA damage and more repair activity may lead to less exact repair; since Bcr-Abl also up-regulates anti-apoptosis genes BCL2 and BCL-XI, and thus causes G2/M delay, the stage is set to accumulate DNA damage without the mechanisms to eliminate these cells."<sup>77</sup> It is worth noting that BCR-ABL is not the only cause of genetic instability. Chromosomal abnormalities in CML cells may also result from natural stem cell aging. Regardless of the cause, it is evident that CML progression and the CP-to-BC transition in particular are heralded by massive changes in gene expression that alter the phenotype and aggressiveness of the LSC<sup>77,101,102</sup>.

As mentioned earlier, any cancer cell has the potential to become a CSC provided that it becomes self-renewing and can recapitulate the tumor following isolation. Thus, accumulated mutations in BCR-ABL<sup>+</sup> cells activate aberrant self-renewal in GMP and promote progression to blast crisis CML.

The best-characterized self-renewal pathway active in blast crisis LSC is the WNT/ $\beta$ -catenin pathway, which is critical for the self-renewal of normal HSC<sup>127,128</sup>. In contrast to normal hematopoietic progenitors, which don't self-renew, blast crisis GMP are shown to have significant levels of nuclear  $\beta$ -catenin due in part to dysfunctional regulation of its degradation<sup>34,42</sup>. Consistent with these results, elevated nuclear  $\beta$ -catenin increases the self-renewal of blast crisis progenitor cells<sup>34,43</sup>. In addition to this pathway, self-renewal may be activated in blast crisis progenitors by increased Hedgehog and Notch signaling, which are involved in normal stem cell fate determination as well as self-renewal<sup>19,129,130</sup>. Besides activation of self-renewal, blastic transformation is also driven by deregulation of normal differentiation, cell cycle progression and apoptosis<sup>13,77</sup>. Much of this is likely mediated by enhanced BCR-ABL activity<sup>76</sup>, as BCR-ABL expression is elevated in blast crisis cells and associated with increased survival as well as increased resistance to TKIs<sup>131,132</sup>. BCR-ABL-independent genetic and epigenetic changes also likely play a role. For example, the transcriptional repressor BMI1 is overexpressed in blast crisis cells and may contribute to impaired myelopoiesis by downregulation of *Hox* family genes<sup>133,134</sup>. Gene-profiling analysis of CD34<sup>+</sup> CML cells has also highlighted a number of genes involved

in the cell cycle (*GASDD45G*, *FANCG*), differentiation (*CEBA*, *CEBPE*) and survival (*FOXO3A*) that are significantly differentially expressed in blast crisis versus chronic phase<sup>77,101</sup>.

Together, the evidence for increasingly malignant self-renewing blast crisis progenitors has led to a revised model of how LSC drive CML (Figure 1.5). Whereas BCR-ABL expression in HSC is necessary and sufficient to initiate chronic phase disease, it alone cannot fuel CML progression. Instead, BCR-ABL mediates long-term genetic instability and, according to Radich, "is the 'brains' behind the pathogenesis and progression of CML, though along the way it recruits a bevy of accomplices that facilitate resistance and progression."<sup>102</sup> These "accomplices" include aberrant self-renewal pathways, such as WNT/ $\beta$ -catenin, as well as other mutated genes that confer selective advantages to blast crisis LSC such that they are more proliferative and more apoptosis-resistant. Together, these attributes allow blast crisis LSC to outcompete the original cell of origin and to become the dominant LSC clone<sup>36,42,76</sup>. Despite potentially unlimited alterations that could result from BCR-ABL-mediated genetic instability, those so far described consistently fall into discreet functional categories (e.g. self-renewal, differentiation block, etc.)<sup>76,77</sup>. This suggests that targeting these common pathways may be an effective means to eliminate TKI-resistant CML LSC. Targeting the apoptotic pathway represents one such approach that may be particularly useful given that the main mechanism of TKI-killing is apoptosis induction, and given the consistent link between LSC and apoptosis-resistance.

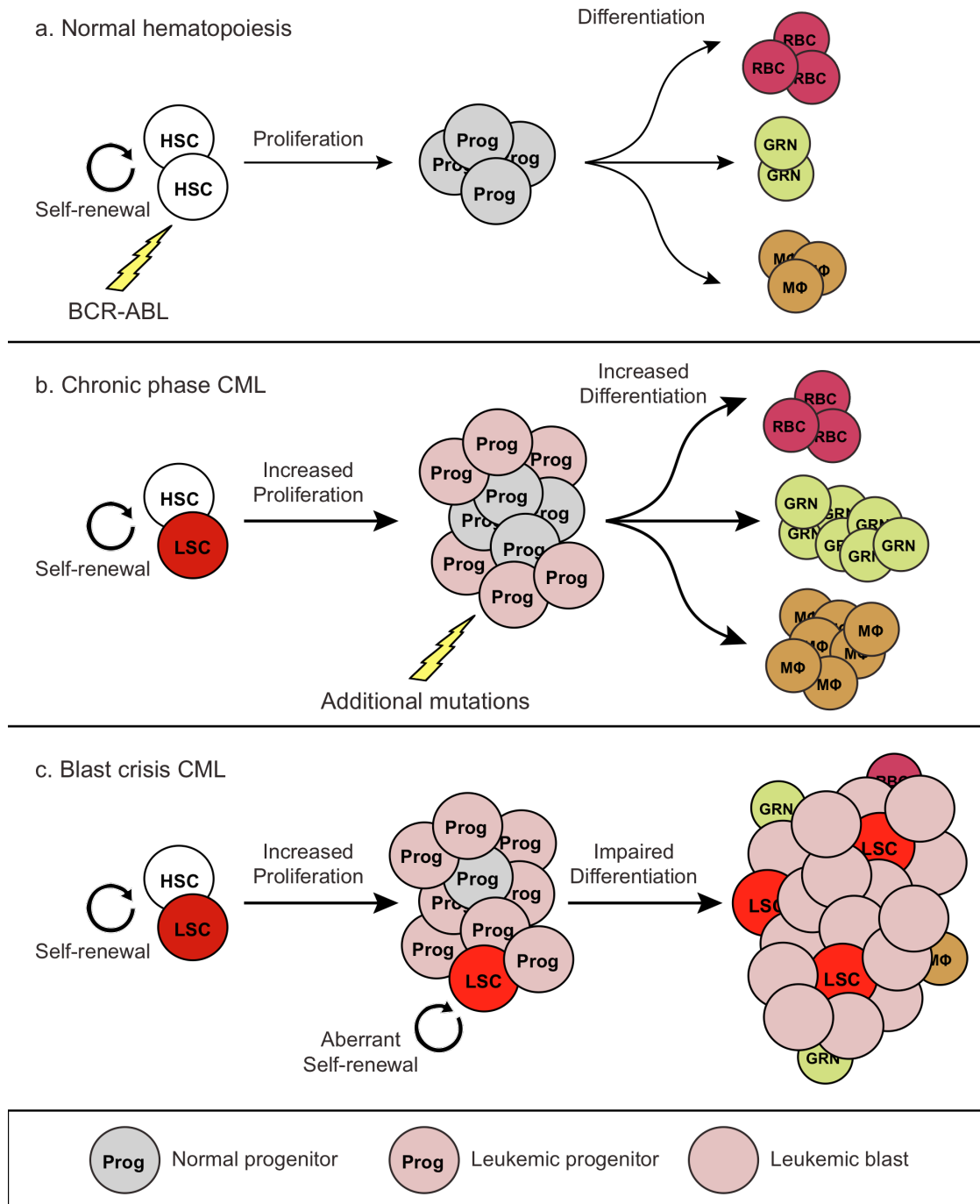


**Figure 1.5. Evolution of CML and development of blast crisis LSC.** **a)** Normal HSC proliferate and differentiate in a highly regulated manner. Acquisition of BCR-ABL generates chronic phase LSC **(b)**, which have unregulated proliferation and differentiation and produce abnormally high numbers of myeloid cells. Over time, additional oncogenic mutations in leukemic progenitors lead to activation of abnormal self-renewal and the generation of blast crisis LSC **(c)**, which are marked by differentiation block and primarily generate poorly differentiated leukemic blasts<sup>36,42</sup>.

### **1.3. Apoptosis deregulation: a potent mechanism for therapy-resistance in cancer**

The term "cell death" immediately brings to mind negative processes - cell death caused by ischemia in heart attack and stroke, cell death associated with neural degeneration and aging, etc. However, programmed cell death via apoptosis is also a normal physiologic process critical for tissue development and homeostasis (reviewed by Fuchs and Steller)<sup>135</sup>. The apoptotic process plays a role, for example, in limb development by removal of interdigital tissue, and in the development of the neural tube and heart by regulating formation of hollow tubes and chambers in solid embryonic precursor tissue. In tissues such as the blood and nervous system where cells are produced in overabundance, apoptosis maintains proper physiologic cell numbers by eliminating older, dysfunctional, and damaged cells. The apoptotic elimination of cells is also a crucial disease-defense mechanism and is responsible for the removal of negatively selected B- and T-cells that recognize auto-antigens as well as oncogenically transformed cells<sup>135-137</sup>. Because of its important physiologic roles apoptosis must be highly regulated, and improper apoptotic responses are associated with many disease processes. Too much apoptosis contributes to neural degeneration, for example, while too little can allow for auto-immunity. Deregulation of apoptosis is also characteristic in cancer development and has recently become an exciting target for anti-cancer therapeutics.



### 1.3.1. Apoptosis versus necrosis

There are two traditional classifications of cell death: necrosis and apoptosis (reviewed by Edinger and Thompson)<sup>138</sup>. In contrast to necrosis, which is energy-independent and largely unregulated, apoptosis is an ATP-dependent process that proceeds in a highly regulated step-wise fashion. Apoptosis is distinguished from necrosis both mechanistically and morphologically. Necrosis generally results from non-specific toxicity that physically damages the cell and compromises the cellular machinery necessary for energy production. This damage causes a "crisis" that leads to the massive depletion of cellular ATP and results in swelling, cytoplasmic vacuolization, fracturing of the plasma membrane and uncontrolled release of pro-inflammatory intracellular contents. In contrast, apoptosis initiation occurs by specific molecular triggers. These activate an intracellular signaling cascade that results in cell shrinkage along with chromatin condensation and nuclear fragmentation. Plasma membrane integrity is maintained throughout apoptosis, and as the cellular components degrade they are compartmentalized into apoptotic bodies that are cleared by non-inflammatory phagocytosis<sup>137-139</sup>.

Despite their differences, apoptosis and necrosis are not mutually exclusive and secondary necrosis can follow from apoptosis if the availability of ATP becomes compromised<sup>139</sup>. Energy depletion may also trigger autophagy, a process whereby the cell "recycles" its own organelles by lysosomal-mediated degradation to conserve ATP<sup>138</sup>. While autophagy is

normally considered a survival mechanism that allows the cell to endure prolonged starvation or growth factor deprivation, there is also evidence that autophagy may promote cell death in the absence of apoptosis initiation. Therefore, there exists a degree of plasticity and cross talk between necrosis, apoptosis and autophagy<sup>138,140</sup>. Nevertheless, apoptosis (and its deregulation) are a central theme in cancer development and its molecular regulation merits more discussion.

### **1.3.2. Mechanisms of apoptosis**

Apoptosis proceeds via two main pathways, extrinsic and intrinsic, depending upon the nature of the pro-death stimulus (reviewed by Elmore and summarized in Figure 1.6)<sup>139</sup>. The extrinsic pathway is triggered by extracellular signals and is transduced by membrane-bound receptors. Extrinsic apoptosis can also be induced by cytotoxic T-cells via an alternative pathway mediated by perforins and granzymes. In contrast, the intrinsic pathway is triggered by intracellular signals activated in response to noxious stimuli that damage cellular components or compromise normal cellular functions. These signals regulate the integrity of the mitochondrial membrane and control the release of pro-apoptotic molecules into the cytoplasm. Following apoptosis initiation both pathways converge on a common pathway, also known as the execution pathway, which culminates in the activation of a proteolytic caspase cascade. Convergence explains why, despite different

mechanisms for initiation, all types of apoptosis are characterized by the same biochemical changes. These changes are directly mediated by caspases and include protein cleavage, protein cross-linking, DNA fragmentation, plasma membrane "flipping" and increased expression of phagocytic recognition markers<sup>137,139,141</sup>.

The term caspase, short for cysteinyl aspartic acid-protease, refers to a family of genes of similar structure and function (thoroughly reviewed by Reidl and Shi)<sup>142</sup>. Caspase genes are highly phylogenetically conserved with homologues found in everything from vertebrates to fruit flies to yeast. In humans there are eleven different caspase genes that are grouped according to their differential role in apoptosis: initiator versus executor. Implicit in the name, all caspase genes encode proteases that cleave target proteins at aspartic acid residues. However, the exact sites of cleavage are specific to individual caspases and are determined by surrounding amino acid sequences. While caspases are broadly expressed, they usually exist in an inactive pro-enzyme form (pro-caspase) and must be proteolytically activated<sup>139,142</sup>. This occurs in a step-wise fashion: first, extrinsic or intrinsic signals stimulate the production of intracellular death-inducing protein complexes. These complexes facilitate auto-activation of initiator caspases (caspase-2, -8, -9, -10). The active initiator caspases then proteolytically cleave and activate executor caspases (caspase-3, -6, -7), which subsequently target and cleave an array of diverse protein substrates.

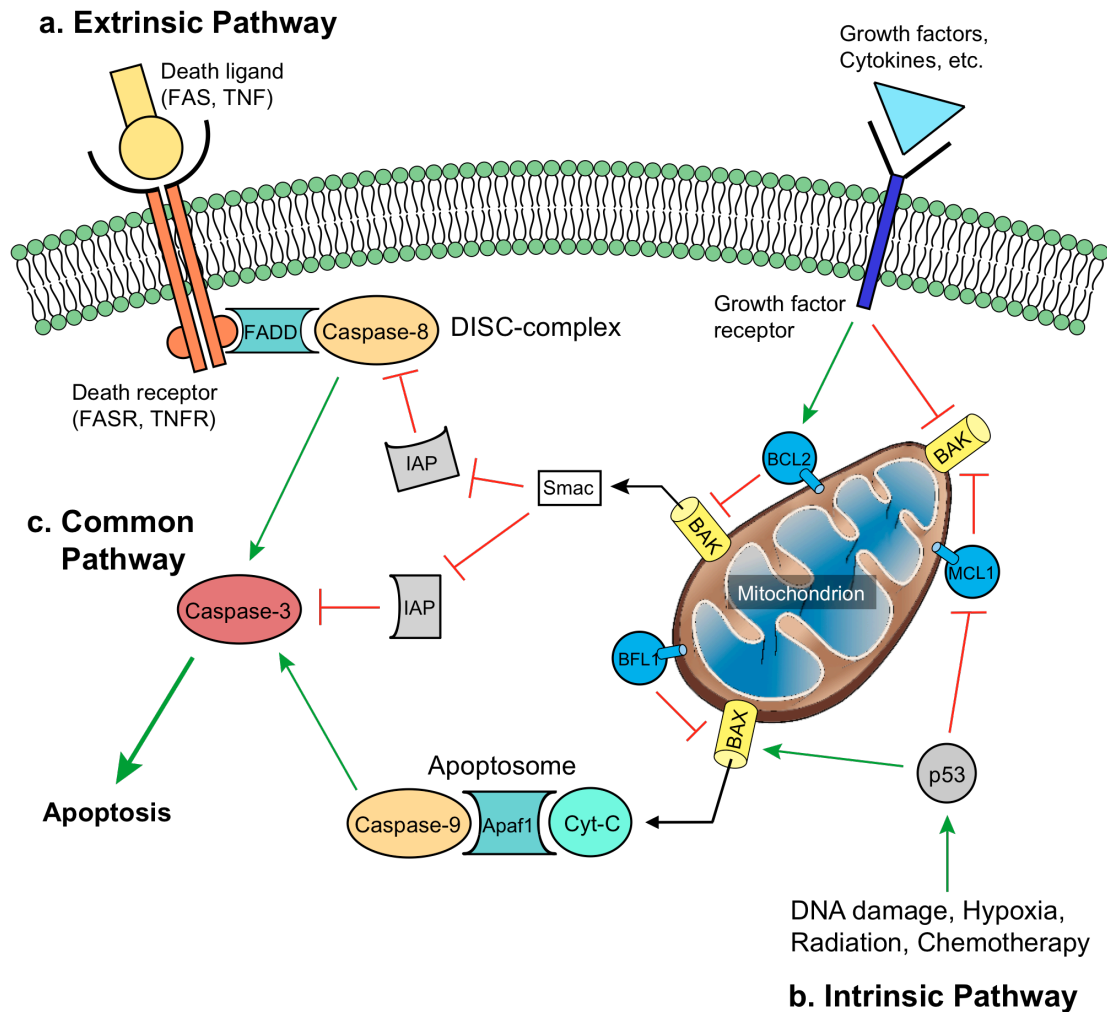


**Figure 1.6.** Overview of the two main pathways of apoptosis: **a)** The extrinsic pathway is activated by extracellular ligands such as FASL and TNF. These ligands bind to and activate death receptors on the cell surface. This triggers a signaling cascade mediated by death domain-containing proteins, such as FADD, that culminates in activation of the DISC complex. The DISC complex facilitates proteolytic cleavage of initiator caspase-8. **b)** The intrinsic pathway is activated by intracellular signals that affect the health of the cell. These signals initiate pore formation in organelles including the mitochondria. Pro-apoptotic mediators, such as cytochrome-C, then leak into the cytoplasm and interact with Apaf1 to form an apoptosome, which facilitates cleavage of initiator caspase-9. Mitochondrial pore formation is also modulated by extracellular signals such as growth factors **c)** The caspase cascade is the common pathway of apoptosis. This pathway is triggered by initiator caspases (such as caspase-8 and -9), which proteolytically cleave and activate executor caspases, such as caspase-3. Activated executor caspases then cleave cellular substrates and are responsible for the biochemical changes that define apoptosis<sup>135,139,141</sup>.

The expression of caspases as pro-enzymes constitutes a molecular safety-lock that prevents cell death by default. This is complemented by reversible expression of inhibitors of apoptosis (IAPs) that directly regulate the enzymatic activity and stability of caspases<sup>142-144</sup>. At the same time, organization of caspases into a proteolytic cascade allows the apoptotic response to be amplified once a pro-death signaling threshold is crossed<sup>139</sup>. In addition, activated executor caspases actually target and cleave upstream initiator caspases in a positive feedback loop. This ensures that apoptosis behaves in an all-or-none fashion<sup>145</sup>. Activation of the caspase cascade can be considered the *coup de grâce* of apoptosis because, once it is triggered, cell death irreversibly proceeds to completion<sup>139,142</sup>. Therefore, tight regulation of the cascade is crucial in order to prevent inadvertent cell death. In addition to IAP-mediated regulation, there is a network of genes that controls apoptosis upstream of initiator caspase activation.

Caspase activation via the extrinsic pathway occurs at the plasma membrane following ligand binding to membrane-bound death receptors (Figure 1.6a). The best described of these receptor-ligand pairs are FAS/FASL as well as TNFR/TNF, which mediate the immunologic clearance of malignant and infected cells<sup>139</sup>. In a classic example, FAS death receptors are expressed on the cell surface in response to infection. The ligand, FASL, is expressed in turn by cytotoxic T-cells responsible for clearing the infection. As the two cells interact the pro-apoptotic ligands bind to their corresponding death receptors. This binding causes receptor aggregation and conformational changes that

expose cytoplasmic death domains on the receptors. Exposure of these domains allows the recruitment of death domain-containing adaptor proteins, such as TRADD and FADD, to the plasma membrane. Localization to the membrane allows the adaptors to recruit pro-caspase-8 along with other proteins that together form a death-inducing signaling complex (DISC). This DISC-complex then facilitates the auto-proteolytic cleavage of pro-caspase-8, an initiator caspase, which in turn triggers the downstream caspase cascade<sup>139,141,146</sup>.

In contrast to extrinsic apoptosis, which is receptor-mediated, intrinsic apoptosis is regulated by diverse pro-death and pro-survival factors that are broadly linked to the overall genetic and metabolic health of the cell. Intracellular noxious stimuli that affect normal cellular function alter the balance of these factors and induce the intrinsic pathway. These stimuli can either be direct damaging forces such as radiation, hypoxia and oxidative stress, or indirect such as the removal of supportive growth factors and cytokines (Figure 1.6b)<sup>137,139,141</sup>. For example, cytotoxic drugs and radiation can cause DNA damage, which activates pro-death proteins such as p53 that directly induce intrinsic apoptosis<sup>147</sup>. On the other hand, the withdrawal of crucial growth factors can indirectly activate apoptosis by the removal of pro-survival signals<sup>139</sup>. Regardless of the exact initiator, intracellular apoptotic stimuli cause the formation of pores in the outer membrane of the mitochondria and endoplasmic reticulum (ER). This allows molecules such as cytochrome-C to leak into the cytoplasm where they complex with Apaf-1 and

pro-caspase-9, another initiator caspase, to form a death-signaling complex called the apoptosome. The newly formed apoptosome facilitates auto-proteolytic activation of pro-caspase-9, which then triggers the caspase cascade by cleavage of downstream executor caspases-6 and -3<sup>139,141</sup>. Along with cytochrome-C, other pro-apoptotic molecules are released from organellar pores and contribute to caspase-mediated processes. These include IAP inhibitors such as Smac/DIABLO and DNA fragmenting enzymes such as AIF and endonuclease G. In addition, release of Ca<sup>2+</sup> ions from the ER causes metabolic stress, which can potentiate apoptosis<sup>139,141,148</sup>. As the major molecular event of intrinsic apoptosis, organellar pore formation must be tightly regulated. This is primarily accomplished at the mitochondrial membrane by the BCL2 family of genes. This family, which encodes an array of pro-death and pro-survival proteins, directly regulates pore formation and thus facilitates release or sequestration of the key components of intrinsic apoptosis<sup>139,141,149,150</sup>.

### **1.3.3. The BCL2 gene family**

The BCL2 family includes over 20 proteins involved in apoptosis regulation (extensively reviewed by Cory and Adams)<sup>151</sup>. The archetypical function of this protein family is to either promote or inhibit the formation of pores in the mitochondrial and ER membranes in response to upstream apoptotic or survival signals. Consistent with these functions, many BCL2

family proteins contain transmembrane domains that localize them to the organellar membrane. However, a significant number of BCL2 family proteins do not contain such domains and are cytoplasmically localized. These cytoplasmic proteins generally function to modulate pore formation by the membrane-bound subset. Despite a variety of exact structures, BCL2 family proteins all share one or more common functional domains, called BCL2-homology (BH) domains. These domains allow BCL2 family proteins to interact with each other as heterodimers, and are crucial for the regulatory function of the proteins. The number and type of BH domains can be used to roughly classify the BCL2 family into functional sub-groups: the pore-forming group (e.g. BAX, BAK), the pro-survival group (e.g. BCL2, MCL1, BCLX) and the BH3-only death-inducing group (e.g. BAD, BID, BIM) (summarized in Figure 1.7).

Pore-forming BCL2 family members, BAX and BAK, are pro-death proteins that contain three BH domains (BH1-BH3) and a transmembrane domain. BAX and BAK are expressed in most cell types and are essential for intrinsic apoptosis. Upon activation by apoptotic stimuli, BAX and BAK form homo-oligomers that constitute molecular pores. These pores lead to mitochondrial outer-membrane permeabilization (MOMP), which then allows release of cytochrome-C into the cytoplasm as described previously. In the absence of apoptotic stimuli, BAX and BAK are held in an inactive state by heterodimerization with the pro-survival group of BCL2 family proteins. These proteins, which include BCL2, MCL1, BCLX, and BFL1, each contain four BH



domains (BH1-BH4) and a transmembrane domain and interact with BAX and BAK via the shared BH3 domain. If BAX and BAK are normally held inactive how can they oligomerize to form the mitochondrial pore? The answer lies with the third group of the BCL2 family, the BH3-only proteins.

BH3-only genes are by far the most diverse of the BCL2 family and encode both cytoplasmic proteins (BAD, BID) as well as membrane proteins (BIM, PUMA, NOXA). These proteins are pro-death and interact, via BH3 domains, with the other BCL2 family proteins in a complex network. Shamas-Din and colleagues have explained the workings of this network in their proposed "Embedded-Together model"<sup>152</sup>. In this model, BH3 proteins come in two flavors: activators and sensitizers. Activators interact with and directly induce BAX and BAK oligomerization. They, like BAX and BAK, are inhibited under normal conditions by heterodimerization with pro-survival BCL2 proteins. In contrast, sensitizers solely interact with the pro-survival group. This interaction displaces BAX and BAK as well as activator BH3 proteins and allows them to execute MOMP. Together this network can be thought of as a molecular lock and key that regulates the opening of the membrane pore; Pro-survival BCL2 proteins are the lock, BH3 only proteins are the key, BAX and BAK are the door. Unlocking the mitochondrial door to apoptosis centers on which BCL2 proteins are active and which are inactive.

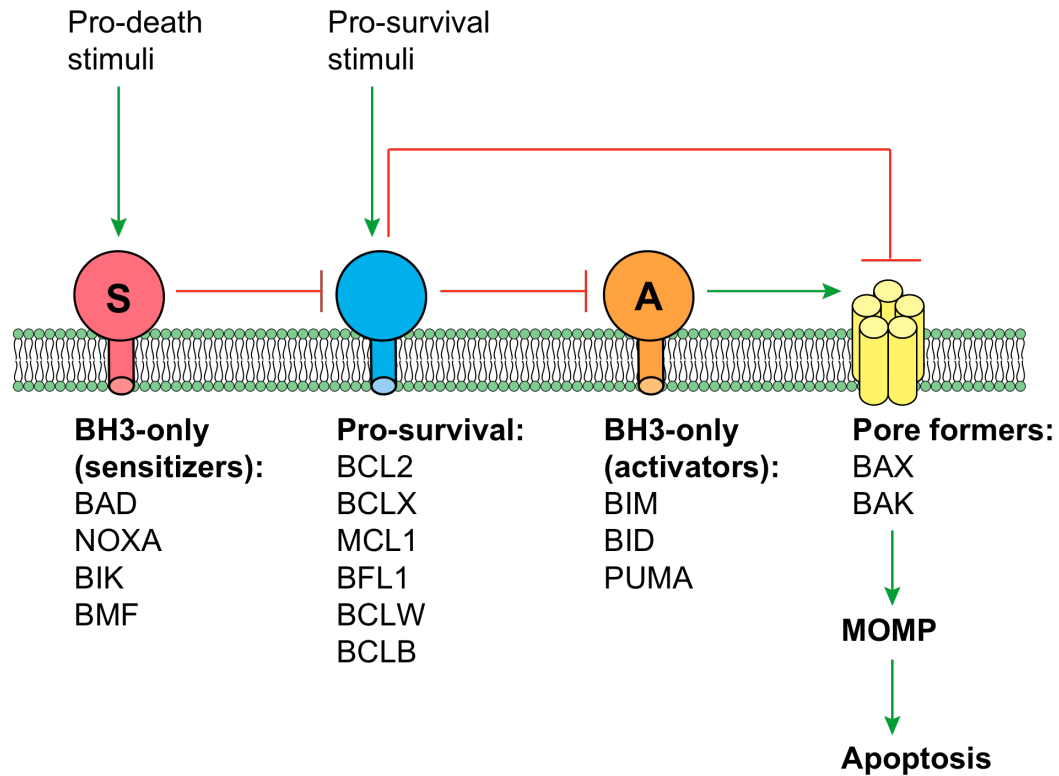


**Figure 1.7. Overview of BCL2 family protein organization:** BCL2 family proteins fall into 4 different functional groups. These subgroups regulate mitochondrial outer-membrane permeabilization (MOMP) by heterodimerization. In the absence of pro-survival stimuli, pore-formers and activators are free and interact with each other to potentiate intrinsic apoptosis. The pro-survival group inhibits this process by binding to and sequestering both activators and pore-formers. This inhibition is removed in turn by sensitizers, which are activated in response to pro-death stimuli. Upon activation, sensitizers translocate to the membrane and bind to the pro-survival proteins. This displaces pore-formers and activators, which are then free to initiate MOMP once-again. Whether apoptosis is initiated or not depends upon the relative abundance of each group in the membrane as well as the protein's activation state as determined by post-translation modifications (see below)<sup>150,152</sup>.

#### 1.3.4. BCL2 family regulation

BCL2 family gene regulation occurs at both the mRNA and protein levels. Several pro-survival genes such as BCL2 and BCLX are transcriptionally upregulated in response to supportive cytokines such as IL-3 and GM-CSF<sup>153,154</sup>. Likewise, many pathways involved in proliferation and self-renewal, such as PI3K/AKT, JAK/STAT, WNT/ $\beta$ -catenin and Hedgehog target and upregulate pro-survival BCL2 family genes<sup>155-158</sup>. In similar but opposite fashion, death stimuli alter the balance of expressed BCL2 family genes. The transcription factor p53, for example, is activated in response to DNA damage and mediates apoptosis in part by transcriptional upregulation of pro-death PUMA, NOXA, BAX and BAK, and transcriptional repression of pro-survival BCL2 and BCLX<sup>151,159</sup>. BCL2 family mRNA expression is also regulated post-transcriptionally by splicing and micro-RNAs. BCL2 family genes encode a rather large variety of splice variants. For some genes, such as MCL1 and BCLX, alternative splicing produces shorter variants that lack transmembrane domains and have functions antithetical to the full-length variant<sup>160,161</sup>. Other variants are less well studied but presumably have functional differences that may modulate the apoptotic balance of the cell. This balance may also be dynamically adjusted by micro-RNAs. miR-15, -16 and -181b, for example, bind to and promote degradation of BCL2 and MCL1 mRNA in response to cytotoxic drugs<sup>162,163</sup>.

BCL2 family proteins can also be altered post-translationally. These modifications occur in response to pro-death or pro-survival signals and change the activity and stability of the proteins. In response to growth factors, BCL2 is phosphorylated on its variable loop domain by kinases such as ERK, which enhances its pro-survival activity and prevents inhibition by p53<sup>164,165</sup>. BCL2 phosphorylation is reversed by protein phosphatase 2A (PP2A) following DNA damage<sup>166</sup>. Phosphorylation of MCL1 by GSK3 $\beta$  increases the protein's turnover by targeting it for proteolytic degradation<sup>167,168</sup>. Interestingly, MCL1 phosphorylation on other residues by ERK or JNK actually stabilizes the protein<sup>168,169</sup>. Consistent with this effect, activated ERK also promotes survival by phosphorylation and degradation of pro-death BIM<sup>170</sup>. In addition to these modifications, BCL2 family proteins can be cleaved by caspases. In the case of BCL2, caspase-mediated cleavage not only inhibits the protein's pro-survival function but also converts it into a BH3-only pro-death protein. This generates a positive feedback-loop that potentiates intrinsic apoptosis<sup>171,172</sup>. Finally, BCL2 family proteins can be modified in other ways such as by deamidation, which reduces BCLX<sub>L</sub> activity following DNA damage<sup>173</sup>. Much of the regulation of the BCL2 family was discovered in the context of cancer where perturbations tilt the balance toward survival and contribute to apoptosis resistance.

### 1.3.5. BCL2 family deregulation in cancer and CML

Altered expression of BCL2 family genes is an extremely common hallmark of cancer and contributes to tumorigenesis in several ways<sup>150,174</sup>. In some blood malignancies, such as follicular lymphoma, overexpression of BCL2 occurs due to translocation of its genetic locus<sup>175</sup>. In many other cancers activated oncogenes stimulate proliferation pathways that lead to overexpression or over-activation of pro-survival BCL2 family genes<sup>149,150</sup>. Deletion of p53 is probably the most common genetic aberration of cancer and leads to loss of pro-death BCL2 family transcription and activation<sup>137,147,176</sup>. Moreover, deletion or inactivation of other tumor suppressors such as PP2A and miR-15 and -16 removes inhibitory controls on BCL2 and other pro-survival genes<sup>162,177</sup>. Recent evidence also suggests that splicing is globally altered in cancer, and alternative splicing of BCL2 genes, which encode several variants, may change the apoptotic balance of the cell<sup>178,179</sup>.

Together, alterations in BCL2-mediated apoptosis can lead to growth factor independence and can allow cells to endure harsh or foreign environments such as those in metastatic sites<sup>137,180</sup>. Furthermore, these changes prevent cells from dying in response to mutagenesis and oncogene activation. Instead tumor cells can accumulate mutations and become more malignant over time. Myc-mediated leukemia, for example, is accelerated by overexpression of any of the six pro-survival BCL2 family genes<sup>181</sup>. Finally, because most drugs exert their cytotoxic effects by inducing the intrinsic apoptotic pathway, alterations in BCL2 family expression are fundamentally

linked to chemotherapy resistance<sup>182</sup>, a problem especially for relapsed disease. Many of these perturbations are known to play a role in CML development. Moreover CML LSC, which are defined in part by their ability to endure toxic insult, likely have abnormal BCL2 family expression as well.

In CML, changes in BCL2 family expression have been heavily linked to BCR-ABL. BCL2, MCL1 and BCLX are upregulated in CML cell lines downstream of BCR-ABL kinase activity<sup>183-186</sup>. This regulation likely occurs in part via activation of BCR-ABL target pathways such as PI3K-AKT, RAS and JAK-STAT. For example, the PI3K and RAS pathways phosphorylate and inactivate the pro-death mediator BAD<sup>187,188</sup>, while JAK-STAT signaling induces transcription of pro-survival BCLX<sub>L</sub><sup>189</sup>. On the other hand, inhibition of BCR-ABL reverses these effects and leads to cell death by engagement of the intrinsic apoptosis pathway. For example, BCLX<sub>L</sub> is transcriptionally suppressed while pro-death BIM, BMF and BAD are activated following treatment with TKIs<sup>189-191</sup>. Consistent with these data, TKI-resistance occurs by overexpression of BCL2 or loss of BIM and BAD<sup>191</sup>. Likewise, resistance is mediated by niche-dependent signaling that upregulates MCL1 and BCLX<sub>L</sub><sup>192</sup>. The fact that advanced disease is more refractory to TKIs suggests that BCL2 family gene expression and activity is increasingly perturbed over time in CML.

As described previously, the CML CP-BC transition is characterized by numerous genetic mutations and expression changes<sup>76,102</sup>. Not surprisingly, many of the affected genes have connections to the BCL2 family. The most obvious link is to BCR-ABL, which is more highly expressed in blast

crisis<sup>131,132</sup>. Deletions and point mutations that compromise p53 function are also commonly observed with progression<sup>193</sup>. Furthermore, blast crisis cells often have inactivation and decreased expression of other tumor suppressors, including PP2A and FOXO3A, which inhibit pro-survival BCL2 family genes<sup>177,194</sup>. The sum of these genetic changes swings the regulatory pendulum even further toward survival and likely contributes to the therapy-refractory nature of advanced disease. However, do aberrations in BCL2 family expression also explain chemotherapy resistance in LSC?

Intriguingly, despite a wealth of data on BCL2 family genes in cancer and CML, relatively little has been published on the expression of these genes in the LSC population specifically. What has been well established is that LSC are resistant to TKI treatment. Moreover, evidence suggests that this resistance is BCR-ABL-independent because primitive CML cells are insensitive to TKI-mediated cell death even with significant BCR-ABL inhibition<sup>39,111</sup>. In normal hematopoiesis it has been demonstrated that upregulation of pro-survival BCL2 protects HSC from radiation and cytotoxic drugs<sup>195,196</sup>. Furthermore, many studies of normal and malignant stem cells have linked resistance to quiescence<sup>117,118</sup>. In AML upregulation of pro-survival BCL2 expression is directly linked to chemo-resistance of primitive G<sub>0</sub> cells<sup>197</sup>. However, changes in BCL2 expression have not been definitively linked to quiescence nor to therapy resistance in CML LSC. Nevertheless, these data suggest that the BCL2 family may be an important mediator of LSC

survival in CML and could represent an important target for eliminating TKI-resistant LSC that drive CML relapse.

### **1.3.6. Molecular targeting of the BCL2 family**

Realization of the important role of apoptosis-resistance in cancer has led to development of therapeutic molecules that can target apoptotic pathways. Examples include small molecules that activate caspases and p53 or inhibit IAPs<sup>198-200</sup>. For the BCL2 family, antisense oligo-nucleotides have been used to sensitize cells to cytotoxic drugs by removing the pro-survival brakes to the pathway<sup>201</sup>. In addition, a new class of drugs called BH3 mimetics, targets the intrinsic pathway by direct inhibition of pro-survival BCL2 family proteins. As the name suggests, these drugs are molecular mimics that act analogously to BH3-only BCL2 proteins. By binding to pro-survival family members, BH3 mimetics displace sequestered pro-death proteins that are then free to activate intrinsic apoptosis<sup>202,203</sup>. In malignancies that are oncogenically addicted to pro-survival BCL2, BH3 mimetics alone can initiate apoptosis, and two of these drugs, ABT-263 and obatoclax, are currently in clinical trials as monotherapy for cancer<sup>203-206</sup>. These drugs may also have utility in malignancies marked by activation of several oncogenic pathways, where they can function as chemo-sensitizers<sup>203,207,208</sup>. In these cancers, BH3 mimetics unlock the door to apoptosis, but there must be additional stimuli to push the cell through that door.



The best-studied BH3 mimetics, ABT-737 and ABT-263, are potent and specific inhibitors of BCL2 and BCLX<sub>L</sub><sup>202,204</sup>. However, these drugs do not inhibit all pro-survival BCL2 family proteins due to structural differences in the BH3-pocket of the different proteins<sup>203,205</sup>. This is clinically significant because some cancers rely on proteins other than BCL2, and ABT-resistance may emerge by compensatory upregulation of MCL1 and BFL1<sup>174,209-211</sup>. ABT-resistance can be overcome by antisense RNA or drugs that downregulate MCL1<sup>212,213</sup>. However, a better strategy may be to inhibit all six pro-survival BCL2 family proteins simultaneously.

Obatoclax is one such pan-BCL2 inhibitor that has shown promise in clinical trials<sup>203</sup>. However, this compound is significantly less potent than ABT-drugs and may not specifically activate intrinsic apoptosis<sup>203,214</sup>. Recently, a new subset of pan-active BH3 mimetics has been developed by chemical modification of gossypol, a naturally occurring molecule derived from cottonseed oil. These compounds are unique because they can bind to and inhibit all pro-survival BCL2 family proteins, including MCL1 and BFL1<sup>215-217</sup>. The lead compound in this group, sabutoclax (BI-97C1), also retains high potency and specificity against the pro-survival BCL2 family<sup>217</sup>. Sabutoclax is therefore a novel new therapeutic for treating cancers which rely on MCL1 or BFL1 expression as well as those which express an array of pro-survival BCL2 family proteins<sup>174,217,218</sup>.

#### **1.4. Summary: targeting the BCL2 family in CML LSC**

The advent of TKIs has dramatically improved the lives of most patients suffering from CML. This success has also paved the way for the development of targeted molecular therapies for many other cancers. Despite these significant advances, a majority of CML patients remain un-cured and at risk for relapse. In addition, lifelong therapy with TKIs represents a significant burden to the health and financial welfare of patients. Ultimately, our goal must be to find better treatments that can fully cure CML. In line with this goal, the recent combined efforts of many talented researchers and clinicians have led to a vast amount of knowledge concerning drug-resistance, progression and relapse of CML. This in turn has shed light on the important role of LSC in initiating these processes and has challenged us to develop new strategies for targeting and eliminating these malignant stem cells.

An exciting strategy is to target the molecules that LSC rely on for their survival and drug-resistance. The BCL2 gene family, known to play a role in CML pathogenesis and TKI-resistance, is strongly implicated in this role. Moreover, many of the pathways involved in CML progression converge on the BCL2 family and modulate either the expression or activation of these genes. Inhibiting this gene family may therefore represent an effective means to eliminate LSC and prevent CML progression and relapse. BH3 mimetics are potent inhibitors of the BCL2 family that synergize with other chemotherapeutic agents. Among these, sabutoclax (BI-97C1) is a novel

compound that targets all six pro-survival BCL2 family proteins with high potency and selectivity. Sabutoclax can sensitize drug-resistant cancer cells to therapy and could be used to target LSC.

Despite previous data concerning BCL2 family expression in CML, comprehensive analysis of these genes and their splice isoforms has not yet been done in LSC specifically. It also remains unknown how BCL2 family expression changes with CML progression and how it compares to that in normal hematopoietic stem and progenitor cells. While data suggests that BH3 mimetics may be effective for CML, it has not been established whether these drugs can eliminate LSC. Moreover, it is unknown whether there is any therapeutic window between LSC and normal HSC killing. Finally, it has not been demonstrated whether inhibition of BCL2 family genes may be able to overcome niche-mediated TKI resistance.

Thus we set out to determine which BCL2 family genes are expressed in CML LSC and how this expression changes with disease progression. We also investigated how expression of these genes may contribute to LSC survival and TKI resistance, especially *in vivo*. Finally, we tested whether sabutoclax could target LSC in supportive niches and whether this drug could be used in combination with a TKI to eliminate resistant CML LSC. Our results are detailed in chapter 2.

## **2. Niche targeting of human blast crisis leukemia stem cells with a novel pan-BCL2 inhibitor**

Leukemic stem cells (LSC) play a pivotal role in chronic myeloid leukemia (CML) development and blast crisis (BC) progression. Many studies have demonstrated that LSC are highly resistant to standard treatments and are responsible for CML relapse following therapy. The BCL2 family of genes encodes a diverse set of pro-survival and pro-death proteins that regulate intrinsic apoptosis at the mitochondrial membrane. Moreover, abnormal expression of these genes has been directly linked to apoptosis and chemotherapy resistance. Based on these data, we hypothesized that LSC survival and therapy resistance may be mediated, in part, through abnormal expression and alternative splicing of the BCL2 family. Concordantly, we hypothesized that drug-resistant LSC may be sensitive to a pan-BCL2 inhibitor.

To elucidate BCL2 family regulators of BC LSC maintenance and survival, we performed splice isoform-specific qRT-PCR, full transcriptome RNA-sequencing, nanoproteomics, stromal co-culture and LSC xenotransplantation analyses. Cumulatively, these studies show that malignant reprogramming of myeloid progenitors into self-renewing LSC is characterized by upregulation and alternative splicing of multiple pro-survival

BCL2 family genes. Furthermore, enhanced pro-survival gene expression is correlated with increased LSC quiescence and resistance to tyrosine kinase inhibitors (TKIs) that is dependent on engraftment in the bone marrow niche. In accordance with these data, a novel pan-BCL2 inhibitor, sabutoclax (BI-97C1), targets BC LSC at doses that spare normal progenitors. Moreover, sabutoclax sensitizes BC LSC to treatment with TKIs. These findings underscore the importance of BCL2 family gene expression in the microenvironmental maintenance of BC LSC and suggest that niche targeted inhibition of pro-survival BCL2 family proteins may represent a principal component of a therapeutic strategy to eliminate dormant LSC.

## 2.1. Introduction

Leukemia stem cells (LSC), first described in acute myeloid leukemia (AML)<sup>24</sup>, subvert stem cell properties, such as quiescence, self-renewal and enhanced survival, which render them resistant to conventional therapy<sup>18,219</sup>. Chronic myeloid leukemia (CML) represents an important paradigm for dissecting the role of LSC in therapeutic resistance because it is initiated by a single well-defined genetic alteration, the BCR-ABL fusion gene, which can be molecularly targeted<sup>106</sup>. Although BCR-ABL-targeted tyrosine kinase inhibitors (TKIs) eradicate the bulk of CML cells, they frequently fail to eliminate quiescent, niche-resident LSC that drive relapse<sup>39,111,118,220</sup> and progression following TKI discontinuation<sup>11,36,112,221</sup>. Despite improved overall survival<sup>108</sup>, there remains no curative pharmacologic therapy for CML, in part, because the genetic and epigenetic drivers of BC LSC generation remain to be elucidated.

Evidence from primary CML patient samples demonstrates that expression of BCR-ABL1 in hematopoietic stem cells (HSC)<sup>46</sup> initiates chronic phase (CP) but is not sufficient to drive progression to blast crisis (BC)<sup>101</sup>. Both mouse transgenic model and xenotransplantation data show that activation of stem cell signaling pathways, including WNT/ $\beta$ -catenin<sup>34,42,128,222</sup>, Hedgehog<sup>129</sup> and the intrinsic apoptotic pathway regulated by the BCL2 gene family<sup>223</sup>, promote BC transformation<sup>34,42,43,130</sup>. Malignant reprogramming of BCR-ABL1 expressing granulocyte-macrophage progenitors into self-renewing BC LSC

occurs, in some cases, as a consequence of alternative splicing of GSK3 $\beta$ , a negative regulator of WNT/ $\beta$ -catenin and MCL1<sup>34,224</sup>. While recent reports reveal that mutations in splicing genes promote progression of myeloid malignancies to acute leukemia<sup>179</sup>, alternative splicing-mediated alterations in the transcriptome may also enable BC transformation in a malignant microenvironment.

Because CML becomes increasingly refractory to TKIs during disease progression to BC<sup>225,226</sup>, understanding the epigenetic mechanisms that drive BC LSC maintenance and contribute to therapeutic resistance is essential. TKI resistance is regulated by diverse BCR-ABL1-dependent and independent mechanisms. Mutations in the BCR-ABL1 kinase domain and enhanced BCR-ABL1 transcription are observed in patients with variable TKI compliance, which represents a major concern for long-term TKI therapy<sup>115,227</sup>. In addition, several studies suggest that LSC quiescence induction by the stem cell niche is a major component of therapeutic resistance<sup>37-39,41,118</sup>. Although, recent evidence shows that increased expression of BCL2 family members contributes to CML pathogenesis, the precise nature of BCL2 splice isoform usage had not been examined even though a number of isoforms have antithetical functions<sup>160</sup>.

The BCL2 family encodes a diverse set of genes that integrate pro-survival and pro-death stimuli and modulate the permeability of the mitochondrial membrane<sup>228</sup>. Activation of mitochondrial outer membrane permeability (MOMP) results in activation of a caspase cascade triggering

apoptosis. Pro-survival BCL2 family genes contribute to leukemogenesis<sup>181</sup>, CML progression<sup>223</sup>, TKI resistance<sup>183,184,189,197,223</sup> and hematopoietic stem and progenitor cell survival<sup>196,229</sup> by direct inhibition of MOMP. Expression of BCL2 family genes has also been linked to bone marrow niche-dependent TKI resistance *in vitro*<sup>192</sup>. However, the requirement for pro-survival BCL2 family genes expression in human BC LSC maintenance has not been elucidated. Moreover, the role of niche-dependent BCL2 isoform expression has not been delineated in the context of LSC quiescence induction and TKI resistance *in vivo*. Thus we compared BCL2 family expression in FACS-purified CML progenitors from normal, CP and BC patients and in LSC engrafted in different hematopoietic niches. We also investigated whether LSC could be targeted with a novel BCL2 inhibitor and whether this inhibition could overcome niche-dependent TKI resistance.



## 2.2. Results

### 2.2.1. Pro-survival BCL2 family expression is increased in primary CML LSC with progression to BC

Several studies have linked BCL2 family upregulation with CML survival, however most have focused on BCR-ABL-expressing cell lines<sup>183,185,186</sup> or bulk CD34<sup>+</sup> cells<sup>101,184,189</sup> rather than bona fide CML LSC. To gain insight into the role of the BCL2 family in LSC, we performed gene expression analysis on FACS-sorted normal, CP and BC progenitors (patient sample information - Table 2.1; FACS sorting scheme - Figure 2.1). BC samples were highly enriched in CD123<sup>+</sup>CD45RA<sup>+</sup> granulocyte-macrophage progenitors (GMP), previously shown to harbor aberrant self-renewal potential<sup>33,40</sup>, compared to normal and CP samples, which were instead enriched in CD123<sup>+</sup>CD45RA<sup>-</sup> common myeloid progenitors (CMP) and CD123<sup>-</sup>CD45RA<sup>-</sup> megakaryocyte-erythrocyte progenitors (MEP) respectively (Figure 2.2). Because myeloid progenitor phenotypes were highly variable in different samples, it was not possible to sort sufficient CMP, GMP and MEP from each patient sample for gene expression analysis. Instead, we focused on the CD34<sup>+</sup>CD38<sup>+</sup> progenitor population that could be consistently sorted from all samples.

*BCL2* family genes encode splice variants with opposing functions<sup>178</sup>, however, there is relatively little information on *BCL2* splice isoform expression in human BC LSC. Therefore, we devised splice-isoform specific primers for

qRT-PCR and novel analysis tools for full-transcriptome RNA sequencing to scrutinize *BCL2* family isoform expression in sorted primary normal, CP and BC progenitors. BC LSC expressed significantly higher levels of *BCR-ABL* and pro-survival *BCL2<sub>L</sub>*, *MCL1<sub>L</sub>*, *BCLX<sub>L</sub>* and *BFL1<sub>L</sub>* than CP progenitors (Figure 2.3a), as well as significantly higher *BCL2<sub>L</sub>*, *BCLX<sub>L</sub>* and *BFL1<sub>L</sub>* than normal progenitors (Figure 2.3b). *MCL1<sub>L</sub>* expression was slightly lower in BC compared to normal progenitors, however both qRT-PCR and RNA sequencing revealed significant overrepresentation of long compared with short isoforms of *MCL1* in CP and BC progenitors compared to normal progenitors (Figure 2.4). Together these data demonstrate that pro-survival *BCL2* family genes are globally upregulated in CML LSC with disease progression. These data also suggest that *BCL2* family splicing is altered in CML compared to normal hematopoiesis.

Because *BCR-ABL* induces *BCL2* family gene expression in CML cell lines<sup>183,184,189</sup>, we examined whether pro-survival *BCL2* family expression was correlated with *BCR-ABL* expression in CML progenitors. There was a striking correlation between *BCR-ABL* and *BCLX<sub>L</sub>* transcript levels in CML progenitors that was also observed in lentiviral *BCR-ABL*-transduced progenitors (Figure 2.5a) suggesting that increased *BCLX<sub>L</sub>* expression in BC LSC is primarily driven by *BCR-ABL* amplification. However, we observed no significant correlations with any other *BCL2* family genes (figure 2.5b) suggesting that increased expression of these genes in BC LSC is independent of *BCR-ABL* amplification.

Next, we examined BCL2 family protein expression in CML progenitor cells. BCL2 and MCL1 protein levels were upregulated in BC LSC versus CP progenitors, comparable to qRT-PCR results, as determined by intracellular flow cytometry (Figure 2.6a and Figure 2.6b). We also compared the stem ( $lin^-CD34^+CD38^-$ ) and progenitor ( $lin^-CD34^+CD38^+$ ) populations and observed the highest BCL2 protein expression in BC LSC (Figure 2.6c). Both BCL2 protein and mRNA expression in CML progenitors were correlated with CD123<sup>+</sup> progenitor expansion, suggesting that increased BCL2 expression is a marker of disease progression. Importantly, this trend was not observed with normal progenitors (Figure 2.6d and 2.6e).

To gain further insight into apoptosis regulation in primary LSC we compared gene expression in normal, CP and BC progenitors using whole-transcriptome RNA sequencing. Unsupervised, whole-gene analysis revealed that normal, CP and BC samples cluster separately with regard to the apoptotic pathway genes with the exception of sample BC-05, which derived from a patient in the midst of CP-BC transition and clustered with chronic phase samples. (Figure 2.7a; for a full list of significantly differentially expressed genes see Appendix Tables A.1-A.3). Consistent with our other results, there was a trend toward increased expression of multiple pro-survival *BCL2* family genes in BC compared to normal progenitors (Figure 2.8). However, BC progenitors also had increased expression of several pro-apoptosis *BCL2* family genes including *BAD*, *BIM*, *BIK*, *PUMA* and *NOXA*. Interestingly, many other pro-apoptosis genes were also significantly

upregulated in BC compared to normal progenitors (Figure 2.7b and Table A.1) including caspase genes (*CASP3* and *CASP8*) responsible for apoptosis execution<sup>230</sup>, members of the TNF receptor super-family (*FAS* and *TNFRSF25*) that activate extrinsic apoptosis in response to extracellular inflammatory and immune stimuli<sup>146,231</sup>, death-domain containing adaptor proteins (*CRADD*, *LRDD* and *TRADD*) that recruit and activate initiator caspases<sup>232-234</sup> and *TP53*, which activates intrinsic apoptosis in response to DNA-damage and other intracellular stresses<sup>147,235</sup>.

We also compared CP and BC progenitor transcriptome expression (Figure 2.7b and Table A.3). Similar to the above results, BC progenitors had increased expression of a number of pro-death genes encoding TNF super-family receptors (*TNFRSF1B*, *TNFRSF21* and *FAS*) and apoptosis adaptor proteins (*CRADD* and *PYCARD*). In addition, this analysis identified several genes involved in signal transduction that were significantly increased in BC progenitors (Figure A.1), including *PI3K*, *JAK* and *RAS*, which are known to promote apoptosis resistance by regulation of the *BCL2* family<sup>155,173,236</sup>, and which could account for why BC progenitors have increased expression of multiple pro-survival *BCL2* family genes. At the same time, we observed decreased expression of proliferation genes such as cyclin-D and *MYC* (Figure A.1), which suggests that BC progenitors may be in a more quiescent state than their counterparts in CP.

Finally, we compared apoptosis-gene splice isoform expression in the sorted progenitors. Normal, CP and BC progenitors clustered separately with

regard to splice isoform expression, and this analysis revealed a 23-isoform signature that distinguished normal from CML samples (Figure 2.9a). Notable isoforms that were upregulated in CML versus normal cells included those of *YWHAZ*, which encodes a pro-survival 14-3-3 protein that inhibits BAD<sup>237</sup>, *CFLAR*, which inhibits FAS-mediated apoptosis<sup>238,239</sup>, *DIABLO*, which encodes a pro-death inhibitor of inhibitor-of-apoptosis (IAP) proteins<sup>148</sup>, and *CASP8AP2*, which encodes an adaptor protein required for caspase-8 activation<sup>240</sup>. Multiple isoforms of *CASP8* and an isoform of *PMAIP1* (*NOXA*), a BH3-only BCL2 family gene<sup>241</sup>, were also significantly increased in CML cells. In addition to these isoforms, there were several isoforms that were significantly differentially expressed between BC and CP progenitors (Figure 2.9b). Many of these were consistent with genes identified previously including caspases (*CASP1*, *CASP7*, *CASP8*) and TNF super-family receptors (*TNFRSF1B*, *TNFRSF21*, *FAS*). Other notable upregulated isoforms included *LTA* a pro-inflammatory cytokine of the TNF family<sup>242</sup>, and *HRK* (*HARAKIRI*) a death-promoting gene that interacts with BCL2 and BCLX<sub>L</sub> in the mitochondrial membrane<sup>243</sup>. Among the downregulated isoforms was *BIRC5*, which encodes the IAP survivin<sup>143</sup>. Isoforms of two BH3-only BCL2 family genes were also differentially expressed with *BCL2L14* upregulated and *BCL2L11* (*BIM*) downregulated in BC progenitors. Interestingly, there were some genes with individual splice isoforms both upregulated and downregulated in BC progenitors. An example was *RIPK2* (highlighted in blue in Figure 2.9a), which encodes a kinase that activates NF- $\kappa$ B<sup>244</sup>. To our knowledge there have been

no publications that describe the function of the individual splice isoforms of *RIPK2*. Therefore it is difficult to speculate whether there is any functional consequence of this splice isoform switching in BC LSC. Nevertheless, these data together with our analyses of *MCL1* splice isoforms (Figure 2.4) suggest that alternative splicing may contribute to apoptosis-gene alteration in BC LSC. Overall these RNA sequencing data point to a number of additional apoptosis-gene candidates that may be altered in CML progenitor cells upon transformation, and with progression to BC.

**Table 2.1.** CML patient sample characteristics

<b>ID</b>	<b>Date</b>	<b>Sex/Age</b>	<b>Sample type</b>	<b>WBCs (K/mL)</b>	<b>% Blasts, PB</b>	<b>Treatment</b>
C001	26 Oct 07	N/A	Chronic Phase	N/A	N/A	N/A
C002	09 Jan 07	M	Chronic Phase	689	4%	Imatinib
C003	N/A	N/A	Chronic Phase	N/A	N/A	N/A
C004	05 Feb 07	F	Chronic Phase	N/A	N/A	N/A
C01	13 Nov 08	M/60	Chronic Phase	189	1.4%	none
C02	23 May 08	F/63	Chronic Phase	326	5%	none
C03	10 Dec 99	M/57	Chronic Phase	49	4.1%	none
C04	14 Oct 08	M/44	Chronic Phase	306	5.8%	none
C05	21 Sep 09	M/26	Chronic Phase	231	<1%	none
C06	25 Sep 09	F/68	Chronic Phase	88	<5%	Imatinib
C07	25 Mar 07	F/33	Chronic Phase	37.1	<1%	N/A
C08	29 Jan 99	M/56	Chronic Phase	381	<5%	Imatinib
C11	14 Jan 09	F/44	Chronic Phase	9.5	<1%	Hydroxyurea
C12	26 Aug 09	N/A	Chronic Phase	390	N/A	N/A
C13	21 Sep 07	F/50	Chronic Phase	N/A	N/A	Imatinib
B001	15 May 08	M/50	Blast Crisis	N/A	N/A	N/A
B002	N/A	N/A	Blast Crisis	N/A	N/A	N/A
B04	29 Jul 08	M/20	Blast Crisis	622	68%	Imatinib
B05	08 Dec 03	M/51	Blast Crisis	82.4	32%	Imatinib
B06	26 Oct 93	M/30	Blast Crisis	170	94.1%	Hydroxyurea
B07	29 Oct 93	M/48	Blast Crisis	209	86.1%	Hydroxyurea
B08	27 Jul 00	M/53	Blast Crisis	98	82.6%	Hydroxyurea
B09	17 Oct 91	M/65	Blast Crisis	72	41.7%	none
B10	21 Sep 93	M/40	Blast Crisis	133	82%	none
B11	16 Mar 06	M/31	Blast Crisis	40.1	79%	Hydroxyurea
B12	26 Jul 09	F/47	Blast Crisis	262	45%	Hydroxyurea
B13	16 May 08	M/49	Blast Crisis	8.4	15%	Imatinib
B14	16 Apr 04	M/40	Blast Crisis	47.7	47%	none
B15	8 Mar 05	F/31	Blast Crisis	11.4	55%	none
B16	22 Jul 02	F/52	Blast Crisis	60.3	14%	none
B20	N/A	?/37	Blast Crisis	N/A	N/A	N/A
B26	N/A	?/78	Blast Crisis	N/A	N/A	N/A

N/A - data not available

WBCs = white blood cell count

PB = peripheral blood

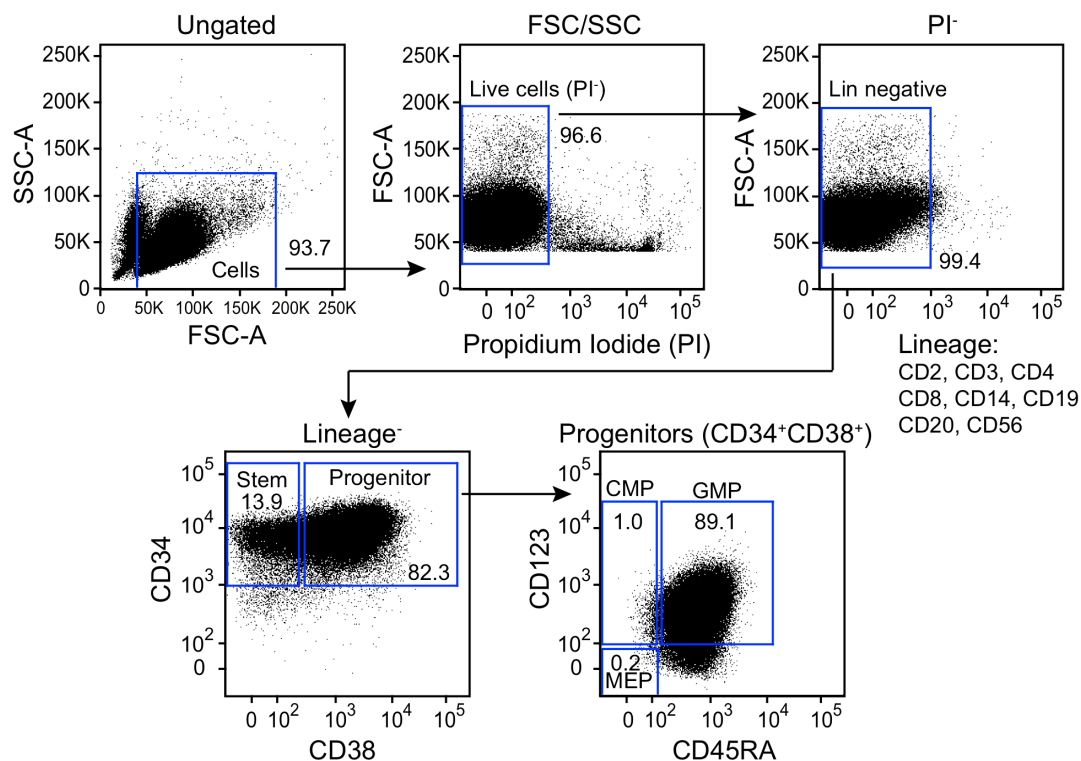


**Figure 2.1.** FACS, progenitor analysis scheme: Representative FACS plots of a BC sample showing the gating scheme used for progenitor analysis and sorting.

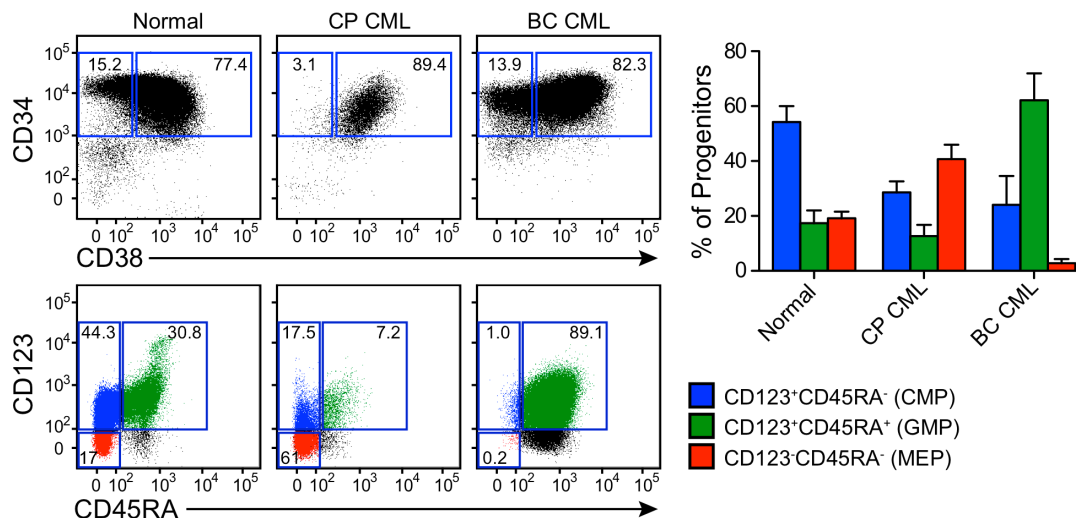


**Figure 2.2.** BC samples are enriched in granulocyte-macrophage progenitors (GMP). Left: Representative FACS plots of lineage negative cells (top row) and myeloid progenitors (bottom row) in normal, CP and BC samples. Right: Quantification of myeloid progenitor types in normal (n=4), CP (n=8) and BC (n=8) samples.



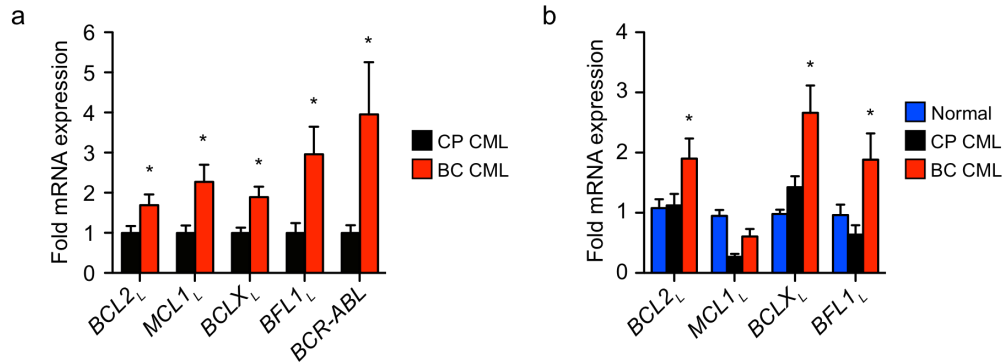


**Figure 2.3.** *BC progenitors express high levels of BCL2 family mRNAs.* **a)** qRT-PCR of pro-survival (long isoforms) BCL2, MCL1, BCLX, BFL1 and BCR-ABL mRNAs in primary CP (black, n=13) and BC (red, n=11) progenitors. **b)** CP and BC expression compared to that of normal (black, n=16) progenitors. All values are normalized to human HPRT mRNA expression. Graphs show mean  $\pm$  SEM; \*  $p < 0.05$  by unpaired t-test.

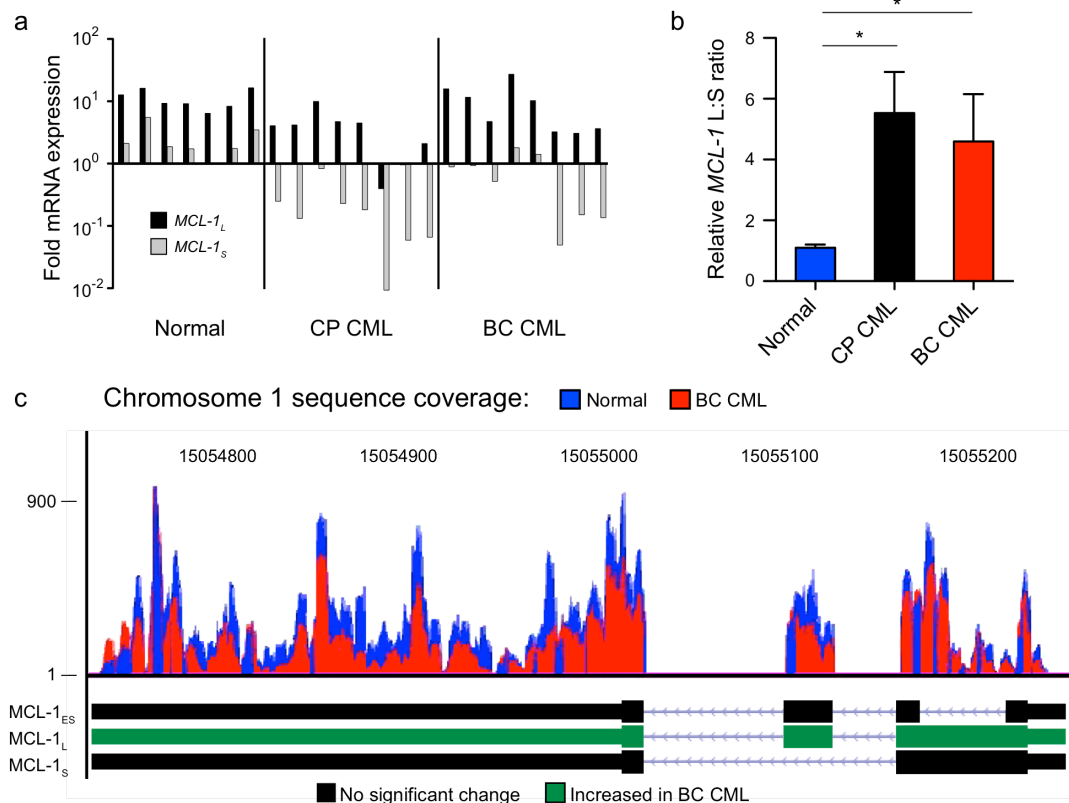


**Figure 2.4.** The  $MCL1$  L:S isoform balance is switched in normal versus CML progenitors. **a)** RT-qPCR of  $MCL1_L$  and  $MCL1_S$  in normal, CP and BC progenitors. **b)**  $MCL1_L:MCL1_S$  ratio in normal (n=7), CP (n=8) and BC progenitors. **c)** Whole transcriptome sequencing of FACS-sorted progenitor cells from a normal and a BC sample showing representative sequence coverage histograms for the chromosome 1,  $MCL1$  locus.

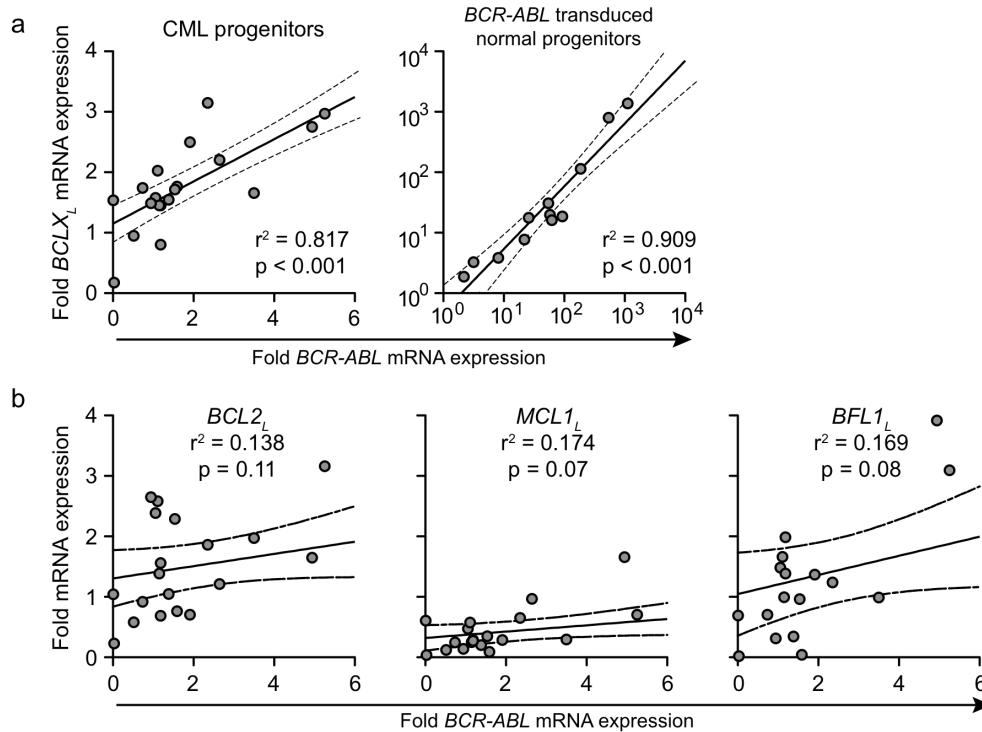


**Figure 2.5.**  $BCLX_L$  but not other  $BCL2$  family member mRNA expression is correlated with  $BCR-ABL$  expression in CML progenitors. **a)** Correlation between  $BCR-ABL$  mRNA expression and  $BCLX_L$  mRNA expression in progenitors. *Left:* Primary CP and BC samples ( $n=20$ ). *Right:*  $BCR-ABL$  transduced normal progenitor colonies ( $n=12$ ). **b)** Correlation between  $BCR-ABL$  mRNA expression and  $BCL2_L$ ,  $MCL1_L$  and  $BFL1_L$  mRNA expression in primary CP and BC samples ( $n=20$  for each graph). All graphs depict best-fit line and 95% confidence intervals by Pearson correlation analysis.

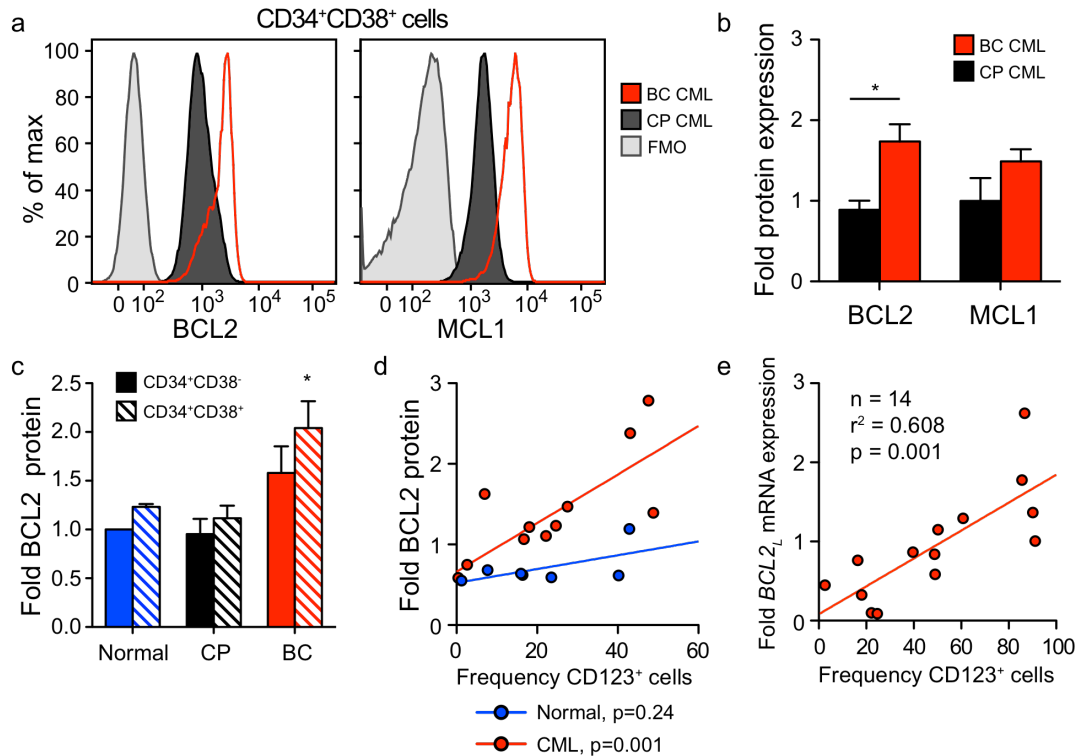


**Figure 2.6.** *BCL2* family protein expression is increased in BC progenitors and is correlated with CD123<sup>+</sup> cell expansion. **a)** Representative FACS histograms of BCL2 and MCL1 protein expression in CP versus BC progenitors. **b)** Quantitative intracellular FACS analysis of total BCL2 and MCL1 protein in primary CP and BC progenitors. BCL2 - n=6 CP and n=7 BC; MCL1 - n=3 CP and n=4 BC. Graph shows mean  $\pm$  SEM; \*  $p < 0.05$  by unpaired t-test. **c)** BCL2 protein expression in primary normal (blue, n=6) CP (black, n=6) and BC (red, n=7) stem cells (CD34<sup>+</sup>CD38<sup>-</sup>) and progenitor cells (CD34<sup>+</sup>CD38<sup>+</sup>). Graph shows mean  $\pm$  SEM; \*  $p < 0.05$  by ANOVA and Tukey post-hoc analysis. **d)** Correlation between BCL2 protein expression and CD123<sup>+</sup> cell frequency in primary CML (red, n=13) and normal (blue, n=6) progenitors. Graph shows best-fit lines; In general linear regression models the frequency of CD123<sup>+</sup> cells is associated with BCL2 expression in CML ( $r^2=0.557$ ,  $p=0.001$ ) but not in normal ( $r^2=0.365$ ,  $p=0.24$ ). **e)** Correlation between CD123<sup>+</sup> cell frequency and BCL2<sub>L</sub> mRNA expression in CML progenitors (n=14).  $r^2=0.608$ ,  $p=0.001$  by Pearson correlation analysis.

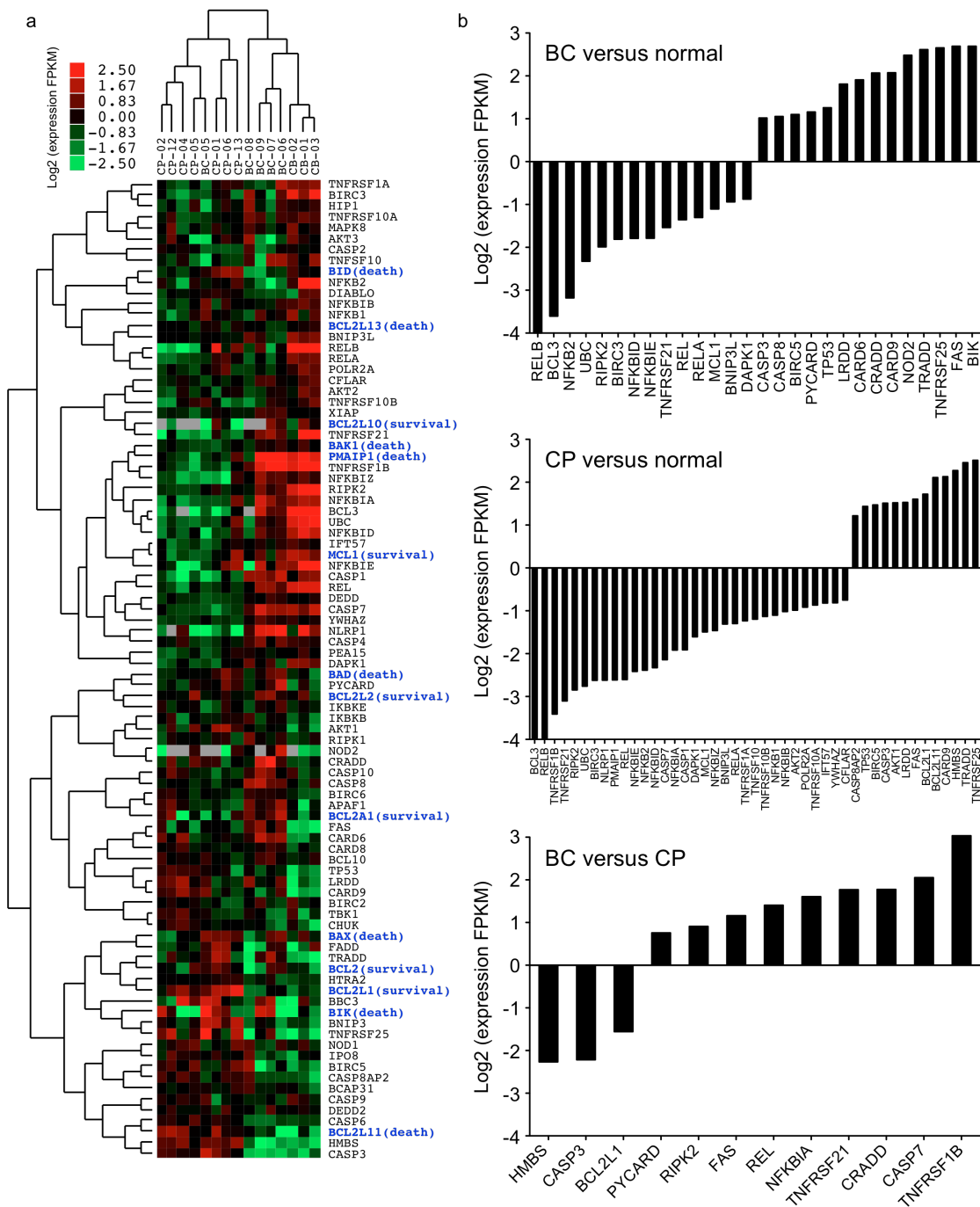


**Figure 2.7. Normal, CP and BC progenitors differentially express apoptosis genes. a)** Clustering of expression of apoptosis related genes in normal (n=3), CP CML (n=7) and BC CML (n=5) progenitors measured by RNA sequencing analysis. Heat-map shows relative fragments per kilobase of exon per million fragments mapped (FPKM). BCL2 family genes are highlighted in blue and designated as either pro-survival or pro-death. **b)** Significantly differentially expressed genes (p<0.05) in BC versus normal (top), CP versus normal (middle) and BC versus CP progenitors (bottom). Graphs show average fold FPKM.

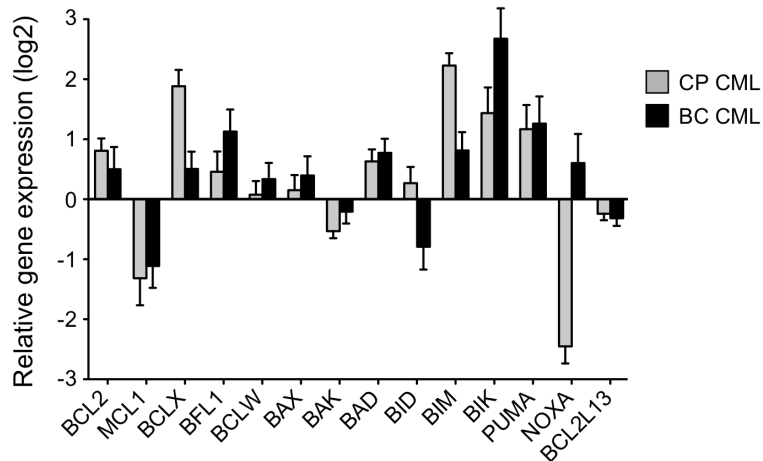


**Figure 2.8.** *BCL2 family gene expression is generally increased in CML compared to normal progenitors.* Relative fold expression of BCL2 family genes in CP (n=7) and BC (n=5) compared to normal (n=3) progenitors measured by RNA sequencing analysis. Graph shows mean  $\pm$  SEM for each gene relative to normal progenitors, which are set at 1.

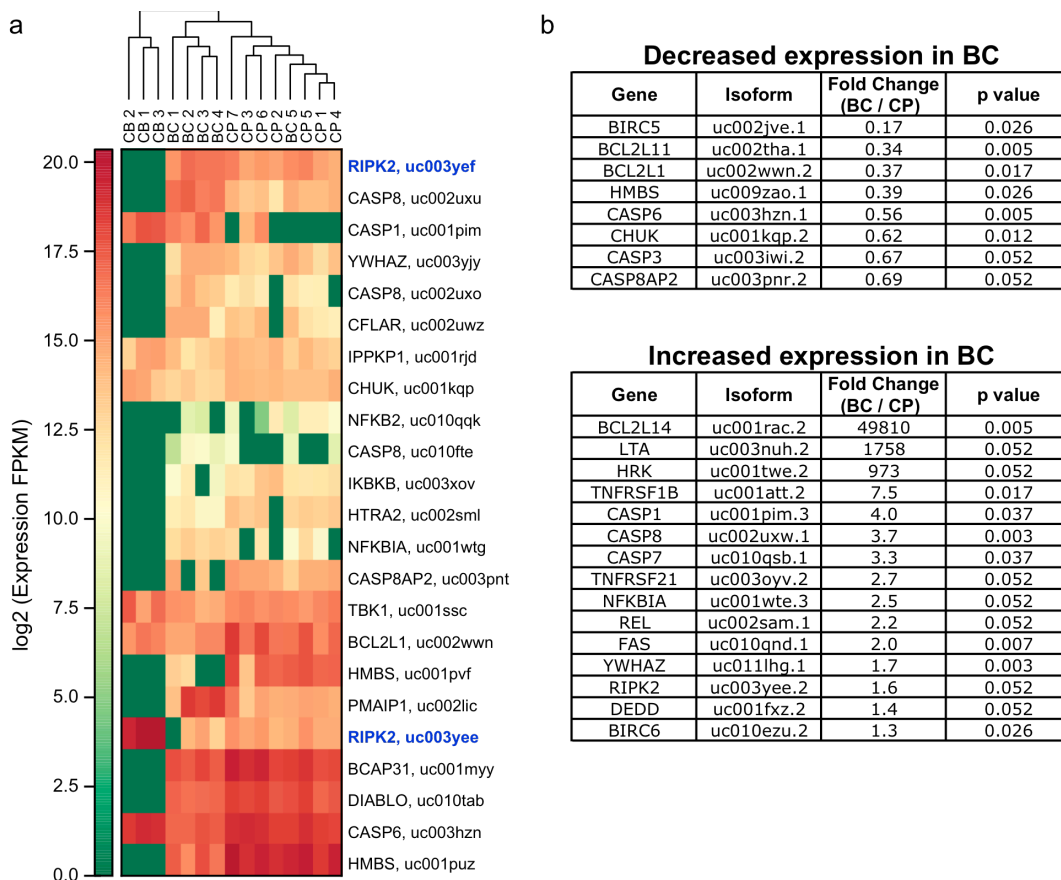


**Figure 2.9.** Normal, CP and BC progenitors differentially express apoptosis-gene splice isoforms. **a)** Clustering of splice isoform expression in normal (n=3), CP (n=7) and BC (n=5) progenitors. Heat-map shows relative FPKM. Two splice isoforms of RIPK2, which are oppositely upregulated and downregulated, are highlighted in blue. **b)** Table of significantly downregulated and upregulated splice-isoforms in BC compared to CP progenitors.

### 2.2.2. The bone marrow niche protects BC LSC from the TKI, dasatinib

In addition to altered *BCL2* isoform expression, recent studies suggest that supportive microenvironments render LSC quiescent and resistant to therapy<sup>37,41,118,192</sup>. To investigate how the microenvironment contributes to LSC survival, we examined BC LSC in various hematopoietic niches using a xenograft model. To establish this model, primary CD34<sup>+</sup> BC cells were isolated using magnetic bead selection and transplanted intrahepatically into neonatal RAG2<sup>-/-</sup>γ<sub>c</sub><sup>-/-</sup> mice<sup>33</sup> (experimental design - Figure 2.10). Transplanted mice typically developed BC CML at approximately 6-10 weeks post-transplant, and disease was characterized by the formation of diffuse myeloid sarcomas (Figure 2.11a) and engraftment of human CD45<sup>+</sup> and CD34<sup>+</sup>CD38<sup>+</sup> leukemic cells in all hematopoietic tissues (Figure 2.11b and Table 2.2).

To quantitatively assess whether resistant LSC had a predilection for a particular microenvironment, BC transplanted mice were treated orally with dasatinib, a high potency TKI, and leukemic engraftment was measured immediately following a 2-week treatment period (Figure 2.12). Dasatinib was extremely effective at killing BC leukemic cells *in vivo* and we observed marked decreases in the leukemic engraftment of the liver (the site of transplant, Figure 2.12c), the myeloid sarcoma burden (Figure 2.12d) and the spleen size (Figure 2.12e) of dasatinib-treated animals. Spleen and blood leukemic engraftment was also dramatically diminished by dasatinib treatment (Figure 2.12f). However, despite these effects, a sizable dasatinib-resistant



population remained in the bone marrow after treatment (Figure 2.12f). This resistant population was especially evident when engraftment of CD34<sup>+</sup>CD38<sup>+</sup> cells was measured, and at lower doses there was no significant change in this population (Figure 2.12g). To test whether the dasatinib-resistant population contained functional LSC, we serially transplanted whole bone marrow derived from the treated animals into secondary recipients. Strikingly, mice transplanted with vehicle- and dasatinib-treated marrow developed nearly identical levels of disease (Figure 2.13a). Moreover, mice that received dasatinib-treated marrow had no significant survival advantage over those that received vehicle-treated marrow (Figure 2.13b). Together, these data demonstrate that the bone marrow protects functional BC LSC from the cytotoxic effects of TKIs.

Importantly, bone marrow-associated resistance was not simply due to higher disease burden in the marrow because high-level human engraftment and comparable progenitor engraftment were detected in all hematopoietic tissues (Figure 2.12a-b). Furthermore, myeloid sarcomas had the highest levels of engraftment and yet were extremely sensitive to dasatinib (Figure 2.12d). Marrow TKI-resistance was also not due to a lack of drug availability because FACS-sorted CD34<sup>+</sup>CD38<sup>+</sup> cells from the marrow of dasatinib-treated mice had significantly reduced CRKL phosphorylation (Figure 2.14), a direct measure of BCR-ABL kinase activity. This suggests that dasatinib inhibits BCR-ABL, but fails to kill marrow LSC due to the activity of other compensatory, BCR-ABL-independent protective pathways.

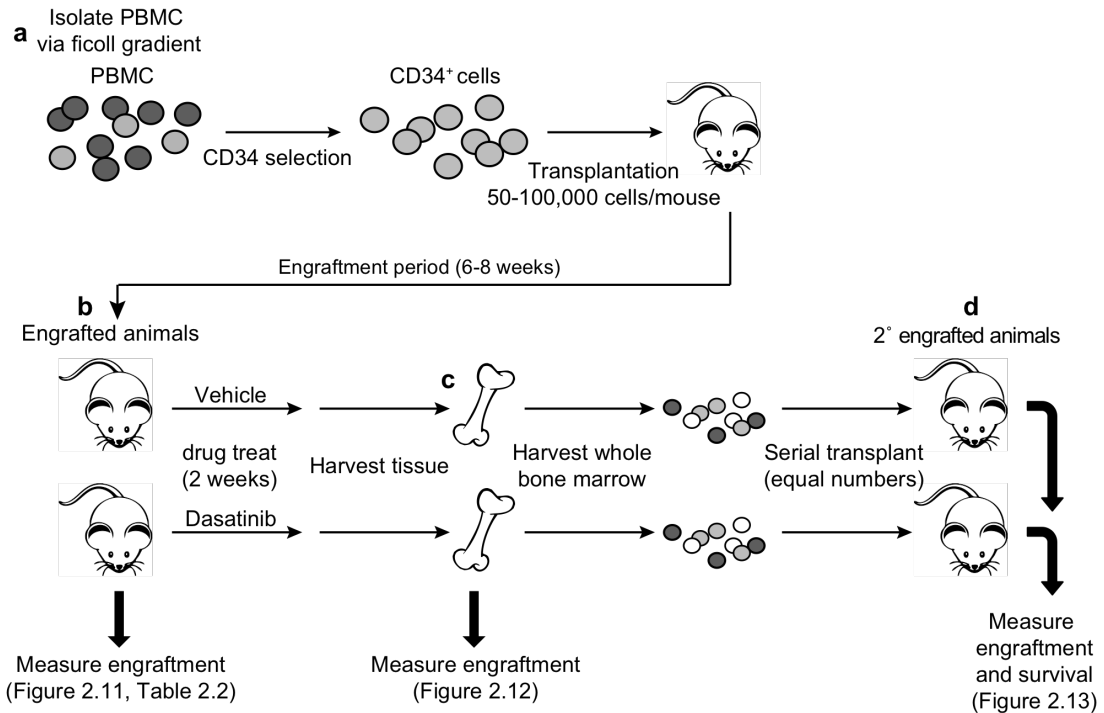


**Figure 2.10. Experimental design for measuring the effects of dasatinib on BC LSC *in vivo*:** **a)** Peripheral blood mononuclear cells (PBMC) were isolated using a ficoll-gradient and CD34<sup>+</sup> cells were purified using magnetic bead selection (MACS). 50-100,000 CD34<sup>+</sup> cells were transplanted into neonatal RAG2<sup>-/-</sup>γ<sub>c</sub><sup>-/-</sup> mice. **b)** After a 6-8 week engraftment period, transplanted mice were sacrificed to measure total human and progenitor engraftment in the hematopoietic organs. Two cohorts of engrafted mice were left alive and were treated for 2 weeks with dasatinib (oral, 1 dose per day) or vehicle. **c)** After the 2-week dosing period treated mice were sacrificed and engraftment was measured in the hematopoietic organs. Whole bone marrow cells were isolated from dasatinib- and vehicle-treated mice and were transplanted into secondary recipients. **d)** The survival of the secondary recipients was recorded and engraftment was verified in secondary bone marrow post-mortem.

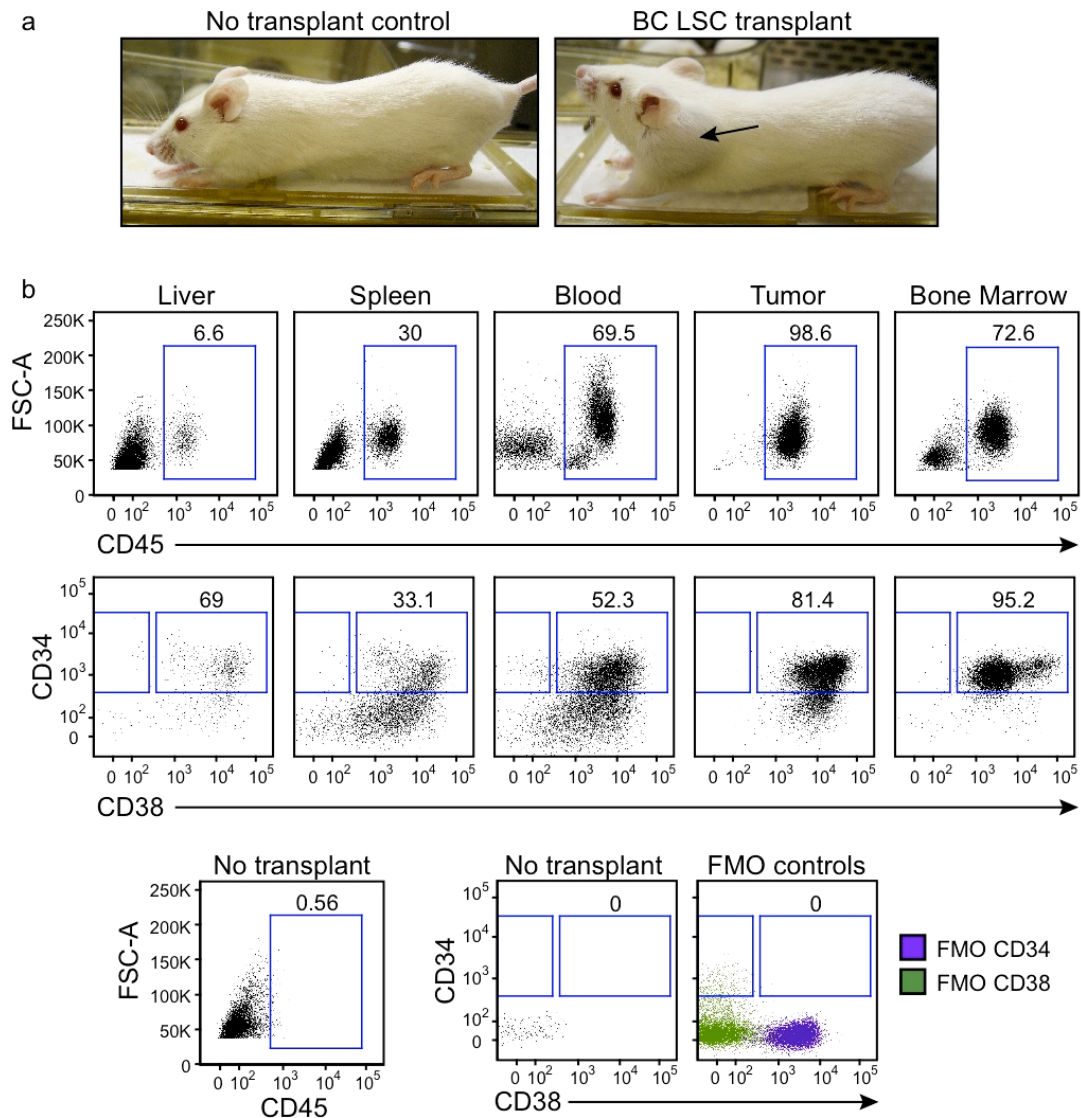


**Figure 2.11.** Transplanted BC CML cells form myeloid sarcomas and engraft all hematopoietic niches. **a)** Representative photographs of control and BC LSC transplanted animals. The arrow denotes a large, subcutaneous myeloid sarcoma. **b)** Representative FACS plots of total human engraftment ( $CD45^+$  cells, top row) and progenitor engraftment ( $CD34^+CD38^+$  cells, middle row) in mouse hematopoietic tissues and myeloid sarcomas ("tumor"). The bottom row shows gating in no-transplant control bone marrow and fluorescence minus one (FMO) controls.

**Table 2.2.** Frequency of engraftment of human leukemic cell populations in BC LSC transplanted mice

Population	Frequency	Tissue				
		Liver	Spleen	Blood	Tumor	Marrow
CD45 <sup>+</sup>	Mean	17.7	31.7	47.7	64.4	57.0
	SEM	2.8	3.6	6.0	6.4	5.6
	n	44	52	31	22	52
CD45 <sup>+</sup> CD34 <sup>+</sup> CD38 <sup>+</sup> ("progenitor")	Mean	7.7	11.4	7.6	46.3	27.1
	SEM	2.0	1.6	1.8	7.9	4.5
	n	39	49	31	22	49
CD45 <sup>+</sup> CD34 <sup>+</sup> CD38 <sup>-</sup> ("stem")	Mean	0.32	0.74	0.46	0.04	0.14
	SEM	0.06	0.16	0.11	0.008	0.04
	n	39	49	31	22	49

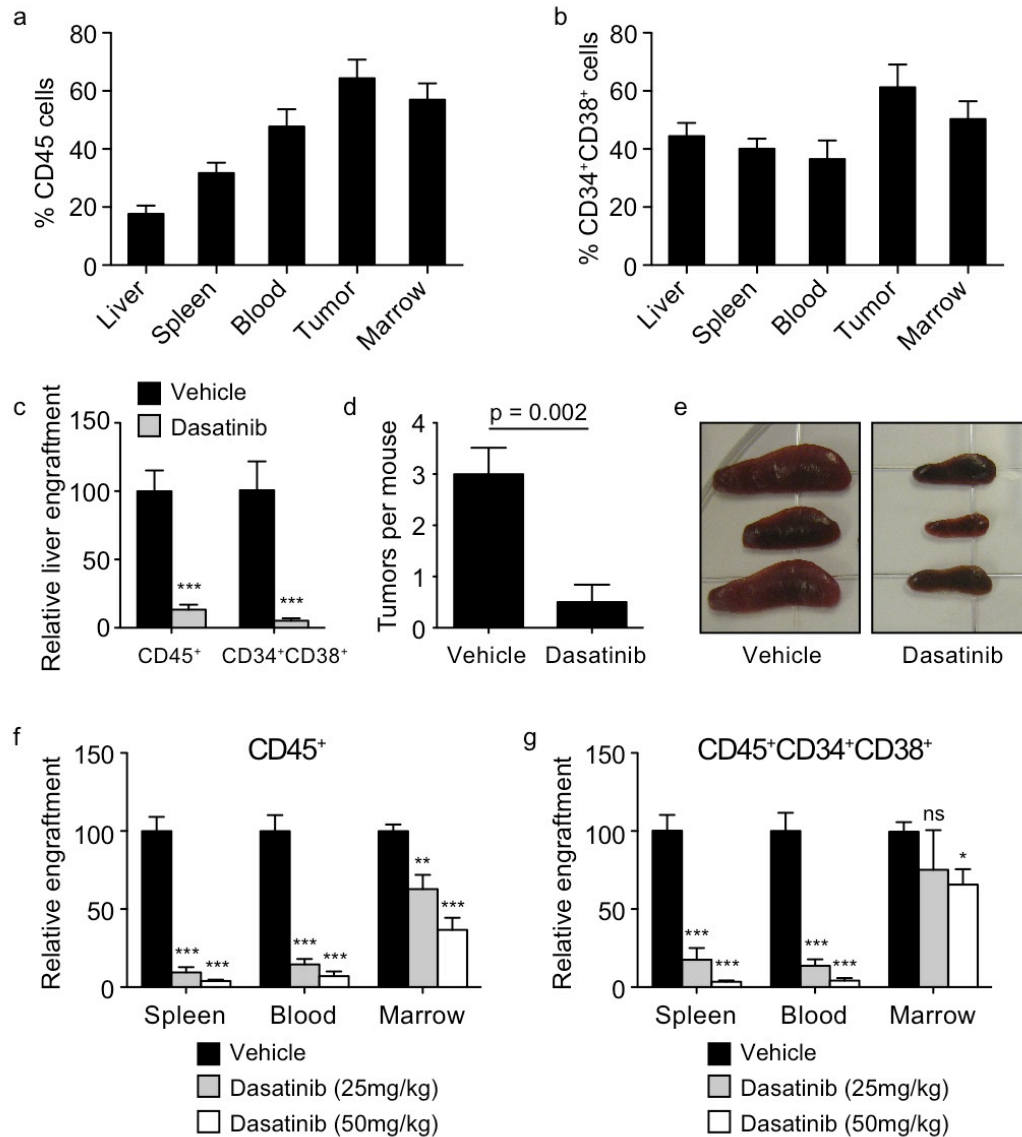


**Figure 2.12.** Bone marrow engrafted BC LSC, but not those in other niches, are resistant to dasatinib. **a)** Total human CD45 engraftment in liver, spleen, blood, tumor, and bone marrow of BC transplanted mice (see Table 2.2 for n). **b)** Engraftment of CD34<sup>+</sup>CD38<sup>+</sup> cells in the hematopoietic tissues (see Table 2.2 for n). **c)** Relative engraftment of CD45<sup>+</sup> and CD34<sup>+</sup>CD38<sup>+</sup> cells in the liver following treatment with vehicle (n=11) or dasatinib (50mg/kg, n=13). **d)** Number of myeloid sarcomas found in vehicle (n=6) and dasatinib (n=6) treated mice. **e)** Representative images of spleens harvested from vehicle and dasatinib treated mice. **f)** Relative engraftment of CD45<sup>+</sup> cells in spleen, blood and bone marrow following treatment with vehicle (n=22), 25mg/kg dasatinib (n=10) and 50mg/kg dasatinib (n=14). **g)** Relative engraftment of CD45<sup>+</sup>CD34<sup>+</sup>CD38<sup>+</sup> cells in hematopoietic tissues following the same treatments (n=29, 9 and 20 respectively). All graphs show mean +/- SEM. Panels c, f and g are normalized to vehicle controls. Statistical analyses are by unpaired t-test or ANOVA with Tukey post-hoc tests; \* p<0.05, \*\* p<0.01, \*\*\* p<0.001.

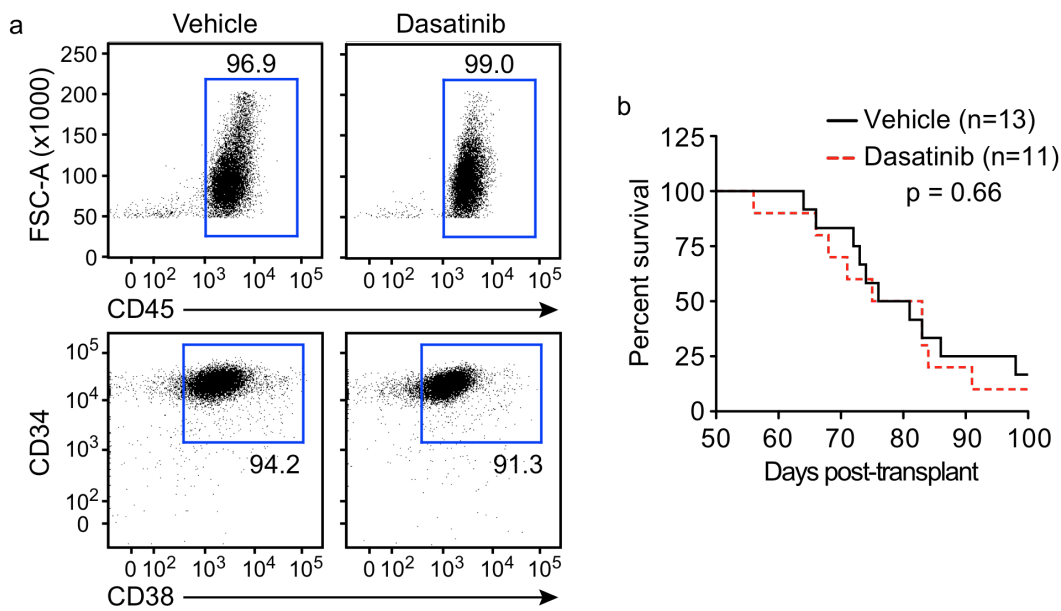


**Figure 2.13.** *Dasatinib treatment does not prevent BC CML relapse in secondary transplanted animals. a)* Representative FACS plots showing engraftment of CD45<sup>+</sup> (top row) and CD34<sup>+</sup>CD38<sup>+</sup> (bottom row) cells in the marrow of mice that were serially transplanted with whole bone marrow derived from vehicle and dasatinib (25mg/kg) treated primary mice. **b)** Survival of mice serially transplanted with vehicle (n=13) and dasatinib (25mg/kg, n=11) treated bone marrow. Statistical analysis is by log-rank test.

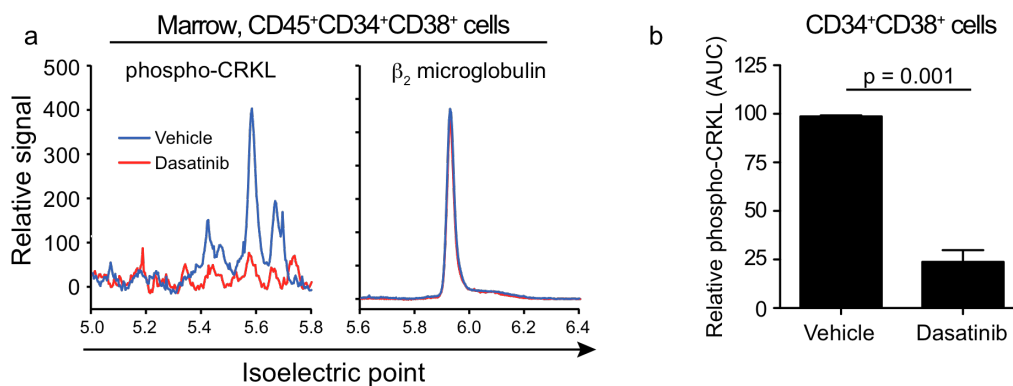


**Figure 2.14.** *Dasatinib significantly reduces BCR-ABL activity in bone marrow engrafted LSC. a)* Quantitative proteomic analysis of phospho-CRKL (left) and β<sub>2</sub> microglobulin (right) in FACS-sorted BC progenitors engrafted in mouse bone marrow after treatment with vehicle or dasatinib. **b)** Quantification of total area under the curve (AUC) of phospho-CRKL peaks in vehicle and dasatinib treated samples. All values are normalized to levels of β<sub>2</sub> microglobulin. Graph shows mean +/- SEM from 5 replicate measurements and statistical analysis by unpaired t-test.

### **2.2.3. Bone marrow LSC are induced into quiescence by TKI-treatment**

Chemotherapy resistance in leukemia has been previously linked to LSC quiescence<sup>117,118</sup>. To investigate whether quiescence-induction could account for the protective effect of the marrow on BC LSC in our model, we measured and compared the cell-cycle status of cells engrafted in the various hematopoietic niches. First, to test whether quiescent LSC are preferentially localized to a particular niche, we transplanted a cohort of mice with CD34<sup>+</sup> BC cells pre-labeled with DiR, a membrane-bound fluorescent dye. DiR is similar in function to carboxyfluorescein succinimidyl ester (CFSE); it is lost from cell membranes with every sequential cell division and only persists in non-dividing cells. Following an 18-week engraftment period, transplanted mice were sacrificed and DiR fluorescence was measured in human leukemic cells in the different hematopoietic tissues (tumor, liver, spleen and bone marrow - Figure 2.15a-b). DiR positive cells were detectable in the spleen and marrow only suggesting that these tissues are niches for quiescent LSC.

The spleen and marrow both contain quiescent cells but respond very differently to dasatinib (Figure 2.12). This suggests either that there are more quiescent cells in the marrow or that quiescence prior to treatment does not necessarily equal drug-resistance. To investigate these possibilities we quantified quiescent BC cells in the spleen and marrow environments in more detail using Ki-67/7-AAD flow-cytometric analysis. We also monitored whether there was a change in the quiescence of cells in each niche after treatment with dasatinib. Consistent with our DiR data, this analysis demonstrated a

distinct population of  $G_0$  ( $Ki-67^{low}7-AAD^{low}$ )  $CD45^+CD34^+CD38^+$  BC cells engrafted in both the spleen and marrow environments (Figure 2.15c). However, to our surprise, there were significantly more  $G_0$  progenitor cells in the spleen than in the bone marrow of untreated animals (Figure 2.15d). These data indicate that the quiescent state alone is not sufficient to protect BC progenitors from dasatinib-mediated cytotoxicity. However, spleen and marrow-engrafted cells differed greatly in their cell-cycle response to dasatinib. While there was no significant change in spleen-engrafted cells (Figure 2.16a-b), dasatinib treatment led to a dramatic increase in the  $G_0$  progenitor population in the bone marrow (Figure 2.16c-d). Because there was little change in the overall number of engrafted bone marrow progenitors (Figure 2.12), these results suggest that marrow LSC are induced into quiescence by TKI treatment. This quiescent state likely contributes to the protection of marrow LSC in the continued presence of the TKI.

Quiescent, drug-resistant LSC have recently been described in AML xenograft models in association with the bone marrow endosteal niche<sup>40,41</sup>, a location previously described as a niche for normal bone marrow stem cells<sup>245,246</sup>. To investigate whether this phenomenon may also apply to BC LSC we examined BC-engrafted bone marrow by immunohistochemistry and immunofluorescence using human progenitor markers (CD45, CD34 and CD38) and the cell cycle markers Ki-67 and phospho-Histone H3 (pHis-H3). This analysis demonstrated uniform engraftment of  $CD45^+CD34^+CD38^+$  leukemic cells throughout the marrow space (Figure 2.17) Notably, despite this



ubiquitous pattern of engraftment, analysis of both pHis-H3 and Ki-67 staining revealed a distinct population of quiescent leukemic cells adjacent to the endosteum (Figure 2.17a-b). Quantification of pHis-H3 staining confirmed that mitotic cells were significantly more frequent in the central zone compared to the endosteum of the marrow (Figure 2.17c). These data suggest that quiescent BC LSC preferentially reside in the endosteal bone marrow niche of untreated animals. We also examined marrow sections after treatment with dasatinib. Consistent with our other data, analysis of dasatinib treated marrow sections showed a dramatic decrease in Ki67 staining indicating induction of quiescence (Figure 2.17d). These results corroborate our FACS data and demonstrate that quiescent LSC are highly enriched in the bone marrow environment following dasatinib treatment.

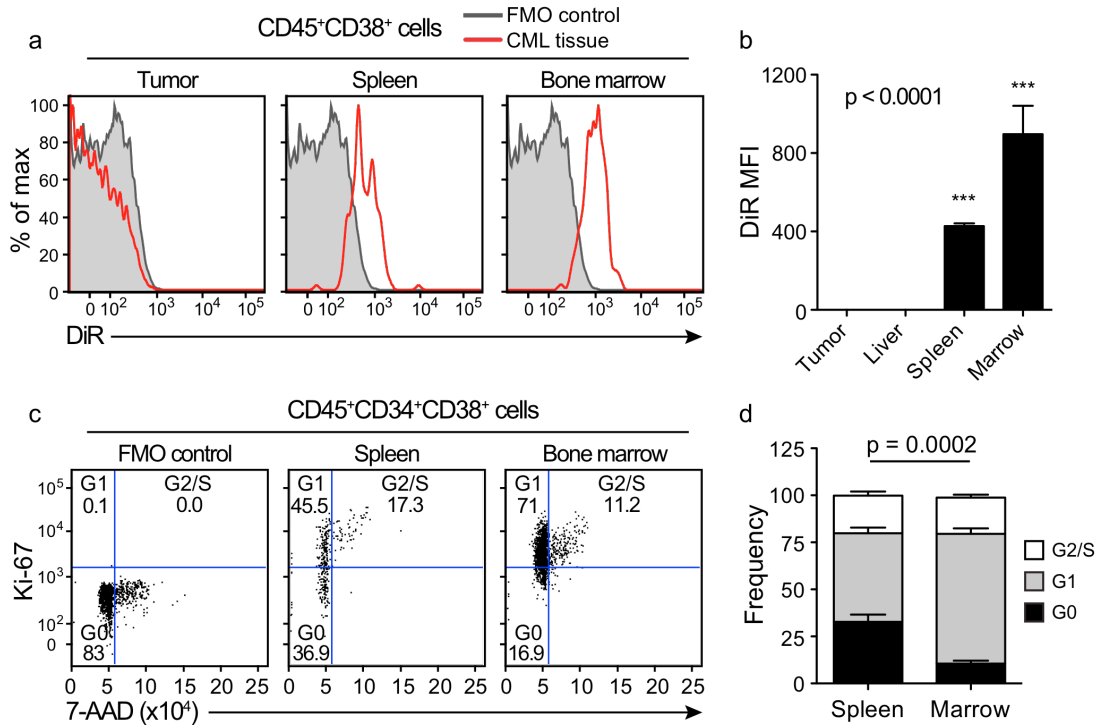


**Figure 2.15.** Quiescent BC LSC are engrafted in both spleen and marrow but are more frequent in the spleen. **a)** Representative FACS histograms of DiR signal retention in CD45<sup>+</sup>CD38<sup>+</sup> BC cells engrafted in tumor, spleen, and bone marrow at 18 weeks post-transplant. **b)** DiR mean fluorescence intensity (MFI) of CD45<sup>+</sup>CD38<sup>+</sup> BC cells engrafted in tumor (n=4), liver (n=4), spleen (n=3), and bone marrow (n=2). Graph shows mean +/- SEM. Statistical analysis is by ANOVA; \*\*\* p<0.001 by Tukey post-hoc analysis. **c)** Representative FACS plots showing cell cycle analysis of CD45<sup>+</sup>CD34<sup>+</sup>CD38<sup>+</sup> BC cells engrafted in spleen and bone marrow. A Ki-67 FMO-control is shown at far left. **d)** Quantification of the frequency of G2/S, G1 and G0 CD45<sup>+</sup>CD34<sup>+</sup>CD38<sup>+</sup> BC cells engrafted in spleen (n=10) and bone marrow (n=10). Statistical comparison is shown for the G0 population by unpaired t-test.

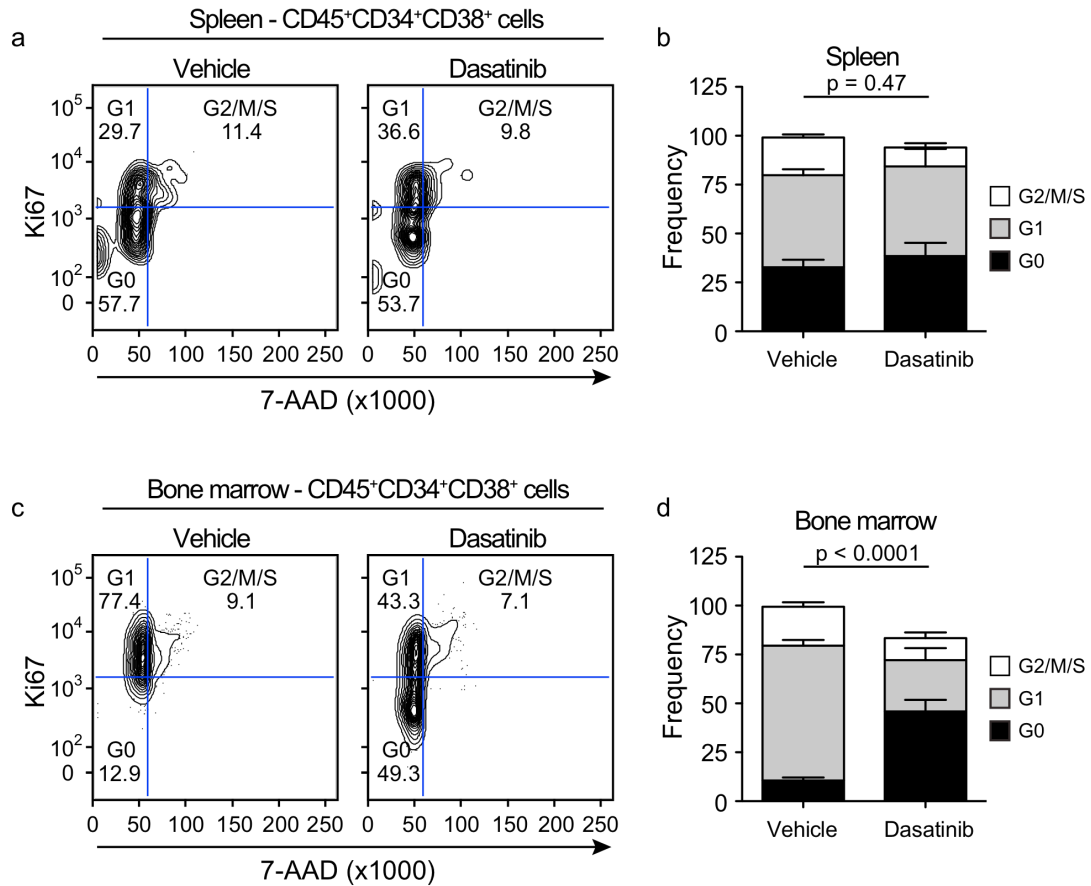


**Figure 2.16.** Dasatinib treatment enriches for quiescent BC LSC in the marrow but not the spleen. **a and c**) Representative FACS plots showing cell cycle analysis of CD45<sup>+</sup>CD34<sup>+</sup>CD38<sup>+</sup> BC cells engrafted in spleen (top row) and bone marrow (bottom row) following vehicle and dasatinib treatment. **b and d**) Quantification of G2/S, G1 and G0 CD45<sup>+</sup>CD34<sup>+</sup>CD38<sup>+</sup> BC cells engrafted in spleen and bone marrow following treatment with vehicle (n=10) and dasatinib (n=10). Both graphs show mean +/- SEM. Statistical comparisons are shown for the G0 population by unpaired t-test.

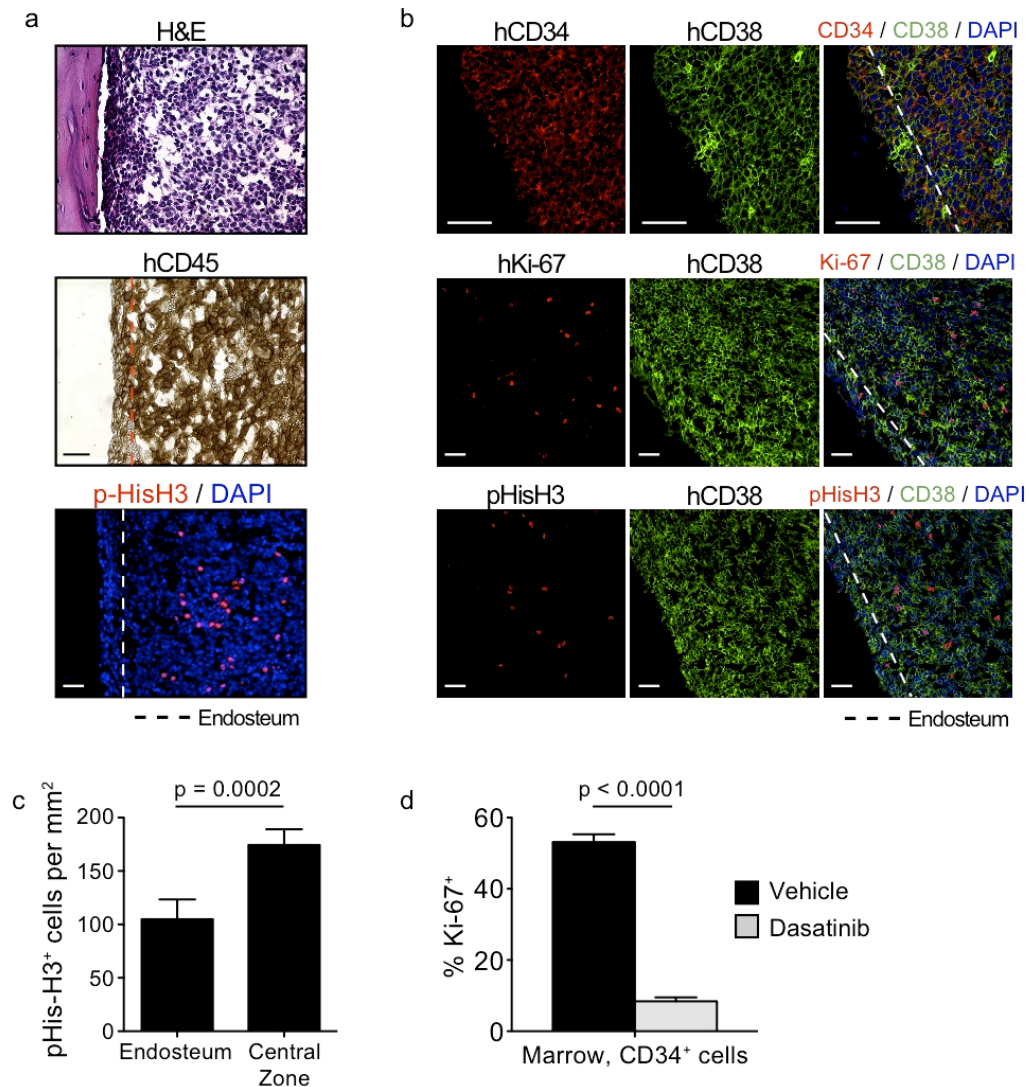


**Figure 2.17.** Quiescent bone marrow niche LSC are enriched in the endosteal region and following dasatinib treatment. **a and b)** Representative histological analyses of BC engrafted bone marrow showing H&E, human specific CD45, CD34, CD38 and Ki-67 and pHis-H3 staining. The dotted lines delineate the endosteal region (defined as 5 cell widths (~50 $\mu$ m) from the marrow edge). All scale bars equal 50 $\mu$ m. **c)** Quantification of endosteal pHis-H3 staining. Graph shows the mean +/- SEM number of pHis-H3 positive cells per area for the endosteum versus the central zone for a total of 30 separate fields (15 bones, 2 fields per bone). Statistical analysis is by paired t-test. **d)** Quantification of CD34<sup>+</sup>Ki-67<sup>+</sup> cells in BC transplanted bones following vehicle (n=3) or dasatinib (25mg/kg, n=3) treatment. Graph shows mean +/- SEM. Statistical analysis is by unpaired t-test.

#### 2.2.4. Dasatinib-resistant LSC express pro-survival BCL2 family genes

Because pro-survival *BCL2* family gene upregulation has been linked with chemotherapy resistance<sup>185,196,197</sup> and because we observed striking chemoprotection of BC LSC in the marrow niche, we hypothesized that the marrow microenvironment may promote *BCL2* family expression in engrafted LSC. We analyzed *BCL2* family expression in CD45<sup>+</sup>CD34<sup>+</sup>CD38<sup>+</sup>lin<sup>-</sup> cells sorted from spleen and marrow, using an apoptosis pathway qRT-PCR array (Figure 2.18a). Pro-survival *BCL2* was significantly upregulated in marrow while *MCL1*, *BCLX*, *BFL1* and *BCLW* were expressed but not significantly different between the two niches. These findings were confirmed by splice-isoform specific qRT-PCR and intracellular flow cytometric analysis of BCL2 protein (Figure 2.18b). In contrast, several pro-apoptotic genes were significantly downregulated in marrow LSC, including *BAX*, *BAK* and *BIM*, and there was a trend towards decreased *BAD* and *BID* expression. These data suggest that the survival versus death balance of BCL2 family genes favors a more pro-survival phenotype in marrow-niche LSC.

To investigate whether BCL2 expressing LSC may be localized to particular spaces within the marrow, we next examined the distribution of BCL2 family protein expression by immunohistochemical and immunofluorescence analysis. We also examined BC engrafted bones following dasatinib treatment to determine whether marrow niche BCL2 expression may correspond with dasatinib-resistance. Consistent with our

qRT-PCR analysis, BC cells in the marrow were found to express both BCL2 and MCL1 protein (Figure 2.19a). Moreover, BCL2 and MCL1 staining was highly correlated with CD34 and CD38 staining throughout the marrow space (Figure 2.19a) as well as the endosteal region (Figure 2.19b). Intriguingly, CD34<sup>+</sup>BCL2<sup>+</sup>MCL1<sup>+</sup> BC cells were more frequent in the epiphysis compared to the diaphysis of engrafted bones (Figure 2.19a and 2.20a). However, despite this predilection for the epiphysis, both bone regions became significantly enriched in BCL2<sup>+</sup> and MCL1<sup>+</sup> BC cells following dasatinib treatment (Figure 2.20b). This effect was not due to activation of BCL2 expression because dasatinib treatment did not significantly change BCL2 expression per cell as measured by intracellular FACS analysis (Figure 2.20c). These data suggest that dasatinib enriches for BCL2<sup>+</sup> and MCL1<sup>+</sup> cells by killing non-expressing cells in the marrow. Dasatinib resistance in the marrow niche is therefore associated with selection of BCL2 family expressing LSC in addition to quiescence-induction (Figure 2.16 and 2.17).

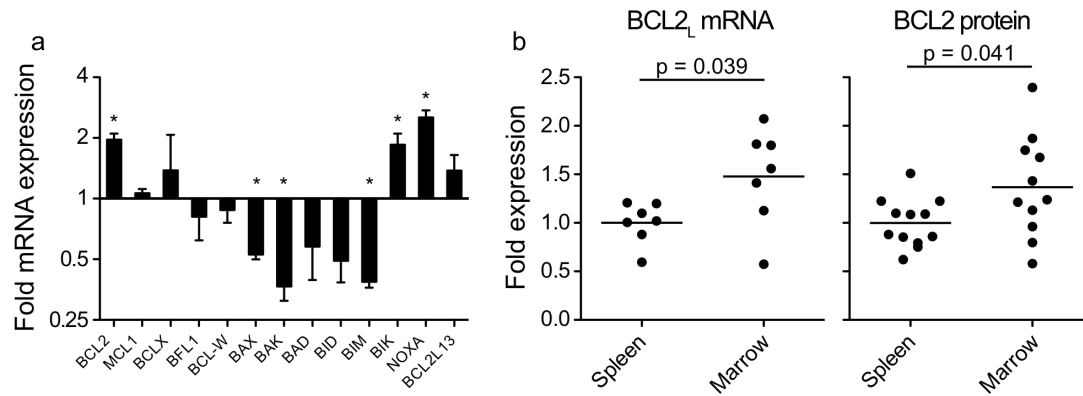


**Figure 2.18.** Marrow LSC differentially express BCL2 family genes compared to spleen LSC. **a)** BCL2 family qRT-PCR array data of FACS-sorted progenitors from engrafted mice (n=3). The graph depicts fold expression in marrow-engrafted progenitors relative to spleen-engrafted progenitors, which are set at 1. All bars are mean +/- SEM; \* p<0.05 by unpaired t-test. **b)** BCL2<sub>L</sub> mRNA isoform expression and BCL2 protein expression in marrow versus spleen-engrafted BC progenitors. Statistical analysis for both graphs is by paired t-test.

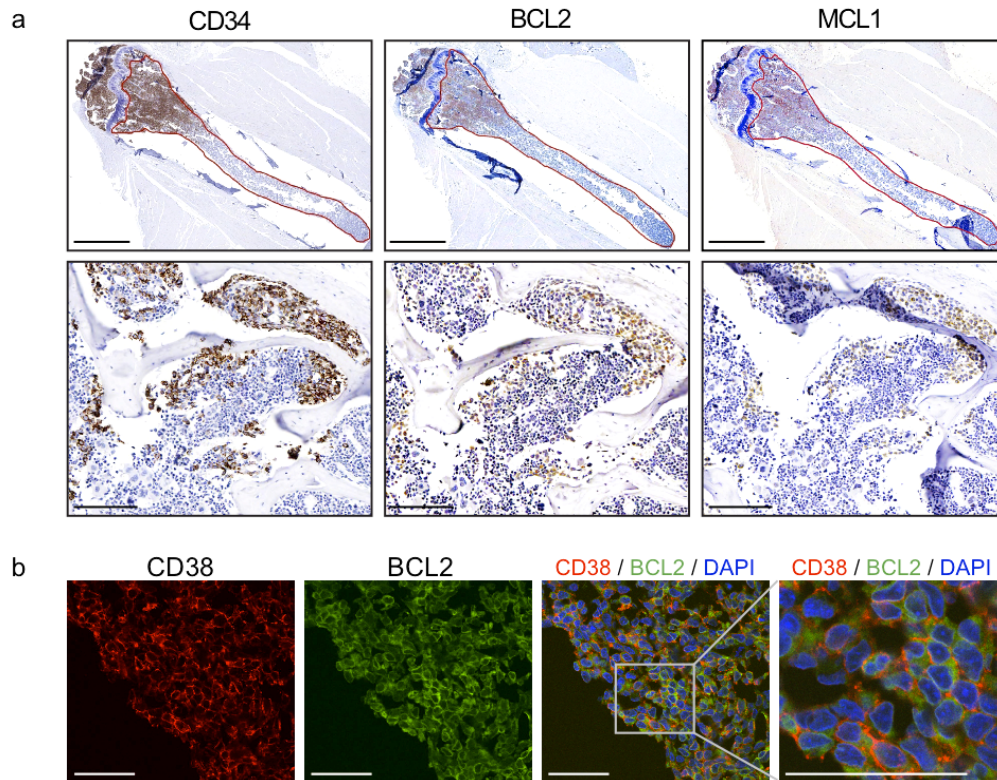


**Figure 2.19.** Marrow  $CD34^+$  LSC express *BCL2* and *MCL1* protein. **a)** Representative immunohistochemical analyses of gross (top) and endosteal (bottom) engraftment of human  $CD34^+$ ,  $BCL2^+$  and  $MCL1^+$  cells in mouse bone marrow. Scale bars equal 1mm in low-magnification images and 100 $\mu$ m in high-magnification images. **b)** Representative immunofluorescence analyses of CD38 and BCL2 co-staining in marrow and endosteal niche (far right) engrafted BC cells. Scale bars equal 50 $\mu$ m.



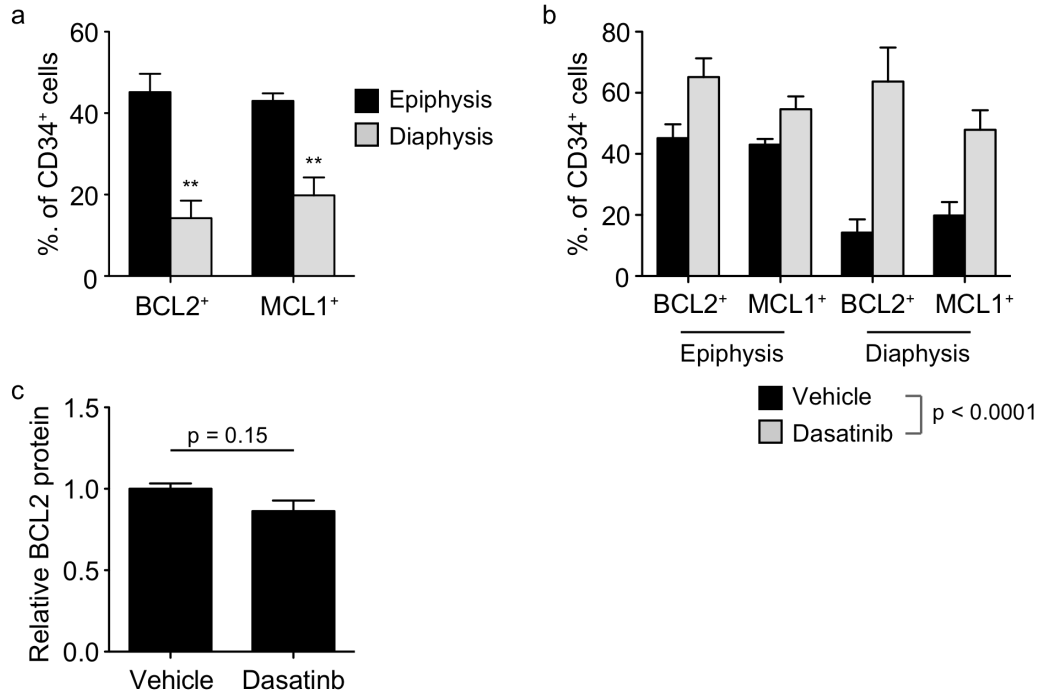


**Figure 2.20.** *BCL2* family expressing BC LSC are more frequent in the epiphyseal region and are highly enriched following dasatinib treatment. **a)** Quantification of CD34<sup>+</sup>BCL2<sup>+</sup> and CD34<sup>+</sup>MCL1<sup>+</sup> cells engrafted in the epiphysis and diaphysis of untreated BC engrafted bone marrow (n=3 per group). Statistical analyses are by unpaired t-test; \*\* p < 0.01. **b)** Frequency of CD34<sup>+</sup>BCL2<sup>+</sup> and CD34<sup>+</sup>MCL1<sup>+</sup> BC cells in the epiphysis and diaphysis of vehicle- (n=3) and dasatinib- treated (25mg/kg, n=3) bone marrow. Statistical analysis is by 2-way ANOVA. **c)** Relative BCL2 protein expression in CD34<sup>+</sup>CD38<sup>+</sup> BC cells engrafted in bone marrow and treated with vehicle (n=2) and dasatinib (n=3). Statistical analysis is by unpaired t-test. All graphs show mean +/- SEM

### 2.2.5. BC LSC are sensitive to sabutoclax, a pan-BCL2 family inhibitor

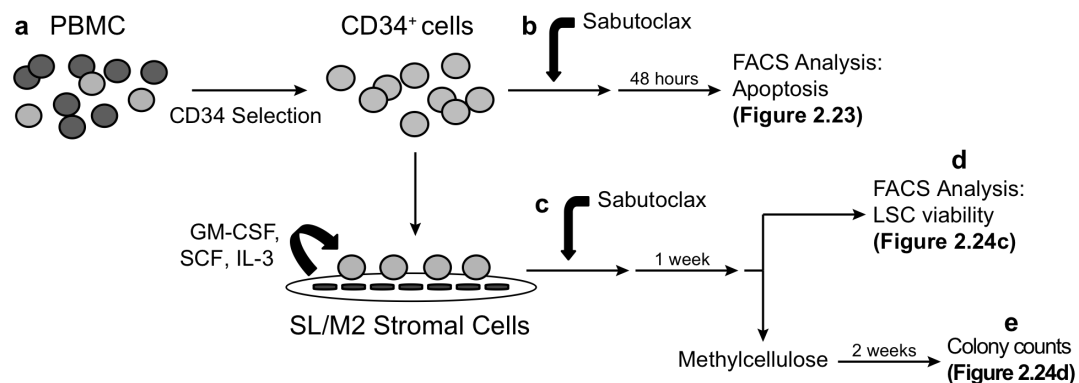
Expression of multiple pro-survival *BCL2* genes in primary and marrow niche-engrafted BC LSC suggested that inhibition of these genes may target BC LSC in protective niches. Therefore, we tested a novel pan-BCL2 inhibitor, sabutoclax (BI-97C1), which is an optically pure derivative of apogossypol that inhibits all pro-survival BCL2 family proteins<sup>216,217</sup>, on BC LSC *in vitro* (experimental design: Figure 2.21).

First, we determined the specificity and efficacy of sabutoclax against the BCL2 family and tested its ability to induce apoptosis. Using a fluorescence polarization assay, we measured the potency of sabutoclax in dissociating a BIM-peptide from the different BCL2 family proteins. As a positive control, we also tested ABT-737, a potent and specific BCL2 and BCLX<sub>L</sub> inhibitor<sup>202</sup>. As expected, ABT-737 inhibited BIM binding to BCL2 and BCLX<sub>L</sub> but had no effect on binding to MCL1 and BFL1 (Figure 2.22a). In contrast, sabutoclax dissociated BIM from BCL2, MCL1, BCLX<sub>L</sub> and BFL1 proteins at sub-micromolar concentrations (Table 2.3 and Figure 2.22b). Sabutoclax induced apoptosis in K562 cells, a BCR-ABL-dependent leukemia cell line, in a dose-dependent manner as measured by the accumulation of cleaved caspase-3, a marker of activation of the intrinsic apoptotic pathway (Figure 2.23a). In this assay, sabutoclax-induced caspase-3 activation was similar to that induced by ABT-737. Sabutoclax also induced apoptosis in primary CD34<sup>+</sup>CD38<sup>+</sup> BC CML cells (Figure 2.23b-c). Together these data

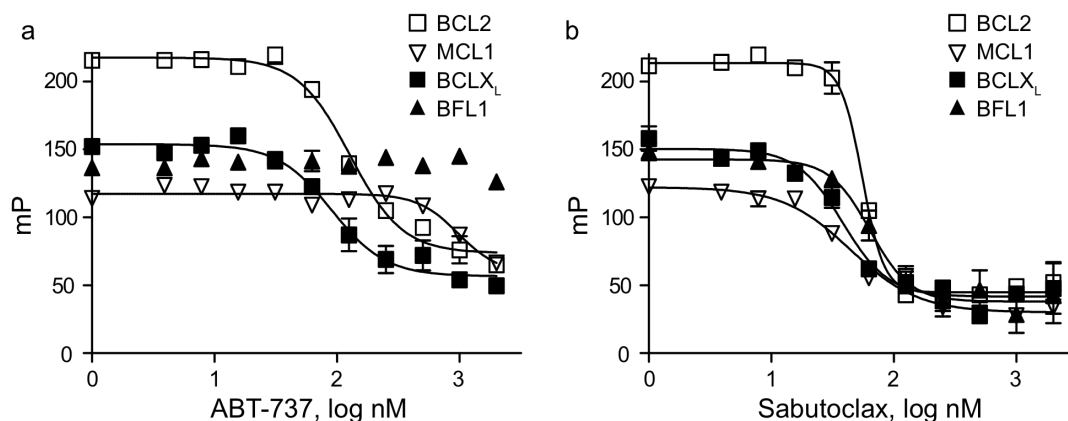
demonstrate that sabutoclax is a specific BCL2 family inhibitor that activates the intrinsic apoptotic pathway in CML cell lines and immature CML progenitors.

Because BC LSC are chemo-protected in supportive microenvironments, we tested the anti-LSC efficacy of sabutoclax in a genetically engineered SL/M2 stromal co-culture system that secretes human GM-CSF, SCF and IL-3 and supports long-term survival of self-renewing LSC<sup>247</sup> (Figure 2.21). BC LSC had increased expression of pro-survival *BCL2<sub>L</sub>*, *MCL1<sub>L</sub>*, *BCLX<sub>L</sub>* and *BFL1<sub>L</sub>* in the presence of SL/M2 stroma (Figure 2.24a). Notably, upregulation of these genes was similar when LSC were cultured in SL/M2 conditioned media indicating that increased *BCL2* family gene expression was likely due to the secreted factors from the stroma rather than cell-cell interactions. Despite stroma-induced pan-upregulation of pro-survival *BCL2* genes, sabutoclax treatment led to a dose-dependent reduction in LSC survival (Figure 2.24b-c) and LSC colony formation (Figure 2.24d). In both assays BC LSC were more sensitive to sabutoclax than normal progenitors (Table 2.3) suggesting that, despite expression of the *BCL2* family, normal progenitors are less dependent upon these genes for their survival. Consistent with these data, ABT-737 treatment was also more effective in killing BC LSC than normal progenitors (Table 2.3 and Figure 2.25). In addition, lentiviral-mediated short-hairpin RNA knockdown of *BCL2* reduced BC LSC clonogenicity but not that of normal progenitors (Figure 2.26). In these experiments, *BCL2* knockdown alone did not completely abrogate BC colony

formation, possibly because of relatively low knockdown efficiency (~50%). Also, colony inhibition by sabutoclax and ABT-737 was partially dependent on the stromal microenvironment as both drugs were significantly more effective in the absence of stroma (Figure 2.24d and Figure 2.25b). However, in both conditions sabutoclax was significantly more potent against LSC than ABT-737 (Table 2.3). Furthermore, in the presence of stroma, only sabutoclax was more effective against BC LSC than normal progenitor cells. Taken together, these data suggest that knockdown or inhibition of multiple BCL2 proteins may be required to selectively eradicate BC LSC, especially in supportive microenvironments.

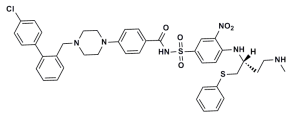
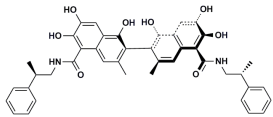


**Figure 2.21.** *Experimental design for in vitro sabutoclax treatment:* **a)** CD34<sup>+</sup> BC cells were isolated and purified by ficoll-gradient and MACS and cultured either alone or in the presence of SL/M2 stromal cells. **b)** CD34<sup>+</sup> BC cells were treated with sabutoclax for 48 hours and apoptosis was measured by FACS. **c)** For the co-cultured cells, sabutoclax treatment was given for 1-week. Following the treatment period the co-cultures were harvested and split for analysis of viable progenitors by FACS (**d**) or for colony assay (**e**). To measure colony formation, treated cells were plated on methylcellulose and colonies were counted following an additional 2-week growth period.



**Figure 2.22.** Sabutoclax inhibits multiple BCL2 family proteins with high potency. Fluorescence polarization assay analysis of ABT-737 (a) and sabutoclax (b) against BCL2, MCL1, BCLX<sub>L</sub> and BFL1 protein bound to a BIM peptide. Graph shows mean FITC fluorescence +/- SD from 2 replicate measurements.

**Table 2.3.** Characteristics of ABT-737 and sabutoclax and efficacy against normal and BC progenitors cultured *in vitro*

		<b>ABT-737</b>	<b>Sabutoclax (BI-97C1)</b>
<b>Structure</b>			
<b>EC<sub>50</sub> (μM), BCL2 family proteins</b>	BCL2	0.13	0.055
	BCLX <sub>L</sub>	0.09	0.038
	MCL1	>1	0.044
	BFL1	>20	0.064
<b>IC<sub>50</sub> (nM), FACS assay</b>	Normal	2079	210
	BC CML	249.7	42.8
	p value	0.01	0.008
<b>IC<sub>50</sub> (nM), Colony assay (with stroma)</b>	Normal	155.2	436.9
	BC CML	102	27.8
	p value	0.66	<0.0001

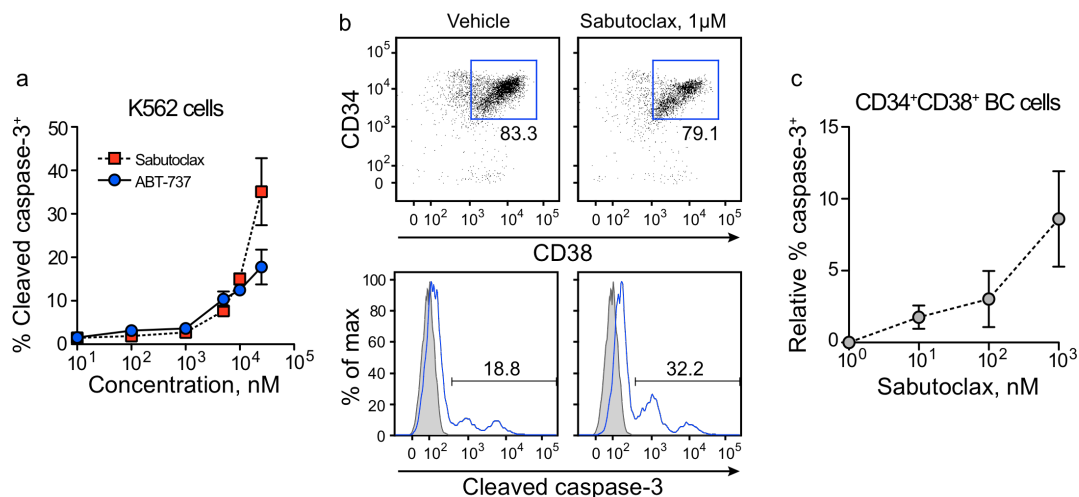


**Figure 2.23. Sabutoclax induces caspase-3 cleavage in CML cells. a)** Percent of cleaved caspase-3 positive K562 cells following treatment with different doses of ABT-737 and sabutoclax. Graph shows mean  $\pm$  SEM from 3 independent experiments. **b)** Representative FACS plots of vehicle and sabutoclax treated BC cells. The top row shows gating of CD34<sup>+</sup>CD38<sup>+</sup> cells while the bottom row shows fluorescence histograms of cleaved caspase-3. **c)** Relative percent of cleaved caspase-3 positive BC CD34<sup>+</sup>CD38<sup>+</sup> cells following treatment with different doses of sabutoclax. Values are normalized to vehicle baseline. Graph shows mean  $\pm$  SEM from 3 independent experiments.

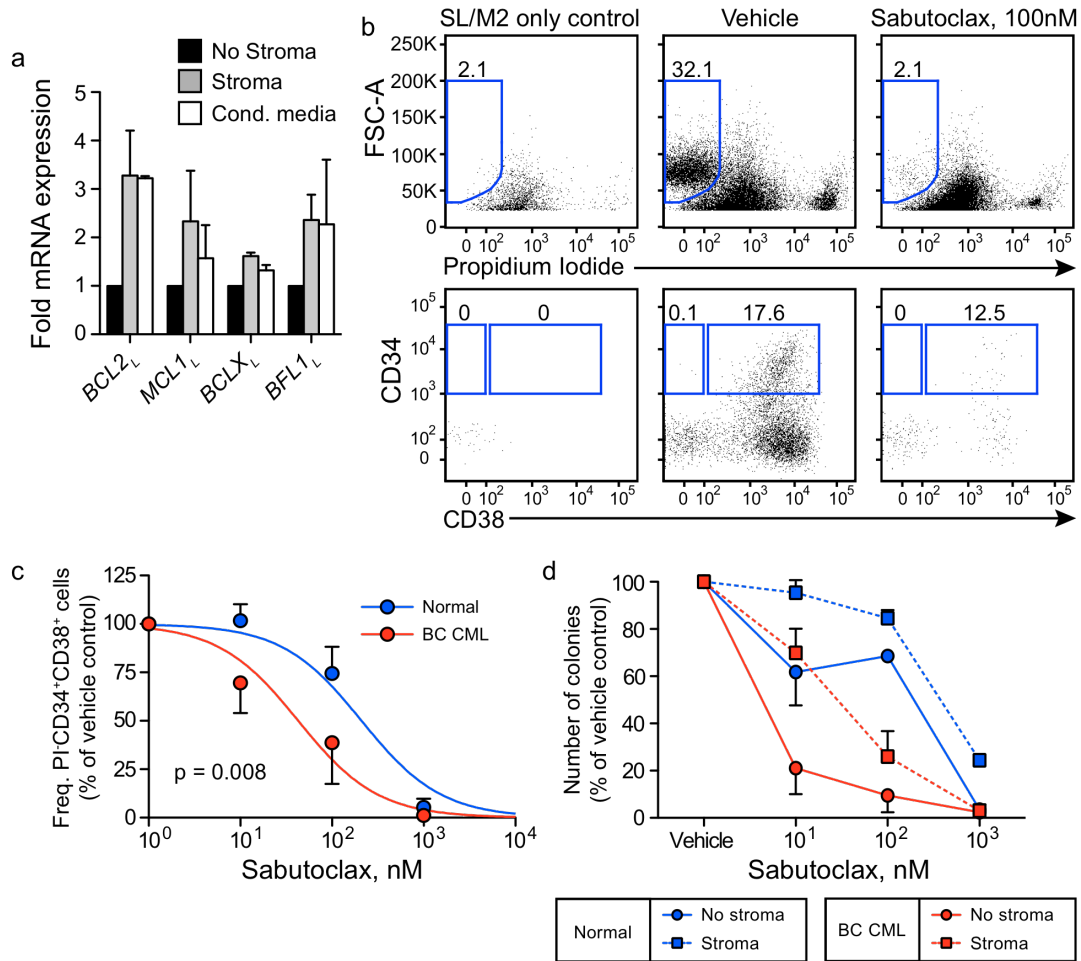


**Figure 2.24. Sabutoclax targets BC LSC in the context of a protective bone marrow microenvironment.** **a)** qRT-PCR of pro-survival *BCL2* family transcripts in FACS-sorted BC progenitors after 1 week of culture in the presence of SL/M2 stroma (n=4 experiments) or SL/M2 conditioned media (n=2 experiments). Values are normalized to no-stroma control. Graph shows mean  $\pm$  SEM. **b)** Representative FACS plots of BC cells cultured on SL/M2 stromal cells and treated with either vehicle or sabutoclax compared to SL/M2 only control cultures. The top row shows gating of live cells while the bottom row shows gating of progenitor cells. **c)** FACS analysis of normal and BC progenitors cultured on SL/M2 bone marrow stroma in the presence of sabutoclax. Values are expressed as percent of vehicle treated control. Graph shows mean  $\pm$  SEM from 5 different normal and BC samples and statistical comparisons by non-linear regression analysis. **d)** Total colonies formed by normal and BC progenitors following sabutoclax treatment in the presence and absence of SL/M2 stroma. Values are expressed as percent of vehicle treated control. Graph shows mean  $\pm$  SEM from 3 different normal and 4 BC samples.

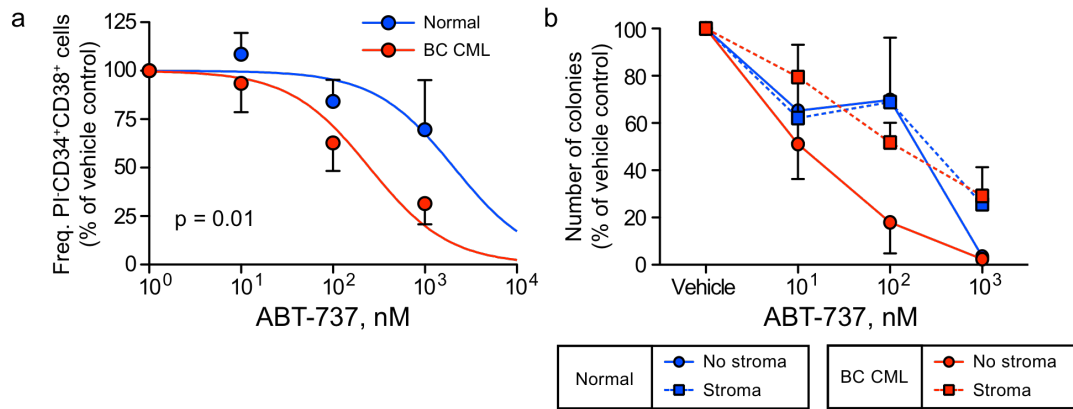


**Figure 2.25. ABT-737 targets BC LSC in vitro. a)** FACS analysis of normal (n=5) and BC (n=5) progenitors cultured on SL/M2 bone marrow stroma in the presence of ABT-737. **b)** Total colonies formed by normal (n=2) and BC (n=3) progenitors following ABT-737 treatment in the presence and absence of SL/M2 stroma. Values for both graphs are expressed as percent of vehicle treated control. Both graphs show mean +/- SEM. Statistical comparison is by non-linear regression analysis.



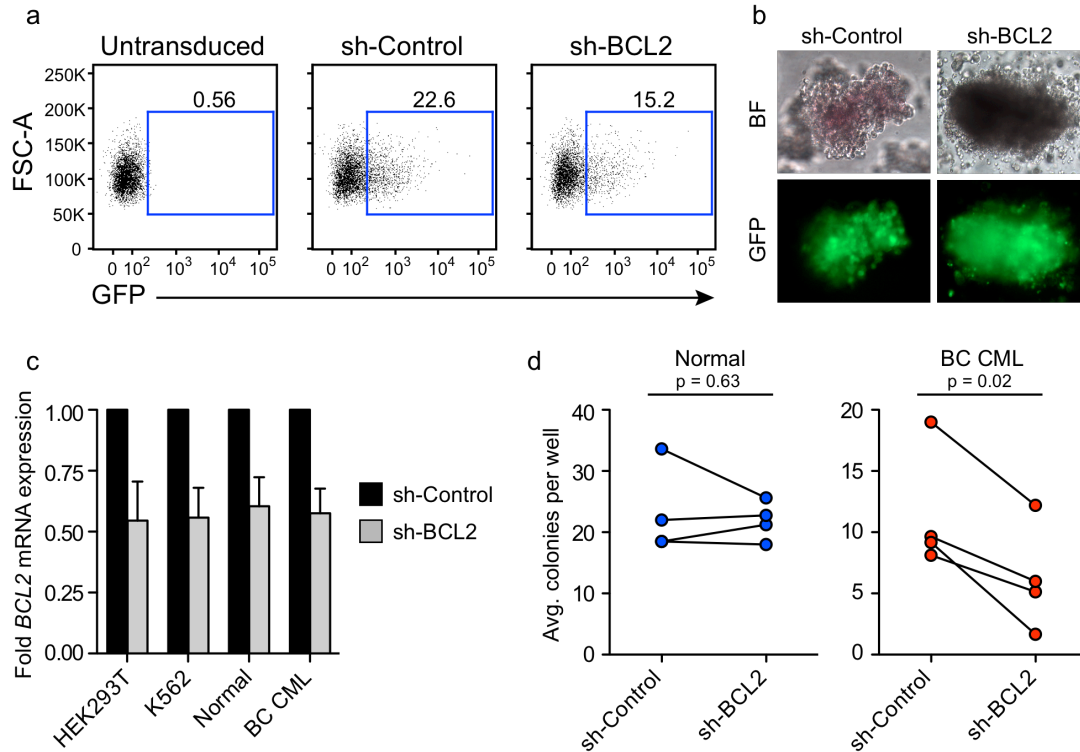


**Figure 2.26.** *shRNA-mediated knockdown of BCL2 inhibits BC but not normal colony formation.* **a)** Representative FACS plots of untransduced versus sh-Control and sh-BCL2 transduced progenitors. **b)** Representative colonies from control or sh-BCL2 transduced progenitors. **c)** qRT-PCR of *BCL2<sub>L</sub>* mRNA in HEK293T and K562 cell lines as well as primary normal and BC cells following transduction with control and sh-BCL2 lentivirus (n=5 experiments for cells lines; n=3 colonies for each primary sample type). **d)** Number of colonies formed by normal or BC progenitors following transduction with control or sh-BCL2 lentivirus. Graph shows average colonies per well for 4 different normal and BC samples and statistical analysis by paired t-test.

### 2.2.6. Sabutoclax sensitizes marrow-niche engrafted BC LSC to dasatinib

To examine the necessity of pro-survival *BCL2* family expression for LSC engraftment, we tested the efficacy of sabutoclax against LSC *in vivo* (experimental design: Figure 2.27). In BC-transplanted mice, sabutoclax (5mg/kg) significantly reduced LSC engraftment in all hematopoietic tissues (Table 2.4 and Figure 2.28a-b). Consistent with our *in vitro* results, there was no significant reduction in normal progenitor engraftment following sabutoclax treatment, while marrow LSC burden was significantly reduced (Figure 2.28c). Sabutoclax-treated marrow also had reduced numbers of BCL2 and MCL1 immunopositive cells (Figure 2.29a-b), a slight increase in G<sub>2</sub>/S cells (Figure 2.29c), and increased TUNEL<sup>+</sup> cells (Figure 2.29d), suggesting that quiescent, BCL2 expressing LSC were killed by apoptosis.

We next examined whether sabutoclax could sensitize marrow niche LSC to dasatinib. First, we quantified the TKI-sensitizing effects of sabutoclax in the presence of human LSC-supportive cytokines that are not secreted by the mouse marrow. Equal numbers of human BC LSC were sorted from sabutoclax or vehicle treated marrow into SL/M2 stromal co-cultures in the presence of dasatinib (Figure 2.30a). In this *ex vivo* assay, sabutoclax pre-treated progenitors were more sensitive to dasatinib than vehicle pre-treated controls (Figure 2.30b). Next, BC-engrafted mice were treated with sabutoclax (1.25mg/kg), dasatinib (25mg/kg) or a combination of the two drugs and LSC engraftment was analyzed by FACS. While dasatinib and sabutoclax alone

had no significant effect on marrow LSC engraftment at these lower doses, there was significant reduction in marrow LSC after combination treatment compared to vehicle treated controls (Table 2.5 and Figure 2.31a). At higher doses (50mg/kg dasatinib, 2.5mg/kg sabutoclax), this difference was more pronounced and there was ~90% reduction in LSC burden following combination treatment (Table 2.5 and Figure 2.31c). We examined combination treated marrow in more detail by immunohistochemical analysis. Compared to dasatinib treatment alone, combination-treated marrows had significantly reduced expression of BCL2 and MCL1 protein (Figure 3.32b) as well as a trend toward increased Ki67 expression (Figure 3.32a). These results suggest that sabutoclax sensitizes quiescent, BCL2 family-expressing cells to dasatinib-mediated cell death. Finally, to test whether functional LSC had truly been eliminated, we serially transplanted treated bone marrow into secondary recipients and monitored survival time. Mice that received combination-treated marrow had a significant survival advantage compared to those that received dasatinib-treated marrow at both doses tested (Figure 2.31b-d). Overall our data demonstrate that dasatinib alone, while effective at reducing primary leukemic burden, does not significantly eradicate bone marrow-resident LSC. In contrast, combined dasatinib and sabutoclax therapy significantly inhibits both primary and serial LSC engraftment suggesting that TKI-resistance has been abrogated. Consistent with this effect, combination treatment decreases the burden of quiescent and BCL2 expressing cells in the marrow, which are enriched following dasatinib treatment alone.

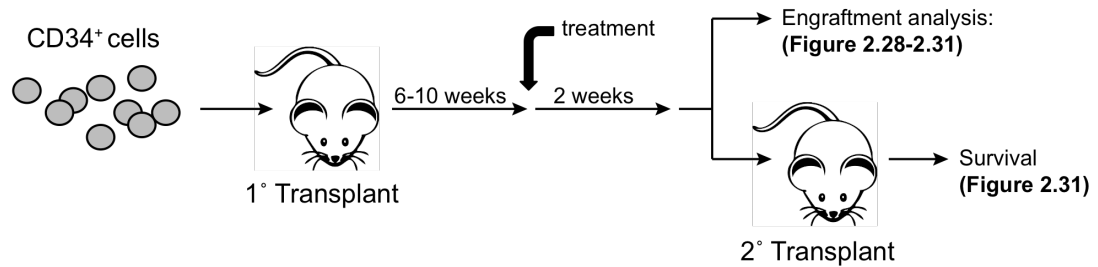


**Figure 2.27.** *Experimental design for in vivo sabutoclax and combination treatment:* CD34<sup>+</sup> BC cells were isolated by ficoll-gradient and MACS and transplanted into neonatal RAG2<sup>-/-</sup>γ<sub>c</sub><sup>-/-</sup> mice. Following a 6-10 week engraftment period, the transplanted mice were split into cohorts and treated with sabutoclax (IP, 3 doses per week), dasatinib (oral, 1 dose per day), sabutoclax + dasatinib, or vehicle for 2 weeks. After treatment, the mice were sacrificed and engraftment was measured by FACS. In addition, whole bone marrow was harvested from the different cohorts mice and transplanted into secondary recipients. Survival was followed in the secondary recipients and engraftment was verified by FACS post-mortem.

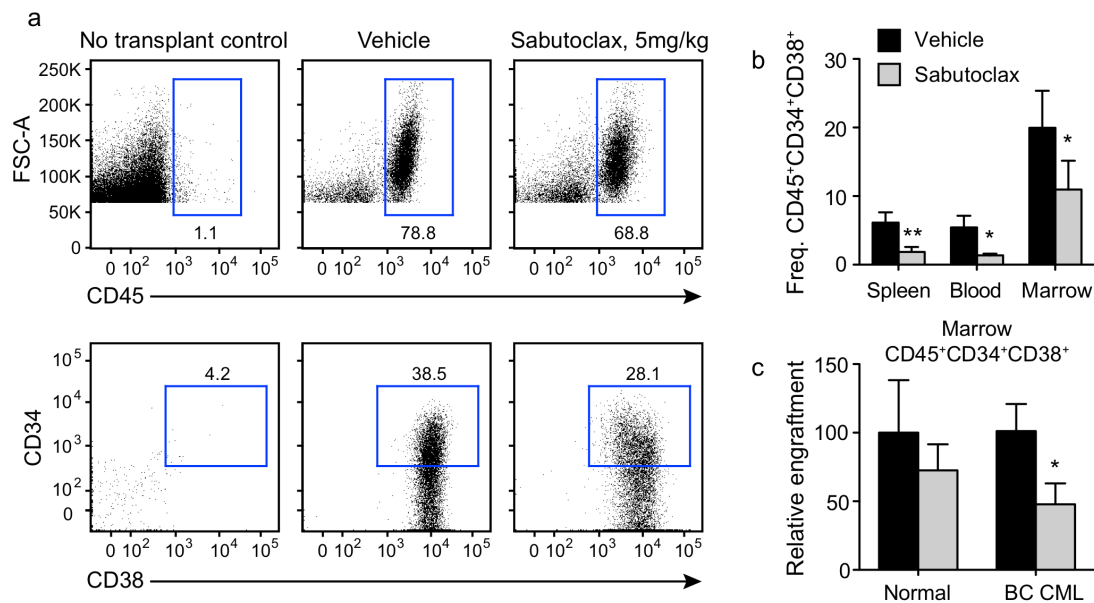


**Figure 2.28.** *Sabutoclax targets engrafted BC LSC in vivo.* **a**) Representative FACS plots of BC cells engrafted in mouse bone marrow showing gating and measurement of human CD45<sup>+</sup> cells and progenitors after treatment with either vehicle or sabutoclax for 2 weeks and compared to no-transplant control marrow (left column). **b**) Engraftment of BC progenitors in spleen, blood and bone marrow following vehicle (n=27) and sabutoclax treatment (5mg/kg, n=26). **c**) Relative engraftment of normal and BC progenitors in bone marrow following vehicle and sabutoclax treatment (5mg/kg). Normal: vehicle n=6, sabutoclax n=6. Graphs **b** and **c** show mean +/- SEM for 3 different BC patient samples. \* p < 0.05, \*\* p < 0.01 by Mann Whitney test.

**Table 2.4.** Sabutoclax effects on BC LSC engraftment *in vivo*

Treatment	Mean (SEM) engraftment of CD34 <sup>+</sup> CD38 <sup>+</sup> cells		
	Spleen	Blood	Marrow
Vehicle (n=27)	4.92 (1.2)	5.44 (1.7)	15.54 (4.5)
Sabutoclax (n=26)	1.39 (0.5)	1.36 (0.3)	8.02 (3.2)
p value (Mann Whitney test)	0.001	0.043	0.026

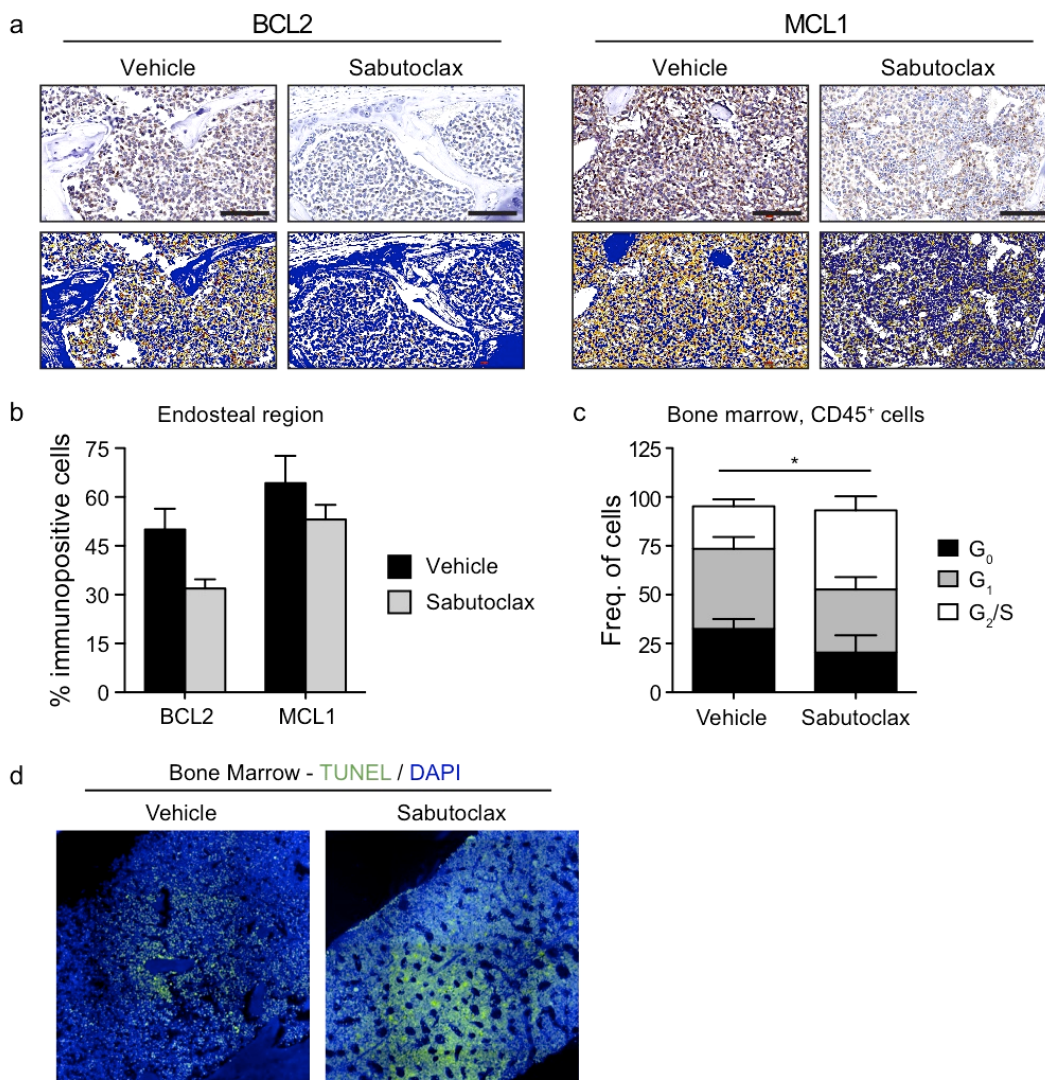


**Figure 2.29.** Sabutoclax targets quiescent,  $BCL2^+MCL1^+$  marrow LSC. **a)** Representative images of BCL2 and MCL1 immunohistochemical staining in BC engrafted bone marrow following vehicle and sabutoclax treatment. The top row shows raw bright-field images while the bottom row shows pseudocoloring for quantification. Scale bars equal 100 $\mu$ m. **b)** Quantification of BCL2<sup>+</sup> and MCL1<sup>+</sup> cells in the endosteum of BC engrafted bone marrow following vehicle (n=3) and sabutoclax (5mg/kg, n=3) treatment. Graph shows mean  $\pm$  SEM. **c)** FACS-cell cycle analysis of human CD45<sup>+</sup> BC cells in the marrow of vehicle (n=6) and sabutoclax (5mg/kg, n=5) treated mice. Graph shows mean  $\pm$  SEM. \* p<0.05 by unpaired t-test. **d)** Representative images of TUNEL staining of BC-engrafted bone marrow following treatment with vehicle or sabutoclax (5mg/kg).

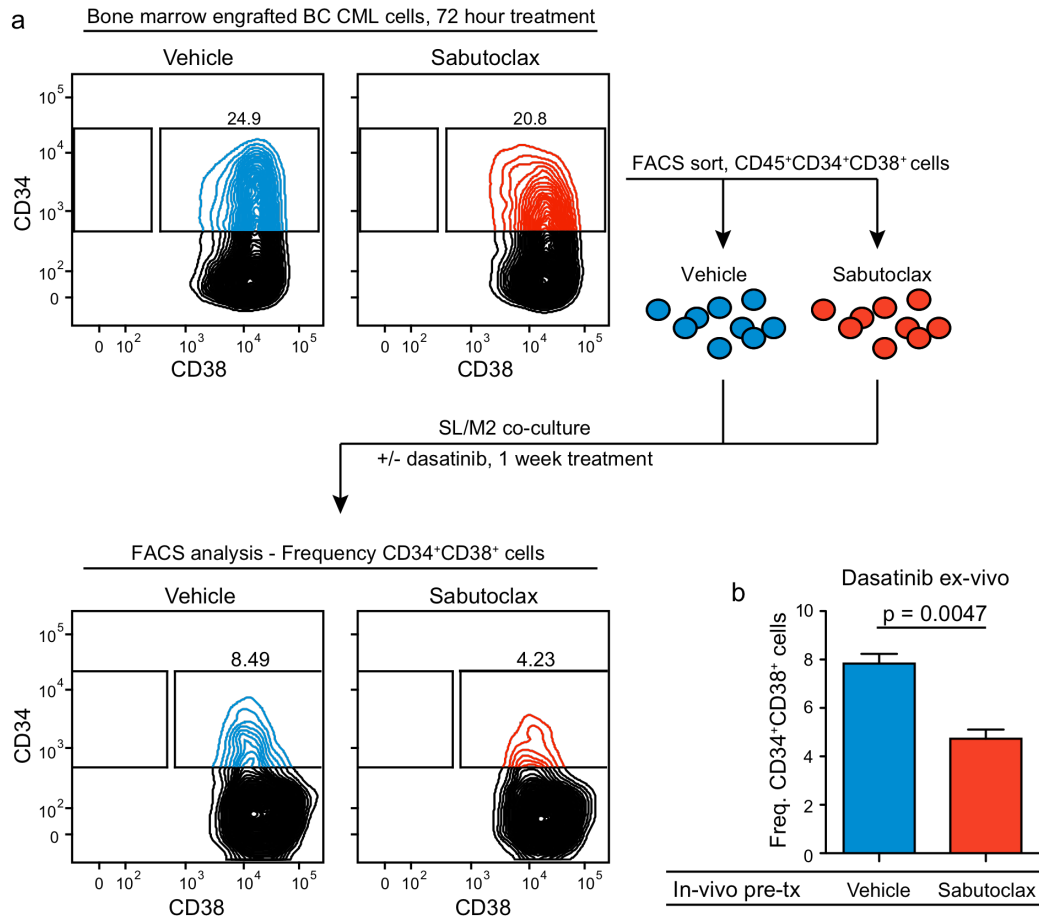
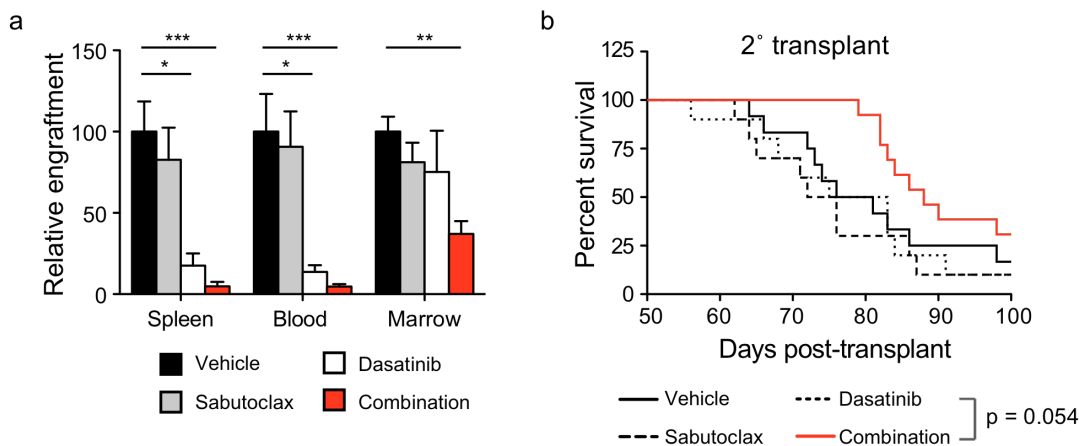


**Figure 2.30.** *In vivo* sabutoclax pre-treatment sensitizes BC LSC to dasatinib *ex vivo*. **a)** Scheme and representative FACS plots of vehicle or sabutoclax pre-treated BC progenitors before and after *ex vivo* treatment with dasatinib for 1 week in SL/M2 co-culture. **b)** Frequency of live BC progenitors from vehicle (n=3) or sabutoclax (5mg/kg, n=3) pre-treated mice following dasatinib treatment *ex vivo* (250nM). Graph shows mean +/- SEM with statistical analysis by unpaired t-test.

## Low dose



## High dose

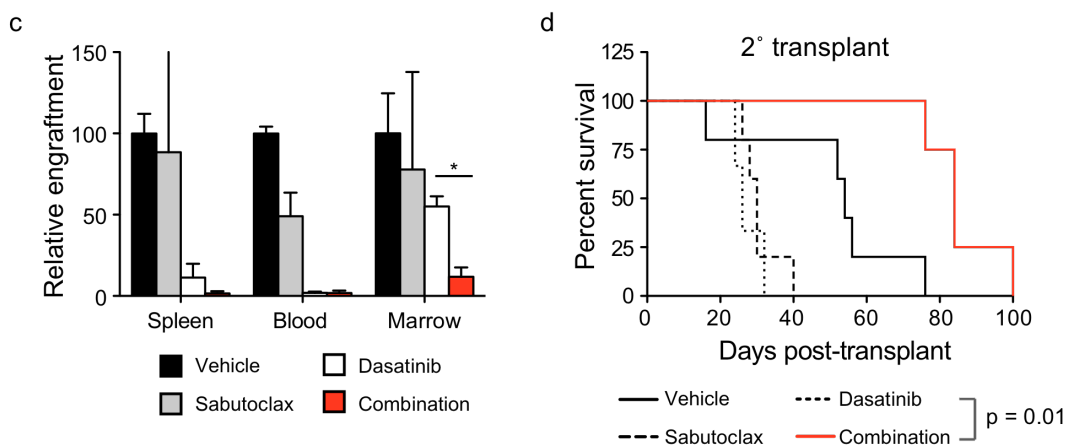


**Figure 2.31. Sabutoclax in combination with dasatinib targets marrow engrafted BC LSC.** **a)** Relative engraftment of BC progenitors in spleen, blood and bone marrow following treatment with vehicle (n=9), sabutoclax (1.25mg/kg, n=9), dasatinib (25mg/kg, n=9) and sabutoclax in combination with dasatinib (n=11). Graph shows mean +/- SEM. \* p<0.05, \*\* p<0.01, \*\*\* p<0.001 by Kruskal-Wallis test with Dunn's post-hoc analysis. **b)** Survival of mice following serial transplant with vehicle (n=12), sabutoclax (n=10), dasatinib (n=10) or combination (n=13) treated whole bone marrow. Statistical analysis is shown for dasatinib versus combination by log-rank test. **c)** Relative engraftment of BC progenitors in hematopoietic tissues following treatment with vehicle (n=2), sabutoclax (2.5mg, n=2), dasatinib (50mg/kg, n=3) and sabutoclax in combination with dasatinib (n=2). Graph shows mean +/- SEM. \* p<0.05 by unpaired t-test. **d)** Survival of mice following serially transplant with vehicle (n=5), sabutoclax (n=5), dasatinib (n=3) or combination (n=4)-treated whole bone marrow. Statistical analysis is shown for dasatinib versus combination by log-rank test.



**Table 2.5.** Sabutoclax + dasatinib combination effects on BC LSC engraftment *in vivo*

	Mean (SEM) engraftment of CD34 <sup>+</sup> CD38 <sup>+</sup> cells			
<b>Low Dose Treatment</b>	<b>Spleen</b>	<b>Blood</b>	<b>Marrow</b>	<b>2° TP - Median survival (days)</b>
Vehicle (n=10)	16.8 (3.7)	12.5 (4.8)	35.4 (12.4)	78.5 (n=12)
Sabutoclax (n=9)	12 (2.7)	11.0 (3.8)	34.2 (12.5)	74 (n=10)
Dasatinib (n=9)	2.0 (0.8)	2.1 (0.9)	28.8 (10.7)	79 (n=10)
Combination (n=11)	0.6 (0.3)	0.6 (0.3)	15.5 (6.0)	88 (n=13)
p value (dasatinib vs. combination)	0.07	0.07	0.22	0.054
<b>High Dose Treatment</b>	<b>Spleen</b>	<b>Blood</b>	<b>Marrow</b>	<b>2° TP - Median survival (days)</b>
Vehicle (n=2)	10.3 (0.4)	27.7 (3.4)	38.58 (9.6)	57 (n=5)
Sabutoclax (n=2)	5.1 (1.5)	24.5 (17.6)	30.01 (23.2)	45 (n=5)
Dasatinib (n=3)	0.2 (0.07)	3.1 (2.4)	21.23 (2.4)	43 (n=3)
Combination (n=2)	0.19 (0.16)	0.4 (0.37)	4.54 (2.3)	72 (n=4)
p value (dasatinib vs. combination)	0.91	0.44	0.018	0.01

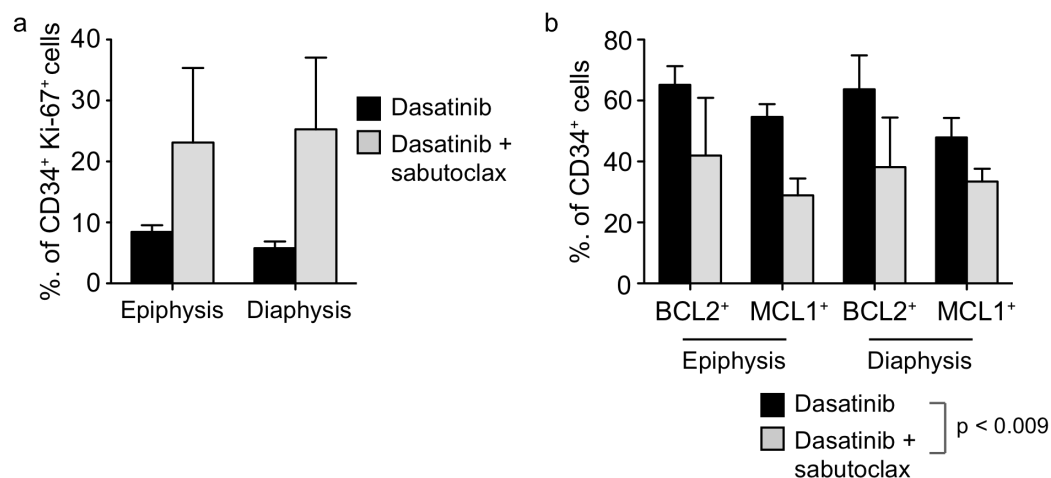


**Figure 2.32.** Sabutoclax targets quiescent, BCL2<sup>+</sup> and MCL1<sup>+</sup> BC LSC enriched by dasatinib treatment. **a)** IHC-based quantification of CD34<sup>+</sup>Ki-67<sup>+</sup> BC cells in the epiphysis and diaphysis of bone marrow treated with dasatinib alone (25mg/kg, n=3) and dasatinib + sabutoclax (1.25mg/kg, n=3). **b)** Frequency of CD34<sup>+</sup>BCL2<sup>+</sup> and CD34<sup>+</sup>MCL1<sup>+</sup> BC cells in the epiphysis and diaphysis of bone marrow treated with dasatinib alone (25mg/kg, n=3) and dasatinib + sabutoclax (1.25mg/kg, n=3). Statistical analysis is by 2-way ANOVA.

### 2.3. Summary and discussion

Malignant reprogramming of human myeloid progenitors by dysregulation of apoptosis is an important molecular mechanism driving blastic transformation and therapeutic resistance of CML LSC. By analyzing FACS-sorted CD34<sup>+</sup>CD38<sup>+</sup>lin<sup>-</sup> cells from primary patient samples, we demonstrate that BC LSC harbor increased expression of multiple pro-survival *BCL2* family genes compared to both CP and normal progenitors. Moreover, this pro-survival gene expression is further upregulated upon co-culture with cytokine-secreting bone marrow stroma or engraftment into the bone marrow niche. These data are consistent with previous reports demonstrating increased *BCL2* family expression in CML cells<sup>183,184,189</sup> and upregulation via niche-dependent signals<sup>192</sup>. However, our study is unique in that we show pan-*BCL2* upregulation in phenotypically and functionally defined BC LSC and we demonstrate that niche-dependent *BCL2* expression is associated with TKI-resistance *in vivo*. We are also the first to examine isoform-specific *BCL2* family expression in CML, which is important given that the *BCL2* family is spliced into variants with antithetical functions<sup>160,161</sup>. Alternative splicing of apoptosis genes thus represents a novel mechanism that may skew the balance of pro-death and pro-survival factors and contribute to apoptosis-resistance in LSC.

In addition to altered *BCL2* family expression, we identify a number of other apoptosis-related genes that are differentially expressed between

normal, CP and BC progenitors. Surprisingly, many of the genes and isoforms that are upregulated in BC LSC are pro-apoptotic. At the same time, this is balanced by increased expression of pro-survival signaling kinases, such as PI3K and JAK (Figure A.1), increased BCR-ABL expression (Figure 2.3) and increased expression of multiple pro-survival BCL2 family genes (Figure 2.3 and 2.6). Together these results suggest that BC LSC may be primed for both extrinsic and intrinsic apoptosis, but that they are unable to initiate caspase-cascade activation because of the presence of numerous pro-survival factors. This apoptosis-priming may be due to global genetic instability, which is caused by the prolonged presence of BCR-ABL<sup>126,248,249</sup>, and which likely leads to activation of apoptosis regulators such as p53 (summarized in Figure 2.33). Apoptosis-priming may also explain why BC LSC are sensitive to BCL2 inhibition while normal progenitors are more resistant (Figure 2.24-2.26): BC LSC appear to be under a greater degree of pro-apoptotic pressure. Notably, a number of the genes differentially expressed in BC progenitors are regulators of NF- $\kappa$ B signaling. The NF- $\kappa$ B signaling complex regulates innate immune responses downstream of TNF receptor activation<sup>250</sup> and promotes apoptosis-resistance in response to toxic stimuli by transcriptional activation of pro-survival genes<sup>251,252</sup>. Thus, deregulation of this pathway could represent another important mechanism for promoting LSC survival as well as a mechanism for how LSC evade immune clearance by TNF receptor-mediated pathways.

Using a RAG2<sup>-/-</sup>γc<sup>-/-</sup> xenograft model of BC CML, we demonstrate that phenotypic LSC are protected from TKI-mediated cell death when engrafted in the marrow microenvironment compared with extramedullary hematopoietic niches suggesting that LSC are subject to marrow-specific cytoprotection (summarized in Figure 2.34). This niche-specific protection is independent of BCR-ABL kinase activity as demonstrated by nanoproteomic phospho-CRKL analysis. Thus, while dasatinib treatment effectively reduces overall leukemic burden in BC-engrafted mice, it does not fully eliminate LSC and mice serially transplanted with dasatinib-treated bone marrow rapidly develop CML (Figure 2.13). These data add to previous findings that CML LSC are not oncogenically addicted to BCR-ABL and instead depend on BCR-ABL-independent survival mechanisms<sup>39</sup>. Our findings expand on this concept by identifying pro-survival *BCL2* family expression as an important niche-specific survival mechanism and molecular target for CML LSC. The mechanisms that underlie these expression changes will be important for future study.

Using cell cycle and immunofluorescence analysis of engrafted bone marrow we show that quiescent CML LSC engraft the bone marrow niche and are enriched in the endosteal region, consistent with studies done in AML xenograft models<sup>39</sup>. Moreover, immunohistochemical analysis demonstrates that endosteal niche LSC express pro-survival *BCL2* and *MCL1* proteins. Strikingly, dasatinib treatment enriches for quiescent bone marrow LSC. Quiescent stem cells are known to have enhanced engraftment potential<sup>118</sup>, which could explain why mice serially transplanted with dasatinib-treated

marrow still develop CML despite receiving fewer phenotypic LSC. Our results suggest that BCL2 family expression may also be associated with this enhanced transplant-ability because dasatinib also enriches for BCL2 and MCL1 expressing cells in the marrow.

In contrast to dasatinib, BC LSC in stromal co-culture or the marrow are sensitive to a novel pan-BCL2 inhibitor, sabutoclax<sup>216,217</sup>. Sabutoclax also sensitizes marrow-niche LSC to TKI-treatment suggesting that bone marrow-specific TKI protection is predicated, at least in part, on BCL2 family expression in the niche that can be overcome with a pan-inhibitor. Also, unlike dasatinib, sabutoclax treatment does not significantly enrich for marrow G<sub>0</sub> cells despite reducing LSC engraftment, indicating that quiescent cells are targeted with this compound. This is evidenced by our observation that in combination-treated marrow there is a trend toward more frequent Ki67<sup>+</sup> LSC compared to dasatinib-treated marrow (Figure 2.32). Finally, combination treatment significantly improves the survival of serially transplanted mice (Figure 2.31) indicating that significant numbers of functional LSC have been eliminated.

While BCL2 inhibition has been previously explored for CML, most studies have focused on CML cell lines<sup>191,253</sup> or primary CD34<sup>+</sup> cells grown in culture<sup>254</sup> rather than primary, self-renewing CML BC LSC in selective niches. Moreover, published reports do not address the potential antithetical roles of BCL2 family splice isoforms or the role of the malignant microenvironment in promoting LSC survival. Furthermore, treatment with ABT-737<sup>191,254</sup>, a potent

BCL2 and BCLX<sub>L</sub> inhibitor, does not inhibit MCL1<sub>L</sub> or BFL1<sup>202,217</sup>, which have been shown to accelerate leukemogenesis<sup>181</sup>, mediate resistance<sup>210-212</sup> and which are upregulated in CML progenitors during progression from CP to BC (Figure 2.3 and 2.6). Because inhibition of both subfamilies of pro-survival BCL2 family proteins is necessary for apoptosis initiation<sup>255</sup>, inhibition strategies that include MCL1 would be expected to be more successful than those that only target BCL2<sup>174</sup>. Pan-BCL2 inhibition may therefore prove more effective at targeting LSC that express multiple BCL2 family proteins and upregulate these genes in response to niche-dependent stimuli *in vivo*. In addition, our findings may also have relevance for the elimination of solid tumor cells where metastasis and survival in the metastatic niche are mediated by pro-survival BCL2 family expression<sup>180</sup>. Thus, pan-BCL2 inhibition with novel small molecules like sabutoclax could provide an important new component of combination therapies that target a broad array of CSC residing in protective niches.

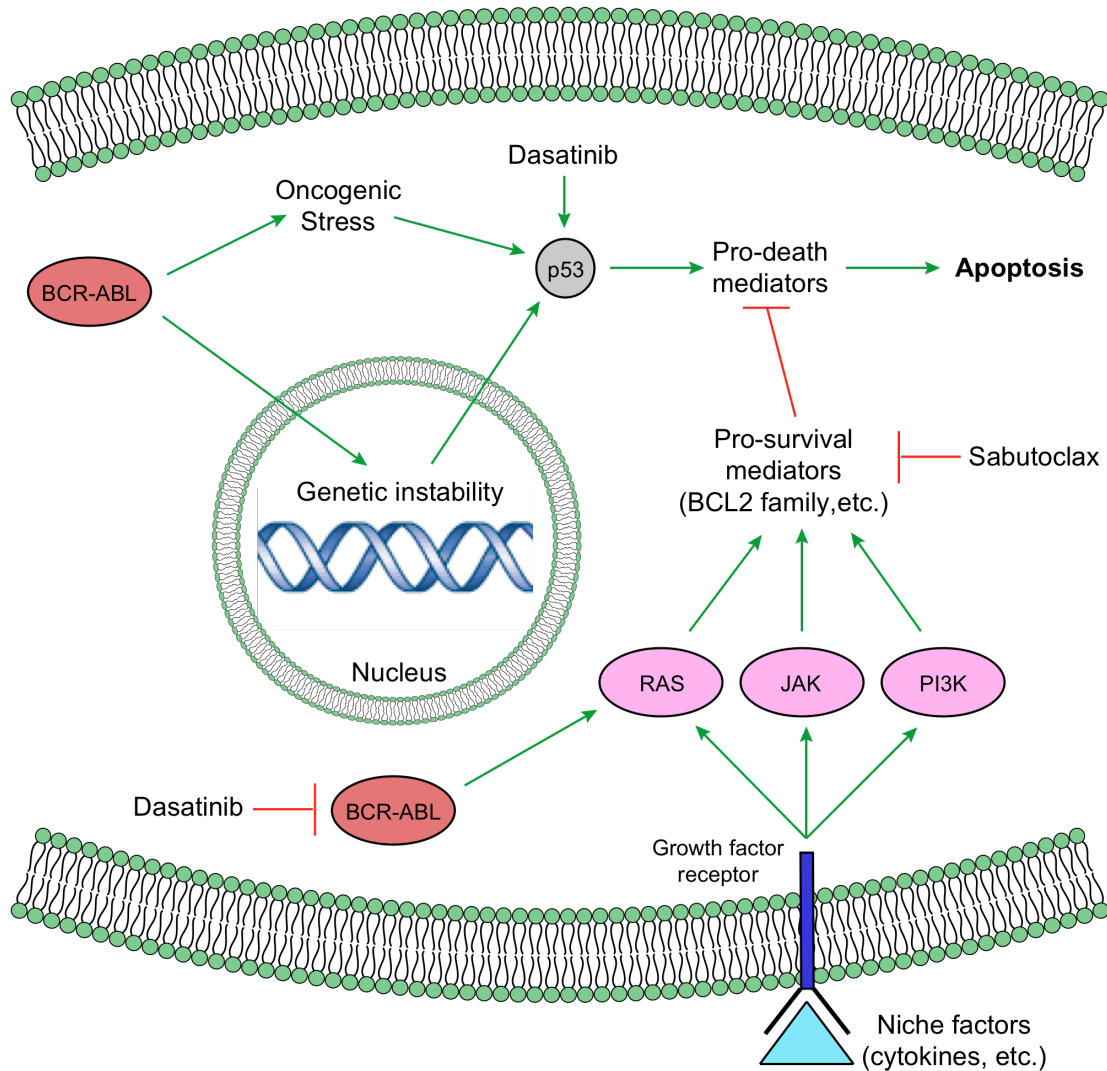


**Figure 2.33.** Proposed model for BCL2 family regulation of BC LSC survival and TKI-resistance: BC LSC are primed for apoptosis due to the prolonged effects of BCR-ABL, which induces genetic instability and oncogenic stress, and leads to the upregulation of regulators such as p53 and other pro-apoptotic genes. However, BC LSC fail to initiate intrinsic apoptosis due to concurrent upregulation of pro-survival mediators (such as BCL2 family genes) via upregulation of BCR-ABL and other pro-survival pathways such as RAS, JAK, and PI3K-mediated signaling. BC LSC are sensitive to BCL2 inhibition because it removes the pro-survival component thereby allowing apoptosis to proceed. Apoptosis can also be initiated by dasatinib, which activates pro-death mediators via p53 and inhibits pro-survival mediators by blocking BCR-ABL. In the niche, additional survival pathways are active (via cytokines and other niche factors) and converge to activate pro-survival BCL2 family genes. These pathways compensate for the pro-death activity of dasatinib and mediate niche-dependent TKI-resistance. Sabutoclax is effective in the niche because it inhibits this compensatory pro-survival stimulation thus sensitizing LSC to the effects of dasatinib.



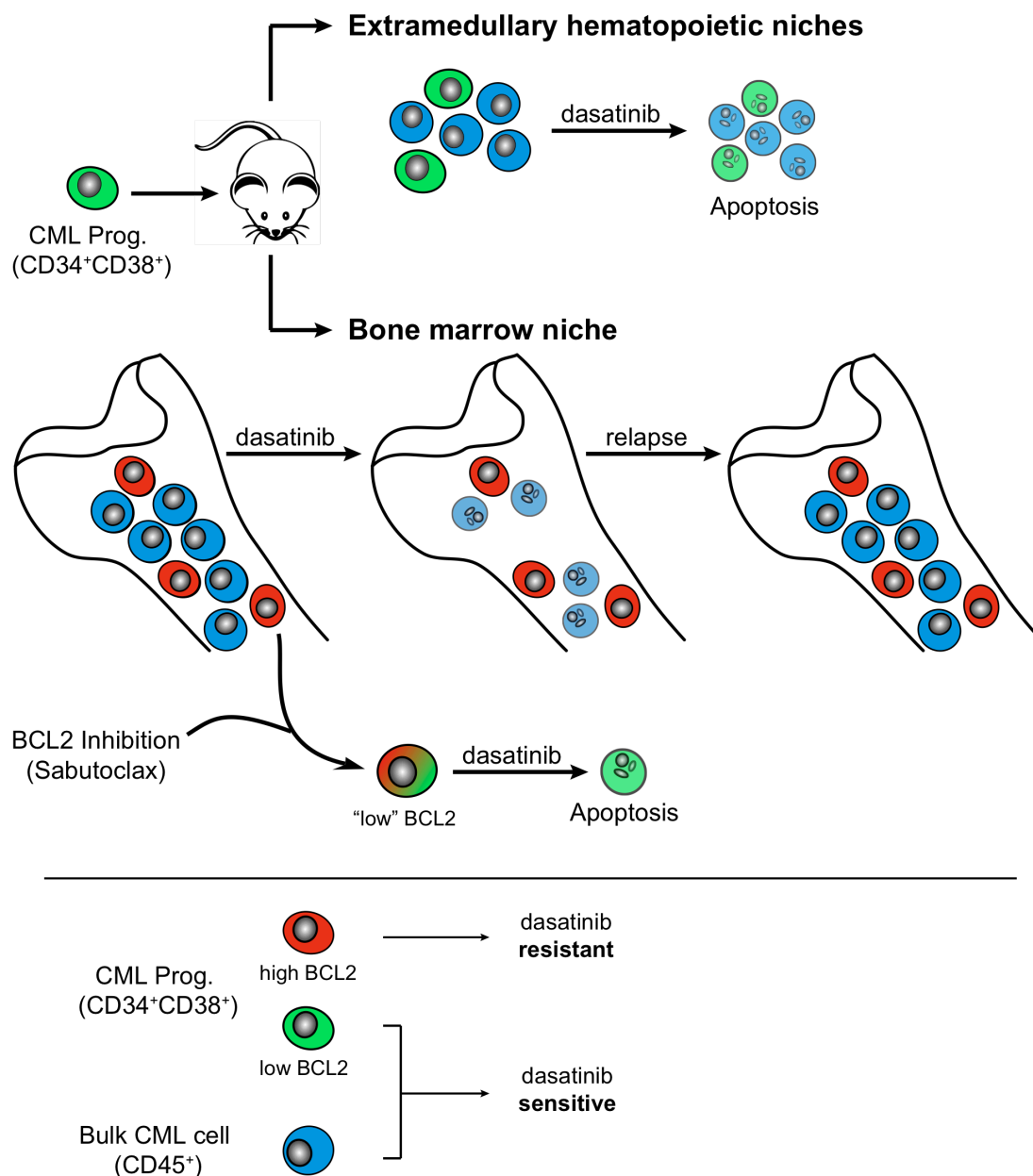


**Figure 2.34.** Summary: Sabutoclax sensitizes bone marrow-niche engrafted BC LSC to dasatinib-mediated apoptosis. While transplanted BC progenitors engraft multiple hematopoietic niches, these cells are differentially sensitive to dasatinib depending on their *in vivo* location. Both progenitors and bulk CML cells are highly sensitive to dasatinib in extramedullary niches including spleen, liver and blood while progenitors engrafted in bone marrow are dasatinib-resistant. This resistance is associated with an increased pro-survival gene signature including upregulated BCL2 expression. However, bone marrow engrafted LSC are sensitive to the pan-BCL2 inhibitor, sabutoclax, which also sensitizes these cells to treatment with dasatinib. Thus sabutoclax may be useful in combination with dasatinib to target CML in all niches.

## **2.4. Materials and Methods**

### **2.4.1. Patient sample preparation and FACS sorting**

Normal cord blood and adult peripheral blood samples were purchased from All Cells. CML samples were obtained from consenting patients at the University of California San Diego, Stanford University, the University of Toronto Health Network, MD Anderson and the University of Bologna according to Institutional Review Board approved protocols. CD34<sup>+</sup> cells were initially purified by magnetic bead separation (MACS; Miltenyi, Bergisch Gladbach, Germany) followed by FACS progenitor purification using human-specific CD34 and CD38 antibodies as previously described<sup>33,40</sup>. Peripheral blood mononuclear cells (PBMC) were extracted from peripheral blood following Ficoll density centrifugation, CD34<sup>+</sup> selected, stained with fluorescent conjugated antibodies, and analyzed and purified and analyzed using a FACS Aria and Flowjo software as described previously<sup>33,40</sup>.

### **2.4.2. Quantitative RT-PCR**

20,000-50,000 hematopoietic progenitor cells were sorted from the indicated cell populations using FACS Aria, total RNA was isolated and cDNA was synthesized as described previously<sup>33,40</sup>. Quantitative PCR (qRT-PCR) was performed in duplicate on an iCycler using SYBR GreenER Super Mix (Life Technologies, Carlsbad, California), 5ng of template mRNA and 0.4mM

of each forward and reverse primer. Splice isoform-specific primers were designed for *BCL2*, *MCL1*, *BCLX*, and *BFL1* and isoform specificity was confirmed by sequencing of each PCR product. The following primers were used:

*BCL2<sub>L</sub>* Forward: atgtgtgtggagagcgtcaa

*BCL2<sub>L</sub>* Reverse: tcagagacagccaggagaaa

*MCL1<sub>L</sub>* Forward: agacctacgacgggttg

*MCL1<sub>L</sub>* Reverse: aatcctgccccagtttgta

*MCL1<sub>S</sub>* Forward: gaggaggacgagttgtaccg

*MCL1<sub>S</sub>* Reverse: actccacaacccatccttg

*BCLX<sub>L</sub>* Forward: catggcagcagtaaagcaag

*BCLX<sub>L</sub>* Reverse: gaaggagaaaaaggccacaa

*BFL1<sub>L</sub>* Forward: gctgggaaaatggctttg

*BFL1<sub>L</sub>* Reverse: tcagaaaaattaggccggttt

*BCR-ABL* Forward: ctccagactgtccacagcat

*BCR-ABL* Reverse: ccctgaggctcaaagtcaga

*HPRT* Forward: cgtcttgctcgagatgtgatg

*HPRT* Reverse: ttatagcccccttgagcac

mRNA levels for each transcript were normalized to HPRT and compared using the delta-delta CT method<sup>256</sup>.

### 2.4.3. Transcriptome sequencing and analysis

50,000 normal and BC CML progenitor cells were sorted directly into RLT buffer as described above. For each sample, approximately 100ng of total RNA was treated using a RiboMinus standard protocol (Life Technologies, #K155002). The SOLiD™ Total RNA-Seq kit (Applied Biosystems, #4445374) was used to prepare libraries. Samples were run on SOLiD v.3 plus instruments with a target read number of > 50 million 50bp unpaired reads/sample.

We used a two-pass procedure to first remove mouse-derived RNA-seq reads and to remove adapter sequence within RNA-seq reads. In the first pass, we aligned all reads to the mm9 and hg19 mouse and human genome reference sequences using v0.12.7 of bowtie. We disregarded from further analysis any reads that aligned to the mouse genome with fewer mismatches and any reads that mapped to tRNA or rRNA genes or to the mitochondrion. Unmapped reads were subjected to SOLiD P1 and P2 adapter trimming with v1.0 of the cutadapt program. In the second pass, the adapter-trimmed sequences were re-filtered against the mouse genome and tRNA, rRNA, and mitochondrion as in pass one. The hg19-aligned sequences from pass one and pass two and the unmapped reads from pass two were combined into one set of sequences. We aligned this pooled set of sequences to the hg19 RefSeq transcriptome using v0.6.4f of bfast+bwa bwaln in three steps, where in steps two and three the unaligned reads from the previous step were 3' trimmed by 5bp. We converted the transcriptome alignment coordinates of

each aligned read to hg19 genome coordinates using a custom script (Barrett and Frazer 2012, unpublished). Finally, we used these coordinate-converted reads and the RefSeq isoform models as input to v1.0.3 of the cuffdiff program from the Cufflinks software suite to compute differential expression.

#### **2.4.4. BCL2 and MCL1 FACS-protein analyses**

Normal, CP CML and BC CML CD34<sup>+</sup> selected cells were stained with lineage antibodies and progenitor antibodies as described previously<sup>33,40</sup>, and fixed with 0.8% paraformaldehyde (PFA) for 10 min. Fixed cells were washed and stained overnight with a FITC-conjugated mouse monoclonal antibody specific for human BCL2 (Dako, #F7053) or isotype-control antibody diluted in 0.15% Saponin (TCI America). For MCL1 analysis, cells were stained with a monoclonal rabbit antibody specific for human MCL1 (Abcam #ab32087)<sup>257</sup> or isotype-control antibody conjugated to alexa-405 (Zenon kit, Life Technologies). The next day, cells were washed and analyzed using a FACS Aria and Flowjo software. Mean fluorescence intensity (MFI) for BCL2 and MCL1 was measured for each CML sample<sup>257,258</sup> and normalized to a normal cord blood control sample in the same experiment.

#### **2.4.5. *In vivo* analyses**

Immunocompromised RAG2<sup>-/-</sup>y<sub>c</sub><sup>-/-</sup> mice were bred and maintained in the University of California San Diego Moores Cancer Center vivarium.

Neonatal mice were transplanted intrahepatically with 50,000-200,000 CD34<sup>+</sup> cells according to our previously published methods<sup>33,40</sup>. Transplanted mice were screened for tumor formation or human engraftment in peripheral blood by FACS at 6-8 weeks post-transplant. Upon detection of tumors, peripheral blood engraftment, or at 8-12 weeks post-transplant engrafted mice were treated for 2 weeks with dasatinib (daily, 50mg/kg/day in 50% PEG, 50% PBS by oral gavage), sabutoclax (3 days per week, 5mg/kg/day in 10% EtOH, 10% Cremaphor EL (Sigma Aldrich) 80% PBS by IP injection), or drug vehicles. Twenty-four hours post-treatment (10-14 weeks post-transplant), mice were euthanized and single cell suspensions of hematopoietic tissues were analyzed for human engraftment by FACS as described previously<sup>33,40</sup>. For *in vivo* combination studies, dasatinib was used at 25 or 50mg/kg while sabutoclax was used at 1.25 or 2.5mg/kg with the same dosing regimen described above. For serial transplantation, whole mouse bone marrows were pooled from mice in the same treatment group. Total bone marrow cells were counted using Guava ViaCount Reagent and analysis on a Guava PCA system (Millipore) and transplanted in equal numbers into secondary neonatal recipients by intrahepatic injection. 250,000-500,000 whole bone marrow cells per mouse were transplanted.

#### **2.4.6. DiR staining and measurement by FACS**

50,000 CD34<sup>+</sup> CML cells were isolated as described previously and stained with 4mg/mL DiR (Life Technologies) in PBS according to the manufacturer's specifications. DiR stained cells were then washed and transplanted into neonatal mice. After 18 weeks, mice were sacrificed and hematopoietic tissues were analyzed by FACS for human DiR<sup>+</sup> cells. DiR MFI was measured in human CD38<sup>+</sup>lin<sup>-</sup>PI<sup>-</sup> cells engrafted in each tissue.

#### **2.4.7. FACS cell cycle analysis**

Single cell suspensions of bone marrow cells from mice treated with sabutoclax or vehicle were immunostained with Alexa405-conjugated anti-human CD45 (Life Technologies), Alexa647-anti-human CD38 (AbD Serotec) and biotin-anti-human CD34 (Life Technologies) plus Alexa488-streptavidin (Life Technologies) in 2% fetal bovine serum/ PBS- followed by live cell staining using the LIVE/DEAD® Fixable Near-IR Dead Cell Stain Kit (Life Technologies). Surface-stained cells were fixed in 70% ethanol overnight. Fixed, surface-stained cells were immunostained with PE-conjugated anti-Ki-67 (BD Biosciences) in 0.15% saponin/ 2% fetal bovine serum/ PBS-, washed twice in saponin-containing staining media and incubated with 7-AAD (Life Technologies, 10µg/mL in 0.1M sodium citrate/ 5mM EDTA pH8.0/ 0.15M NaCl/ 0.5% BSA/ 0.02% saponin). Stained samples were analyzed using a MACSQuant (Miltenyi Biotec) and FlowJo software.

#### **2.4.8. Bone marrow IHC and IF**

For IHC, femurs were harvested from transplanted, treated animals, fixed and decalcified in Cal-Ex II (Fisher Scientific, Fair Lawn, NJ) for 48 hrs, followed by standard tissue processing, paraffin-embedding and sectioning. Paraffin tissue sections were deparaffinized, rehydrated, and boiled in antigen retrieval solution (BD, California) (pH 6.0) for 10 min to retrieve antigen. Tissues were blocked with 5% bovine serum albumin (BSA) and 0.25% Triton X-100 in PBS for 30 min and incubated with primary antibody in PBS with 1% BSA at 4 °C for 16 h. Primary antibodies used were human CD45 (Abcam) and Ki-67 (BD). IHC staining was then carried out with LSAB System-HRP Kit (Dako Cytomation, Hamburg, Germany) according to manufacturer's protocol using methyl green (Sigma Aldrich) as counterstaining. Omission of primary antibodies was used as a negative control and showed no staining. All sections were mounted before examination using a Nikon Eclipse E600 microscope.

For IF, femurs were fixed in 4% PFA (EMS, Hatfield, PA) for 1 hour, decalcified in 0.23M EDTA pH 7.0 for 4 days by changing the decalcifying solution twice daily, dehydrated in 30% sucrose and frozen in OCT. For immunostaining, cryoprotected tissue was sectioned at 10mm, washed with PBS<sup>-</sup>, fixed with 4% PFA for 10 minutes and rinsed with PBS<sup>-</sup>. Sections were incubated with 5% normal donkey serum/0.2% Triton X-100 for 1 hour at room temperature followed by incubation with primary antibodies overnight at 4°C. Mouse antibodies were used with MOM kit (Vector, Burlingame, CA). Mouse



antibodies were used with MOM kit (Vector, Burlingame, CA). Primary antibodies used were anti-phospho-histone H3, Ser10 (1:500, Cell Signaling, Inc.), anti-human Ki-67 (1:300, Spring Bioscience), anti-human CD34 (1:250, BD Biosciences), Alexa 647-conjugated anti-human CD38 (1:25, Serotec) and FITC-conjugated anti human BCL2 (1:25, Dako). Slides were washed in PBS and incubated with secondary antibody (Alexa 594-conjugated donkey anti-mouse or rabbit, Invitrogen) for 1 hour at room temperature. Stained sections were mounted using Prolong® Gold antifade with DAPI (Invitrogen). Epifluorescent images were acquired using confocal microscopy (Zeiss LSM510 or Olympus Fluoview FV10i) and Adobe Photoshop CS5.

Quantification of phospho-histone H3 was performed as follows: first, the endosteum was defined as the region within 50 $\mu$ m (approximately 5 cell-widths) from the edge of the marrow. The area of this 50 $\mu$ m-wide strip and the area of the remaining marrow tissue were then measured using Image-J software. Finally, the number of phospho-histone H3 positive cells in each region was counted and the frequency of these cells was calculated as the number of positive cells per area of tissue.

For apoptosis analysis, bone marrows were stained using the ApopTag fluorescein *in situ* TUNEL apoptosis detection kit (Chemicon, #S7110) following the manufacturer's protocol. Sections were mounted as above. Images were acquired using an Applied Imaging Ariol SL-50 automated scanning microscope and image analysis system.

#### **2.4.9. Nanofluidic phospho-proteomic immunoassay**

NPI experiments were performed with the Nanopro 1000 instrument (Cell Biosciences) and all samples were run in triplicate at least. Briefly, for each capillary analysis, 4nl of 10mg/mL lysate was diluted to 0.2 mg/mL in 200nl HNG (20mM HEPES pH 7.5, 25mM NaCl, 0.1%, 10% glycerol, Sigma Phosphatase Inhibitor Cocktail 1 diluted 1:100 and Calbiochem Protease Inhibitor diluted 1:100). 200nl sample mix containing internal pl standards was added. The Firefly system first performed a charge-based separation (isoelectric focusing) in a 5-cm-long, 100-micron-inner-diameter capillary. Predicted pls were calculated with Scansite. Each sample was run on a panel of different pH gradients (pH 3–10 and pH 2–11) to optimize the resolution of different peak patterns. After separation and photo-activated in-capillary immobilization, CRKL was detected using CRKL-specific antibody (Cell Signaling Technology). B2-microglubulin antibody (Upstate) was used to normalize the amount of loaded protein. Phosphorylation peaks were quantified by manually selecting the start and end of each peak and a flat baseline and calculating the area under the curve (AUC). The NPI data was normalized to B2M by dividing the measured peak area for the protein of interest by the measured peak area for B2M.

#### **2.4.10. RT-PCR apoptosis array**

FACS-sorted progenitors cells were analyzed using OpenArray "nanoplate" technology (Life Technologies). Briefly, 20,000 progenitor cells were sorted from the bone marrow and spleen of BC engrafted mice into lysis buffer (Cell-to-Ct kit, Life Technologies) followed by DNase treatment and reverse transcription reaction. 20ul of cDNA was pre-amplified for 12 cycles with a pool of gene-specific Taqman assays spotted on Taqman Apoptosis OpenArray. The diluted (1:20) pre-amplified cDNA (1.5ul) was mixed with GeneFast Taqman PCR mix (3.5ul) (Life Technologies, Inc) and dispensed into the OpenArray plate. Twenty-four cDNA samples were tested simultaneously per OpenArray plate. Real-time PCR occurred in a computer-controlled imagin NT OpenArray thermal cycler. The amplification curves for each through-hole in the array were constructed from collected images, from which cycle threshold ( $C_T$ ) was computed and used for further data analysis. Gene levels were normalized to the geometric mean of *RPLPO*, *ACTB*, *PPIA*, *PGK1* and *B2M* and compared using the delta-delta CT method.

#### **2.4.11. Bone marrow BCL2 and MCL1 IHC analysis**

Bone specimens were fixed and mildly decalcified in Bouin's solution (Sigma-Aldrich, St. Louis, MO) for 8 h at room temperature, then postfixed in zinc-containing buffered formalin (Z-Fix; Anatech Ltd., Battle Creek, MI) for 3 days at +4°C, and embedded in paraffin. Dewaxed tissue sections (4–5µm)

were immunostained as previously reported<sup>259</sup> using mouse monoclonal antibody to CD34 (Dako Cytomation, Carpinteria, CA) and rabbit polyclonal BCL2 and MCL1 antibodies raised in the Reed laboratory against synthetic peptides<sup>260,261</sup>. The slides were scanned at an absolute magnification of 400× (resolution of 0.25 µm/pixel (100,000 pix/in.)) using the Aperio ScanScope CS system (Aperio Technologies, Vista, CA). The Spectrum Analysis algorithm package and ImageScope analysis software (version 9; Aperio Technologies, Inc.) were applied to quantify IHC stainings<sup>262</sup>.

#### **2.4.12. SL/M2 co-culture**

The mouse bone marrow stromal cell lines M2-10B4 (M2) and SL/SL (SL) were provided by StemCell Technologies on behalf of Dr. Donna Hogge in the Terry Fox Laboratory (Vancouver, British Columbia) and maintained according to previously published methods<sup>247</sup>. One day prior to co-culture, the cell lines were treated with mitomycin-C (1mg/mL for 3 hours) and plated in a 1:1 mixture at a total concentration of 100,000/mL. 10,000-20,000 CD34<sup>+</sup> CML or normal cells were plated on top of the adherent SL/M2 cells, cultured for 1-4 weeks in Myelocult H5100 media (StemCell Technologies) and the frequency of live human progenitor cells was quantified by FACS.

#### **2.4.13. Competitive peptide displacement assays**

Briefly, 20nM of GST-BCL2 proteins were incubated with sabutoclax

or ABT-737 at various concentrations for 5 minutes at room temperature in PBS. 15nM FITC-Bim BH3 peptide (FITC-Ahx-DMRPEIWIAQELRRIGDEFNAYYAR) was added and fluorescence polarization was measured after 10 minutes as described previously<sup>205</sup>. EC<sub>50</sub> determinations were generated by fitting the experimental data using a sigmoidal dose-response nonlinear regression model.

#### **2.4.14. *In vitro* drug treatment and apoptosis analysis**

Cultures of CD34<sup>+</sup> CML and normal cells were maintained alone in Stempro media (Invitrogen) or on SL/M2 stroma as described above. One day after plating, cultured cells were treated with different concentrations of sabutoclax diluted in DMSO. After 1 week of culture, live CD45<sup>+</sup>CD34<sup>+</sup>CD38<sup>+</sup>lin<sup>-</sup> cells were quantified by FACS analysis. For analysis of apoptosis, treated cells were harvested after 24 hours and analyzed for activated caspase-3 by FACS using the NucView-488 assay (Biotium, Hayward, California) according to the manufacturer's specifications. Best-fit lines and IC<sub>50</sub> determinations were generated by fitting the experimental data using a sigmoidal dose-response nonlinear regression model with vehicle controls set at 1nM to facilitate plotting the data on a log-scale.

#### **2.4.15. Colony assays**

Following *in vitro* culture in Stempro media or with SL/M2 stroma, human cells were harvested, counted by trypan blue exclusion or by using Guava ViaCount Reagent and analysis on a Guava PCA system (Millipore), and 100-200 cells were plated per well of a 24-well plate in Methocult media (Stemcell Technologies). After 2 weeks, total colonies were counted.

#### **2.4.16. Lentivirus transduction**

SMARTVector 2.0 lentiviral particles containing shRNA specific to human BCL2 and control shRNA were purchased from Thermo-Dharmacon (Lafayette, Colorado, #SK-003307). shBCL2 lentiviruses were tested by transduction of 293T cells and K562 cells and knockdown of ~50% of BCL2 transcripts was confirmed by qRT-PCR on the transduced cells. Transduction was then performed on FACS-sorted CD34<sup>+</sup>CD38<sup>+</sup>lin<sup>-</sup>PI<sup>-</sup> CML and normal cells using our previously published methods<sup>33</sup>. shBCL2 and shControl transduced cells were FACS-sorted into Methocult media (20-50 cells per well of a 96-well plate, 5-10 wells per condition) and total colonies were counted for each condition after 2 weeks of culture.

#### **2.4.17. *Ex vivo* drug treatment**

Neonatal mice were transplanted with 100,00 CD34<sup>+</sup> BC cells and were treated with 5mg/kg sabutoclax (n=3) or vehicle (n=3) starting at 8 weeks

post-transplant as previously described. After 72 hours of treatment the mice were sacrificed, bone marrow was harvested, and progenitors were FACS-sorted from each individual mouse. 10,000-20,000 sorted progenitors from the individual mice were then distributed per well onto confluent SL/M2 stroma in 24-well plates and treated with increasing doses of dasatinib for 1 week. After the 1-week treatment the co-cultures were harvested and analyzed for live BC progenitor cells by FACS as described above.

#### **2.4.18. Statistical analysis**

Statistical analyses were performed with the aid of Microsoft Excel, SAS version 9.2 and Graphpad Prism software and are indicated in the figure legends.

Chapter 2, in part, has been submitted to Nature Medicine for publication. Daniel J. Goff, Angela Court-Recart, Alice Y. Shih, Anil Sadarangani, Christian L. Barrett, Hye-Jung Chun, Maryla Krajewska, Heather Leu, Jun Wei, Dayong Zhai, Ifat Geron, Qingfei Jiang, Ryan Chuang, Larisa Balaian, Jason Gotlib, Mark Minden, Giovanni Martinelli, Annelie E. Schairer, Wenxue Ma, Jessica Rusert, Kim-Hien Dao, Kamran Shazand, John D. McPherson, Peggy Wentworth, Christina A. M. Jamieson, Sheldon R. Morris, Lawrence S.B. Goldstein, Thomas J. Hudson, Marco Marra, Kelly A. Frazer, Kristen M. Smith, Maurizio Pellecchia, John C. Reed, and Catriona H.M. Jamieson. "Niche targeting of human blast crisis leukemia stem cells with a novel pan-BCL2 inhibitor." The dissertation author is the primary investigator and author of the manuscript.



### 3. Conclusions and future studies

Cancer prevention, diagnosis and treatment have undoubtedly improved over the last 30 years. However, despite our best efforts, many cancers remain incurable and relapse continues to be a huge clinical problem. Recent advances in cell sorting and methods for assaying tumorigenic cells *in vivo* have led to the discovery of putative CSC in many malignancies. These cells are believed to be directly responsible for cancer recurrence because they can survive treatment and re-proliferate to form a new tumor. While traditional therapies can delay recurrence, they are not curative because they do not specifically target the CSC population. Development of curative therapies for these malignancies will therefore require an understanding of how CSC evade current treatment regimens so that they may be better and more specifically targeted.

CML is a relatively rare cancer but represents an important tool for studying CSC-driven malignancy. Because the genetic cause of CML is well understood and its cellular origin has been phenotypically characterized, CML LSC can be readily quantified and purified for molecular analyses. In addition, because the disease progresses through distinguishable stages that can be modeled *in vivo*, CML affords an opportunity to study how CSC evolve over time. Because CML LSC are characteristically resistant to therapy, the study of these cells can shed light on the molecular mechanisms that contribute to CSC survival and cancer relapse. These studies may in turn lead

to novel therapeutic approaches for efficiently and specifically eliminating CML LSC and potentially CSC in general.

Our recent studies of CML identify aberrant BCL2 family gene expression as an important mediator of LSC survival and therapy-resistance. By analysis of BCL2 family mRNA and protein in functionally-defined and FACS-purified LSC derived from primary CML patients we demonstrate that pro-survival BCL2 family genes are globally upregulated in BC LSC and that increased expression of these genes is a hallmark of disease progression. Furthermore, we show that pro-survival BCL2 expression is induced by supportive microenvironments, such as the bone marrow, and correlates with niche-specific quiescence and TKI protection. Consistent with these findings, we demonstrate that sabutoclax, a novel pan-BCL2 inhibitor, can kill BC LSC in protective microenvironments. Moreover, sabutoclax is more effective against LSC than normal progenitor cells. Finally, we show that sabutoclax can sensitize bone marrow niche-LSC to TKI-mediated cell death, and in combination with dasatinib, significantly delays disease relapse in secondarily transplanted mice.

Overall our results suggest that pro-survival BCL2 proteins are important molecular targets for eliminating CML LSC. At the same time, these results raise several questions about the role of BCL2 family gene expression in CML development and progression. It also remains to be determined exactly how BCL2 family expression increases in BC LSC. While our results suggest that BCL2 expression mediates niche-dependent TKI resistance,

there are likely other mechanisms that also contribute to resistance in the marrow environment. Finally, our findings are potentially clinically significant because they suggest that a BCL2 inhibitor may be useful in conjunction with standard treatments for CML. This may be especially relevant for the treatment of patients with advanced disease who do not typically respond to TKIs alone. However, despite these obvious clinical implications, further preclinical studies will be necessary to optimize the therapeutic effect of combination treatment. More work must also be done to determine how best to identify candidates for treatment and how best to monitor treatment efficacy. Together, this information may allow for BCL2 targeting strategies to be more broadly translated to the treatment of other CSC-driven malignancies.

### **3.1. Exploring further the role of individual BCL2 family genes in CML**

#### **LSC survival and maintenance**

Our *in vitro* studies using sabutoclax, ABT-737 and shRNA demonstrate clearly that clonogenic BC CML cells rely on BCL2 for their survival. This has been further echoed by Mak and colleagues who show that ABT-737 can target CD34<sup>+</sup> CML cells *in vitro*<sup>254</sup>. However, we also show that primary CML LSC simultaneously express 5 different pro-survival BCL2 family genes (BCL2, MCL1, BCLX, BFL1, BCLW - Figure 2.3 and 2.8). This, together with the fact that sabutoclax more potently inhibits LSC than ABT-737 (Table 2.3), suggests that other pro-survival genes besides BCL2 are also important

mediators of LSC survival. These data raise important questions regarding the role of individual BCL2 family genes in LSC: are only some genes functionally significant while others are just bystanders? Or, do all pro-survival BCL2 family genes contribute equally to CML LSC survival? What about TKI-resistance?

In addition to their role in inducing apoptosis resistance, BCL2 family genes may also contribute to other stem cell functions, such as self-renewal, quiescence and differentiation. MCL1, for example, has been previously shown to be required for normal HSC self-renewal rather than survival<sup>257</sup>. Likewise, forced BCL2 expression maintains embryonic stem cell self-renewal in the absence of feeder cells<sup>263</sup>. BCL2 and BCLX have also been linked with quiescence, as overexpression of these genes lengthens G<sub>1</sub> and promotes entry into the G<sub>0</sub> phase of the cell cycle<sup>264-266</sup>. Consistent with these data, we show that quiescence induction in CML LSC occurs in parallel with enrichment of BCL2 family-expressing cells (Figure 2.20). However, whether MCL1 and other BCL2 family genes directly contribute to CML LSC self-renewal and quiescence has not yet been elucidated. Moreover, if BCL2 family genes do contribute to these functions in LSC, are they simply redundant or do they each play a unique role in the biology of CML LSC?

Whereas expression of BCL2 genes may promote stem cell maintenance, loss could contribute to differentiation. Evidence for this comes from experiments performed in our lab using apogossypol, a lower potency pan-BCL2 inhibitor. In these experiments, apogossypol treatment led to a dose-dependent enrichment of lineage positive cells both *in vitro* and *in vivo*

(Figure 3.1a-c, e). There was also a shift in the frequency of myeloid progenitors from CMP to GMP, a more differentiated progenitor subtype (Figure 3.1d). Both effects were specific to apogossypol and were not observed when cells were treated with dasatinib (Figure 3.1e). These results suggest that loss of BCL2 family function may induce LSC differentiation. Furthermore, that these same effects were not observed with sabutoclax suggests that the degree of BCL2 inhibition may determine whether the response is apoptosis or differentiation induction. However, if apogossypol truly does induce differentiation is it predominantly by inhibition of one BCL2 family gene or many at the same time?

To begin to answer these questions we have put together a library of shRNAs that target the different pro-survival BCL2 family genes. Using this library, it will hopefully be possible to determine the relative importance of each gene for LSC survival, as well as other stem cell functions such as self-renewal, quiescence and differentiation. Furthermore, the relative importance of the different genes in mediating TKI-resistance can be assayed by challenging cultured LSC with dasatinib following shRNA knockdown. Sequential knockdown of the BCL2 family genes can also be used to determine which are necessary for LSC survival, engraftment and TKI-resistance *in vivo*.

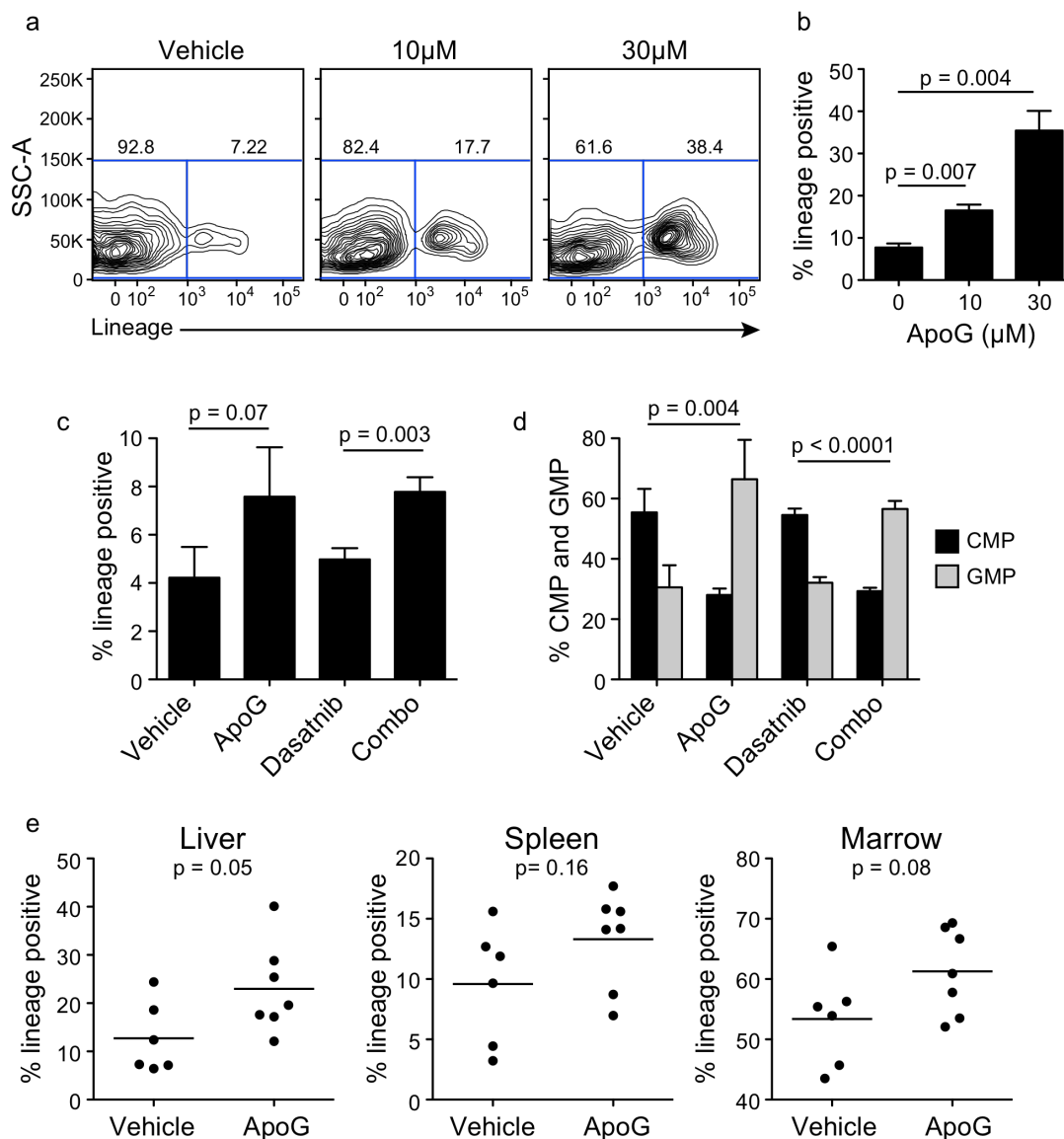


**Figure 3.1. Apogossypol treatment induces "differentiation" of blast crisis progenitors.** **a)** Representative FACS plots of vehicle and apogossypol treated blast crisis cells cultured *in vitro*. **b)** Quantification of lineage positive blast crisis cells following treatment with either vehicle or two different doses of apogossypol. Graph shows a representative experiment; n=3 replicate wells per condition. **c,d)** Quantification of lineage positive cells, CMP and GMP following treatment with vehicle, apogossypol, dasatinib and both drugs in combination. Both graphs show a representative experiment; n=3 replicate wells per condition. **e)** Quantification of lineage positive cells engrafted in the liver, spleen and marrow of blast crisis transplanted mice following treatment with vehicle (n=6 mice) and apogossypol (60mg/kg, n=6 mice). All statistical analyses are by unpaired t-test.

### 3.2. The role of BCL2 family genes in CML progression

In addition to the above questions, there is still much that needs to be established concerning the role of BCL2 family genes in CML progression. Our data demonstrate that pro-survival BCL2 family gene expression is increased in blast crisis myeloid progenitors compared to those in chronic phase. However, the question remains: does this increased expression cause progression or is it simply a result of progression?

Evidence for a causative role has come from studies of transgenic overexpression of BCL2 and BCR-ABL in murine HSC. In these experiments, BCR-ABL alone induced chronic phase CML, but was not sufficient to trigger blast crisis. However, the addition of BCL2 led to the development of blast crisis-like acute leukemia<sup>223</sup>. Mechanistically, how might BCL2 contribute to the oncogenic effects of BCR-ABL? The most likely explanation is that it compensates for BCR-ABL-mediated activation of cell-death pathways. This effect has been demonstrated, for example, in MYC-driven leukemia, which is greatly enhanced by co-expression of any of the pro-survival BCL2 family genes<sup>181</sup>. Similarly, over-activation of self-renewal pathways such as WNT/ $\beta$ -catenin is toxic and depletes the stem cell population<sup>267</sup> unless it occurs in the background of BCL2 overexpression<sup>127</sup>. Despite these data, a causative role for most of the pro-survival BCL2 family genes has not yet been described for CML progression. To address this we are assembling a library of overexpression vectors for each gene that can be tested alongside BCR-ABL

(Figure 3.2a-c). Using these vectors it will be possible to test and compare the potency of the different BCL2 family genes in promoting BCR-ABL-mediated leukemogenesis. Furthermore, the importance of these genes for blast crisis LSC development can be tested by forcing overexpression in chronic phase progenitors and measuring colony formation, replating and transplantation potential.

At this point we have performed preliminary experiments on BCL2 overexpression in normal cord blood and chronic phase CML CD34<sup>+</sup> cells. In these experiments BCL2 overexpression alone had no effect on overall colony numbers in either sample type (Figure 3.2d). However, there was a trend toward increased replating efficiency in both types of progenitor cells upon overexpression of BCL2 (Figure 3.2e). Intriguingly, other experiments in our lab have recently demonstrated that forced overexpression of BCR-ABL actually decreases the self-renewal of normal CD34<sup>+</sup> cells both *in vitro* and *in vivo* (Angela Court-Recart and Jessica Ruser, unpublished data). An implication of these results is that BCR-ABL expression must occur in concert with some other factor(s) in order to induce transformation of normal progenitors. Whether BCL2 is this factor can be tested by co-overexpression of BCR-ABL together with BCL2. Going forward, it would also be interesting to test whether and to what extent the other BCL2 family genes may protect against BCR-ABL-mediated reduction in self-renewal.



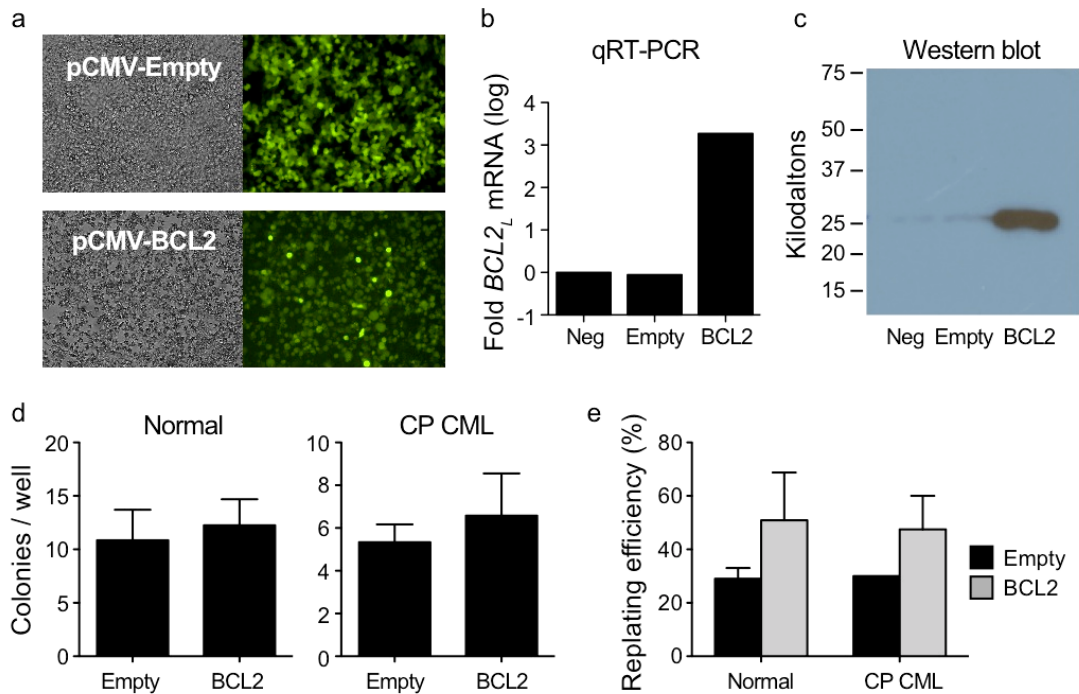


**Figure 3.2.** Effects of BCL2 overexpression on normal and chronic phase progenitor colony formation and replating: **a)** Representative bright-field and fluorescence images of empty vector and pCMV-BCL2 transfected HEK293T cells. **b)** Relative BCL2<sub>L</sub> mRNA expression in empty vector and pCMV-BCL2 transfected HEK293T cells compared to untransfected control cells. **c)** Western blot analysis of BCL2 protein in empty vector and pCMV-BCL2 transfected HEK293T cells. **d)** Number of colonies per well formed by normal and CP CML progenitors following transduction with pCMV-BCL2 and empty vector control lentivirus. **e)** Replating efficiency of normal and CP CML colonies following transduction with pCMV-BCL2 and empty vector control lentivirus. Panel **d** and **e** show mean  $\pm$  SEM for 2 independent experiments.

### 3.3. Mechanisms of BCL2 family upregulation in BC LSC

Our data clearly show that pro-survival BCL2 genes are globally upregulated in the progenitor population with CML progression. However, the exact mechanism for their increased expression remains unclear. One possibility is that GMP, which are enriched in blast crisis, normally express more of these genes than other myeloid progenitors. In this case increased expression would simply reflect expansion of the GMP population. To investigate this possibility, we measured BCL2 protein levels in different progenitor populations using intracellular FACS. This analysis demonstrated that CD123<sup>+</sup> cells (GMP/CMP) express similar amounts of BCL2 protein as CD123<sup>-</sup> cells (MEP) in the same sample (Figure 3.3a). Moreover, we observed the same trends for increased BCL2 expression in both the stem and progenitor populations (Figure 3.3b), and BCL2 protein expression was ~1.5-2 fold increased in blast crisis GMP/CMP (CD34<sup>+</sup>CD38<sup>+</sup>CD123<sup>+</sup>) specifically (Figure 3.3c). Together these data suggest that increased BCL2 protein in blast crisis reflects changes in gene expression within individual stem and progenitor cells rather than just enrichment of the GMP population.

How might intracellular BCL2 family expression increase in CML progenitors over time? Our data show that BCL2 and MCL1 protein and mRNA levels are increased in CP versus BC progenitors to a similar degree (Figure 2.3 and 2.6). This suggests that changes in expression are due to increased transcription. BCR-ABL would be the most obvious candidate for

causing these changes because it is upregulated in blast crisis LSC (Figure 2.3) and has been previously shown to transcriptionally regulate pro-survival BCL2 family genes<sup>183-185</sup>. However, correlation analysis between BCR-ABL and the BCL2 family demonstrated that only BCLX<sub>L</sub> expression was closely linked to BCR-ABL levels in these cells (Figure 2.5). While we cannot rule out that increased BCR-ABL activity may account for the observed changes, these data suggest that increased BCL2 family expression is independent of BCR-ABL. Numerous other oncogenic signaling pathways transcriptionally regulate the BCL2 family. Many of these are activated in LSC and may promote CML progression including the WNT/ $\beta$ -catenin<sup>34,42,43</sup>, JAK-STAT (Angela Court-Recart et al., manuscript in preparation) and Sonic-Hedgehog<sup>129</sup> (Alice Shih et al., manuscript in preparation) signaling pathways. In addition, whole-transcriptome RNA-sequencing analysis suggests that PI3K and RAS signaling is upregulated in blast crisis LSC (Figure A.1). These and our other RNA sequencing results must still be validated, but for now suggest that increased expression of BCL2 family genes is the result of complex redundancy and overlap between many activated signaling pathways. The actual pattern of these pathways is likely patient-specific, which could account for the heterogeneity of BCL2 family expression observed in primary patient samples.

In addition to increased transcription, CML progression could also be associated with changes in BCL2 family protein modifications. Many of the pathways described above, for example, also affect BCL2 family protein

stability and activity by phosphorylation<sup>164</sup>. One potentially interesting regulator of the BCL2 family is GSK3 $\beta$ , a kinase downstream of WNT and PI3K that is differentially spliced in blast crisis LSC<sup>34</sup>. While GSK3 $\beta$  is known to modulate MCL1 stability<sup>224,268</sup>, whether this enzyme also regulates other BCL2 family proteins has not been reported. There have also been no reports as to how GSK3 $\beta$  may affect BCL2 expression in CML LSC. In preliminary experiments, we have observed that overexpression of full-length GSK3 $\beta$  decreases BCL2 protein levels in LSC (Figure 3.4). However, this effect is diminished when the splice variant is used. These data suggest that GSK3 $\beta$  mis-splicing may contribute to blast crisis LSC function by upregulation of BCL2. Whether this is due to changes in protein stability, similar to the regulation of MCL1, remains to be determined. Nevertheless, altered GSK3 $\beta$  splicing represents a potential novel mechanism for increased BCL2 expression in CML LSC. In addition to investigating this pathway, we are also exploring whether BCL2 phosphorylation patterns may be globally altered in LSC. To do this, we are developing methods to quantify different BCL2 protein modifications using a nano-fluidics proteomics assay (Figure 3.5).

Finally, there are several unexplored mechanisms that could account for increased BCL2 family expression in blast crisis LSC. For example, genetic instability could lead to chromosomal duplications that affect BCL2 family genes. Instability could also lead to point mutations in promoters or coding regions of these genes that could affect transcription or mRNA stability. At the epigenome level there is evidence that CML progression is associated with

chromatin remodeling and altered methylation<sup>269,270</sup>. These epigenetic changes could directly affect BCL2 family genes or could lead to loss of suppressors such as miRNAs<sup>271</sup>, some of which are known to regulate BCL2 family expression<sup>162</sup>. To explore some of these mechanisms we are currently performing full-exome sequencing as well as copy number variation (CNV) analysis on FACS-sorted CML progenitors. Analysis of miRNAs using an expression-array could also be used to identify which miRNAs may be differentially expressed with CML progression, while methylation changes could be assayed by whole-genome bi-sulfite sequencing. However, for the time being it is unknown whether any of these mechanisms contribute to changes in BCL2 family expression in CML LSC.

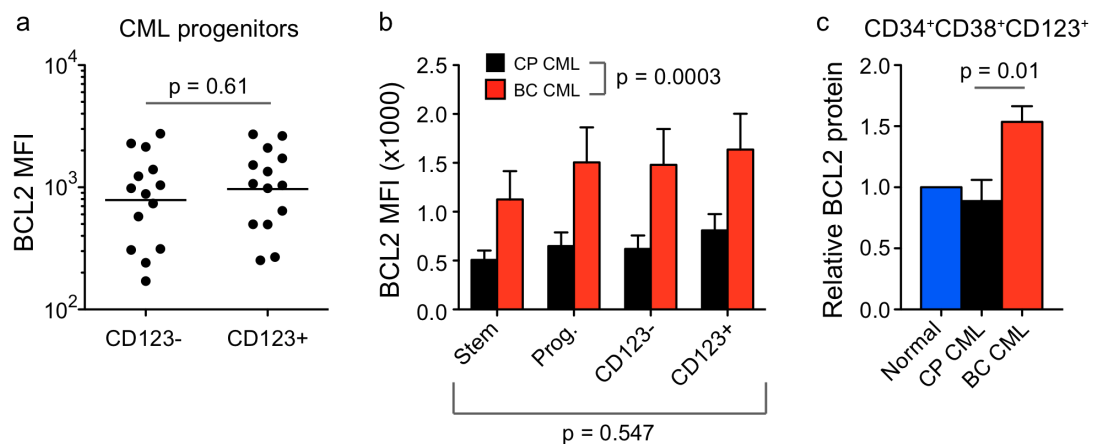


**Figure 3.3.** *BCL2* protein expression in different primitive populations: **a)** BCL2 mean fluorescence intensity (MFI) of CD123<sup>-</sup> and CD123<sup>+</sup> progenitor fractions of 13 primary CML samples. Graph shows median with statistical analysis by Mann Whitney test. **b)** BCL2 MFI of stem (CD34<sup>+</sup>CD38<sup>-</sup>), progenitor (CD34<sup>+</sup>CD38<sup>+</sup>), CD123<sup>-</sup> progenitor and CD123<sup>+</sup> progenitor cells in primary CP (n=6) and BC (n=7) samples. Graph shows mean +/- SEM. Statistical analyses are by 2-way ANOVA. **c)** Relative BCL2 protein expression in CD123<sup>+</sup> progenitors from CP (n=6) and BC (n=7) samples versus that in normal samples (n=6). Graph shows mean +/- SEM. Statistical analysis is by unpaired t-test.

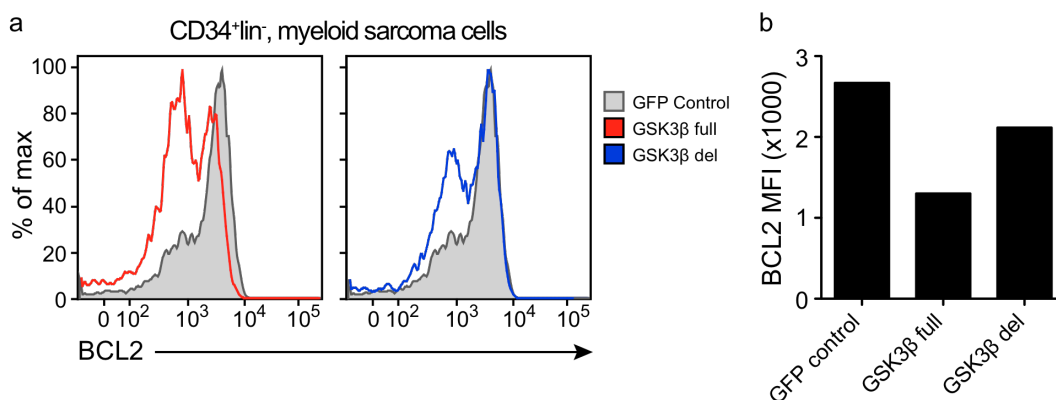


**Figure 3.4.** A novel deletion variant of GSK3 $\beta$  has impaired ability to downregulate BCL2 protein expression. **a)** Representative FACS plots showing BCL2 expression in CD34<sup>+</sup> myeloid sarcoma cells following transduction with GSK3 $\beta$ -full length and GSK3 $\beta$ -deletion encoding lentiviruses compared to control lentivirus<sup>34</sup>. **b)** BCL2 MFI in control versus GSK3 $\beta$ -full length and -deletion transduced CD34<sup>+</sup> myeloid sarcoma cells.

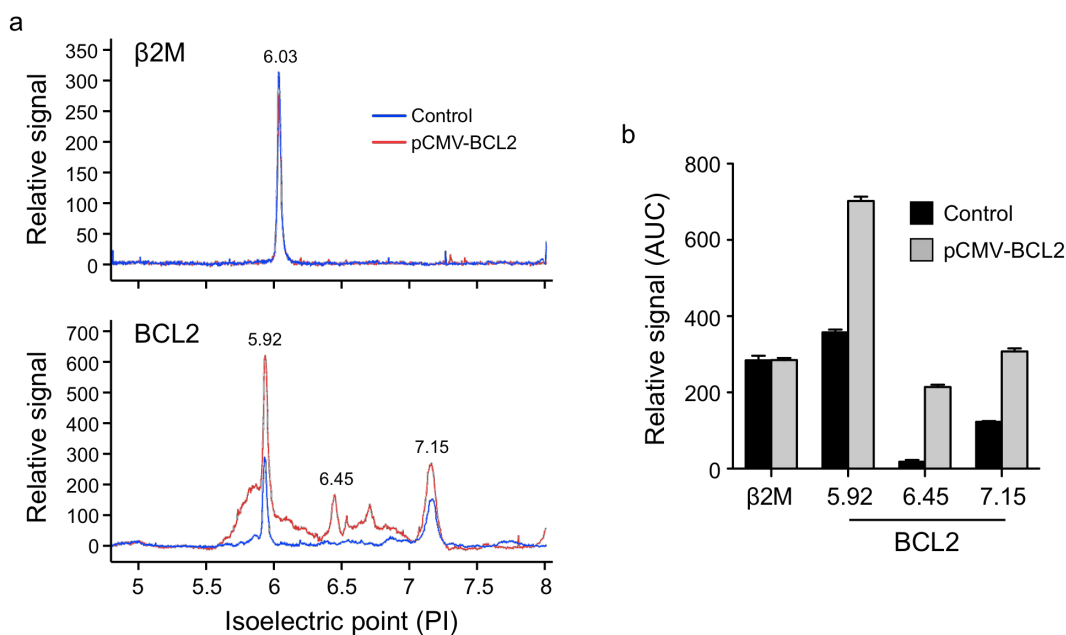


**Figure 3.5.** BCL2 protein variants can be detected and quantified using nanofluidic-proteomic analysis. **a)** Representative traces of BCL2 signal in control and pCMV-BCL2 transfected HEK293T cells. **b)** Quantification of  $\beta$ 2M and different BCL2 protein peaks in control versus pCMV-BCL2 transfected HEK293T cells. Graph shows mean  $\pm$  SEM for 3 replicate readings per condition.

### 3.4. The role of the niche in regulating LSC survival

One of our most important findings is that the marrow niche can regulate CML LSC sensitivity to TKI-treatment. Specifically, our data show that LSC engrafted in the bone marrow are highly resistant to dasatinib while those in other hematopoietic niches (liver, spleen, blood, and tumor) are sensitive (Figure 2.12). Because the BCL2 family has been previously linked to TKI-resistance in CML<sup>191</sup>, we investigated whether these genes play a role in niche-mediated LSC resistance in our xenograft models. Using qRT-PCR and immunohistochemical analysis, we show that bone marrow LSC express multiple pro-survival BCL2 family genes. Bone marrow LSC also have increased expression of BCL2 mRNA and protein, and decreased expression of several pro-death BH3-only genes (Figure 2.18 and 2.19). Thus bone marrow TKI-resistance is correlated with a shift in the balance of BCL2 family gene expression that favors a more pro-survival phenotype. Consistent with these data, bone marrow TKI-resistance is reduced by co-treatment with a pan-BCL2 inhibitor. Together these results indicate that the marrow niche mediates TKI-resistance, in part, by regulation of BCL2 family genes. However, these data also raise some important questions: 1) By what mechanisms does the niche modulate BCL2 family expression in LSC? 2) Could niche resistance be explained by other mechanisms as well? 3) Which, if any, of these mechanisms might play a role in the bone marrow of actual CML patients?

Niche-mediated changes in BCL2 expression could result from several different mechanisms. The most obvious possibilities are factors secreted or expressed on the surface of stromal cells within the niche. Cytokines such as IL-3, GM-CSF and SCF, for example, are known to exert their pro-survival effects via induction of BCL2 family genes<sup>153,154,272</sup>. These soluble factors have also been shown to mediate resistance to BCR-ABL inhibition via upregulation of genes such as BCLX<sub>L</sub> and MCL1<sup>192</sup>. Our data demonstrate that these pathways are active in CML LSC because co-culture on SL/M2 stromal cells, which secrete several cytokines<sup>247</sup>, leads to induction of multiple BCL2 family genes *in vitro* (Figure 2.24a). In addition to soluble factors, adhesion molecules are known regulators of BCL2 family genes. Among these are integrins that induce transcription of BCL2 via RAS, PI3K-AKT and ERK-dependent pathways<sup>273-275</sup>. Integrins also contribute to contact-dependent protection of leukemia cells from chemotherapeutic drugs<sup>276</sup>. Likewise, adherence to bone marrow fibronectin via VLA-4 promotes leukemia cell survival by activation of PI3K and downstream BCL2<sup>277</sup>. CXCR4, an inflammatory chemokine receptor, plays an interesting role in mediating cross talk between cytokine- and adherence-dependent survival. This receptor is upregulated in response to soluble factors from the marrow microenvironment. CXCR4 signaling in turn induces expression of integrins that promote survival as described above. This signaling cascade may be especially important for drug-resistance in CML because it is activated in response to TKIs and appears to trigger LSC homing to the bone marrow niche<sup>278</sup>. Overall, these



data suggest that marrow-induced BCL2 expression in our models may be the product of both cytokine- and adhesion-dependent signaling. To investigate which exact mechanisms are at work, we are in the process of analyzing CML LSC sorted from bone marrow versus spleen by RNA sequencing. We are also comparing marrow LSC before and after dasatinib-treatment, and marrow-engrafted LSC to the same phenotypic cells pre-transplant (Figure 3.6 - progenitors and 3.7 - stem cells). In addition to these analyses it would be informative to know precisely which cytokines are active in the bone marrow compared to the other hematopoietic environments of our mouse models.

Other mechanisms could also explain the niche-resistance we observe *in vivo*. One possibility is niche-specific hypoxia. The marrow is a naturally hypoxic environment that has been shown to diminish BCR-ABL protein levels and select for cells resistant to TKIs<sup>279-281</sup>. Hypoxia also induces transcriptional regulators such as HIF-1 $\alpha$ , which enhances CML cell metabolism and appears to be required for survival of LSC<sup>282,283</sup>. However, hypoxia alone may not explain dasatinib-resistance in our models. In these mice, CML cells form myeloid sarcomas that are characterized by disorganized vasculature and large areas of necrosis. These tumors are presumably hypoxic, yet cells in the tumor niche remain very responsive to dasatinib (Figure 2.12d). These data suggest either that hypoxia is not sufficient to drive resistance in this model or that cells in the tumors have a defective hypoxic response. This discrepancy could be resolved by sorting

cells from both the tumor and marrow niches, and comparing the hypoxic responses of each subset in culture.

Another possible mechanism for resistance could be that TKIs do not efficiently penetrate into the marrow niche. Our data suggest that this is probably not the case because marrow LSC have dramatically reduced phosphorylated CRKL levels following dasatinib treatment (Figure 2.14). However, it remains possible that specific zones in the niche may be more or less permissive to TKIs. If so, we would expect resistant LSC to be enriched within specific areas of the marrow. On the other hand, specific patterns of LSC resistance could also be explained by location-specific quiescence induction. In this case the drug adequately reaches the target cells but fails to damage the cells because they are in an inactive state. This mechanism has been demonstrated in AML xenografts. In these models quiescent cells are enriched in the endosteal region, and the pattern of quiescence matches the pattern of drug-resistance<sup>40,41</sup>. Consistent with these results, we observe enrichment of quiescent cells in the endosteal region of our CML-transplanted mice (Figure 2.17). Moreover, both FACS analysis and IHC demonstrate that the percentage of quiescent CML LSC in the marrow greatly increases following dasatinib treatment (Figure 2.16 and 2.17). Despite these data, it is not clear whether the quiescent fraction increases because of selective enrichment of previously non-dividing cells or because of TKI-mediated induction of quiescence in cycling cells. It also remains to be determined whether the patterns of LSC resistance and quiescence overlap within the

endosteal region. Alternatively, resistance and quiescence of CML LSC could correspond with engraftment in other bone marrow niches, such as the perivascular niche<sup>284</sup>. To investigate these different possibilities, we plan to examine the patterns of LSC engraftment and quiescence in the marrow following dasatinib treatment. The fate of quiescent LSC could also be tracked by pre-labeling bone marrow engrafted cells with bromodeoxyuridine (BrdU) prior to treating with dasatinib.

In contrast to the mechanisms described above, a different explanation for our observations could be that the cells engrafted in the marrow and spleen are fundamentally different, and thus have variable intrinsic resistance to TKIs. This would imply that, rather than niche-specific induction of survival pathways, there is instead preferential homing of inherently resistant cells to the marrow. Our data for this is inconclusive at this point. For example, FACS analysis of human cells engrafted in the different hematopoietic niches shows that they are phenotypically indistinguishable in some models, but phenotypically different in others (Figure 3.8). Despite these patient-specific differences, both types of models behave similarly in response to dasatinib -the resistant population is largely restricted to the marrow (Figure 3.9).

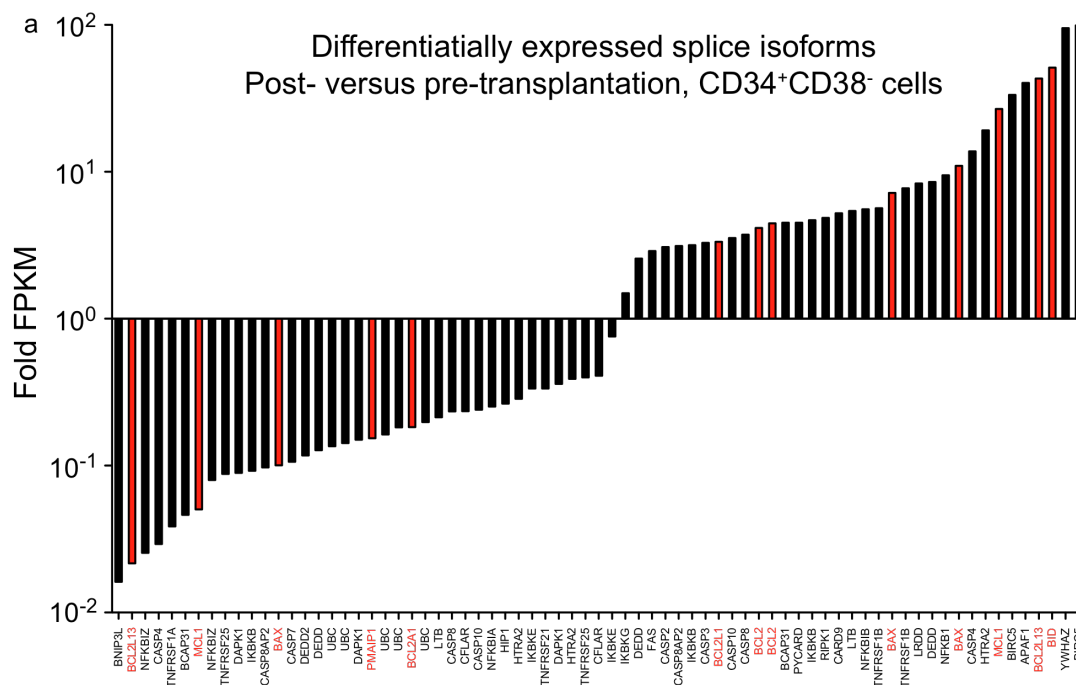
Our phenotypic characterization is admittedly limited and could be improved by the analysis of additional markers. In the end, detailed characterization may reveal that bone marrow engrafted cells are indeed unique compared to those in other niches. At the same time it should be noted

that phenotype is not necessarily static and does not necessarily define the cell's function. For example, melanoma cells differentially express an array of surface markers that can be used to sort sub-populations of marker-positive and -negative cells. However, after separation both sub-populations can re-establish a homeostatic mix of marker-positive and -negative cells, and these surface markers turn out to be useless for selecting tumor-initiating cells from bulk cells. These data demonstrate that, at least in melanoma, surface marker expression is dynamic and fluctuating<sup>22,23</sup>. Based on this we cannot say with certainty that CML cells in the bone marrow are unique just because their surface marker expression is different. It is plausible that CML LSC are abundant in all the hematopoietic niches but simply change their surface marker expression in response to local micro-environmental cues. Ultimately, the only way to distinguish whether LSC are exclusive to one niche would be to test the ability of cells from all niches to serially transplant secondary recipients. On this point we know from experience that cells derived from the different niches can serially transplant CML. Moreover, serially engrafted CML cells can be detected in every hematopoietic tissue following transplant, regardless of the source material. These data suggest that each niche contains similarly functional CML LSC. However, a strict quantitative assessment of the number of LSC residing in each niche has not yet been performed. To make this assessment, limiting dilution assays should be done using identical CML progenitors sorted from each microenvironment. Because of patient heterogeneity, it would also be best if this analysis were done for

every patient independently. This assay would also allow for a qualitative analysis of how the cells from each niche compare with regards to homing and phenotype.

Finally, as a complement to all of the studies discussed above, the role of other survival mechanisms should also be investigated both in primary CML progenitors as well as in the different hematopoietic microenvironments. Our RNA-sequencing data suggest that many novel apoptosis related genes and splice isoforms may be dysregulated in primary (Figure 2.8 and 2.9) and marrow-engrafted BC cells (Figure 3.6 and 3.7). However the relative expression profiles and function of these genes will have to be verified using more traditional assays. In addition, BCL2-dependent and other resistance mechanisms should be confirmed in the marrow of actual CML patients. We propose to do this, in part, by adapting our immunofluorescence and immunohistochemistry assays for use on human marrow sections. Expression analyses could also be performed on phenotypic LSC sorted from the same patient before and after TKI treatment, and comparing blood and bone marrow. In addition to confirming whether the BCL2 family and other genes are expressed in human marrow-resident LSC, these studies may be helpful for establishing the cause of resistance as well as for predicting how best to overcome that resistance in individual patients.





b

Decreased expression post-TP				Increased expression post-TP			
Gene	Isoform	Fold Change (Post/Pre)	p value	Gene	Isoform	Fold Change (Post/Pre)	p value
BNIP3L	uc010luh.1	0.016	4.08E-06	BIRC5	uc002jvf.2	99.17	2.17E-04
BCL2L13	uc002zmz.2	0.022	2.93E-06	YWHAZ	uc003yiw.2	95.11	8.54E-05
NFKBIZ	uc010hpo.2	0.026	8.25E-05	TFRC	uc003fwa.3	61.75	7.91E-05
CASP4	uc010ruv.1	0.029	7.69E-04	BID	uc002znd.1	51.19	1.21E-04
TNFRSF1A	uc010sev.1	0.039	1.15E-04	BCL2L13	uc002zmv.2	43.20	8.67E-05
BCAP31	uc011myy.1	0.046	2.53E-04	APAF1	uc001tgc.2	40.27	5.63E-05
MCL1	uc010pch.1	0.050	3.96E-11	BIRC5	uc002jvg.2	33.41	8.96E-11
NFKBIZ	uc003dvp.2	0.080	4.29E-09	MCL1	uc001eva.2	26.77	2.66E-04
TNFRSF25	uc001ang.2	0.088	4.93E-03	HTRA2	uc002smn.1	19.18	6.08E-04
DAPK1	uc004app.2	0.089	6.01E-04	CASP4	uc001pib.1	13.80	2.05E-03

**Figure 3.7.** Engraftment in the bone marrow niche alters the expression of several *BCL2* family and other apoptosis genes in BC stem cells. **a)** Fold change of significantly differentially expressed splice isoforms in bone marrow engrafted BC stem cells (CD34<sup>+</sup>CD38<sup>-</sup> cells) versus pre-transplantation stem cells. *BCL2* family isoforms are highlighted in red. **b)** Summary of the top-10 splice isoforms with decreased and increased expression in BC stem cells following engraftment in the marrow.

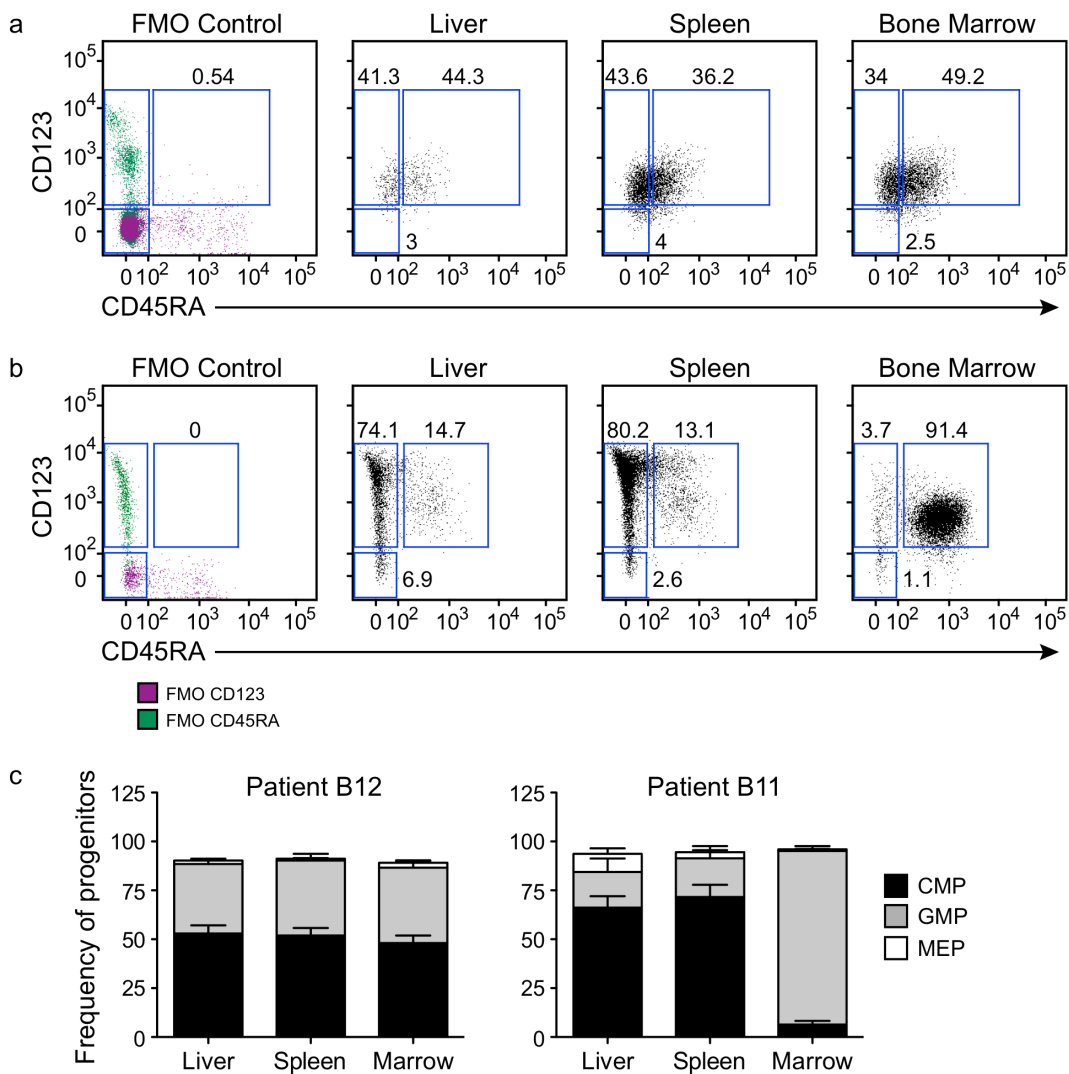


**Figure 3.8.** The phenotype of engrafted BC CML progenitors is either niche-independent or niche-dependent, depending on the patient sample. **a)** Representative FACS plots showing the phenotype of human progenitor cells engrafted in the liver, spleen and bone marrow of BC transplanted mice. The top row shows patient B12 while the bottom row shows patient B11. Gating is also shown for FMO controls (far left column). **b)** Quantification of phenotypic CMP, GMP and MEP engrafted in the liver, spleen and marrow of mice transplanted with patient B12 (n=8 mice) or patient B11 (n=6 mice)-derived progenitors. Graphs show mean  $\pm$  SEM.



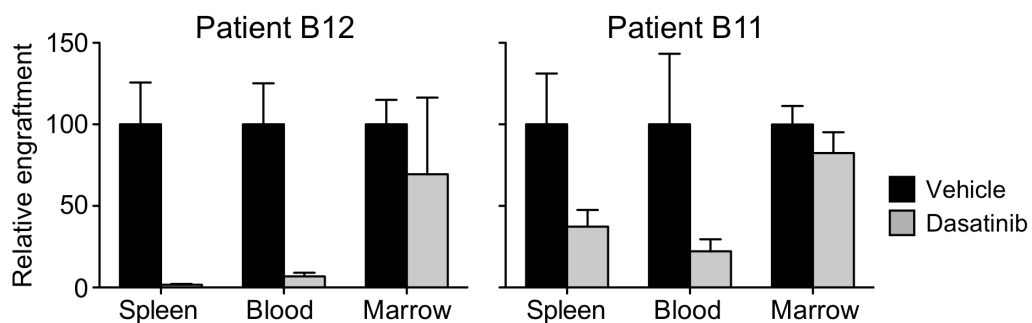


**Figure 3.9.** Bone marrow engrafted BC CML progenitors are consistently resistant to dasatinib regardless of the patient sample. Relative tissue engraftment of CD45<sup>+</sup> CD34<sup>+</sup>CD38<sup>+</sup> BC cells derived from two different patients following treatment with vehicle (n=5 and n=4 respectively) and dasatinib (25mg/kg, n=5 and n=4 respectively). Both graphs show mean +/- SEM. All values are normalized to vehicle treatment.

### 3.5. Optimizing BCL2 family inhibition for targeting BC LSC

As described in chapter 2.2.6, we tested two different sub-therapeutic doses of sabutoclax (1.25mg/kg and 2.5mg/kg) in combination with dasatinib *in vivo*. This strategy was useful because it helped to better resolve the differences between single agent and combination treatment. Our data clearly demonstrate a therapeutic benefit from the combination and show that the benefit is dose-dependent. This result is especially apparent in the serial transplant experiments where low dose combination treatment delays relapse by ~1-2 weeks, while high dose combination treatment delays relapse by ~1 month (Figure 2.31). However, at the doses we tested LSC were not completely eliminated, because mice serially transplanted with combination-treated marrow eventually succumbed to leukemia (Figure 3.10). Obviously, the next step will be to optimize the doses of both drugs in an attempt to eliminate all possible LSC. Unfortunately, sabutoclax and combination toxicity is also likely to become a significant issue.

In our hands, 5mg/kg sabutoclax was the maximally tolerable dose for a 2 week, 3 doses per week, IP-dosing regimen. At this dose, sabutoclax toxicity was manifest by local inflammation at the site of IP injection along with moderate wasting and weight loss due to diarrhea (Figure 3.11a-b). In most cases these effects improved over time as the mice adjusted to dosing. However, at higher doses toxicity was much more pronounced and irreversible. Higher doses also induced significant intestinal and fat necrosis

that was observed upon necropsy. While 5mg/kg sabutoclax was tolerated, the addition of 50mg/kg dasatinib was poorly tolerated and led to the re-emergence of profound gut toxicity. Histological analysis of mice treated with these doses of sabutoclax and dasatinib showed marked shortening and destruction of the intestinal villi. While villi damage was apparent with sabutoclax alone, it was greatly exaggerated by the addition of dasatinib (Figure 3.11c). This toxicity was lessened but still significant at 2.5mg/kg sabutoclax (which is why there were few primary mice treated at this dose). Toxicity was minimal when the doses of both drugs were halved (final dose: 1.25mg/kg sabutoclax and 25mg/kg dasatinib, figure 2.31a-b). These data suggest that, in addition to a combined therapeutic effect, sabutoclax and dasatinib have a combined toxicity profile. This of course has serious ramifications for the potential to translate sabutoclax to clinical use. However, improvements in sabutoclax formulation and dosing may largely alleviate these problems.

Recent experiments have demonstrated that sabutoclax may be more efficacious and less toxic when administered intravenously (IV). In our hands, 10-20mg/kg single agent sabutoclax was tolerated using IV dosing, albeit with some weight loss. Moreover, at 5-10mg/kg, sabutoclax could be safely administered in combination with 25mg/kg dasatinib with little toxicity. This suggests that combination toxicity is largely a local effect and can be avoided by systemic administration of the drug. IV dosing has the added advantage of increasing the bioavailability of sabutoclax. Pharmacokinetic studies by our

colleagues at the Burnham Institute have shown that IP administered sabutoclax is only ~20% bioavailable compared to IV administered drug. IV sabutoclax also has a relatively long half-life in plasma (~15 hours) which could allow for less frequent dosing. Together, these data suggest that by switching to an IV dosing regimen we may be able to significantly minimize toxicity and dramatically increase the therapeutic effect of combination treatment. Thus future experiments will focus on optimizing dasatinib/sabutoclax treatment *in vivo* using this modified dosing scheme.

Despite its promise, sabutoclax is not the only BH3 mimetic that could be used to treat LSC. ABT-737 and obatoclax, for example, have also been shown to synergize with other chemotherapeutics to kill cancer cells<sup>207,208,254</sup>. Our data show that sabutoclax is more potent than ABT (Table 2.3), presumably because ABT fails to inhibit MCL1 and BFL1, which we show are expressed in CML LSC (Figure 2.3). However, it is plausible that LSC from some patients may rely exclusively on BCL2. In these cases combination treatment with ABT may be perfectly adequate. This raises the point that genetic profiling of a patient's LSC could be used to predict which BH3 mimetic would be the most efficacious. Along these lines, it would be worthwhile to have a detailed comparison of the efficacy and toxicity profiles of all the different BH3 mimetics against LSC *in vivo*. In the end, these data would ideally assist us in choosing the best BH3 mimetic for a particular patient.

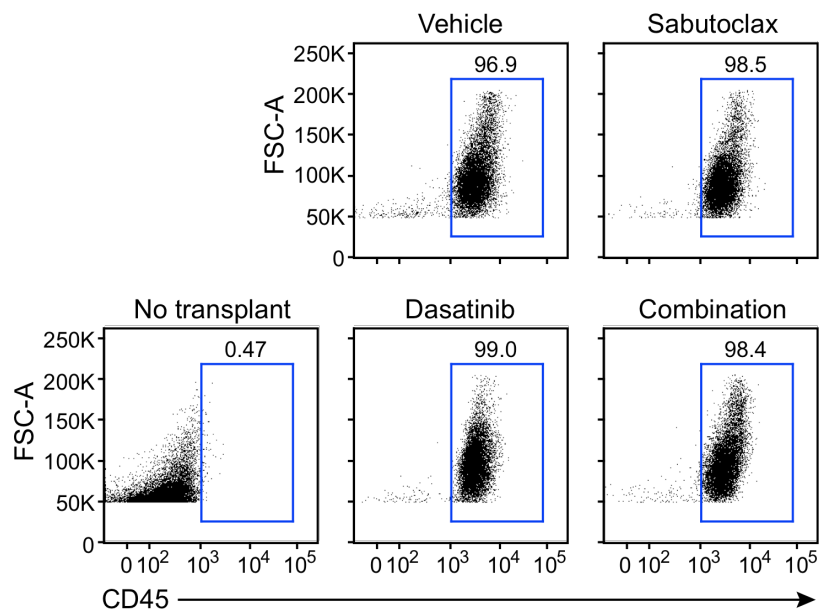


**Figure 3.10.** Mice serially transplanted with treated bone marrow ultimately develop high-level leukemic engraftment. Representative FACS plots of mice serially transplanted with vehicle, sabutoclax, dasatinib and combination-treated whole bone marrow showing engraftment of human CD45<sup>+</sup> cells.

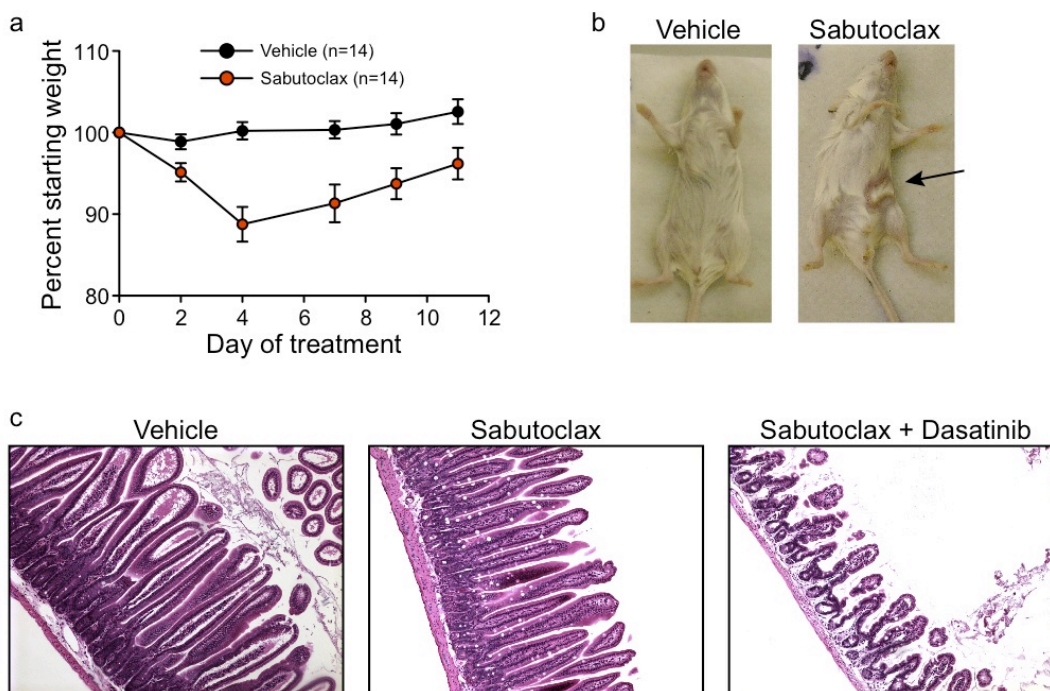


**Figure 3.11. Sabutoclax toxicity in single agent and combination treatment: a)** Change in body weight of mice treated with vehicle (n=14 mice) versus sabutoclax (5mg/kg, n=14 mice). **b)** Local tissue inflammation observed at the site of sabutoclax injection (denoted by the arrow). A vehicle treated control mouse is included for comparison. **c)** H&E stained sections of small intestine harvested from vehicle, sabutoclax (2.5mg/kg) and combination (2.5mg/kg sabutoclax, 50mg/kg dasatinib) treated mice. Note the extensive shortening of the intestinal villi in the combination treated mouse.

### 3.6. Translating BCL2 inhibition to other CSC-driven malignancies

Overall, our studies demonstrate that BCL2 family genes are important mediators of LSC survival in blast crisis CML. We also show that LSC are resistant to standard TKI-treatment and that this resistance is driven in part by engraftment into the bone marrow niche, which induces upregulation of pro-survival BCL2. Importantly, we demonstrate that niche-dependent drug resistance can be overcome by using a pan-BCL2 inhibitor and that targeting of the BCL2 family sensitizes functional LSC to standard therapeutic agents, which they normally evade. Thus our data suggest that BCL2 inhibition may be a cornerstone of combination therapies that can target and eradicate drug-resistant CML LSC. Since CML is a paradigm for CSC-driven malignancy, the next question is whether we can translate this combination approach to treating CSC in other cancers?

BCL2 family genes are expressed by a large variety of hematologic malignancies and solid tumors, and many of these cancers are sensitive to BCL2 family inhibitors, at least *in vitro*<sup>174,181,228</sup>. Moreover, CSC have now been identified in a number of these tumor types<sup>285</sup>. However, a link between BCL2 family expression and CSC function has not yet been established in most malignancies. Chemotherapy resistance and relapse are common themes in cancer, and many of these problems could conceivably depend upon subsets of CSC that express various amounts of pro-survival BCL2 genes. Therefore going forward, it would be interesting to apply our techniques

to survey BCL2 family expression in different CSC-driven cancers, especially those with a high risk of drug-resistance and relapse. Because leukemia cells are readily FACS-sortable, we plan to first extend our analysis into phenotypic LSC from these malignancies, including AML and myelodysplastic syndrome (MDS).

In addition to their importance for the function of CSC, our data suggest that expression of BCL2 family genes may be particularly relevant to protective niches. Presumably, there other CSC-driven cancers where niche-specific BCL2 expression is responsible for increased survival and drug-resistance. We plan to explore this possibility in other xenograft models, such as multiple myeloma, AML and T-ALL, which also engraft various hematopoietic niches. This concept may also extend to the survival of solid tumor CSC in metastatic niches, where cells must endure a harsh transition to a new microenvironment<sup>180</sup>. It would be very interesting to examine to what extent BCL2 family expression plays a role in metastasis and whether metastatic disease may be particularly susceptible to BCL2 inhibition. Along these lines, we have begun investigating pro-survival BCL2 family expression in primary prostate cancer cells xenografted into bone, one of the most common metastatic sites for this disease<sup>286</sup>. In these models, androgen-dependent prostate cancer cells cannot grow in castrated animals if they are transplanted subcutaneously, but readily proliferate when transplanted into the bone marrow (Christina Jamieson, manuscript in preparation). This result indicates that the marrow environment provides a pro-survival stimulus to



these cells that compensates for the lack of androgens. Using qRT-PCR analysis of cells derived from castrated versus intact animals, we observed that castration was associated with significant upregulation of pro-survival BCL2 in bone-engrafted cells (Figure 3.12). These data suggest that the niche induces BCL2 expression, which may in turn promote resistance to the sudden lack of androgens that comes with castration. This raises the possibility of using a BCL2 family antagonist to target bone-metastatic prostate cancer. Interestingly, prostate cancer cells were recently shown to be sensitive to sabutoclax *in vivo*<sup>218</sup>, though it was not shown whether these results extend to androgen-dependent cells or whether sabutoclax may target bone-metastatic prostate cancer cells. It would therefore be interesting to further investigate the role of the BCL2 family in this model and in driving apoptosis-resistance in other metastatic cancers.

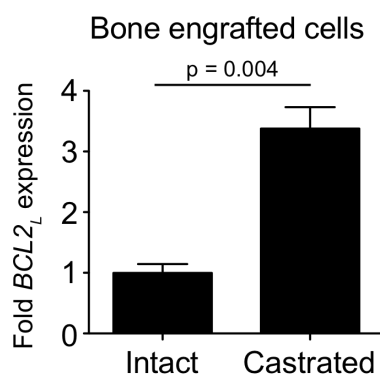


**Figure 3.12.** Pro-survival BCL2 expression is increased in bone marrow engrafted prostate cancer cells following castration. qRT-PCR analysis showing relative BCL2<sub>L</sub> mRNA expression in prostate cancer cells harvested from the bone of intact (n=3) versus castrated (n=3) mice. Graph show mean ± SEM. Statistical analysis is by unpaired t-test.

### 3.7. Summary

The last decades have provided significant advances to the treatment of cancer. Unfortunately, despite an impressive repertoire of therapeutics, cures for most cancers have, tragically, remained elusive. However, there is reason to be optimistic. Many studies have illuminated the role of CSC in driving cancer development and relapse. These studies suggest that by dealing effectively with CSC we may be able to completely eradicate some malignancies. There is thus great interest in uncovering the mechanisms that these cells use to evade treatment. These results may in turn lead directly to the development of therapeutic strategies that can be used to overcome CSC.

Our studies are significant because they demonstrate a role for the BCL2 family in promoting the progression, drug-resistance and relapse of blast crisis CML. Moreover, our data show that these processes are driven by LSC that reside in the protective bone marrow niche, and show that these cells can be effectively targeted with standard therapeutic agents if the BCL2 family is inhibited simultaneously. These results are important not just because of their clinical implications for CML, but because of their potential application to other malignant processes. Whether involved in drug-resistance or metastasis, apoptosis-resistance is a critical recurring theme in cancer. Our data thus provide a platform for using a pan-BCL2 inhibitor as a means to disrupt this resistance in CSC. In a broader sense, this strategy may ultimately prove useful for eliminating CSC in general.

# APPENDIX

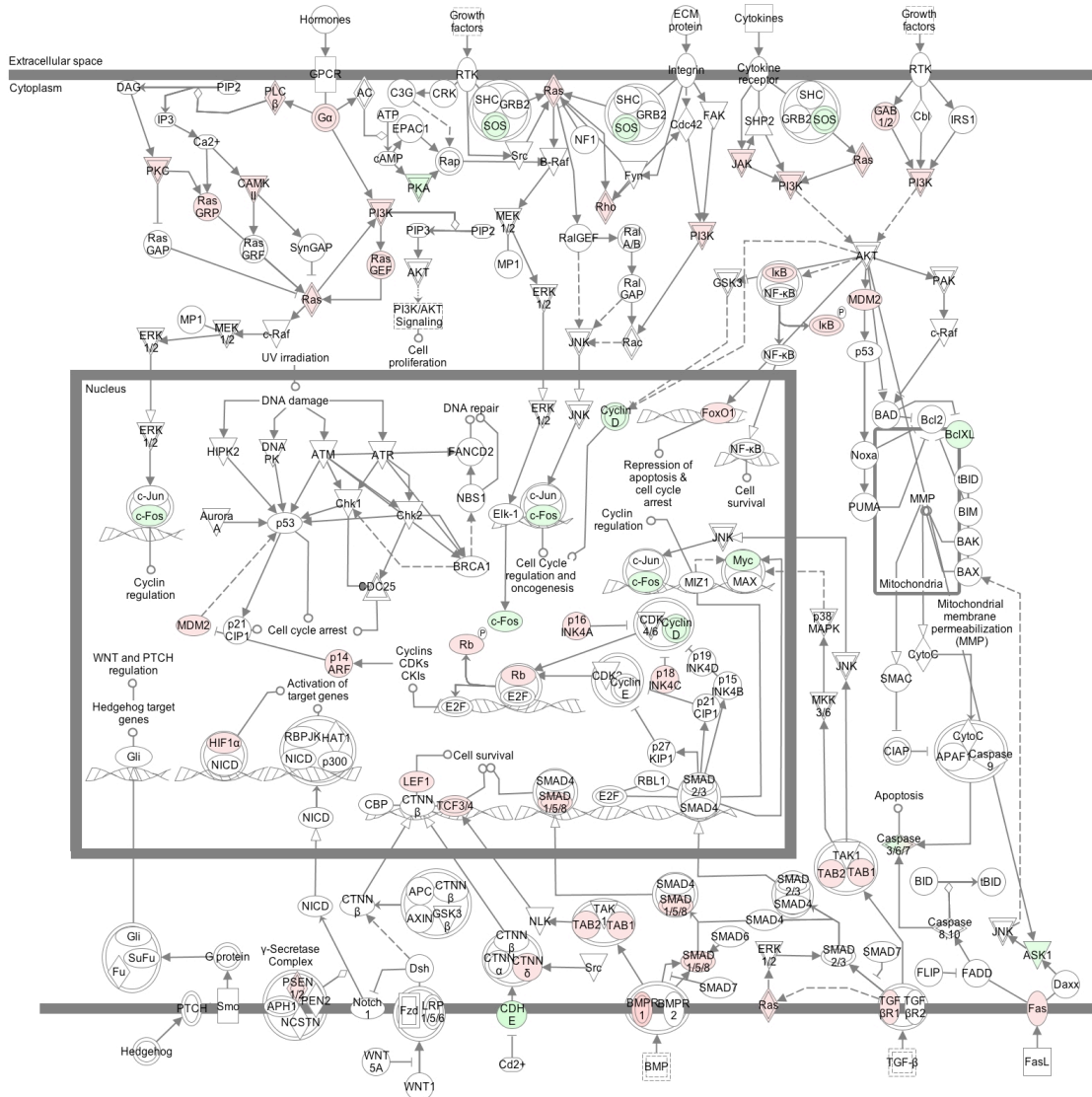


**Figure A.1.** BC progenitors differentially express several genes involved in cancer signaling. Diagram of common signaling pathways involved in cancer and demonstrating genes significantly different in BC (n=5) versus CP (n=7) progenitors. White = no change; Red = significantly increased expression; Green = significantly decreased expression.

**Table A.1.** Apoptosis genes significantly differentially expressed in normal versus BC progenitors

Gene	Expression (FPKM)*		Fold	p value	q value
	Normal mean	BC mean			
ENSG00000150991_UBC	127080	25355	0.20	1.9E-11	1.8E-09
ENSG00000104856_RELB	3745	206	0.05	1.1E-08	6.0E-07
ENSG00000104312_RIPK2	57362	14463	0.25	3.3E-08	1.6E-06
ENSG00000215788_TNFRSF25	911	5732	6.30	2.2E-07	8.6E-06
ENSG00000026103_FAS	650	4204	6.46	9.3E-07	3.0E-05
ENSG00000069399_BCL3	2351	193	0.08	1.7E-06	5.0E-05
ENSG00000169372_CRADD	1275	5350	4.20	2.5E-05	5.2E-04
ENSG00000187796_CARD9	1168	4919	4.21	3.9E-05	7.5E-04
ENSG00000077150_NFKB2	1443	159	0.11	1.5E-04	2.3E-03
ENSG00000023445_BIRC3	7461	2127	0.29	3.6E-04	4.7E-03
ENSG00000141510_TP53	11577	27698	2.39	5.8E-04	6.8E-03
ENSG00000177595_LRDD	1255	4395	3.50	5.9E-04	6.9E-03
ENSG00000162924_REL	17343	6778	0.39	5.9E-04	6.9E-03
ENSG00000132357_CARD6	681	2559	3.76	7.3E-04	8.3E-03
ENSG00000146072_TNFRSF21	10091	3475	0.34	7.8E-04	8.7E-03
ENSG00000167604_NFKBID	3896	1127	0.29	1.0E-03	1.1E-02
ENSG00000164305_CASP3	9787	19813	2.02	2.0E-03	1.8E-02
ENSG00000064012_CASP8	13152	27291	2.08	2.3E-03	2.1E-02
ENSG00000143384_MCL1	17271	8036	0.47	2.4E-03	2.2E-02
ENSG00000100290_BIK	108	696	6.47	2.4E-03	2.2E-02
ENSG00000103490_PYCARD	10232	22817	2.23	3.5E-03	2.8E-02
ENSG00000104765_BNIP3L	54185	28276	0.52	4.3E-03	3.3E-02
ENSG00000146232_NFKBIE	1922	556	0.29	7.5E-03	5.0E-02
ENSG00000102871_TRADD	80	491	6.11	9.3E-03	6.0E-02
ENSG00000173039_RELA	4841	1961	0.41	9.7E-03	6.1E-02
ENSG00000167207_NOD2	71	396	5.58	1.2E-02	7.3E-02
ENSG00000089685_BIRC5	4744	10176	2.15	1.4E-02	8.1E-02
ENSG00000196730_DAPK1	16614	9059	0.55	1.6E-02	8.6E-02

\* FPKM = fragments per kilobase of exon per million fragments mapped

**Table A.2.** Apoptosis genes significantly differentially expressed in normal versus CP progenitors

Gene	Expression (FPKM)*		Fold	p value	q value
	Normal mean	CP mean			
ENSG00000150991_UBC	132886	19622	0.15	8.1E-29	2.8E-26
ENSG00000104312_RIPK2	59966	8332	0.14	6.3E-26	1.7E-23
ENSG00000069399_BCL3	2459	41	0.02	5.1E-20	7.1E-18
ENSG00000141682_PMAIP1	21015	3434	0.16	1.6E-16	1.5E-14
ENSG00000146072_TNFRSF21	10537	1225	0.12	3.3E-16	3.0E-14
ENSG00000162924_REL	18137	2981	0.16	1.5E-15	1.2E-13
ENSG00000028137_TNFRSF1B	6412	603	0.09	6.5E-15	4.9E-13
ENSG00000104856_RELB	3915	241	0.06	1.1E-14	7.8E-13
ENSG00000100906_NFKBIA	39690	10512	0.26	4.6E-12	2.3E-10
ENSG00000023445_BIRC3	7809	1268	0.16	1.1E-10	4.3E-09
ENSG00000149397_HMBS	5186	25069	4.83	1.1E-10	4.3E-09
ENSG00000167604_NFKBID	4073	811	0.20	2.2E-07	4.3E-06
ENSG00000165806_CASP7	6186	1402	0.23	2.7E-07	5.1E-06
ENSG00000215788_TNFRSF25	950	5419	5.70	3.1E-07	5.8E-06
ENSG00000196730_DAPK1	17380	5711	0.33	3.5E-07	6.6E-06
ENSG00000104765_BNIP3L	56696	22887	0.40	5.1E-07	9.0E-06
ENSG00000164305_CASP3	10241	29193	2.85	1.0E-06	1.7E-05
ENSG00000143384_MCL1	18069	6422	0.36	1.4E-06	2.2E-05
ENSG00000144802_NFKBIZ	16269	5915	0.36	1.8E-06	2.8E-05
ENSG00000187796_CARD9	1220	5336	4.37	3.0E-06	4.4E-05
ENSG00000141510_TP53	12095	32727	2.71	1.0E-05	1.3E-04
ENSG00000171552_BCL2L1	2831	9332	3.30	1.2E-05	1.4E-04
ENSG00000146232_NFKBIE	2008	377	0.19	1.8E-05	2.1E-04
ENSG00000137752_CASP1	3761	1001	0.27	2.8E-05	3.0E-04
ENSG00000077150_NFKB2	1507	289	0.19	5.5E-05	5.5E-04

\* FPKM = fragments per kilobase of exon per million fragments mapped

**Table A.2. (continued)** Apoptosis genes significantly differentially expressed in normal versus CP progenitors

Gene	Expression (FPKM)		Fold	p value	q value
	Normal mean	CP mean			
ENSG00000089685_BIRC5	4957	13726	2.77	1.1E-04	9.6E-04
ENSG00000170233_NLRP1	635	103	0.16	5.5E-04	3.9E-03
ENSG00000067182_TNFRSF1A	8584	3650	0.43	5.8E-04	4.1E-03
ENSG00000153094_BCL2L1	406	1752	4.32	8.9E-04	5.9E-03
ENSG00000164924_YWHAZ	76153	43300	0.57	1.1E-03	7.0E-03
ENSG00000173039_RELA	5064	2058	0.41	1.4E-03	8.6E-03
ENSG00000177595_LRDD	1311	3782	2.89	1.7E-03	9.9E-03
ENSG00000118412_CASP8AP2	4152	9645	2.32	2.5E-03	1.4E-02
ENSG00000109320_NFKB1	8001	3726	0.47	2.5E-03	1.4E-02
ENSG00000142208_AKT1	1239	3556	2.87	2.9E-03	1.5E-02
ENSG00000026103_FAS	680	2068	3.04	4.6E-03	2.3E-02
ENSG00000120889_TNFRSF10B	5493	2508	0.46	5.5E-03	2.6E-02
ENSG00000181222_POLR2A	10591	5616	0.53	5.7E-03	2.7E-02
ENSG00000114446_IFT57	14161	8020	0.57	7.9E-03	3.5E-02
ENSG00000104825_NFKBIB	4195	2073	0.49	1.0E-02	4.4E-02
ENSG00000121858_TNFSF10	3448	1504	0.44	1.1E-02	4.4E-02
ENSG00000102871_TRADD	84	461	5.49	1.1E-02	4.6E-02
ENSG00000105221_AKT2	4650	2348	0.50	1.4E-02	5.5E-02
ENSG00000003402_CFLAR	17199	10238	0.60	1.8E-02	6.6E-02
ENSG00000104689_TNFRSF10A	3670	2012	0.55	2.8E-02	9.2E-02

\* FPKM = fragments per kilobase of exon per million fragments mapped

**Table A.3.** Apoptosis genes significantly differentially expressed in CP versus BC progenitors

Gene	Expression (FPKM)*		Fold	p value	q value
	CP mean	BC mean			
ENSG00000028137_TNFRSF1B	628	6288	10.01	1.1E-11	2.7E-10
ENSG00000149397_HMBS	26150	5430	0.21	2.3E-07	3.3E-06
ENSG00000164305_CASP3	30542	6559	0.21	4.1E-07	5.6E-06
ENSG00000100906_NFKBIA	11030	33554	3.04	5.3E-07	7.1E-06
ENSG00000165806_CASP7	1450	6004	4.14	1.3E-05	1.5E-04
ENSG00000169372_CRADD	1911	6528	3.42	3.9E-05	3.9E-04
ENSG00000146072_TNFRSF21	1297	4419	3.41	3.1E-04	2.6E-03
ENSG00000162924_REL	3118	8245	2.64	5.9E-04	4.5E-03
ENSG00000171552_BCL2L1	9835	3333	0.34	1.1E-03	7.8E-03
ENSG00000104312_RIPK2	8728	16355	1.87	9.8E-03	4.8E-02
ENSG00000026103_FAS	2153	4802	2.23	2.1E-02	8.9E-02
ENSG00000103490_PYCARD	15557	26256	1.69	2.3E-02	9.5E-02

\* FPKM = fragments per kilobase of exon per million fragments mapped

## REFERENCES

1. Ries, L.A.G., Melbert, D., Krapcho, M., Stinchcomb, D.G., Howlader, N., Horner, M.J., Mariotto, A., Miller, B.A., Feuer, E.J., Altekruse, S.F., Lewis, D.R., Clegg, L., Eisner, M.P., Reichman, M. & Edwards, B.K. SEER Cancer Statistics Review, 1975-2005. [http://seer.cancer.gov/csr/1975\\_2005/](http://seer.cancer.gov/csr/1975_2005/) (2008).
2. The top 10 causes of death. *World Health Organization*, <http://www.who.int/mediacentre/factsheets/fs310/en/index.html>; Last updated June 2011; Accessed January 2012.
3. Siegel, R., Naishadham, D. & Jemal, A. Cancer statistics, 2012. *CA Cancer J Clin* **62**, 10-29 (2012).
4. Age-Adjusted SEER Incidence Rates. *National Cancer Institute*, <http://seer.cancer.gov/faststats/selections.php?run=runit&output=1&data=1&statistic=1&cancer=1&year=201101&race=201101&sex=201101&series=age&age=201115;201175;201141;201160;201166>; Accessed January 2012.
5. Facts 2012. *Leukemia & Lymphoma Society*, <http://www.lls.org/content/nationalcontent/resourcecenter/freeducationmaterials/generalcancer/pdf/facts.pdf>; Accessed January 2012.
6. Chabner, B.A. & Roberts, T.G., Jr. Timeline: Chemotherapy and the war on cancer. *Nat Rev Cancer* **5**, 65-72 (2005).
7. Aktipis, C.A., Kwan, V.S., Johnson, K.A., Neuberg, S.L. & Maley, C.C. Overlooking evolution: a systematic analysis of cancer relapse and therapeutic resistance research. *PLoS One* **6**, e26100 (2011).
8. Roninson, I.B., Chin, J.E., Choi, K.G., Gros, P., Housman, D.E., Fojo, A., Shen, D.W., Gottesman, M.M. & Pastan, I. Isolation of human mdr DNA sequences amplified in multidrug-resistant KB carcinoma cells. *Proc Natl Acad Sci U S A* **83**, 4538-4542 (1986).
9. Gallo, O., Chiarelli, I., Bianchi, S., Calzolari, A., Simonetti, L. & Porfirio, B. Loss of p53 gene mutation after irradiation is associated with increased aggressiveness in recurring head and neck cancer. *Clin Cancer Res* **2**, 1577-1582 (1996).
10. Yamashita, H., Toyama, T., Nishio, M., Ando, Y., Hamaguchi, M., Zhang, Z., Kobayashi, S., Fujii, Y. & Iwase, H. p53 protein accumulation predicts resistance to endocrine therapy and decreased post-relapse survival in metastatic breast cancer. *Breast Cancer Res* **8**, R48 (2006).



11. Deininger, M. Resistance and relapse with imatinib in CML: causes and consequences. *J Natl Compr Canc Netw* **6 Suppl 2**, S11-S21 (2008).
12. Eyler, C.E. & Rich, J.N. Survival of the fittest: cancer stem cells in therapeutic resistance and angiogenesis. *J Clin Oncol* **26**, 2839-2845 (2008).
13. Kavalierchik, E., Goff, D. & Jamieson, C.H. Chronic myeloid leukemia stem cells. *J Clin Oncol* **26**, 2911-2915 (2008).
14. Pajonk, F., Vlashi, E. & McBride, W.H. Radiation resistance of cancer stem cells: the 4 R's of radiobiology revisited. *Stem Cells* **28**, 639-648 (2010).
15. O'Brien, C.S., Farnie, G., Howell, S.J. & Clarke, R.B. Breast cancer stem cells and their role in resistance to endocrine therapy. *Horm Cancer* **2**, 91-103 (2011).
16. Clarke, M.F., Dick, J.E., Dirks, P.B., Eaves, C.J., Jamieson, C.H., Jones, D.L., Visvader, J., Weissman, I.L. & Wahl, G.M. Cancer stem cells--perspectives on current status and future directions: AACR Workshop on cancer stem cells. *Cancer Res* **66**, 9339-9344 (2006).
17. O'Brien, C.A., Kreso, A. & Jamieson, C.H. Cancer stem cells and self-renewal. *Clin Cancer Res* **16**, 3113-3120 (2010).
18. Visvader, J.E. Cells of origin in cancer. *Nature* **469**, 314-322 (2011).
19. Takebe, N., Harris, P.J., Warren, R.Q. & Ivy, S.P. Targeting cancer stem cells by inhibiting Wnt, Notch, and Hedgehog pathways. *Nat Rev Clin Oncol* **8**, 97-106 (2011).
20. Nowell, P.C. The clonal evolution of tumor cell populations. *Science* **194**, 23-28 (1976).
21. Greaves, M. Cancer stem cells: back to Darwin? *Semin Cancer Biol* **20**, 65-70 (2010).
22. Quintana, E., Shackleton, M., Sabel, M.S., Fullen, D.R., Johnson, T.M. & Morrison, S.J. Efficient tumour formation by single human melanoma cells. *Nature* **456**, 593-598 (2008).
23. Shackleton, M., Quintana, E., Fearon, E.R. & Morrison, S.J. Heterogeneity in cancer: cancer stem cells versus clonal evolution. *Cell* **138**, 822-829 (2009).

24. Lapidot, T., Sirard, C., Vormoor, J., Murdoch, B., Hoang, T., Caceres-Cortes, J., Minden, M., Paterson, B., Caligiuri, M.A. & Dick, J.E. A cell initiating human acute myeloid leukaemia after transplantation into SCID mice. *Nature* **367**, 645-648 (1994).
25. Bonnet, D. & Dick, J.E. Human acute myeloid leukemia is organized as a hierarchy that originates from a primitive hematopoietic cell. *Nat Med* **3**, 730-737 (1997).
26. Nguyen, L.V., Vanner, R., Dirks, P. & Eaves, C.J. Cancer stem cells: an evolving concept. *Nat Rev Cancer* (2012).
27. Reya, T., Morrison, S.J., Clarke, M.F. & Weissman, I.L. Stem cells, cancer, and cancer stem cells. *Nature* **414**, 105-111 (2001).
28. Mintz, B. & Illmensee, K. Normal genetically mosaic mice produced from malignant teratocarcinoma cells. *Proc Natl Acad Sci U S A* **72**, 3585-3589 (1975).
29. Illmensee, K. & Mintz, B. Totipotency and normal differentiation of single teratocarcinoma cells cloned by injection into blastocysts. *Proc Natl Acad Sci U S A* **73**, 549-553 (1976).
30. Fearon, E.R., Burke, P.J., Schiffer, C.A., Zehnbauser, B.A. & Vogelstein, B. Differentiation of leukemia cells to polymorphonuclear leukocytes in patients with acute nonlymphocytic leukemia. *N Engl J Med* **315**, 15-24 (1986).
31. Barabe, F., Kennedy, J.A., Hope, K.J. & Dick, J.E. Modeling the initiation and progression of human acute leukemia in mice. *Science* **316**, 600-604 (2007).
32. Wang, J.C., Lapidot, T., Cashman, J.D., Doedens, M., Addy, L., Sutherland, D.R., Nayar, R., Laraya, P., Minden, M., Keating, A., Eaves, A.C., Eaves, C.J. & Dick, J.E. High level engraftment of NOD/SCID mice by primitive normal and leukemic hematopoietic cells from patients with chronic myeloid leukemia in chronic phase. *Blood* **91**, 2406-2414 (1998).
33. Al-Hajj, M., Wicha, M.S., Benito-Hernandez, A., Morrison, S.J. & Clarke, M.F. Prospective identification of tumorigenic breast cancer cells. *Proc Natl Acad Sci U S A* **100**, 3983-3988 (2003).
34. Abrahamsson, A.E., Geron, I., Gotlib, J., Dao, K.H., Barroga, C.F., Newton, I.G., Giles, F.J., Durocher, J., Creusot, R.S., Karimi, M., Jones, C., Zehnder, J.L., Keating, A., Negrin, R.S., Weissman, I.L. &

- Jamieson, C.H. Glycogen synthase kinase 3beta missplicing contributes to leukemia stem cell generation. *Proc Natl Acad Sci U S A* **106**, 3925-3929 (2009).
35. Rasheed, Z.A., Kowalski, J., Smith, B.D. & Matsui, W. Concise review: Emerging concepts in clinical targeting of cancer stem cells. *Stem Cells* **29**, 883-887 (2011).
  36. Stuart, S.A., Minami, Y. & Wang, J.Y. The CML stem cell: evolution of the progenitor. *Cell Cycle* **8**, 1338-1343 (2009).
  37. Holyoake, T., Jiang, X., Eaves, C. & Eaves, A. Isolation of a highly quiescent subpopulation of primitive leukemic cells in chronic myeloid leukemia. *Blood* **94**, 2056-2064 (1999).
  38. Forsberg, E.C., Passegue, E., Prohaska, S.S., Wagers, A.J., Koeva, M., Stuart, J.M. & Weissman, I.L. Molecular signatures of quiescent, mobilized and leukemia-initiating hematopoietic stem cells. *PLoS One* **5**, e8785 (2010).
  39. Corbin, A.S., Agarwal, A., Loriaux, M., Cortes, J., Deininger, M.W. & Druker, B.J. Human chronic myeloid leukemia stem cells are insensitive to imatinib despite inhibition of BCR-ABL activity. *J Clin Invest* **121**, 396-409 (2011).
  40. Saito, Y., Kitamura, H., Hijikata, A., Tomizawa-Murasawa, M., Tanaka, S., Takagi, S., Uchida, N., Suzuki, N., Sone, A., Najima, Y., Ozawa, H., Wake, A., Taniguchi, S., Shultz, L.D., Ohara, O. & Ishikawa, F. Identification of Therapeutic Targets for Quiescent, Chemotherapy-Resistant Human Leukemia Stem Cells. *Science Translational Medicine* **2**(2010).
  41. Saito, Y., Uchida, N., Tanaka, S., Suzuki, N., Tomizawa-Murasawa, M., Sone, A., Najima, Y., Takagi, S., Aoki, Y., Wake, A., Taniguchi, S., Shultz, L.D. & Ishikawa, F. Induction of cell cycle entry eliminates human leukemia stem cells in a mouse model of AML. *Nat Biotechnol* **28**, 275-280 (2010).
  42. Jamieson, C.H., Ailles, L.E., Dylla, S.J., Muijtjens, M., Jones, C., Zehnder, J.L., Gotlib, J., Li, K., Manz, M.G., Keating, A., Sawyers, C.L. & Weissman, I.L. Granulocyte-macrophage progenitors as candidate leukemic stem cells in blast-crisis CML. *N Engl J Med* **351**, 657-667 (2004).
  43. Minami, Y., Stuart, S.A., Ikawa, T., Jiang, Y., Banno, A., Hunton, I.C., Young, D.J., Naoe, T., Murre, C., Jamieson, C.H. & Wang, J.Y. BCR-

ABL-transformed GMP as myeloid leukemic stem cells. *Proc Natl Acad Sci U S A* **105**, 17967-17972 (2008).

44. Fialkow, P.J., Gartler, S.M. & Yoshida, A. Clonal origin of chronic myelocytic leukemia in man. *Proc Natl Acad Sci U S A* **58**, 1468-1471 (1967).
45. Fialkow, P.J., Jacobson, R.J. & Papayannopoulou, T. Chronic myelocytic leukemia: clonal origin in a stem cell common to the granulocyte, erythrocyte, platelet and monocyte/macrophage. *Am J Med* **63**, 125-130 (1977).
46. Martin, P.J., Najfeld, V., Hansen, J.A., Penfold, G.K., Jacobson, R.J. & Fialkow, P.J. Involvement of the B-lymphoid system in chronic myelogenous leukaemia. *Nature* **287**, 49-50 (1980).
47. Sirard, C., Lapidot, T., Vormoor, J., Cashman, J.D., Doedens, M., Murdoch, B., Jamal, N., Messner, H., Addey, L., Minden, M., Laraya, P., Keating, A., Eaves, A., Lansdorp, P.M., Eaves, C.J. & Dick, J.E. Normal and leukemic SCID-repopulating cells (SRC) coexist in the bone marrow and peripheral blood from CML patients in chronic phase, whereas leukemic SRC are detected in blast crisis. *Blood* **87**, 1539-1548 (1996).
48. Naugler, C.T. Population genetics of cancer cell clones: possible implications of cancer stem cells. *Theor Biol Med Model* **7**, 42 (2010).
49. Williams, R.T., den Besten, W. & Sherr, C.J. Cytokine-dependent imatinib resistance in mouse BCR-ABL+, Arf-null lymphoblastic leukemia. *Genes Dev* **21**, 2283-2287 (2007).
50. Kelly, P.N., Dakic, A., Adams, J.M., Nutt, S.L. & Strasser, A. Tumor growth need not be driven by rare cancer stem cells. *Science* **317**, 337 (2007).
51. Krivtsov, A.V., Twomey, D., Feng, Z., Stubbs, M.C., Wang, Y., Faber, J., Levine, J.E., Wang, J., Hahn, W.C., Gilliland, D.G., Golub, T.R. & Armstrong, S.A. Transformation from committed progenitor to leukaemia stem cell initiated by MLL-AF9. *Nature* **442**, 818-822 (2006).
52. Yahata, T., Ando, K., Sato, T., Miyatake, H., Nakamura, Y., MUGURUMA, Y., Kato, S. & Hotta, T. A highly sensitive strategy for SCID-repopulating cell assay by direct injection of primitive human hematopoietic cells into NOD/SCID mice bone marrow. *Blood* **101**, 2905-2913 (2003).

53. McKenzie, J.L., Gan, O.I., Doedens, M. & Dick, J.E. Human short-term repopulating stem cells are efficiently detected following intrafemoral transplantation into NOD/SCID recipients depleted of CD122+ cells. *Blood* **106**, 1259-1261 (2005).
54. Feuring-Buske, M., Gerhard, B., Cashman, J., Humphries, R.K., Eaves, C.J. & Hogge, D.E. Improved engraftment of human acute myeloid leukemia progenitor cells in beta 2-microglobulin-deficient NOD/SCID mice and in NOD/SCID mice transgenic for human growth factors. *Leukemia* **17**, 760-763 (2003).
55. Kennedy, J.A., Barabe, F., Poepl, A.G., Wang, J.C. & Dick, J.E. Comment on "Tumor growth need not be driven by rare cancer stem cells". *Science* **318**, 1722; author reply 1722 (2007).
56. Singh, S.K., Hawkins, C., Clarke, I.D., Squire, J.A., Bayani, J., Hide, T., Henkelman, R.M., Cusimano, M.D. & Dirks, P.B. Identification of human brain tumour initiating cells. *Nature* **432**, 396-401 (2004).
57. Yuan, X., Curtin, J., Xiong, Y., Liu, G., Waschmann-Hogiu, S., Farkas, D.L., Black, K.L. & Yu, J.S. Isolation of cancer stem cells from adult glioblastoma multiforme. *Oncogene* **23**, 9392-9400 (2004).
58. Eramo, A., Lotti, F., Sette, G., Piloizzi, E., Biffoni, M., Di Virgilio, A., Conticello, C., Ruco, L., Peschle, C. & De Maria, R. Identification and expansion of the tumorigenic lung cancer stem cell population. *Cell Death Differ* **15**, 504-514 (2008).
59. Ponti, D., Costa, A., Zaffaroni, N., Pratesi, G., Petrangolini, G., Coradini, D., Pilotti, S., Pierotti, M.A. & Daidone, M.G. Isolation and in vitro propagation of tumorigenic breast cancer cells with stem/progenitor cell properties. *Cancer Res* **65**, 5506-5511 (2005).
60. O'Brien, C.A., Pollett, A., Gallinger, S. & Dick, J.E. A human colon cancer cell capable of initiating tumour growth in immunodeficient mice. *Nature* **445**, 106-110 (2007).
61. Ricci-Vitiani, L., Lombardi, D.G., Piloizzi, E., Biffoni, M., Todaro, M., Peschle, C. & De Maria, R. Identification and expansion of human colon-cancer-initiating cells. *Nature* **445**, 111-115 (2007).
62. Passegue, E., Jamieson, C.H., Ailles, L.E. & Weissman, I.L. Normal and leukemic hematopoiesis: are leukemias a stem cell disorder or a reacquisition of stem cell characteristics? *Proc Natl Acad Sci U S A* **100 Suppl 1**, 11842-11849 (2003).

63. Kondo, M., Wagers, A.J., Manz, M.G., Prohaska, S.S., Scherer, D.C., Beilhack, G.F., Shizuru, J.A. & Weissman, I.L. Biology of hematopoietic stem cells and progenitors: implications for clinical application. *Annu Rev Immunol* **21**, 759-806 (2003).
64. Steinman, R.A. Cell cycle regulators and hematopoiesis. *Oncogene* **21**, 3403-3413 (2002).
65. Rossi, D.J., Jamieson, C.H. & Weissman, I.L. Stems cells and the pathways to aging and cancer. *Cell* **132**, 681-696 (2008).
66. Krause, D.S. Regulation of hematopoietic stem cell fate. *Oncogene* **21**, 3262-3269 (2002).
67. Orkin, S.H. & Zon, L.I. Hematopoiesis: an evolving paradigm for stem cell biology. *Cell* **132**, 631-644 (2008).
68. Zhu, J. & Emerson, S.G. Hematopoietic cytokines, transcription factors and lineage commitment. *Oncogene* **21**, 3295-3313 (2002).
69. Robb, L. Cytokine receptors and hematopoietic differentiation. *Oncogene* **26**, 6715-6723 (2007).
70. Chateauvieux, S., Grigorakaki, C., Morceau, F., Dicato, M. & Diederich, M. Erythropoietin, erythropoiesis and beyond. *Biochem Pharmacol* **82**, 1291-1303 (2011).
71. Spivak, J.L. Narrative review: Thrombocytosis, polycythemia vera, and JAK2 mutations: The phenotypic mimicry of chronic myeloproliferation. *Ann Intern Med* **152**, 300-306 (2010).
72. Faderl, S., Talpaz, M., Estrov, Z., O'Brien, S., Kurzrock, R. & Kantarjian, H.M. The biology of chronic myeloid leukemia. *N Engl J Med* **341**, 164-172 (1999).
73. Druker, B.J. Translation of the Philadelphia chromosome into therapy for CML. *Blood* **112**, 4808-4817 (2008).
74. Deininger, M.W. Chronic myeloid leukemia: an historical perspective. *Hematology Am Soc Hematol Educ Program*, 418 (2008).
75. Goldman, J.M. Chronic myeloid leukemia: a historical perspective. *Semin Hematol* **47**, 302-311 (2010).
76. Perrotti, D., Jamieson, C., Goldman, J. & Skorski, T. Chronic myeloid leukemia: mechanisms of blastic transformation. *J Clin Invest* **120**, 2254-2264 (2010).

77. Radich, J.P. The Biology of CML blast crisis. *Hematology Am Soc Hematol Educ Program*, 384-391 (2007).
78. Nowell, P.C. & Hungerford, D.A. Chromosome studies on normal and leukemic human leukocytes. *J Natl Cancer Inst* **25**, 85-109 (1960).
79. Rowley, J.D. Letter: A new consistent chromosomal abnormality in chronic myelogenous leukaemia identified by quinacrine fluorescence and Giemsa staining. *Nature* **243**, 290-293 (1973).
80. de Klein, A., van Kessel, A.G., Grosveld, G., Bartram, C.R., Hagemeijer, A., Bootsma, D., Spurr, N.K., Heisterkamp, N., Groffen, J. & Stephenson, J.R. A cellular oncogene is translocated to the Philadelphia chromosome in chronic myelocytic leukaemia. *Nature* **300**, 765-767 (1982).
81. Groffen, J., Stephenson, J.R., Heisterkamp, N., de Klein, A., Bartram, C.R. & Grosveld, G. Philadelphia chromosomal breakpoints are clustered within a limited region, bcr, on chromosome 22. *Cell* **36**, 93-99 (1984).
82. Heisterkamp, N., Stam, K., Groffen, J., de Klein, A. & Grosveld, G. Structural organization of the bcr gene and its role in the Ph' translocation. *Nature* **315**, 758-761 (1985).
83. Shtivelman, E., Lifshitz, B., Gale, R.P. & Canaani, E. Fused transcript of abl and bcr genes in chronic myelogenous leukaemia. *Nature* **315**, 550-554 (1985).
84. Ben-Neriah, Y., Daley, G.Q., Mes-Masson, A.M., Witte, O.N. & Baltimore, D. The chronic myelogenous leukemia-specific P210 protein is the product of the bcr/abl hybrid gene. *Science* **233**, 212-214 (1986).
85. Wang, J.Y., Prywes, R. & Baltimore, D. Structure and function of the Abelson murine leukemia virus transforming gene. *Prog Clin Biol Res* **119**, 57-63 (1983).
86. Wang, J.Y., Ledley, F., Goff, S., Lee, R., Groner, Y. & Baltimore, D. The mouse c-abl locus: molecular cloning and characterization. *Cell* **36**, 349-356 (1984).
87. Konopka, J.B., Watanabe, S.M. & Witte, O.N. An alteration of the human c-abl protein in K562 leukemia cells unmasks associated tyrosine kinase activity. *Cell* **37**, 1035-1042 (1984).

88. Lugo, T.G., Pendergast, A.M., Muller, A.J. & Witte, O.N. Tyrosine kinase activity and transformation potency of bcr-abl oncogene products. *Science* **247**, 1079-1082 (1990).
89. Daley, G.Q., Van Etten, R.A. & Baltimore, D. Induction of chronic myelogenous leukemia in mice by the P210bcr/abl gene of the Philadelphia chromosome. *Science* **247**, 824-830 (1990).
90. Heisterkamp, N., Jenster, G., ten Hoeve, J., Zovich, D., Pattengale, P.K. & Groffen, J. Acute leukaemia in bcr/abl transgenic mice. *Nature* **344**, 251-253 (1990).
91. Deininger, M.W., Goldman, J.M. & Melo, J.V. The molecular biology of chronic myeloid leukemia. *Blood* **96**, 3343-3356 (2000).
92. Kurzrock, R., Gutterman, J.U. & Talpaz, M. The molecular genetics of Philadelphia chromosome-positive leukemias. *N Engl J Med* **319**, 990-998 (1988).
93. Puil, L., Liu, J., Gish, G., Mbamalu, G., Bowtell, D., Pelicci, P.G., Arlinghaus, R. & Pawson, T. Bcr-Abl oncoproteins bind directly to activators of the Ras signalling pathway. *EMBO J* **13**, 764-773 (1994).
94. Melo, J.V. & Barnes, D.J. Chronic myeloid leukaemia as a model of disease evolution in human cancer. *Nat Rev Cancer* **7**, 441-453 (2007).
95. Skorski, T., Kanakaraj, P., Nieborowska-Skorska, M., Ratajczak, M.Z., Wen, S.C., Zon, G., Gewirtz, A.M., Perussia, B. & Calabretta, B. Phosphatidylinositol-3 kinase activity is regulated by BCR/ABL and is required for the growth of Philadelphia chromosome-positive cells. *Blood* **86**, 726-736 (1995).
96. Skorski, T., Bellacosa, A., Nieborowska-Skorska, M., Majewski, M., Martinez, R., Choi, J.K., Trotta, R., Wlodarski, P., Perrotti, D., Chan, T.O., Wasik, M.A., Tsichlis, P.N. & Calabretta, B. Transformation of hematopoietic cells by BCR/ABL requires activation of a PI-3k/Akt-dependent pathway. *EMBO J* **16**, 6151-6161 (1997).
97. Gordon, M.Y., Dowding, C.R., Riley, G.P., Goldman, J.M. & Greaves, M.F. Altered adhesive interactions with marrow stroma of haematopoietic progenitor cells in chronic myeloid leukaemia. *Nature* **328**, 342-344 (1987).
98. Bhatia, R., Wayner, E.A., McGlave, P.B. & Verfaillie, C.M. Interferon-alpha restores normal adhesion of chronic myelogenous leukemia hematopoietic progenitors to bone marrow stroma by correcting



- impaired beta 1 integrin receptor function. *J Clin Invest* **94**, 384-391 (1994).
99. Verfaillie, C.M., Hurley, R., Lundell, B.I., Zhao, C. & Bhatia, R. Integrin-mediated regulation of hematopoiesis: do BCR/ABL-induced defects in integrin function underlie the abnormal circulation and proliferation of CML progenitors? *Acta Haematol* **97**, 40-52 (1997).
  100. Li, S., Ilaria, R.L., Jr., Million, R.P., Daley, G.Q. & Van Etten, R.A. The P190, P210, and P230 forms of the BCR/ABL oncogene induce a similar chronic myeloid leukemia-like syndrome in mice but have different lymphoid leukemogenic activity. *J Exp Med* **189**, 1399-1412 (1999).
  101. Radich, J.P., Dai, H., Mao, M., Oehler, V., Schelter, J., Druker, B., Sawyers, C., Shah, N., Stock, W., Willman, C.L., Friend, S. & Linsley, P.S. Gene expression changes associated with progression and response in chronic myeloid leukemia. *Proc Natl Acad Sci U S A* **103**, 2794-2799 (2006).
  102. Radich, J.P. The biology of chronic myelogenous leukemia progression: who, what, where, and why? *Hematol Oncol Clin North Am* **25**, 967-980, v (2011).
  103. Pavlu, J., Szydlo, R.M., Goldman, J.M. & Apperley, J.F. Three decades of transplantation for chronic myeloid leukemia: what have we learned? *Blood* **117**, 755-763 (2010).
  104. Buckner, C.D., Clift, R.A., Fefer, A., Neiman, P.E., Storb, R. & Thomas, E.D. Treatment of blastic transformation of chronic granulocytic leukemia by high dose cyclophosphamide, total body irradiation and infusion of cryopreserved autologous marrow. *Exp Hematol* **2**, 138-146 (1974).
  105. Talpaz, M., McCredie, K., Kantarjian, H., Trujillo, J., Keating, M. & Gutterman, J. Chronic myelogenous leukaemia: haematological remissions with alpha interferon. *Br J Haematol* **64**, 87-95 (1986).
  106. Druker, B.J., Talpaz, M., Resta, D.J., Peng, B., Buchdunger, E., Ford, J.M., Lydon, N.B., Kantarjian, H., Capdeville, R., Ohno-Jones, S. & Sawyers, C.L. Efficacy and safety of a specific inhibitor of the BCR-ABL tyrosine kinase in chronic myeloid leukemia. *N Engl J Med* **344**, 1031-1037 (2001).
  107. Druker, B.J., Tamura, S., Buchdunger, E., Ohno, S., Segal, G.M., Fanning, S., Zimmermann, J. & Lydon, N.B. Effects of a selective

inhibitor of the Abl tyrosine kinase on the growth of Bcr-Abl positive cells. *Nat Med* **2**, 561-566 (1996).

108. Druker, B.J., Guilhot, F., O'Brien, S.G., Gathmann, I., Kantarjian, H., Gattermann, N., Deininger, M.W., Silver, R.T., Goldman, J.M., Stone, R.M., Cervantes, F., Hochhaus, A., Powell, B.L., Gabilove, J.L., Rousselot, P., Reiffers, J., Cornelissen, J.J., Hughes, T., Agis, H., Fischer, T., Verhoef, G., Shepherd, J., Saglio, G., Gratwohl, A., Nielsen, J.L., Radich, J.P., Simonsson, B., Taylor, K., Baccarani, M., So, C., Letvak, L. & Larson, R.A. Five-year follow-up of patients receiving imatinib for chronic myeloid leukemia. *N Engl J Med* **355**, 2408-2417 (2006).
109. de Lavallade, H., Apperley, J.F., Khorashad, J.S., Milojkovic, D., Reid, A.G., Bua, M., Szydlo, R., Olavarria, E., Kaeda, J., Goldman, J.M. & Marin, D. Imatinib for newly diagnosed patients with chronic myeloid leukemia: incidence of sustained responses in an intention-to-treat analysis. *J Clin Oncol* **26**, 3358-3363 (2008).
110. Bhatia, R., Holtz, M., Niu, N., Gray, R., Snyder, D.S., Sawyers, C.L., Arber, D.A., Slovak, M.L. & Forman, S.J. Persistence of malignant hematopoietic progenitors in chronic myelogenous leukemia patients in complete cytogenetic remission following imatinib mesylate treatment. *Blood* **101**, 4701-4707 (2003).
111. Abe, A., Minami, Y., Hayakawa, F., Kitamura, K., Nomura, Y., Murata, M., Katsumi, A., Kiyoi, H., Jamieson, C.H., Wang, J.Y. & Naoe, T. Retention but significant reduction of BCR-ABL transcript in hematopoietic stem cells in chronic myelogenous leukemia after imatinib therapy. *Int J Hematol* **88**, 471-475 (2008).
112. Cortes, J., O'Brien, S. & Kantarjian, H. Discontinuation of imatinib therapy after achieving a molecular response. *Blood* **104**, 2204-2205 (2004).
113. Rousselot, P., Huguet, F., Rea, D., Legros, L., Cayuela, J.M., Maarek, O., Blanchet, O., Marit, G., Gluckman, E., Reiffers, J., Gardembas, M. & Mahon, F.X. Imatinib mesylate discontinuation in patients with chronic myelogenous leukemia in complete molecular remission for more than 2 years. *Blood* **109**, 58-60 (2007).
114. Mahon, F.X., Rea, D., Guilhot, J., Guilhot, F., Huguet, F., Nicolini, F., Legros, L., Charbonnier, A., Guerci, A., Varet, B., Etienne, G., Reiffers, J. & Rousselot, P. Discontinuation of imatinib in patients with chronic myeloid leukaemia who have maintained complete molecular remission

for at least 2 years: the prospective, multicentre Stop Imatinib (STIM) trial. *Lancet Oncol* **11**, 1029-1035 (2010).

115. Jabbour, E., Kantarjian, H., Jones, D., Talpaz, M., Bekele, N., O'Brien, S., Zhou, X., Luthra, R., Garcia-Manero, G., Giles, F., Rios, M.B., Verstovsek, S. & Cortes, J. Frequency and clinical significance of BCR-ABL mutations in patients with chronic myeloid leukemia treated with imatinib mesylate. *Leukemia* **20**, 1767-1773 (2006).
116. Shah, N.P., Skaggs, B.J., Branford, S., Hughes, T.P., Nicoll, J.M., Paquette, R.L. & Sawyers, C.L. Sequential ABL kinase inhibitor therapy selects for compound drug-resistant BCR-ABL mutations with altered oncogenic potency. *J Clin Invest* **117**, 2562-2569 (2007).
117. Graham, S.M., Jorgensen, H.G., Allan, E., Pearson, C., Alcorn, M.J., Richmond, L. & Holyoake, T.L. Primitive, quiescent, Philadelphia-positive stem cells from patients with chronic myeloid leukemia are insensitive to STI571 in vitro. *Blood* **99**, 319-325 (2002).
118. Barnes, D.J. & Melo, J.V. Primitive, quiescent and difficult to kill: the role of non-proliferating stem cells in chronic myeloid leukemia. *Cell Cycle* **5**, 2862-2866 (2006).
119. Michor, F., Hughes, T.P., Iwasa, Y., Branford, S., Shah, N.P., Sawyers, C.L. & Nowak, M.A. Dynamics of chronic myeloid leukaemia. *Nature* **435**, 1267-1270 (2005).
120. Roeder, I., Horn, M., Glauche, I., Hochhaus, A., Mueller, M.C. & Loeffler, M. Dynamic modeling of imatinib-treated chronic myeloid leukemia: functional insights and clinical implications. *Nat Med* **12**, 1181-1184 (2006).
121. Roeder, I. & Glauche, I. Pathogenesis, treatment effects, and resistance dynamics in chronic myeloid leukemia--insights from mathematical model analyses. *J Mol Med (Berl)* **86**, 17-27 (2008).
122. Skorski, T. Oncogenic tyrosine kinases and the DNA-damage response. *Nat Rev Cancer* **2**, 351-360 (2002).
123. Sattler, M., Verma, S., Shrikhande, G., Byrne, C.H., Pride, Y.B., Winkler, T., Greenfield, E.A., Salgia, R. & Griffin, J.D. The BCR/ABL tyrosine kinase induces production of reactive oxygen species in hematopoietic cells. *J Biol Chem* **275**, 24273-24278 (2000).
124. Nowicki, M.O., Falinski, R., Koptyra, M., Slupianek, A., Stoklosa, T., Gloc, E., Nieborowska-Skorska, M., Blasiak, J. & Skorski, T. BCR/ABL

- oncogenic kinase promotes unfaithful repair of the reactive oxygen species-dependent DNA double-strand breaks. *Blood* **104**, 3746-3753 (2004).
125. Slupianek, A., Hoser, G., Majsterek, I., Bronisz, A., Malecki, M., Blasiak, J., Fishel, R. & Skorski, T. Fusion tyrosine kinases induce drug resistance by stimulation of homology-dependent recombination repair, prolongation of G(2)/M phase, and protection from apoptosis. *Mol Cell Biol* **22**, 4189-4201 (2002).
  126. Cramer, K., Nieborowska-Skorska, M., Koptyra, M., Slupianek, A., Penserga, E.T., Eaves, C.J., Aulitzky, W. & Skorski, T. BCR/ABL and other kinases from chronic myeloproliferative disorders stimulate single-strand annealing, an unfaithful DNA double-strand break repair. *Cancer Res* **68**, 6884-6888 (2008).
  127. Reya, T., Duncan, A.W., Ailles, L., Domen, J., Scherer, D.C., Willert, K., Hintz, L., Nusse, R. & Weissman, I.L. A role for Wnt signalling in self-renewal of haematopoietic stem cells. *Nature* **423**, 409-414 (2003).
  128. Zhao, C., Blum, J., Chen, A., Kwon, H.Y., Jung, S.H., Cook, J.M., Lagoo, A. & Reya, T. Loss of beta-catenin impairs the renewal of normal and CML stem cells in vivo. *Cancer Cell* **12**, 528-541 (2007).
  129. Zhao, C., Chen, A., Jamieson, C.H., Fereshteh, M., Abrahamsson, A., Blum, J., Kwon, H.Y., Kim, J., Chute, J.P., Rizzieri, D., Munchhof, M., Vanarsdale, T., Beachy, P.A. & Reya, T. Hedgehog signalling is essential for maintenance of cancer stem cells in myeloid leukaemia. *Nature* (2009).
  130. Ito, T., Kwon, H.Y., Zimdahl, B., Congdon, K.L., Blum, J., Lento, W.E., Zhao, C., Lagoo, A., Gerrard, G., Foroni, L., Goldman, J., Goh, H., Kim, S.H., Kim, D.W., Chuah, C., Oehler, V.G., Radich, J.P., Jordan, C.T. & Reya, T. Regulation of myeloid leukaemia by the cell-fate determinant Musashi. *Nature* **466**, 765-768 (2010).
  131. Barnes, D.J., Schultheis, B., Adedeji, S. & Melo, J.V. Dose-dependent effects of Bcr-Abl in cell line models of different stages of chronic myeloid leukemia. *Oncogene* **24**, 6432-6440 (2005).
  132. Modi, H., McDonald, T., Chu, S., Yee, J.K., Forman, S.J. & Bhatia, R. Role of BCR/ABL gene-expression levels in determining the phenotype and imatinib sensitivity of transformed human hematopoietic cells. *Blood* **109**, 5411-5421 (2007).

133. Mohty, M., Yong, A.S., Szydlo, R.M., Apperley, J.F. & Melo, J.V. The polycomb group BMI1 gene is a molecular marker for predicting prognosis of chronic myeloid leukemia. *Blood* **110**, 380-383 (2007).
134. Cao, R., Tsukada, Y. & Zhang, Y. Role of Bmi-1 and Ring1A in H2A ubiquitylation and Hox gene silencing. *Mol Cell* **20**, 845-854 (2005).
135. Fuchs, Y. & Steller, H. Programmed cell death in animal development and disease. *Cell* **147**, 742-758 (2011).
136. Opferman, J.T. & Korsmeyer, S.J. Apoptosis in the development and maintenance of the immune system. *Nat Immunol* **4**, 410-415 (2003).
137. Wong, R.S. Apoptosis in cancer: from pathogenesis to treatment. *J Exp Clin Cancer Res* **30**, 87 (2011).
138. Edinger, A.L. & Thompson, C.B. Death by design: apoptosis, necrosis and autophagy. *Curr Opin Cell Biol* **16**, 663-669 (2004).
139. Elmore, S. Apoptosis: a review of programmed cell death. *Toxicol Pathol* **35**, 495-516 (2007).
140. Walsh, C.M. & Edinger, A.L. The complex interplay between autophagy, apoptosis, and necrotic signals promotes T-cell homeostasis. *Immunol Rev* **236**, 95-109 (2010).
141. Danial, N.N. & Korsmeyer, S.J. Cell death: critical control points. *Cell* **116**, 205-219 (2004).
142. Riedl, S.J. & Shi, Y. Molecular mechanisms of caspase regulation during apoptosis. *Nat Rev Mol Cell Biol* **5**, 897-907 (2004).
143. Deveraux, Q.L. & Reed, J.C. IAP family proteins--suppressors of apoptosis. *Genes Dev* **13**, 239-252 (1999).
144. Yang, Y.L. & Li, X.M. The IAP family: endogenous caspase inhibitors with multiple biological activities. *Cell Res* **10**, 169-177 (2000).
145. Legewie, S., Bluthgen, N. & Herzog, H. Mathematical modeling identifies inhibitors of apoptosis as mediators of positive feedback and bistability. *PLoS Comput Biol* **2**, e120 (2006).
146. Waring, P. & Mullbacher, A. Cell death induced by the Fas/Fas ligand pathway and its role in pathology. *Immunol Cell Biol* **77**, 312-317 (1999).

147. Vazquez, A., Bond, E.E., Levine, A.J. & Bond, G.L. The genetics of the p53 pathway, apoptosis and cancer therapy. *Nat Rev Drug Discov* **7**, 979-987 (2008).
148. Shiozaki, E.N. & Shi, Y. Caspases, IAPs and Smac/DIABLO: mechanisms from structural biology. *Trends Biochem Sci* **29**, 486-494 (2004).
149. Danial, N.N. BCL-2 family proteins: critical checkpoints of apoptotic cell death. *Clin Cancer Res* **13**, 7254-7263 (2007).
150. Adams, J.M. & Cory, S. The Bcl-2 apoptotic switch in cancer development and therapy. *Oncogene* **26**, 1324-1337 (2007).
151. Cory, S. & Adams, J.M. The Bcl2 family: regulators of the cellular life-or-death switch. *Nat Rev Cancer* **2**, 647-656 (2002).
152. Shamas-Din, A., Brahmabhatt, H., Leber, B. & Andrews, D.W. BH3-only proteins: Orchestrators of apoptosis. *Biochim Biophys Acta* **1813**, 508-520 (2011).
153. Kinoshita, T., Yokota, T., Arai, K. & Miyajima, A. Regulation of Bcl-2 expression by oncogenic Ras protein in hematopoietic cells. *Oncogene* **10**, 2207-2212 (1995).
154. Kinoshita, T., Yokota, T., Arai, K. & Miyajima, A. Suppression of apoptotic death in hematopoietic cells by signalling through the IL-3/GM-CSF receptors. *EMBO J* **14**, 266-275 (1995).
155. Franke, T.F., Hornik, C.P., Segev, L., Shostak, G.A. & Sugimoto, C. PI3K/Akt and apoptosis: size matters. *Oncogene* **22**, 8983-8998 (2003).
156. Li, W.X. Canonical and non-canonical JAK-STAT signaling. *Trends Cell Biol* **18**, 545-551 (2008).
157. Pecina-Slaus, N. Wnt signal transduction pathway and apoptosis: a review. *Cancer Cell Int* **10**, 22 (2010).
158. Bigelow, R.L., Chari, N.S., Uden, A.B., Spurgers, K.B., Lee, S., Roop, D.R., Toftgard, R. & McDonnell, T.J. Transcriptional regulation of bcl-2 mediated by the sonic hedgehog signaling pathway through gli-1. *J Biol Chem* **279**, 1197-1205 (2004).
159. Johnstone, R.W., Ruefli, A.A. & Lowe, S.W. Apoptosis: a link between cancer genetics and chemotherapy. *Cell* **108**, 153-164 (2002).

160. Akgul, C., Moulding, D.A. & Edwards, S.W. Alternative splicing of Bcl-2-related genes: functional consequences and potential therapeutic applications. *Cell Mol Life Sci* **61**, 2189-2199 (2004).
161. Bingle, C.D., Craig, R.W., Swales, B.M., Singleton, V., Zhou, P. & Whyte, M.K. Exon skipping in Mcl-1 results in a bcl-2 homology domain 3 only gene product that promotes cell death. *J Biol Chem* **275**, 22136-22146 (2000).
162. Cimmino, A., Calin, G.A., Fabbri, M., Iorio, M.V., Ferracin, M., Shimizu, M., Wojcik, S.E., Aqeilan, R.I., Zupo, S., Dono, M., Rassenti, L., Alder, H., Volinia, S., Liu, C.G., Kipps, T.J., Negrini, M. & Croce, C.M. miR-15 and miR-16 induce apoptosis by targeting BCL2. *Proc Natl Acad Sci U S A* **102**, 13944-13949 (2005).
163. Visone, R., Veronese, A., Rassenti, L.Z., Balatti, V., Pearl, D.K., Acunzo, M., Volinia, S., Taccioli, C., Kipps, T.J. & Croce, C.M. miR-181b is a biomarker of disease progression in chronic lymphocytic leukemia. *Blood* **118**, 3072-3079 (2011).
164. Willimott, S. & Wagner, S.D. Post-transcriptional and post-translational regulation of Bcl2. *Biochem Soc Trans* **38**, 1571-1575 (2010).
165. Ruvolo, P.P., Deng, X. & May, W.S. Phosphorylation of Bcl2 and regulation of apoptosis. *Leukemia* **15**, 515-522 (2001).
166. Deng, X., Gao, F. & May, W.S. Protein phosphatase 2A inactivates Bcl2's antiapoptotic function by dephosphorylation and up-regulation of Bcl2-p53 binding. *Blood* **113**, 422-428 (2009).
167. Zhao, Y., Altman, B.J., Coloff, J.L., Herman, C.E., Jacobs, S.R., Wieman, H.L., Wofford, J.A., Dimascio, L.N., Ilkayeva, O., Kelekar, A., Reya, T. & Rathmell, J.C. Glycogen synthase kinase 3alpha and 3beta mediate a glucose-sensitive antiapoptotic signaling pathway to stabilize Mcl-1. *Mol Cell Biol* **27**, 4328-4339 (2007).
168. Opferman, J.T. Unraveling MCL-1 degradation. *Cell Death Differ* **13**, 1260-1262 (2006).
169. Domina, A.M., Vrana, J.A., Gregory, M.A., Hann, S.R. & Craig, R.W. MCL1 is phosphorylated in the PEST region and stabilized upon ERK activation in viable cells, and at additional sites with cytotoxic okadaic acid or taxol. *Oncogene* **23**, 5301-5315 (2004).
170. Iglesias-Serret, D., de Frias, M., Santidrian, A.F., Coll-Mulet, L., Cosialls, A.M., Barragan, M., Domingo, A., Gil, J. & Pons, G. Regulation

- of the proapoptotic BH3-only protein BIM by glucocorticoids, survival signals and proteasome in chronic lymphocytic leukemia cells. *Leukemia* **21**, 281-287 (2007).
171. Cheng, E.H., Kirsch, D.G., Clem, R.J., Ravi, R., Kastan, M.B., Bedi, A., Ueno, K. & Hardwick, J.M. Conversion of Bcl-2 to a Bax-like death effector by caspases. *Science* **278**, 1966-1968 (1997).
  172. Liang, Y., Nylander, K.D., Yan, C. & Schor, N.F. Role of caspase 3-dependent Bcl-2 cleavage in potentiation of apoptosis by Bcl-2. *Mol Pharmacol* **61**, 142-149 (2002).
  173. Zhao, R., Follows, G.A., Beer, P.A., Scott, L.M., Huntly, B.J., Green, A.R. & Alexander, D.R. Inhibition of the Bcl-xL deamidation pathway in myeloproliferative disorders. *N Engl J Med* **359**, 2778-2789 (2008).
  174. Placzek, W.J., Wei, J., Kitada, S., Zhai, D., Reed, J.C. & Pellecchia, M. A survey of the anti-apoptotic Bcl-2 subfamily expression in cancer types provides a platform to predict the efficacy of Bcl-2 antagonists in cancer therapy. *Cell Death Dis* **1**, e40 (2010).
  175. Jaeger, U., Karth, G.D., Knapp, S., Friedl, J., Laczika, K. & Kusec, R. Molecular mechanism of the t(14;18)--a model for lymphoid-specific chromosomal translocations. *Leuk Lymphoma* **14**, 197-202 (1994).
  176. Hemann, M.T. & Lowe, S.W. The p53-Bcl-2 connection. *Cell Death Differ* **13**, 1256-1259 (2006).
  177. Neviani, P., Santhanam, R., Trotta, R., Notari, M., Blaser, B.W., Liu, S., Mao, H., Chang, J.S., Galletta, A., Uttam, A., Roy, D.C., Valtieri, M., Bruner-Klisovic, R., Caligiuri, M.A., Bloomfield, C.D., Marcucci, G. & Perrotti, D. The tumor suppressor PP2A is functionally inactivated in blast crisis CML through the inhibitory activity of the BCR/ABL-regulated SET protein. *Cancer Cell* **8**, 355-368 (2005).
  178. Moore, M.J., Wang, Q., Kennedy, C.J. & Silver, P.A. An alternative splicing network links cell-cycle control to apoptosis. *Cell* **142**, 625-636 (2010).
  179. Yoshida, K., Sanada, M., Shiraishi, Y., Nowak, D., Nagata, Y., Yamamoto, R., Sato, Y., Sato-Otsubo, A., Kon, A., Nagasaki, M., Chalkidis, G., Suzuki, Y., Shiosaka, M., Kawahata, R., Yamaguchi, T., Otsu, M., Obara, N., Sakata-Yanagimoto, M., Ishiyama, K., Mori, H., Nolte, F., Hofmann, W.K., Miyawaki, S., Sugano, S., Haferlach, C., Koefler, H.P., Shih, L.Y., Haferlach, T., Chiba, S., Nakauchi, H.,



- Miyano, S. & Ogawa, S. Frequent pathway mutations of splicing machinery in myelodysplasia. *Nature* **478**, 64-69 (2011).
180. Mehlen, P. & Puisieux, A. Metastasis: a question of life or death. *Nat Rev Cancer* **6**, 449-458 (2006).
181. Beverly, L.J. & Varmus, H.E. MYC-induced myeloid leukemogenesis is accelerated by all six members of the antiapoptotic BCL family. *Oncogene* **28**, 1274-1279 (2009).
182. Pommier, Y., Sordet, O., Antony, S., Hayward, R.L. & Kohn, K.W. Apoptosis defects and chemotherapy resistance: molecular interaction maps and networks. *Oncogene* **23**, 2934-2949 (2004).
183. Sanchez-Garcia, I. & Grutz, G. Tumorigenic activity of the BCR-ABL oncogenes is mediated by BCL2. *Proc Natl Acad Sci U S A* **92**, 5287-5291 (1995).
184. Aichberger, K.J., Mayerhofer, M., Krauth, M.T., Skvara, H., Florian, S., Sonneck, K., Akgul, C., Derdak, S., Pickl, W.F., Wacheck, V., Selzer, E., Monia, B.P., Moriggl, R., Valent, P. & Sillaber, C. Identification of mcl-1 as a BCR/ABL-dependent target in chronic myeloid leukemia (CML): evidence for cooperative antileukemic effects of imatinib and mcl-1 antisense oligonucleotides. *Blood* **105**, 3303-3311 (2005).
185. Amarante-Mendes, G.P., McGahon, A.J., Nishioka, W.K., Afar, D.E., Witte, O.N. & Green, D.R. Bcl-2-independent Bcr-Abl-mediated resistance to apoptosis: protection is correlated with up regulation of Bcl-xL. *Oncogene* **16**, 1383-1390 (1998).
186. Gesbert, F. & Griffin, J.D. Bcr/Abl activates transcription of the Bcl-X gene through STAT5. *Blood* **96**, 2269-2276 (2000).
187. del Peso, L., Gonzalez-Garcia, M., Page, C., Herrera, R. & Nunez, G. Interleukin-3-induced phosphorylation of BAD through the protein kinase Akt. *Science* **278**, 687-689 (1997).
188. Wang, H.G., Rapp, U.R. & Reed, J.C. Bcl-2 targets the protein kinase Raf-1 to mitochondria. *Cell* **87**, 629-638 (1996).
189. Horita, M., Andreu, E.J., Benito, A., Arbona, C., Sanz, C., Benet, I., Prosper, F. & Fernandez-Luna, J.L. Blockade of the Bcr-Abl kinase activity induces apoptosis of chronic myelogenous leukemia cells by suppressing signal transducer and activator of transcription 5-dependent expression of Bcl-xL. *J Exp Med* **191**, 977-984 (2000).

190. Oetzel, C., Jonuleit, T., Gotz, A., van der Kuip, H., Michels, H., Duyster, J., Hallek, M. & Aulitzky, W.E. The tyrosine kinase inhibitor CGP 57148 (ST1 571) induces apoptosis in BCR-ABL-positive cells by down-regulating BCL-X. *Clin Cancer Res* **6**, 1958-1968 (2000).
191. Kuroda, J., Puthalakath, H., Cragg, M.S., Kelly, P.N., Bouillet, P., Huang, D.C., Kimura, S., Ottmann, O.G., Druker, B.J., Villunger, A., Roberts, A.W. & Strasser, A. Bim and Bad mediate imatinib-induced killing of Bcr/Abl+ leukemic cells, and resistance due to their loss is overcome by a BH3 mimetic. *Proc Natl Acad Sci U S A* **103**, 14907-14912 (2006).
192. Bewry, N.N., Nair, R.R., Emmons, M.F., Boulware, D., Pinilla-Ibarz, J. & Hazlehurst, L.A. Stat3 contributes to resistance toward BCR-ABL inhibitors in a bone marrow microenvironment model of drug resistance. *Mol Cancer Ther* **7**, 3169-3175 (2008).
193. Ahuja, H., Bar-Eli, M., Advani, S.H., Benchimol, S. & Cline, M.J. Alterations in the p53 gene and the clonal evolution of the blast crisis of chronic myelocytic leukemia. *Proc Natl Acad Sci U S A* **86**, 6783-6787 (1989).
194. Ghaffari, S., Jagani, Z., Kitidis, C., Lodish, H.F. & Khosravi-Far, R. Cytokines and BCR-ABL mediate suppression of TRAIL-induced apoptosis through inhibition of forkhead FOXO3a transcription factor. *Proc Natl Acad Sci U S A* **100**, 6523-6528 (2003).
195. Domen, J., Gandy, K.L. & Weissman, I.L. Systemic overexpression of BCL-2 in the hematopoietic system protects transgenic mice from the consequences of lethal irradiation. *Blood* **91**, 2272-2282 (1998).
196. Domen, J. & Weissman, I.L. Hematopoietic stem cells and other hematopoietic cells show broad resistance to chemotherapeutic agents in vivo when overexpressing bcl-2. *Exp Hematol* **31**, 631-639 (2003).
197. Konopleva, M., Zhao, S., Hu, W., Jiang, S., Snell, V., Weidner, D., Jackson, C.E., Zhang, X., Champlin, R., Estey, E., Reed, J.C. & Andreeff, M. The anti-apoptotic genes Bcl-X(L) and Bcl-2 are over-expressed and contribute to chemoresistance of non-proliferating leukaemic CD34+ cells. *Br J Haematol* **118**, 521-534 (2002).
198. Rohn, J.L. & Noteborn, M.H. The viral death effector Apoptin reveals tumor-specific processes. *Apoptosis* **9**, 315-322 (2004).

199. Sun, H., Liu, L., Lu, J., Qiu, S., Yang, C.Y., Yi, H. & Wang, S. Cyclopeptide Smac mimetics as antagonists of IAP proteins. *Bioorg Med Chem Lett* **20**, 3043-3046 (2010).
200. Lain, S., Hollick, J.J., Campbell, J., Staples, O.D., Higgins, M., Aoubala, M., McCarthy, A., Appleyard, V., Murray, K.E., Baker, L., Thompson, A., Mathers, J., Holland, S.J., Stark, M.J., Pass, G., Woods, J., Lane, D.P. & Westwood, N.J. Discovery, in vivo activity, and mechanism of action of a small-molecule p53 activator. *Cancer Cell* **13**, 454-463 (2008).
201. Ocker, M., Neureiter, D., Lueders, M., Zopf, S., Ganslmayer, M., Hahn, E.G., Herold, C. & Schuppan, D. Variants of bcl-2 specific siRNA for silencing antiapoptotic bcl-2 in pancreatic cancer. *Gut* **54**, 1298-1308 (2005).
202. Oltersdorf, T., Elmore, S.W., Shoemaker, A.R., Armstrong, R.C., Augeri, D.J., Belli, B.A., Bruncko, M., Deckwerth, T.L., Dinges, J., Hajduk, P.J., Joseph, M.K., Kitada, S., Korsmeyer, S.J., Kunzer, A.R., Letai, A., Li, C., Mitten, M.J., Nettesheim, D.G., Ng, S., Nimmer, P.M., O'Connor, J.M., Oleksijew, A., Petros, A.M., Reed, J.C., Shen, W., Tahir, S.K., Thompson, C.B., Tomaselli, K.J., Wang, B., Wendt, M.D., Zhang, H., Fesik, S.W. & Rosenberg, S.H. An inhibitor of Bcl-2 family proteins induces regression of solid tumours. *Nature* **435**, 677-681 (2005).
203. Leber, B., Geng, F., Kale, J. & Andrews, D.W. Drugs targeting Bcl-2 family members as an emerging strategy in cancer. *Expert Rev Mol Med* **12**, e28 (2010).
204. Tse, C., Shoemaker, A.R., Adickes, J., Anderson, M.G., Chen, J., Jin, S., Johnson, E.F., Marsh, K.C., Mitten, M.J., Nimmer, P., Roberts, L., Tahir, S.K., Xiao, Y., Yang, X., Zhang, H., Fesik, S., Rosenberg, S.H. & Elmore, S.W. ABT-263: a potent and orally bioavailable Bcl-2 family inhibitor. *Cancer Res* **68**, 3421-3428 (2008).
205. Zhai, D., Jin, C., Satterthwait, A.C. & Reed, J.C. Comparison of chemical inhibitors of antiapoptotic Bcl-2-family proteins. *Cell Death Differ* **13**, 1419-1421 (2006).
206. O'Brien, S.M., Claxton, D.F., Crump, M., Faderl, S., Kipps, T., Keating, M.J., Viallet, J. & Cheson, B.D. Phase I study of obatoclax mesylate (GX15-070), a small molecule pan-Bcl-2 family antagonist, in patients with advanced chronic lymphocytic leukemia. *Blood* **113**, 299-305 (2009).

207. Lu, M., Wang, J., Li, Y., Berenzon, D., Wang, X., Mascarenhas, J., Xu, M. & Hoffman, R. Treatment with the Bcl-xL inhibitor ABT-737 in combination with interferon {alpha} specifically targets JAK2V617F positive polycythemia vera hematopoietic progenitor cells. *Blood* (2010).
208. Paik, P.K., Rudin, C.M., Pietanza, M.C., Brown, A., Rizvi, N.A., Takebe, N., Travis, W., James, L., Ginsberg, M.S., Juergens, R., Markus, S., Tyson, L., Subzwari, S., Kris, M.G. & Krug, L.M. A phase II study of obatoclax mesylate, a Bcl-2 antagonist, plus topotecan in relapsed small cell lung cancer. *Lung Cancer* **74**, 481-485 (2011).
209. Konopleva, M., Contractor, R., Tsao, T., Samudio, I., Ruvolo, P.P., Kitada, S., Deng, X., Zhai, D., Shi, Y.X., Sneed, T., Verhaegen, M., Soengas, M., Ruvolo, V.R., McQueen, T., Schober, W.D., Watt, J.C., Jiffar, T., Ling, X., Marini, F.C., Harris, D., Dietrich, M., Estrov, Z., McCubrey, J., May, W.S., Reed, J.C. & Andreeff, M. Mechanisms of apoptosis sensitivity and resistance to the BH3 mimetic ABT-737 in acute myeloid leukemia. *Cancer Cell* **10**, 375-388 (2006).
210. Vogler, M., Butterworth, M., Majid, A., Walewska, R.J., Sun, X.M., Dyer, M.J. & Cohen, G.M. Concurrent up-regulation of BCL-XL and BCL2A1 induces approximately 1000-fold resistance to ABT-737 in chronic lymphocytic leukemia. *Blood* **113**, 4403-4413 (2009).
211. Yecies, D., Carlson, N.E., Deng, J. & Letai, A. Acquired resistance to ABT-737 in lymphoma cells that up-regulate MCL-1 and BFL-1. *Blood* **115**, 3304-3313 (2010).
212. Chen, S., Dai, Y., Harada, H., Dent, P. & Grant, S. Mcl-1 down-regulation potentiates ABT-737 lethality by cooperatively inducing Bak activation and Bax translocation. *Cancer Res* **67**, 782-791 (2007).
213. Xu, H. & Krystal, G.W. Actinomycin D decreases Mcl-1 expression and acts synergistically with ABT-737 against small cell lung cancer cell lines. *Clin Cancer Res* **16**, 4392-4400 (2010).
214. Vogler, M., Weber, K., Dinsdale, D., Schmitz, I., Schulze-Osthoff, K., Dyer, M.J. & Cohen, G.M. Different forms of cell death induced by putative BCL2 inhibitors. *Cell Death Differ* **16**, 1030-1039 (2009).
215. Wei, J., Kitada, S., Rega, M.F., Emdadi, A., Yuan, H., Cellitti, J., Stebbins, J.L., Zhai, D., Sun, J., Yang, L., Dahl, R., Zhang, Z., Wu, B., Wang, S., Reed, T.A., Lawrence, N., Sebti, S., Reed, J.C. & Pellecchia, M. Apogossypol derivatives as antagonists of antiapoptotic Bcl-2 family proteins. *Mol Cancer Ther* **8**, 904-913 (2009).

216. Wei, J., Kitada, S., Rega, M.F., Stebbins, J.L., Zhai, D., Cellitti, J., Yuan, H., Emdadi, A., Dahl, R., Zhang, Z., Yang, L., Reed, J.C. & Pellecchia, M. Apogossypol derivatives as pan-active inhibitors of antiapoptotic B-cell lymphoma/leukemia-2 (Bcl-2) family proteins. *J Med Chem* **52**, 4511-4523 (2009).
217. Wei, J., Stebbins, J.L., Kitada, S., Dash, R., Placzek, W., Rega, M.F., Wu, B., Cellitti, J., Zhai, D., Yang, L., Dahl, R., Fisher, P.B., Reed, J.C. & Pellecchia, M. BI-97C1, an optically pure Apogossypol derivative as pan-active inhibitor of antiapoptotic B-cell lymphoma/leukemia-2 (Bcl-2) family proteins. *J Med Chem* **53**, 4166-4176 (2010).
218. Dash, R., Azab, B., Quinn, B.A., Shen, X.N., Wang, X.Y., Das, S.K., Rahmani, M., Wei, J., Hedvat, M., Dent, P., Dmitriev, I.P., Curiel, D.T., Grant, S., Wu, B., Stebbins, J.L., Pellecchia, M., Reed, J.C., Sarkar, D. & Fisher, P.B. An Apogossypol derivative BI-97C1 (sabutoclax) targeting Mcl-1 sensitizes prostate cancer cells to mda-7/IL-24-mediated toxicity. *Proc Natl Acad Sci U S A* (2011).
219. Guzman, M.L., Swiderski, C.F., Howard, D.S., Grimes, B.A., Rossi, R.M., Szilvassy, S.J. & Jordan, C.T. Preferential induction of apoptosis for primary human leukemic stem cells. *Proc Natl Acad Sci U S A* **99**, 16220-16225 (2002).
220. Chomel, J.C., Bonnet, M.L., Sorel, N., Bertrand, A., Meunier, M.C., Fichelson, S., Melkus, M., Bennaceur-Griscelli, A., Guilhot, F. & Turhan, A.G. Leukemic stem cell persistence in chronic myeloid leukemia patients with sustained undetectable molecular residual disease. *Blood* **118**, 3657-3660 (2011).
221. Chomel, J.C. & Turhan, A.G. Chronic myeloid leukemia stem cells in the era of targeted therapies: resistance, persistence and long-term dormancy. *Oncotarget* **2**, 713-727 (2011).
222. McWeeney, S.K., Pemberton, L.C., Loriaux, M.M., Vartanian, K., Willis, S.G., Yochum, G., Wilmot, B., Turpaz, Y., Pillai, R., Druker, B.J., Snead, J.L., Macpartlin, M., O'Brien, S.G., Melo, J.V., Lange, T., Harrington, C.A. & Deininger, M.W. A gene expression signature of CD34+ cells to predict major cytogenetic response in chronic phase chronic myeloid leukemia patients treated with imatinib. *Blood* (2009).
223. Jaiswal, S., Traver, D., Miyamoto, T., Akashi, K., Lagasse, E. & Weissman, I.L. Expression of BCR/ABL and BCL-2 in myeloid progenitors leads to myeloid leukemias. *Proc Natl Acad Sci U S A* **100**, 10002-10007 (2003).

224. Ding, Q., He, X., Xia, W., Hsu, J.M., Chen, C.T., Li, L.Y., Lee, D.F., Yang, J.Y., Xie, X., Liu, J.C. & Hung, M.C. Myeloid cell leukemia-1 inversely correlates with glycogen synthase kinase-3beta activity and associates with poor prognosis in human breast cancer. *Cancer Res* **67**, 4564-4571 (2007).
225. Karbasian Esfahani, M., Morris, E.L., Dutcher, J.P. & Wiernik, P.H. Blastic phase of chronic myelogenous leukemia. *Curr Treat Options Oncol* **7**, 189-199 (2006).
226. Sawyers, C.L., Hochhaus, A., Feldman, E., Goldman, J.M., Miller, C.B., Ottmann, O.G., Schiffer, C.A., Talpaz, M., Guilhot, F., Deininger, M.W., Fischer, T., O'Brien, S.G., Stone, R.M., Gambacorti-Passerini, C.B., Russell, N.H., Reiffers, J.J., Shea, T.C., Chapuis, B., Coutre, S., Tura, S., Morra, E., Larson, R.A., Saven, A., Peschel, C., Gratwohl, A., Mandelli, F., Ben-Am, M., Gathmann, I., Capdeville, R., Paquette, R.L. & Druker, B.J. Imatinib induces hematologic and cytogenetic responses in patients with chronic myelogenous leukemia in myeloid blast crisis: results of a phase II study. *Blood* **99**, 3530-3539 (2002).
227. Hochhaus, A., Kreil, S., Corbin, A.S., La Rosee, P., Muller, M.C., Lahaye, T., Hanfstein, B., Schoch, C., Cross, N.C., Berger, U., Gschaidmeier, H., Druker, B.J. & Hehlmann, R. Molecular and chromosomal mechanisms of resistance to imatinib (STI571) therapy. *Leukemia* **16**, 2190-2196 (2002).
228. Reed, J.C. Bcl-2-family proteins and hematologic malignancies: history and future prospects. *Blood* **111**, 3322-3330 (2008).
229. Milyavsky, M., Gan, O.I., Trottier, M., Komosa, M., Tabach, O., Notta, F., Lechman, E., Hermans, K.G., Eppert, K., Konovalova, Z., Ornatsky, O., Domany, E., Meyn, M.S. & Dick, J.E. A distinctive DNA damage response in human hematopoietic stem cells reveals an apoptosis-independent role for p53 in self-renewal. *Cell Stem Cell* **7**, 186-197 (2010).
230. Kumar, S. Caspase function in programmed cell death. *Cell Death Differ* **14**, 32-43 (2007).
231. Slebioda, T.J., Rowley, T.F., Ferdinand, J.R., Willoughby, J.E., Buchan, S.L., Taraban, V.Y. & Al-Shamkhani, A. Triggering of TNFRSF25 promotes CD8 T-cell responses and anti-tumor immunity. *Eur J Immunol* **41**, 2606-2611 (2011).

232. Tinel, A. & Tschopp, J. The PIDDosome, a protein complex implicated in activation of caspase-2 in response to genotoxic stress. *Science* **304**, 843-846 (2004).
233. Hasegawa, H., Yamada, Y., Tsukasaki, K., Mori, N., Tsuruda, K., Sasaki, D., Usui, T., Osaka, A., Atogami, S., Ishikawa, C., Machijima, Y., Sawada, S., Hayashi, T., Miyazaki, Y. & Kamihira, S. LBH589, a deacetylase inhibitor, induces apoptosis in adult T-cell leukemia/lymphoma cells via activation of a novel RAIDD-caspase-2 pathway. *Leukemia* **25**, 575-587 (2011).
234. Pobezinskaya, Y.L., Choksi, S., Morgan, M.J., Cao, X. & Liu, Z.G. The adaptor protein TRADD is essential for TNF-like ligand 1A/death receptor 3 signaling. *J Immunol* **186**, 5212-5216 (2011).
235. Meek, D.W. Tumour suppression by p53: a role for the DNA damage response? *Nat Rev Cancer* **9**, 714-723 (2009).
236. Steelman, L.S., Chappell, W.H., Abrams, S.L., Kempf, R.C., Long, J., Laidler, P., Mijatovic, S., Maksimovic-Ivanic, D., Stivala, F., Mazzarino, M.C., Donia, M., Fagone, P., Malaponte, G., Nicoletti, F., Libra, M., Milella, M., Tafuri, A., Bonati, A., Basecke, J., Cocco, L., Evangelisti, C., Martelli, A.M., Montalto, G., Cervello, M. & McCubrey, J.A. Roles of the Raf/MEK/ERK and PI3K/PTEN/Akt/mTOR pathways in controlling growth and sensitivity to therapy-implications for cancer and aging. *Aging (Albany NY)* **3**, 192-222 (2011).
237. Niemantsverdriet, M., Wagner, K., Visser, M. & Backendorf, C. Cellular functions of 14-3-3 zeta in apoptosis and cell adhesion emphasize its oncogenic character. *Oncogene* **27**, 1315-1319 (2008).
238. Moriyama, H. & Yonehara, S. Rapid up-regulation of c-FLIP expression by BCR signaling through the PI3K/Akt pathway inhibits simultaneously induced Fas-mediated apoptosis in murine B lymphocytes. *Immunol Lett* **109**, 36-46 (2007).
239. Tao, R.H., Berkova, Z., Wise, J.F., Rezaeian, A.H., Daniluk, U., Ao, X., Hawke, D.H., Karp, J.E., Lin, H.K., Mollidrem, J.J. & Samaniego, F. PMLRARalpha binds to Fas and suppresses Fas-mediated apoptosis through recruiting c-FLIP in vivo. *Blood* **118**, 3107-3118 (2011).
240. Imai, Y., Kimura, T., Murakami, A., Yajima, N., Sakamaki, K. & Yonehara, S. The CED-4-homologous protein FLASH is involved in Fas-mediated activation of caspase-8 during apoptosis. *Nature* **398**, 777-785 (1999).

241. Ploner, C., Kofler, R. & Villunger, A. Noxa: at the tip of the balance between life and death. *Oncogene* **27 Suppl 1**, S84-92 (2008).
242. Aggarwal, B.B. Signalling pathways of the TNF superfamily: a double-edged sword. *Nat Rev Immunol* **3**, 745-756 (2003).
243. Nakamura, M., Shimada, K. & Konishi, N. The role of HRK gene in human cancer. *Oncogene* **27 Suppl 1**, S105-113 (2008).
244. Chin, A.I., Dempsey, P.W., Bruhn, K., Miller, J.F., Xu, Y. & Cheng, G. Involvement of receptor-interacting protein 2 in innate and adaptive immune responses. *Nature* **416**, 190-194 (2002).
245. Adams, G.B., Chabner, K.T., Alley, I.R., Olson, D.P., Szczepiorkowski, Z.M., Poznansky, M.C., Kos, C.H., Pollak, M.R., Brown, E.M. & Scadden, D.T. Stem cell engraftment at the endosteal niche is specified by the calcium-sensing receptor. *Nature* **439**, 599-603 (2006).
246. Lo Celso, C., Fleming, H.E., Wu, J.W., Zhao, C.X., Miake-Lye, S., Fujisaki, J., Cote, D., Rowe, D.W., Lin, C.P. & Scadden, D.T. Live-animal tracking of individual haematopoietic stem/progenitor cells in their niche. *Nature* **457**, 92-96 (2009).
247. Hogge, D.E., Lansdorp, P.M., Reid, D., Gerhard, B. & Eaves, C.J. Enhanced detection, maintenance, and differentiation of primitive human hematopoietic cells in cultures containing murine fibroblasts engineered to produce human steel factor, interleukin-3, and granulocyte colony-stimulating factor. *Blood* **88**, 3765-3773 (1996).
248. Dierov, J., Sanchez, P.V., Burke, B.A., Padilla-Nash, H., Putt, M.E., Ried, T. & Carroll, M. BCR/ABL induces chromosomal instability after genotoxic stress and alters the cell death threshold. *Leukemia* **23**, 279-286 (2009).
249. Burke, B.A. & Carroll, M. BCR-ABL: a multi-faceted promoter of DNA mutation in chronic myelogenous leukemia. *Leukemia* **24**, 1105-1112 (2010).
250. Hayden, M.S., West, A.P. & Ghosh, S. NF-kappaB and the immune response. *Oncogene* **25**, 6758-6780 (2006).
251. Van Antwerp, D.J., Martin, S.J., Kafri, T., Green, D.R. & Verma, I.M. Suppression of TNF-alpha-induced apoptosis by NF-kappaB. *Science* **274**, 787-789 (1996).



252. Dutta, J., Fan, Y., Gupta, N., Fan, G. & Gelinas, C. Current insights into the regulation of programmed cell death by NF-kappaB. *Oncogene* **25**, 6800-6816 (2006).
253. Meng, Y., Li, Y., Li, J., Li, H., Fu, J., Liu, Y., Liu, H. & Chen, X. (-)-Gossypol and its combination with imatinib induce apoptosis in human chronic myeloid leukemic cells. *Leuk Lymphoma* **48**, 2204-2212 (2007).
254. Mak, D.H., Wang, R.Y., Schober, W.D., Konopleva, M., Cortes, J., Kantarjian, H., Andreeff, M. & Carter, B.Z. Activation of apoptosis signaling eliminates CD34(+) progenitor cells in blast crisis CML independent of response to tyrosine kinase inhibitors. *Leukemia* (2011).
255. Vogler, M., Dinsdale, D., Dyer, M.J. & Cohen, G.M. Bcl-2 inhibitors: small molecules with a big impact on cancer therapy. *Cell Death Differ* **16**, 360-367 (2009).
256. Schmittgen, T.D. & Livak, K.J. Analyzing real-time PCR data by the comparative C(T) method. *Nat Protoc* **3**, 1101-1108 (2008).
257. Campbell, C.J., Lee, J.B., Levadoux-Martin, M., Wynder, T., Xenocostas, A., Leber, B. & Bhatia, M. The human stem cell hierarchy is defined by a functional dependence on Mcl-1 for self-renewal capacity. *Blood* (2010).
258. van Stijn, A., Kok, A., van der Pol, M.A., Feller, N., Roemen, G.M., Westra, A.H., Ossenkoppele, G.J. & Schuurhuis, G.J. Multiparameter flow cytometric quantification of apoptosis-related protein expression. *Leukemia* **17**, 787-788 (2003).
259. Krajewska, M., Rosenthal, R.E., Mikolajczyk, J., Stennicke, H.R., Wiesenthal, T., Mai, J., Naito, M., Salvesen, G.S., Reed, J.C., Fiskum, G. & Krajewski, S. Early processing of Bid and caspase-6, -8, -10, -14 in the canine brain during cardiac arrest and resuscitation. *Exp Neurol* **189**, 261-279 (2004).
260. Winter, J.N., Weller, E.A., Horning, S.J., Krajewska, M., Variakojis, D., Habermann, T.M., Fisher, R.I., Kurtin, P.J., Macon, W.R., Chhanabhai, M., Felgar, R.E., Hsi, E.D., Medeiros, L.J., Weick, J.K., Reed, J.C. & Gascoyne, R.D. Prognostic significance of Bcl-6 protein expression in DLBCL treated with CHOP or R-CHOP: a prospective correlative study. *Blood* **107**, 4207-4213 (2006).
261. Krajewski, S., Bodrug, S., Gascoyne, R., Berean, K., Krajewska, M. & Reed, J.C. Immunohistochemical analysis of Mcl-1 and Bcl-2 proteins in normal and neoplastic lymph nodes. *Am J Pathol* **145**, 515-525 (1994).

262. Krajewska, M., Smith, L.H., Rong, J., Huang, X., Hyer, M.L., Zeps, N., Iacopetta, B., Linke, S.P., Olson, A.H., Reed, J.C. & Krajewski, S. Image analysis algorithms for immunohistochemical assessment of cell death events and fibrosis in tissue sections. *J Histochem Cytochem* **57**, 649-663 (2009).
263. Yamane, T., Dylla, S.J., Muijtjens, M. & Weissman, I.L. Enforced Bcl-2 expression overrides serum and feeder cell requirements for mouse embryonic stem cell self-renewal. *Proc Natl Acad Sci U S A* **102**, 3312-3317 (2005).
264. Mazel, S., Burtrum, D. & Petrie, H.T. Regulation of cell division cycle progression by bcl-2 expression: a potential mechanism for inhibition of programmed cell death. *J Exp Med* **183**, 2219-2226 (1996).
265. Vairo, G., Innes, K.M. & Adams, J.M. Bcl-2 has a cell cycle inhibitory function separable from its enhancement of cell survival. *Oncogene* **13**, 1511-1519 (1996).
266. Zinkel, S., Gross, A. & Yang, E. BCL2 family in DNA damage and cell cycle control. *Cell Death Differ* **13**, 1351-1359 (2006).
267. Kirstetter, P., Anderson, K., Porse, B.T., Jacobsen, S.E. & Nerlov, C. Activation of the canonical Wnt pathway leads to loss of hematopoietic stem cell repopulation and multilineage differentiation block. *Nat Immunol* **7**, 1048-1056 (2006).
268. Maurer, U., Charvet, C., Wagman, A.S., Dejardin, E. & Green, D.R. Glycogen synthase kinase-3 regulates mitochondrial outer membrane permeabilization and apoptosis by destabilization of MCL-1. *Mol Cell* **21**, 749-760 (2006).
269. Brusa, G., Zuffa, E., Mancini, M., Benvenuti, M., Calonghi, N., Barbieri, E. & Santucci, M.A. P210 Bcr-abl tyrosine kinase interaction with histone deacetylase 1 modifies histone H4 acetylation and chromatin structure of chronic myeloid leukaemia haematopoietic progenitors. *Br J Haematol* **132**, 359-369 (2006).
270. Jelinek, J., Gharibyan, V., Estecio, M.R., Kondo, K., He, R., Chung, W., Lu, Y., Zhang, N., Liang, S., Kantarjian, H.M., Cortes, J.E. & Issa, J.P. Aberrant DNA methylation is associated with disease progression, resistance to imatinib and shortened survival in chronic myelogenous leukemia. *PLoS One* **6**, e22110 (2011).

271. Wong, K.Y., So, C.C., Loong, F., Chung, L.P., Lam, W.W., Liang, R., Li, G.K., Jin, D.Y. & Chim, C.S. Epigenetic inactivation of the miR-124-1 in haematological malignancies. *PLoS One* **6**, e19027 (2011).
272. Dolgachev, V., Thomas, M., Berlin, A. & Lukacs, N.W. Stem cell factor-mediated activation pathways promote murine eosinophil CCL6 production and survival. *J Leukoc Biol* **81**, 1111-1119 (2007).
273. Matter, M.L. & Ruoslahti, E. A signaling pathway from the alpha5beta1 and alpha(v)beta3 integrins that elevates bcl-2 transcription. *J Biol Chem* **276**, 27757-27763 (2001).
274. Lee, B.H. & Ruoslahti, E. alpha5beta1 integrin stimulates Bcl-2 expression and cell survival through Akt, focal adhesion kinase, and Ca<sup>2+</sup>/calmodulin-dependent protein kinase IV. *J Cell Biochem* **95**, 1214-1223 (2005).
275. Tabe, Y., Jin, L., Tsutsumi-Ishii, Y., Xu, Y., McQueen, T., Priebe, W., Mills, G.B., Ohsaka, A., Nagaoka, I., Andreeff, M. & Konopleva, M. Activation of integrin-linked kinase is a critical prosurvival pathway induced in leukemic cells by bone marrow-derived stromal cells. *Cancer Res* **67**, 684-694 (2007).
276. Maffei, R., Fiorcari, S., Bulgarelli, J., Martinelli, S., Castelli, I., Deaglio, S., Debbia, G., Fontana, M., Coluccio, V., Bonacorsi, G., Zucchini, P., Narni, F., Torelli, G., Luppi, M. & Marasca, R. Physical contact with endothelial cells through beta1- and beta2- integrins rescues chronic lymphocytic leukemia from spontaneous and drug-induced apoptosis and induces a peculiar gene expression profile on leukemic cells. *Haematologica* (2011).
277. Matsunaga, T., Takemoto, N., Sato, T., Takimoto, R., Tanaka, I., Fujimi, A., Akiyama, T., Kuroda, H., Kawano, Y., Kobune, M., Kato, J., Hirayama, Y., Sakamaki, S., Kohda, K., Miyake, K. & Niitsu, Y. Interaction between leukemic-cell VLA-4 and stromal fibronectin is a decisive factor for minimal residual disease of acute myelogenous leukemia. *Nat Med* **9**, 1158-1165 (2003).
278. Jin, L., Tabe, Y., Konoplev, S., Xu, Y., Leysath, C.E., Lu, H., Kimura, S., Ohsaka, A., Rios, M.B., Calvert, L., Kantarjian, H., Andreeff, M. & Konopleva, M. CXCR4 up-regulation by imatinib induces chronic myelogenous leukemia (CML) cell migration to bone marrow stroma and promotes survival of quiescent CML cells. *Mol Cancer Ther* **7**, 48-58 (2008).

279. Giuntoli, S., Roviada, E., Barbetti, V., Cipolleschi, M.G., Olivotto, M. & Dello Sbarba, P. Hypoxia suppresses BCR/Abl and selects imatinib-insensitive progenitors within clonal CML populations. *Leukemia* **20**, 1291-1293 (2006).
280. Filippi, I., Naldini, A. & Carraro, F. Role of the hypoxic microenvironment in the antitumor activity of tyrosine kinase inhibitors. *Curr Med Chem* **18**, 2885-2892 (2011).
281. Tanturli, M., Giuntoli, S., Barbetti, V., Roviada, E. & Dello Sbarba, P. Hypoxia selects bortezomib-resistant stem cells of chronic myeloid leukemia. *PLoS One* **6**, e17008 (2011).
282. Zhao, F., Mancuso, A., Bui, T.V., Tong, X., Gruber, J.J., Swider, C.R., Sanchez, P.V., Lum, J.J., Sayed, N., Melo, J.V., Perl, A.E., Carroll, M., Tuttle, S.W. & Thompson, C.B. Imatinib resistance associated with BCR-ABL upregulation is dependent on HIF-1alpha-induced metabolic reprogramming. *Oncogene* **29**, 2962-2972 (2010).
283. Zhang, H., Li, H., Xi, H.S. & Li, S. HIF1alpha is required for survival maintenance of chronic myeloid leukemia stem cells. *Blood* (2012).
284. Ding, L., Saunders, T.L., Enikolopov, G. & Morrison, S.J. Endothelial and perivascular cells maintain haematopoietic stem cells. *Nature* **481**, 457-462 (2012).
285. Hermann, P.C., Bhaskar, S., Cioffi, M. & Heeschen, C. Cancer stem cells in solid tumors. *Semin Cancer Biol* **20**, 77-84 (2010).
286. Raheem, O., Kulidjian, A.A., Wu, C., Jeong, Y.B., Yamaguchi, T., Smith, K.M., Goff, D., Leu, H., Morris, S.R., Cacalano, N.A., Masuda, K., Jamieson, C.H., Kane, C.J. & Jamieson, C.A. A novel patient-derived intra-femoral xenograft model of bone metastatic prostate cancer that recapitulates mixed osteolytic and osteoblastic lesions. *J Transl Med* **9**, 185 (2011).